

SOLAR ULTRA-VIOLET RADIATION AND  
VITAMIN D SYNTHESIS IN MAN

by

A. R. WEBB, B.Sc.

Thesis submitted to the University of Nottingham  
for the degree of Doctor of Philosophy

Department of Physiology and Environmental Science  
University of Nottingham School of Agriculture  
Sutton Bonington, Loughborough, Leics.

July, 1985

**The following Images and Appendix have  
been omitted on request of the  
University –**

**Plate 3.1            pg. 32**

**Loose leaf article Appendix**

## ACKNOWLEDGEMENTS

"In man" : a study of people. The final words of the title reflect the tremendous help and cooperation I have received from human "materials" and, in work which links two branches of science, the assistance that I have had in the unfamiliar world of medicine.

On the side of environmental physics I would like to thank Chris Deuchar for help in building the integrators and Peter Schaare for the RS232 interface. My thanks also go to Dr. Paul Gibson of Glen Creston for work done in his laboratory with the spectroradiometer, and to Professor Gaylon Campbell for the mathematical means of correcting the measurements from this instrument. Ozone measurements were kindly supplied by Mr. Regan of the Meteorological Office, Bracknell.

I am particularly grateful to those brave volunteers who gave their blood for me: Chris Baker, Dick Berry, Martin Crawford, Mandy Fullwood, Mike Harvey, John Pritchard, Liz Rollin, Peter Schaare and Mike Steven. For taking part in the personal exposure trials and for help in numerous other forms I must also mention the following: Roy Bradshaw, John Burgess, Dawn Carter, Andy Chester, Jim Churchman, Jim Craigon, Chris Daniels, Chris Deuchar, Bob Dugdale, John Gigg, Keith Gregson, Jo and Ray Haines-Young, Dave Harris, David Holyoak, Bob Kear, Paul Mather, Andrew MacDonald, Alastair McArthur, Habib Mohammed, John Monteith, Jopie Paruntu, Jackie Savidge, Mary Seddon, Steve Stockley, John and Sandra Winn.

A further group of volunteers was drawn from elderly long-stay patients at Nottingham General Hospital and I wish to express my gratitude to the patients and staff of John Proctor, W.G. Player, Castle, Frank Jacob and Hogarth wards. Drs David Hosking and Gordon Campbell enabled me to work at the hospital and took the blood samples. I thank Rachel Berryman for teaching me the techniques and working with me on the analysis of the samples.

For advice and support, blood and time, I am most grateful to my two supervisors Professor J.L. Monteith and Dr. M.D. Steven. Finally I wish to thank Miss Edna Lord for typing this thesis and NERC for providing financial support.

## ABSTRACT

The solar UVB radiation incident on a horizontal surface was measured and related to more routinely recorded meteorological variables in a study of the UVB climatology of the English East Midlands. Exposure of individuals in this climate was monitored and related to vitamin D status.

On clear days relations were found between the logarithm of UVB intensity  $I_\lambda$  and airmass  $\mu$ , and at 304 nm where ozone amount  $[O_3]$  is the dominant atmospheric attenuating factor  $\partial^2 \ln I_\lambda / \partial \mu \partial [O_3]$  was close to the ozone absorption coefficient for this wavelength. At longer wavelengths other attenuation processes have to be accounted for.

Measurements of the waveband 300-316 nm were compared with irradiation over broader wavebands. On clear days the ratio of UVB to visible irradiance  $I_B/I_V$  was  $4.16 \cos z + x$  where  $z$  is the solar zenith angle and  $x$  is a coefficient which varies from day to day. Similar analysis for the full solar waveband  $I_F$  showed a similar linearity of  $I_B/I_F$  with  $\cos z$  for each day, but both slope and intercept changed between days.

A relation between daily integrated totals of UVB and full solar radiation (300-3000 nm) was found, enabling UVB radiation to be estimated from measurements made with a standard meteorological pyranometer. The best estimates require daily figures for ozone concentration but an approximation may still be made using monthly mean concentrations or climatological averages.

Diffuse UVB radiation was measured and found to be always greater than 0.5 global UVB. The shade-ring correction applicable in this region of the spectrum is ~ 0.01 greater than the geometric correction. Estimates of the anisotropy of UVB sky radiation gave the relative strength of the circumsolar region as 0.36 with an angular width of 0.78 radians.

Polysulphone film was tested and found suitable for use as a personal dosimeter for solar UVB radiation. The UVB exposure of elderly long-stay hospital patients was monitored for a three month period and compared with that of a young healthy population. Plasma 25-hydroxyvitamin D concentrations were measured to assess vitamin D status and the change in plasma 25(OH)D resulting from skin irradiated with solar UVB was found to be  $6.9 \pm 0.4 \text{ ng J}^{-1}$  for the elderly and  $7.3 \pm 3.4 \text{ ng J}^{-1}$  for the young volunteers suggesting little difference between the responses of the elderly and the young. The implication of these figures is that sunlight exposure of a few hours per week is adequate to maintain a healthy vitamin D status.

## C O N T E N T S

|   | Page |
|---|------|
| 1. INTRODUCTION                                     | 1    |
| 2. SOLAR ULTRAVIOLET RADIATION                      | 9    |
| Introduction  | 9    |
| Ozone in the Atmosphere                             | 10   |
| Stratospheric ozone                                 | 10   |
| The Chapman theory                                  | 12   |
| The hydrogen system                                 | 13   |
| The nitrogen system                                 | 13   |
| Chlorine reactions                                  | 14   |
| Tropospheric ozone                                  | 18   |
| Total ozone amount and UVB radiation                | 19   |
| Tropospheric Attenuation of UV Radiation            | 22   |
| Solar UV Radiation Measurements and Models          | 27   |
| 3. VITAMIN D  | 31   |
| Introduction  | 31   |
| Formation and Metabolism                            | 31   |
| The Relative Importance of UVB Irradiation and Diet | 34   |
| Vitamin D Deficiency in the Community               | 37   |
| The elderly   | 37   |
| Asian immigrants                                    | 39   |
| Methods of combatting deficiency                    | 41   |
| The Vitamin D Action Spectrum                       | 43   |
| 4. MATERIALS AND METHODS - CLIMATOLOGY              | 50   |
| The LICOR LI1800 Portable Spectroradiometer         | 50   |
| The SEE 240 Vacuum Photodiode                       | 58   |
| Testing of the SEE 240                              | 60   |
| Calibration   | 69   |

|  |     |
|--|-----|
| 4. (continued)                               |     |
| Diffuse UVB Radiation Measurement            | 75  |
| Broadband measurements                       | 75  |
| Shade-ring correction                        | 75  |
| Spectral measurements                        | 78  |
| ERRORS OF MEASUREMENT                        | 78  |
| LI1800 Portable Spectroradiometer            | 78  |
| The effective UVB response spectrum          | 82  |
| The total error                              | 88  |
| a) Spectral measurements                     | 88  |
| b) Broadband (300-316 nm) measurements       | 89  |
| Spectral sharpening                          | 90  |
| SEE 240/UVB/W Vacuum Photodiode              | 96  |
| Intercalibration of the two SEE 240 sensors  | 99  |
| 5. RESULTS AND DISCUSSION - THE UVB SPECTRUM | 102 |
| Introduction                                 | 102 |
| The UVB Spectrum Throughout the Year         | 103 |
| Spectral correction technique                | 103 |
| Clear-day climatology                        | 103 |
| Spectral attenuation in the atmosphere       | 110 |
| Comparison with UVB Model                    | 118 |
| The model                                    | 118 |
| Correction of measurements                   | 120 |
| Results                                      | 120 |
| 6. THE UVB WAVEBAND (300-316 nm)             | 125 |
| Introduction                                 | 125 |
| Clear-Day Climatology                        | 125 |
| The influence of cloud                       | 129 |

## 6. Continued

|  |     |
|--|-----|
| UVB and its Relation to Broadband Measurements   | 132 |
| Visible radiation on clear days                  | 132 |
| General theory                                   | 135 |
| Spectral measurements                            | 137 |
| Application to ultraviolet and visible radiation | 137 |
| Full solar radiation on clear days               | 141 |
| Daily Totals of UVB and Fullband Solar Radiation | 142 |
| Diffuse UVB Radiation                            | 154 |
| The ratio of diffuse to global radiation         | 155 |
| Anisotropy of UVB radiation                      | 162 |
| Illumination of Vertical Surfaces                | 165 |
| General theory                                   | 165 |
| Daily UVB irradiance of vertical surfaces        | 168 |
| Weekly UVB irradiance of vertical surfaces       | 172 |
| 7. POLYSULPHONE FILM                             | 175 |
| Introduction                                     | 175 |
| Polysulphone Film                                | 175 |
| Calibration                                      | 179 |
| Stability of the film                            | 184 |
| Polysulphone Personal Exposure Trial             | 187 |
| Materials and methods                            | 187 |
| Results  | 190 |
| Occupational Exposure to Solar UVB Radiation     | 195 |
| The volunteers                                   | 195 |
| UVB sunshine hours for the working day           | 196 |
| Occupational and seasonal exposure               | 199 |
| Work and leisure                                 | 202 |
| To distant climes                                | 208 |

|   | Page |
|---|------|
| <b>7. Continued</b>   |      |
| 27 January 1984, Val d' Isere, French Alps,<br>altitude 1400 m, latitude 4.5 <sup>o</sup> N | 209  |
| 18-22 June 1984, Austrian Alps, altitude<br>3000-7000 ft, latitude 47 <sup>o</sup> N        | 210  |
| 23-29 February, 18-24 March 1984 Hyderabad,<br>India, latitude 17.4 <sup>o</sup> N          | 211  |
| Summary   | 213  |
| <b>8. UVB AND VITAMIN D</b>   | 214  |
| Introduction  | 214  |
| Materials and Methods   | 214  |
| Elderly volunteers  | 214  |
| Young volunteers  | 215  |
| Results and discussion  | 216  |
| The Available UVB Radiation Climate   | 217  |
| Individual Exposure   | 222  |
| Vitamin D Status  | 232  |
| The Relation Between UVB Exposure and Vitamin D<br>Status                                   | 237  |
| The Control group   | 237  |
| The Sun-patient group   | 240  |
| The Young group   | 252  |
| Validity of results   | 257  |
| Comparison with other work  | 258  |
| Sunshine Hours and Vitamin D Health   | 259  |
| <b>9. SUMMARY and CONCLUSIONS</b>   | 262  |
| Introduction  | 262  |
| Spectral Measurements   | 262  |
| Broadband Measurements  | 263  |
| Diffuse Radiation   | 266  |
| Personal Exposure   | 268  |
| Vitamin D Status and UVB Exposure   | 270  |
| <b>REFERENCES</b>   | 275  |
| <b>APPENDICES</b>   | 292  |

## LIST of FIGURES

| Figure |  | Page |
|--------|--|------|
| 1.1    | Spectral distribution of solar radiation outside the earth's atmosphere and at the earth's surface.                  | 2    |
| 1.2    | Integrated effective solar UVB irradiance for five sites along the arctic-alpine life zone gradient.                 | 6    |
| 2.1    | a) Average total ozone with latitude and month.<br>b) Sun-path diagram for latitude 52°N.                            | 11   |
| 2.2    | Time variation in total ozone for Europe and North Temperate zone.   | 17   |
| 2.3    | Vertical ozone distribution.   | 20   |
| 2.4    | The measured intensities of UV global radiation as a function of ozone amount for a zenith angle of 45°.             | 21   |
| 2.5    | The annual variation of B/D at noon.   | 24   |
| 3.1    | Formation and metabolism of vitamin D.   | 33   |
| 3.2    | The relative efficiency of various wavelengths in producing vitamin D.   | 44   |
| 3.3    | Possible reactions between pre-vitamin D <sub>3</sub> and its isomers.   | 47   |
| 4.1    | Diagram of LI1800 scanning spectroradiometer.  | 53   |
| 4.2    | The influence of a long wavelength 'tail' on the response of an instrument measuring solar UVB radiation.            | 56   |
| 4.3    | Irradiance of a horizontal surface.  | 57   |
| 4.4    | The response spectrum of the SEE 240/UVB/W sensor and the action spectrum of human erythema and vitamin D synthesis. | 59   |

| Figure |  | Page |
|--------|--|------|
| 4.5    | The measured relative response spectrum of the SEE 240/UVB/W sensor, and the response when multiplied by the solar spectrum. | 61   |
| 4.6    | Temperature calibration and dark reading of the SEE 240/UVB/W sensor.  | 65   |
| 4.7    | Diagram of the SEE 240 mounted for field use.  | 68   |
| 4.8    | Diagram of meteorological site connection for the SEE 240.   | 70   |
| 4.9    | Calibration graph: signal from SEE 240 vs integrated 300-316 nm waveband from LI1800.  | 71   |
| 4.10   | Inter-sensor calibration checks for 2 clear days.  | 76   |
| 4.11   | Seasonal variation of shade-ring corrections at Sutton Bonington.  | 79   |
| 4.12   | The effective response of the LI1800 at $\lambda_0 = 300$ nm.  | 84   |
| 4.13   | $\lambda_{\frac{1}{2}}$ vs $\lambda_0$ for latitude $50^\circ$ , $[O_3] = 327$ matm cm,<br>$z = 50^\circ$ .                  | 84   |
| 4.14   | The quantities involved in the calculation of 'true' irradiance at a wavelength $\lambda_0$ .                                | 91   |
| 4.15   | The measured spectrum and corrected spectra after 2 and 4 iterations of Hoover's analysis.                                   | 93   |
| 4.16   | LI1800 spectra: 1 measured, 2 with spectral correction, 3 with spectral shift.   | 95   |
| 5.1    | The UVB spectrum at noon on clear days in (a) June and (b) December.   | 105  |
| 5.2    | Spectral irradiance values at noon on clear days for 3 wavelengths.  | 106  |
| 5.3    | The diurnal change of irradiance at 3 wavelengths for 3 clear days.  | 109  |

| Figure |  | Page |
|--------|--|------|
| 5.4    | $\ln I_\lambda$ vs $\mu$ at 3 wavelengths for 3 clear days.                                | 112  |
| 5.5    | - $\partial \ln I_\lambda / \partial \mu$ vs ozone concentration $[O_3]$ at 3 wavelengths. | 114  |
| 5.6    | $g$ vs $\mu$ at 3 wavelengths for 11 July 1983.  | 117  |
| 5.7    | Modelled vs measured irradiances at 3 wavelengths.   | 121  |
| 6.1    | UVB irradiance at noon on clear days in 1983 and 1984.                                     | 126  |
| 6.2    | The diurnal change in UVB irradiance for 4 clear days.                                     | 127  |
| 6.3    | The effect of cloud on UVB irradiance in June and December.                                | 130  |
| 6.4    | The changing ratio of UVB to visible radiation with zenith angle for 2 clear days.         | 133  |
| 6.5    | The changing ratio of UVB to fullband radiation with zenith angle on a clear day.          | 143  |
| 6.6    | UVB and full solar waveband daily radiation totals for clear days in 1983 and 1984.        | 145  |
| 6.7    | Daily totals of UVB and fullband radiation for April and November 1984.                    | 146  |
| 6.8    | $\rho$ vs $\cos z_m$ for months in 1983 and 1984.  | 150  |
| 6.9    | Annual cycles of monthly mean ozone amount and $\cos z$ .                                  | 152  |
| 6.10   | Normalised $\rho$ values vs $\cos z_m$ for 1984.   | 153  |
| 6.11   | Daily variation of $(D/I)_B$ with zenith angle for 2 clear days.                           | 158  |

| Figure |   | Page |
|--------|---|------|
| 6.12   | $(D/I)_B$ vs sec z for 2 days.  | 158  |
| 6.13   | $(D/I)_B$ vs $(D/I)_F$ for 2 clear days.  | 161  |
| 6.14   | $(D/I)_B$ vs $(D/I)_F$ for 3 limited ranges of sun angle                                    | 161  |
| 6.15   | $(D_s/D_{s_0})$ vs $1/f'$ for 10 clear days.  | 165  |
| 6.16   | Diagram of direct beam irradiance on a sloping surface.                                     | 167  |
| 6.17   | The irradiation of vertical surfaces normalised to the corresponding horizontal irradiance. | 169  |
| 6.18   | Mean and range of normalised vertical irradiances for part-day exposures.                   | 171  |
| 7.1    | The response spectrum of 40 $\mu\text{m}$ polysulphone film.                                | 177  |
| 7.2    | Polysulphone film badge calibration.  | 182  |
| 7.3    | UV radiation spectrum of laboratory lighting.   | 191  |
| 7.4    | Badge exposure vs grid exposure for weeks 1 and 3.  | 193  |
| 7.5    | Sample exposure grid with summer scale.   | 197  |
| 7.6    | Daily duration of solar UVB radiation on clear days throughout the year.                    | 198  |
| 7.7    | Working week exposure ranges by season and occupational category.                           | 200  |
| 7.8    | Cumulative UVB exposures for 4 volunteers during the two trial periods.                     | 205  |
| 8.1    | Weekly exposures of Control group badges and indoor badges of Young group.                  | 218  |
| 8.2    | The available UVB radiation at Nottingham and Sutton Bonington.                             | 219  |

| Figure |  | Page |
|--------|--|------|
| 8.3    | Weekly exposures of badges for the Sun group and the Young group.  | 225  |
| 8.4    | Total accumulated UVB for the Sun group and Young group.   | 231  |
| 8.5    | First and final plasma 25(OH)D concentrations of the three volunteer groups.                                   | 233  |
| 8.6    | Plasma 25(OH)D concentrations and mean cumulative UVB dose by week for the Control group.                      | 238  |
| 8.7    | Plasma 25(OH)D concentration and cumulative UVB doses by week for the Sun group.                               | 241  |
| 8.8    | Illustration of the change in plasma 25(OH)D concentration and the UVB irradiation to which it was attributed. | 248  |
| 8.9    | Change in plasma 25(OH)D concentration with cumulative UVB exposure for the Sun group.                         | 249  |
| 8.10   | Change in plasma 25(OH)D concentration with cumulative UVB exposure for the Young group.                       | 253  |

LIST of TABLES

| Table |   | Page |
|-------|---|------|
| 2.1   | The short wavelength limit of the solar spectrum as a function of zenith angle in various seasons in Switzerland. | 27   |
| 4.1   | Ratio of measured to 'true' irradiance at 5 wavelengths.  | 85   |
| 4.2   | Effect of zenith angle and ozone amount on $I_{\lambda_1}/I_{\lambda_0}$ .  | 86   |
| 4.3   | Median and measured wavelengths for LI1800.   | 87   |
| 4.4   | Random errors associated with LI1800 measurements.  | 89   |
| 5.1   | $k_\lambda$ and the corresponding values of $\partial^2 \ln I_\lambda / \partial \mu \partial [O_3]$              | 113  |
| 5.2   | Slopes of $g$ vs $\mu$ for 3 wavelengths.   | 116  |
| 5.3   | $\partial \ln I_\lambda / \partial \mu$ for clear days and $\partial g / \partial \mu$ where available.           | 119  |
| 5.4   | Slopes and intercepts of modelled vs measured irradiance plots.   | 122  |
| 6.1   | Gradients and intercepts for $I_B/I_V$ vs $\cos z$ on clear days.   | 134  |
| 6.2   | $\rho$ and $\eta$ for each month of 1983 and 1984.  | 148  |
| 6.3   | Monthly mean ozone values and monthly mean $\cos z_m$ .   | 149  |
| 6.4   | Annual variation of $(D/I)_B$ and $(D/I)_F$ at 1200 GMT on clear days.  | 156  |
| 6.5   | Weekly irradiances on horizontal and vertical surfaces.   | 173  |
| 7.1   | Values of $\alpha$ and $\beta$ for different batches of polysulphone film used in summer and winter.              | 181  |
| 7.2   | Exposure grid scores.   | 188  |

| Table |  | Page |
|-------|--|------|
| 7.3   | UVB radiation under different lighting conditions.   | 190  |
| 7.4   | Normalised vertical irradiance for weeks 1 and 3.  | 194  |
| 7.5   | Classification of June volunteers by age and occupation.                                   | 196  |
| 7.6   | Maximum exposures by occupation in January and June with respect to total indoor exposure. | 201  |
| 7.7   | Occupational percentages of available workday UVB radiation.                               | 207  |
| 7.8   | Occupational percentages of ambient UVB received.  | 207  |
| 7.9   | UVB radiation incident in French Alps and intercepted by skiers.                           | 209  |
| 7.10  | Available and received UVB of outdoor worker in India.                                     | 212  |
| 8.1   | The volunteer groups.  | 216  |
| 8.2   | Cumulative UVB exposures of Sun, Control and Young groups by week of trial.                | 226  |
| 8.3   | Weekly mean and median exposures for exposed subjects.                                     | 228  |
| 8.4   | First and final plasma 25(OH)D values for the three volunteer groups.                      | 232  |
| 8.5   | Plasma 25(OH)D levels for Control and Sun-patients.  | 235  |
| 8.6   | Plasma 25(OH)D concentrations and cumulative UVB for Sun-patients.                         | 243  |
| 8.7   | Proportion of body surface area accounted for by different parts of the body.              | 251  |
| 8.8   | Plasma 25(OH)D levels and cumulative UVB for Young subjects.                               | 254  |

LIST of PLATES

| Plate |  | Page |
|-------|--|------|
| 3.1   | Rachitic children in the 1920's.               | 32   |
| 4.1   | The meteorological site, Sutton Bonington.     | 51   |
| 4.2   | The LICOR portable spectroradiometer.          | 51   |
| 7.1   | Polysulphone film badge.                       | 179  |
| 8.1   | The terrace to which the Sun-group had access. | 220  |
| 8.2   | Patients sitting on the terrace.               | 223  |
| 8.3   | Variation in dress for the Young group.        | 255  |

### PRINCIPAL SYMBOLS USED IN TEXT

|              |   |
|--------------|---|
| B            | direct beam irradiance on a horizontal surface                          |
| $B_\lambda$  | monochromatic direct beam irradiance at wavelength $\lambda$            |
| $B_L$        | direct beam irradiance on a vertical surface                            |
| D            | diffuse irradiance on a horizontal surface                              |
| $D_\lambda$  | monochromatic diffuse irradiance at wavelength $\lambda$                |
| I            | global (direct + diffuse) irradiance on a horizontal surface            |
| $I_\lambda$  | monochromatic global irradiance at wavelength $\lambda$                 |
| $I_B$        | global irradiance in the waveband 300-316 nm                            |
| $I_V$        | global irradiance in the waveband 300-700 nm                            |
| $I_F$        | global irradiance in the waveband 300-3000 nm                           |
| $\Sigma I_B$ | daily integrated total of global irradiance in the waveband 300-316 nm  |
| $\Sigma I_F$ | daily integrated total of global irradiance in the waveband 300-3000 nm |
| $(D/I)_B$    | ratio of diffuse to global irradiance in the waveband 300-316 nm        |
| $(D/I)_F$    | ratio of diffuse to global irradiance in the waveband 300-3000 nm       |
| $[O_3]$      | equivalent depth of the ozone layer                                     |
| b            | Rayleigh scattering coefficient   |
| c            | attenuation coefficient for aerosol and other absorbers                 |
| k            | ozone absorption coefficient  |
| m            | airmass   |
| z            | zenith angle  |
| $\phi$       | azimuth angle   |
| $\lambda$    | wavelength  |

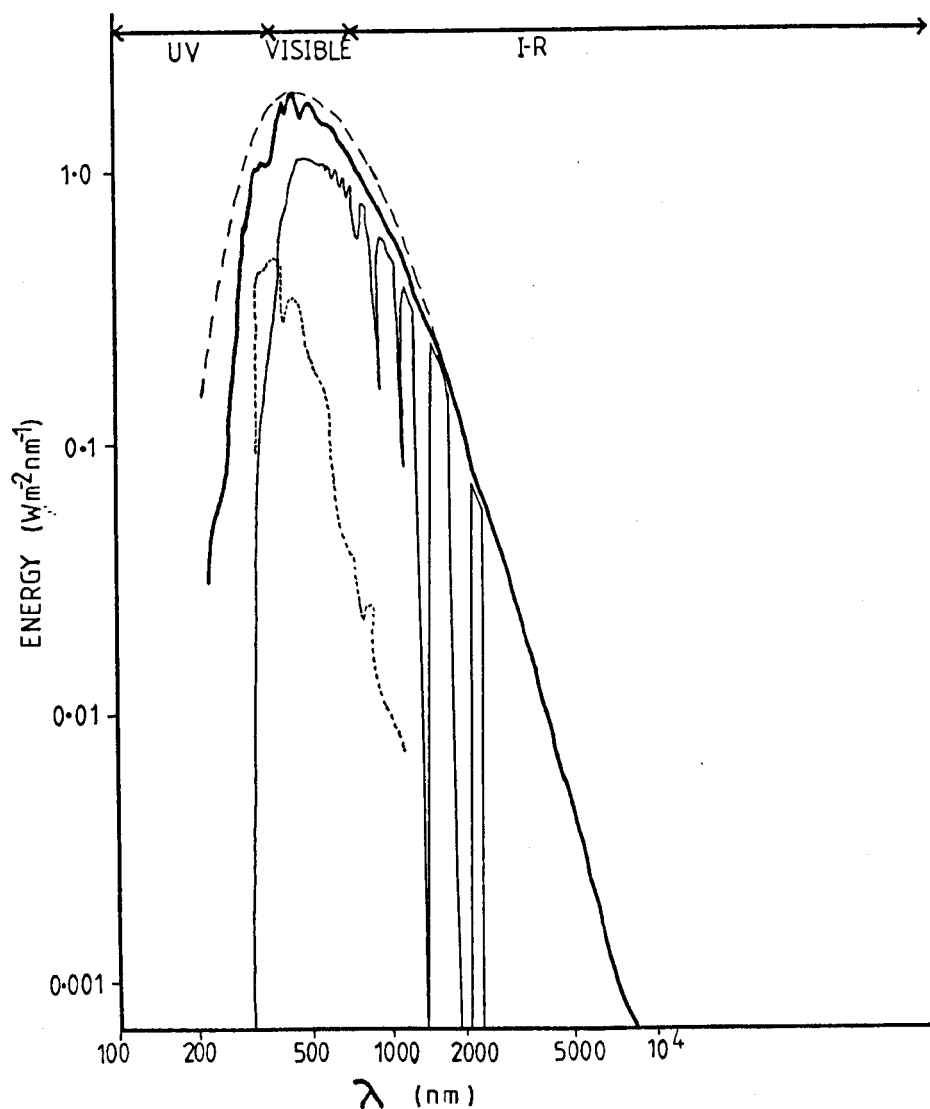
$\mu$  ozone pathlength  
 $\Delta A_{330}$  change in absorbance at a wavelength of 330 nm  
25(OH)D 25 hydroxyvitamin D  
BST British summer time  
GMT Greenwich mean time  
NEI Noise equivalent irradiance

## 1. INTRODUCTION

The short wavelength limit (defined as the wavelength below which no irradiance can be detected) of solar radiation reaching the earth's surface falls in the ultraviolet region of the electromagnetic spectrum at about 290 nm. The Commission International d'Eclairage has defined three regions within the ultraviolet spectrum: UVA (315-400 nm) which contains most of the UV radiation at the earth's surface; UVB (280-315 nm), a small but biologically important spectral region at the short wavelength limit of radiation reaching the earth; and UVC (100-280 nm) which is totally absorbed in the upper atmosphere by oxygen and ozone and is not present in the spectrum at the ground.

Outside the earth's atmosphere the solar spectrum above a wavelength of 400 nm can be approximated by the spectrum of a black body at 6000 K. In the UV region of the spectrum from 200-400 nm the solar emission comes from a region of the sun above the photosphere and corresponds to a lower temperature. For the UVA and UVB bands the radiation can be identified with black body radiation at 5700-5800 K, and at 200 nm the equivalent temperature is 5000 K. The extraterrestrial radiation intensity therefore decreases rapidly with decreasing wavelength below 400 nm: for a solar constant,  $S_0 = 1353 \text{ W m}^{-2}$  (Thekaekara, 1974) the UVA band contains  $7.1\% S_0$ ,  $1.5\% S_0$  <sup>UVB</sup> and UVC 0.5%. Fig. 1.1 shows the spectral distribution of solar radiation outside the atmosphere.

As the UV radiation from the sun penetrates the earth's atmosphere it is depleted in a number of ways: by ozone absorption, Rayleigh scattering, and scattering and absorption by atmospheric aerosol. In consequence, the spectrum of solar radiation at the



— — — Black body radiation at 6000 K

— — Extraterrestrial solar radiation

— — Direct beam solar irradiance at surface

..... Diffuse radiation at earth's surface

Fig. 1.1 Spectral distribution of solar radiation outside the earth's atmosphere and at the earth's surface (Sellers, 1969).

ground has a short wavelength limit around 290 nm and about 90% of UV energy is received in the UVA band.

Wavelengths shorter than 200 nm are removed from the extraterrestrial spectrum by the strong absorption of molecular oxygen. Oxygen is a permanent and major constituent of the atmosphere and is a regular absorber. This process is responsible for the thermal balance of the upper atmosphere.

Above 200 nm ozone becomes the dominant absorber of incident radiation. There are two significant spectral regions for UV absorption: the Hartley band (220-320 nm) and the Huggins band (320-360 nm). The maximum absorption of these two bands occurs at 255 nm, decreasing with increasing wavelength towards 360 nm where the bands are weak. As a result some of the extraterrestrial radiation at the longer wavelength end of these bands (280-360 nm) is able to penetrate to the earth's surface giving the spectrum at the ground shown in Fig. 1.1. The solar spectrum at the earth's surface therefore contains only UVA and UVB radiation.

Although most of the ultraviolet energy is contained in the UVA band, it is the small number of high energy photons in the UVB part of the solar spectrum which are of biological importance. These high energy photons are required to initiate a number of important photochemical and photobiological reactions; an example experienced by many white people is the production of erythema (sunburn) in skin. In man overexposure to UVB is known to encourage skin cancers, but with moderate exposure there are beneficial effects such as the production of vitamin D in skin. Other animals can also develop

cancer on unprotected skin if exposed to strong solar UV radiation, and under weak UV radiation conditions can show signs of vitamin D deficiency.

A review of the effect of environmental levels of UV radiation on plants is given by Klein (1978). Some plants are more sensitive than others to increased UVB, but it has been shown (Teramura, 1980; Tevini, et al., 1982a; Biggs, et al., 1985) that increased UVB radiation inhibits photosynthesis, reduces yield, reduces resistance to disease and increases chlorophyll in agricultural crops. It is possible that the ability of different species to adapt to changing UVB levels (which would result from any change in stratospheric ozone) could alter the natural balance of competition between plants and so change the ecosystem of an area (Bogenreider and Klein, 1982). Some of the consequences of increasing UVB appear to depend simply on the accumulated dose e.g. reduction in seed germination and seedling growth (Tevini, et al., 1982b) but other reactions are more complex: Tevini et al. (1982b) found that photosynthesis was suppressed far more under continual exposure to UVB radiation than when the additional UVB was present in a day/night lighting cycle. A dark repair process appears to operate in the absence of UVB radiation. Other types of damage depend on a peak dose e.g. the inhibition of leaf expansion, and above a certain threshold dose the damage is irreversible (Teramura, 1980; Tevini, et al., 1982a).

Marine ecosystems, as well as those on dry land may be affected by changes in solar UVB radiation. Transmittance in clear oceanic waters is as much as 80%  $m^{-1}$  at 300 nm (Halldal, 1979; Smith and

Baker, 1981). Phytoplankton, which are crucial to the foodchain, are one example of a plant sensitive to UVB radiation and found close to the surface of water bodies. Disruption of the phytoplankton population could alter the whole aquatic ecosystem. A review of literature concerning the impact of UVB radiation upon marine organisms is given by Worrest (1982).

Adaptation to a changed UVB radiation climate is shown by some animals and plants. This often takes the form of altered pigmentation in skin or leaves, and the latter can also alter surface wax layers if radiation changes are gradual. Other reactions which protect against overexposure to UVB e.g. the seeking of shade, leaf orientation, are responses to heat or visible light stress due to total solar radiation load. The present correlation between UVB and total solar radiation provides an indirect protective mechanism. However, a decrease in ozone would increase the proportion of UVB in the total solar spectrum and there would be no adaptation of this wavelength-correlated protection to the increased UVB levels.

While the level of solar UVB radiation is only one aspect of the complex collection of environmental factors which together designate our climates, life in any climate must be able to tolerate all the environmental variables encountered. Man has become adapted to incident UVB radiation levels over an extensive range from tropical to arctic climatic conditions (Fig. 1.2) but individuals are tolerant to different points on this wide scale: in mid-latitudes the north-south doubling distance for the erythema dose of UV radiation is approximately 600 miles (Ellsaeser, 1982). Transported away from

- KEY : 1. Equatorial latitude, elevation 3000-4400 m  
2. Tropical latitude, elevation 3000 m  
3. Temperate latitude, elevation 3350 m  
4. Temperate latitude. elevation 1500 m  
5. Arctic latitude, elevation sea level

For days when solar angles from the zenith are at a minimum for each latitude.

The integral effective irradiance was convoluted following the DNA-damage spectrum and is denoted as DNA-effective irradiance.

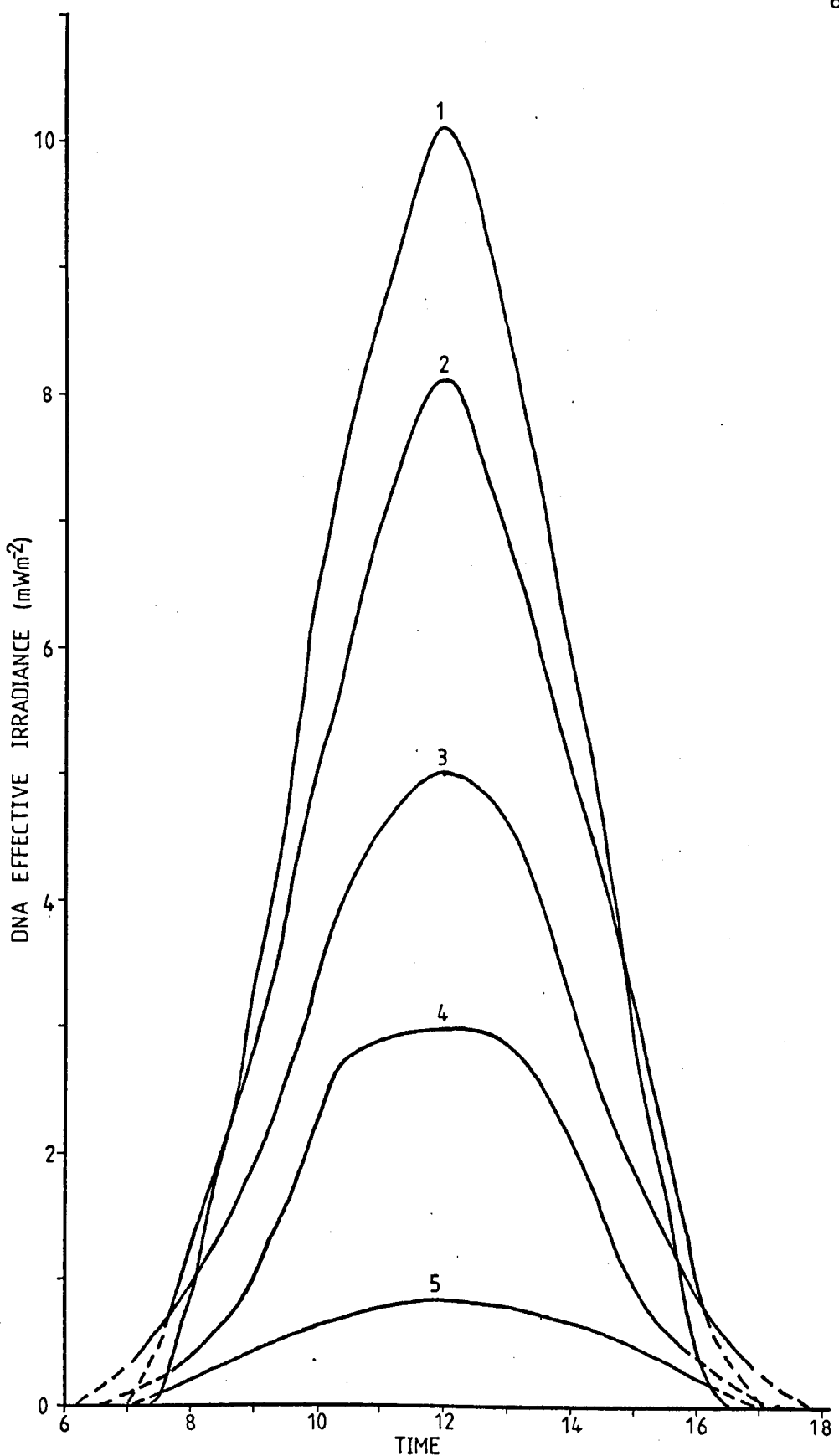


Fig. 1.2 Integrated effective solar UVB irradiance for five sites along the arctic-alpine life zone gradient (Caldwell, *et al.*, 1980)

their natural environment different races may suffer from the change in UVB climate (Farnsworth-Loomis, 1967); skin cancer is more prevalent among caucasian Australians than the indigenous Aborigines; Asians in Britain are more prone to vitamin D deficiency than their white neighbours.

Deficiency of vitamin D, leading to rickets and osteomalacia, still occurs among certain sections of the British population, particularly <sup>Asian</sup> immigrants and the elderly, and recent research (DHSS, 1980) suggests that the safe limits for vitamin D supplementation in the diet are much lower than originally thought. The problem of cutaneous production of vitamin D initiated by ambient UVB radiation has been chosen as a particular application of the measurements of solar UVB radiation presented in this thesis.

One source of vitamin D is the diet, and the amount of the vitamin present in foodstuffs is well documented (Paul and Southgate, 1978). The major unknown factor in the vitamin D status of man is the cutaneous production of the vitamin following UVB irradiation. This factor has three components:

- i) the distribution of effective UVB in the natural environment;
- ii) the exposure of individuals to UVB in a specific environment;
- iii) the production of vitamin D by irradiated skin per unit of incident UVB.

The aim of the experimental programme was to investigate these three factors. Natural UVB incident at Sutton Bonington ( $52^{\circ} 50'N$ ,  $1^{\circ} 15'W$ ) has been measured over a period of 22 months together with the broad band solar radiation in order to relate the UVB radiation to more routinely measured meteorological variables.

The resulting patterns of daily and annual UVB radiation indicate the amount of UVB available (on a horizontal surface) in the natural environment. These measurements are completely general and could be applied to a wide range of topics other than the one studied here.

Personal exposure in an environment depends not only on the climatology of that environment. Few individuals spend all daylight hours unclothed and out of doors, so exposure is considerably less than UV irradiation of a horizontal surface with the same area as the human body. The range of UVB doses received by a population in Sutton Bonington's climate was investigated using personal dosimeter badges of polysulphone film.

The vitamin D status of an individual can be assessed by measuring the level of 25-hydroxyvitamin D ( $25(OH)D$ ), one of the vitamin D metabolites, in blood plasma. This procedure was used in conjunction with polysulphone film badges measuring personal exposure to investigate the in vivo production of vitamin D by UVB irradiated skin.

## 2. SOLAR ULTRAVIOLET RADIATION

### Introduction

Solar radiation reaching the earth's surface at any wavelength depends on the extraterrestrial radiation at that wavelength and the spectral attenuation that occurs along the atmospheric pathlength. Extraterrestrial irradiance over the full solar waveband is generally accepted to be the solar constant  $S_0 = 1353 \text{ W m}^{-2}$  which, despite its name, is the annual average value of radiation outside the atmosphere. Changing sun-earth distance throughout the year results in seasonal variations in  $S_0$  with a maximum of  $1400 \text{ W m}^{-2}$  about January 4 and a minimum of  $1309 \text{ W m}^{-2}$  about July 5 (Thekaekara, 1976). Differing spectral values due to the sun-earth distance are in the same ratio as total irradiance changes.

A further cause of variation in the extraterrestrial radiation would be changes in solar output. The most strongly supported periodic change in solar output follows the 22-year cycle of changing sunspot number, with a maximum solar output being associated with a minimum sunspot number. This theory is based on measurements made from balloon ascents, sightings of solar eclipses, and more recently from satellites. Experimental error, particularly in the earlier measurements, is generally too large to enable firm conclusions to be drawn of a correlation over the full 22-year cycle. Data for half a cycle (1965-1973) suggests that for  $\lambda < 300 \text{ nm}$  the solar output varies considerably with changing sunspot number (Callis, 1979). More recent satellite data also indicate a change in solar output

associated with sunspot number. Decreases in  $S_0$  of about 0.1% were observed by Gough (1980) over periods of 10 days when large sunspot groups appeared on the solar disc; Wilson, et al. (1980) report decreases of up to 0.2% lasting for about a week and highly correlated with the development of sunspot groups.

Extraterrestrial radiation changes of  $\pm 3\%$  (seasonal) and 0.2% (sunspot) have a much modified influence on radiation reaching the earth's surface as atmospheric attenuation varies considerably both daily and annually across the solar spectrum. Absorption by ozone, found mainly in the stratosphere with a maximum concentration at a height of  $\sim 25$  km, is the major attenuating process for UVB radiation. As wavelength increases in the UV part of the spectrum the absorption bands of ozone become weaker and some of the UVB and UVA extraterrestrial radiation is able to reach the earth's surface. The degree of penetration in this spectral region depends on the amount of ozone present in the path of the radiation from sun to earth. Since ozone concentration varies in space and time, and the pathlength for incident radiation changes with latitude and season, the absorption spectrum is a complicated function of both position and time (Fig. 2.1).

### Ozone in the Atmosphere

#### Stratospheric ozone

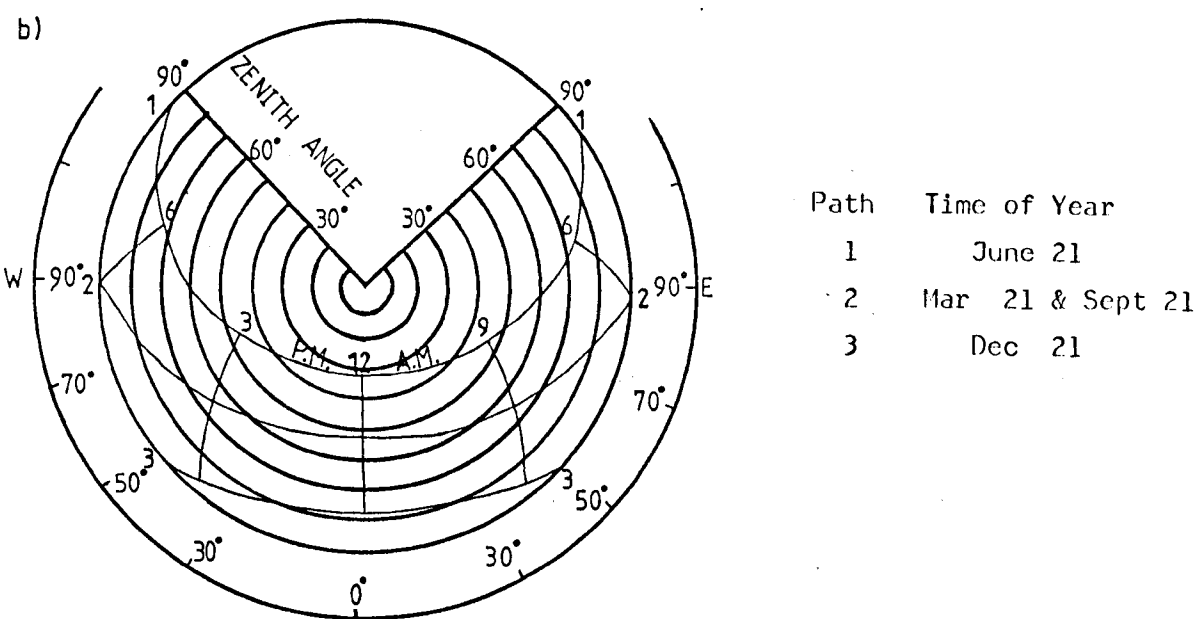
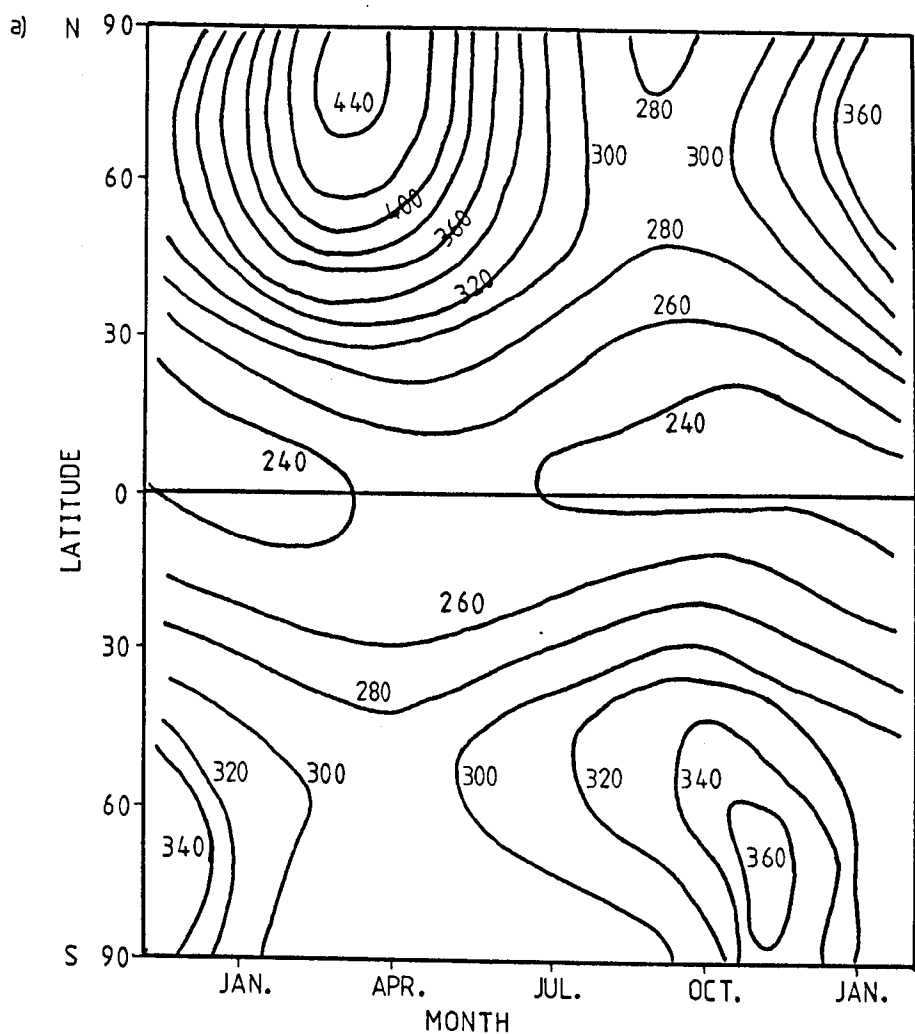
The chemistry of ozone in the atmosphere is driven by the photochemical dissociation of molecular oxygen which requires energy from photons in the UV band ( $\lambda < 242$  nm). Ozone is destroyed by photodissociation ( $\lambda < 320$  nm) or by collision with atmospheric oxygen

Fig. 2.1

a) Average total ozone (matm cm)  
with latitude and month from  
observations made from 1957-1967  
(WMO, 1979).

b) Sun-path diagram for latitude  $52^{\circ}$  N  
(Sellers, 1969).

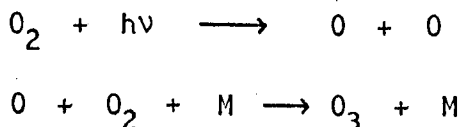
Atmospheric pathlength  $\approx \sec z$  where  
 $z$  is solar zenith angle for  $z \leq 70^{\circ}$ .



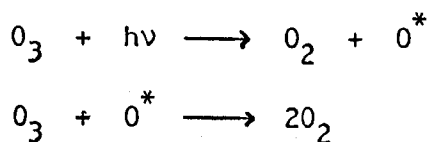
and other chemical constituents until equilibrium is reached. The basic theory of ozone photochemistry was put forward by Chapman in the 1930's, but in recent years it has become clear that other chemical reactions are also important and that the ozone balance is more complicated than originally thought. Hydrogen, nitrogen, chlorine and other halogens all play a part in the destruction of ozone, and a brief summary of ozone reactions is given below.

#### The Chapman theory

Below 80 km molecular oxygen can be photodissociated by solar radiation of  $\lambda < 242$  nm. The resulting oxygen atoms can then bond with other oxygen molecules, in the presence of a third body, M , (mainly N<sub>2</sub>), to form ozone:



Photodissociation of ozone requires solar radiation of  $\lambda < 320$  nm and results in an oxygen molecule and an electronically excited oxygen atom, O<sup>\*</sup>. The latter is able to undergo a destructive reaction with a further ozone molecule:

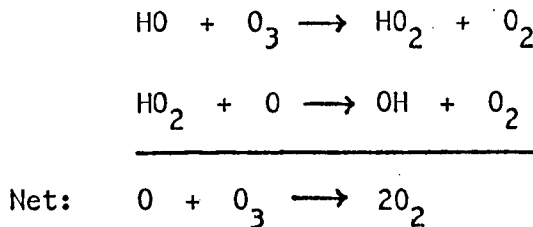


These reactions remove approximately 20% of the ozone formed.

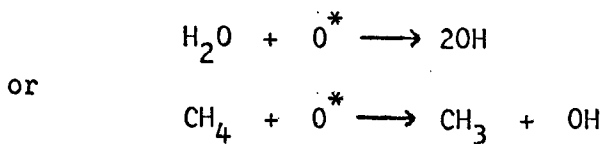
The dominant reaction in the dissociation of ozone (above 40 km) is the hydrogen system, although it removes only about 10% of the total ozone formed.

### The hydrogen system

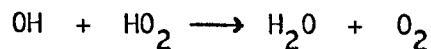
Ozone is eliminated by the following reactions:



The catalyst for this system (OH) remains at the end of the reactions and is available to repeat the process with other ozone molecules. One OH radical can therefore remove many ozone molecules. OH in the atmosphere can result from the photochemistry of water or from methane (diffusing upwards from the earth's surface) reacting with an excited oxygen atom:



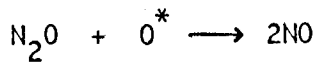
The radical is removed mainly by the reaction:



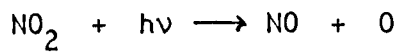
This reaction is one of the most important in the photochemistry of the stratosphere and hence of ozone.

### The nitrogen system

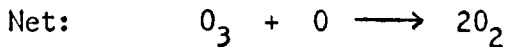
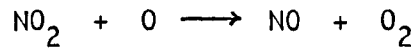
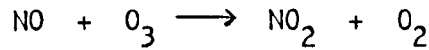
The stratospheric balance of ozone is maintained principally by the nitrogen system, which is responsible for removing approximately 60% of the ozone formed. Nitrous oxide diffuses into the stratosphere from the earth's surface and the following reactions then take place:



and



The nitric oxide NO then acts as a catalyst in ozone depletion:

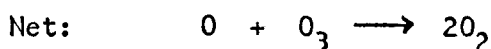
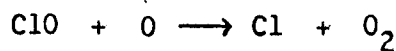
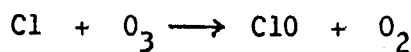


The nitrogen dioxide ( $\text{NO}_2$ ) reacts with OH to form nitric acid ( $\text{HNO}_3$ ) which is washed out of the troposphere.

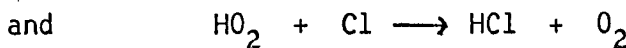
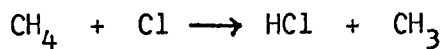
Other less important sources of NO in the stratosphere are lightning in the troposphere followed by upward diffusion, meteorites, cosmic rays, solar proton events and, of man made origin, nuclear explosion and jet engines. The latter source may become a problem if the number of high flying aircraft increases significantly in future years adding further ozone-eliminating catalysts to the stratosphere.

### Chlorine reactions

The action of chlorine has recently attracted much attention because of the man-made contribution to this stratospheric constituent. Chlorine, like nitric oxide, acts as a catalyst in ozone removal:



Catalysis by chlorine is approximately six times as efficient as that by nitric oxide, but conversion of chlorine to hydrogen chloride by:



is also more efficient, so the two catalysts have similar overall efficiencies.

The contribution of natural chlorine to ozone depletion is small (a few percent), but a potentially damaging source has been recognised in man-made chlorofluorocarbons. These chlorofluorocarbons, used in aerosol cans and for refrigeration are inert in the troposphere. However, when they reach a height of about 30 km, near the height of maximum ozone formation, they are dissociated by ultraviolet radiation of  $\lambda = 180-225 \text{ nm}$ , releasing chlorine atoms for ozone catalysis.

The chlorine and nitrogen systems interact through a number of reactions:

- i)  $\text{ClO} + \text{NO} \longrightarrow \text{NO}_2 + \text{Cl}$  then  $\text{NO}_2 + \text{hv} \longrightarrow \text{NO} + \text{O}$
- ii)  $\text{ClO} + \text{NO} \longrightarrow \text{ClNO}_2$
- iii)  $\text{ClO} + \text{NO}_2 \longrightarrow \text{ClNO}_3$

The latter two reactions reduce the rate of ozone depletion that would otherwise be due to the two non-interacting systems. The N.A.S. 1976 report calculated that the chlorine-nitrate interaction would reduce their projected ozone depletion of 14% to 7.5%. Other measurements and calculations (Dave and Halpern, 1976; N.A.S. Committee, 1979; Stordal, *et al.*, 1982) have modified these predictions as the complicated chemistry of the stratosphere is better understood and simulated in models.

Some of the more recent models of the stratospheric ozone balance predict changes in ozone concentrations far smaller than the 16%

depletion forecast by early models. Prather, et al. (1984) using a one dimensional model calculated that if chlorine and bromine emissions remain constant, the resulting ozone depletion would be less than 3%. Schmailzl (1985) predicted changes of the order of  $\pm 2\%$  ozone concentration, a figure of the same magnitude as the naturally occurring ozone fluctuations (Fig. 2.2). The effect of large decreases in ozone (increases in ultraviolet radiation) on various biological systems has been studied by a number of workers (Chapter 3) and generally found to be detrimental. However, biological systems at present cope with much larger short-term fluctuations about the mean amounts of atmospheric ozone: 10% per hour with the passage of a frontal system, 25% seasonally, 5% annually, up to 30% along a latitudinal gradient within the U.S at any time (N.A.S., 1979). Models now forecasting changes in mean ozone concentrations comparable with natural variations suggest that human activity is having less effect on the natural system than originally thought. In support of this Angell and Korshover (1983) studying measurements of total ozone amount (the ozone present in a vertical column through the atmosphere) from 1958-1981 found no evidence of a long-term decrease in hemispheric or global total ozone, although they suggest that there may be changes within different atmospheric layers: an increase in tropospheric ozone (see following section) compensating for a stratospheric decrease. However, the latest report on this subject (Farman, et al., 1985) warns of the danger of predicting global ozone changes from calculations based on one location; the stratospheric circulation should be accounted for. Measurements made in Antarctica (Farman, et al., 1985) show a steady decline of ozone in

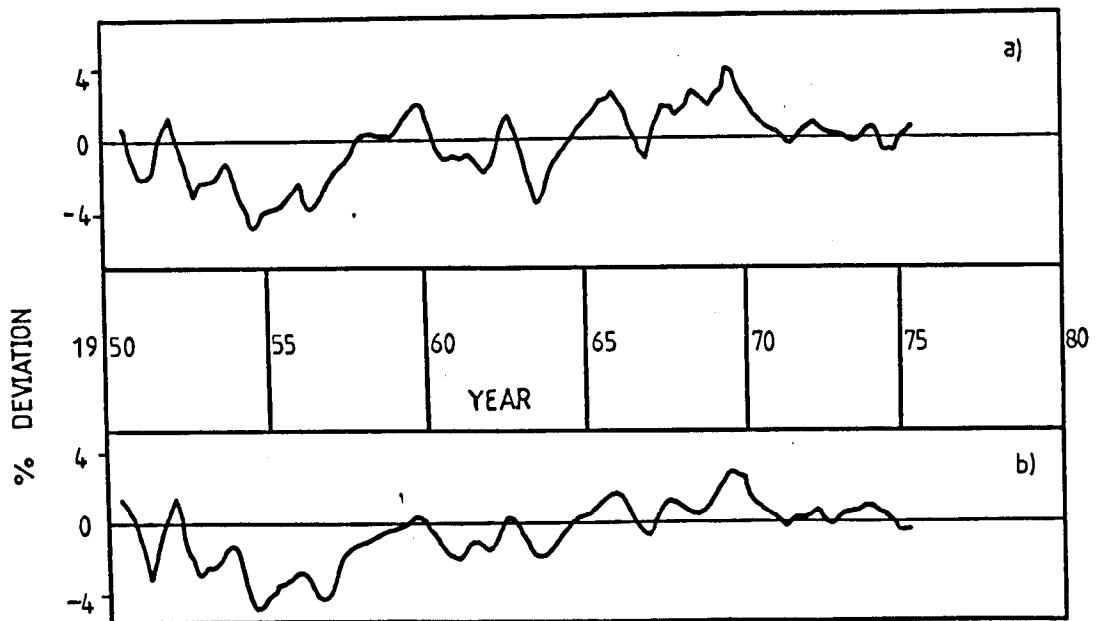


Fig. 2.2 Time variation in total ozone for a) Europe (14 stations), b) North Temperate Zone (33 stations).

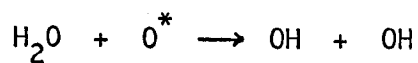
The variation is shown as the percentage deviation from the mean for the total length of record (the annual oscillation has been removed). WMO (1979).

the Antarctic spring since the early 1970's, while the chlorofluorocarbons in the troposphere have increased four to eight fold. The efficiency of chlorine in converting ozone to oxygen is increased by cold so that during the long, cold polar nights Antarctica becomes a sink for the world's ozone which must be recognised when assessing the potential global effects of chlorofluorocarbons.

#### Tropospheric ozone

Discussion so far has concentrated on ozone in the stratosphere, but there is also a small, though relevant, amount of ozone in the troposphere. Changes in tropospheric ozone change the total ozone distribution and cannot be ignored. Tropospheric ozone comes from two sources. It can be transported down from the stratosphere, particularly in middle and high latitudes, or can be photochemically produced. As with the photochemistry of the stratosphere, that of the troposphere is not fully understood, but the same atmospheric constituents, OH, HO<sub>2</sub>, NO and NO<sub>2</sub> are important to the ozone chemistry.

In clean air excited oxygen atoms decompose water vapour to form OH



HO<sub>2</sub> is then formed by reaction with naturally occurring methane.

The HO<sub>2</sub> is important in converting NO to NO<sub>2</sub> by the reaction



Photodissociation of NO<sub>2</sub> then increases the number of single oxygen atoms which are available for ozone production.

In areas of heavy pollution the burning of fossil fuels releases many hydrocarbons which are oxidised, producing  $\text{HO}_2$ . This and other radicals which also provide the  $\text{NO} \rightarrow \text{NO}_2$  conversion can result in greatly increased ozone concentrations in the lowest layers of a polluted atmosphere. The ozone which occurs in this way can be mixed with surrounding air and transported long distances.

#### Total ozone amount and UVB radiation

The overall atmospheric distribution of ozone is given by a combination of these photochemical processes and atmospheric circulation, with the maximum ozone concentration at a height of about 25 km (Fig. 2.3). The total ozone in an atmospheric column shows both seasonal and geographical variation, with a spring maximum ( $\sim 390 \text{ matm. cm}^+$  at  $50^\circ \text{ N}$ ) and autumn minimum ( $\sim 290 \text{ matm cm}$  at  $50^\circ \text{ N}$ ). Total and seasonal amounts both increase with increasing latitude (Fig. 2.1) so that the amount of UV radiation reaching the ground decreases with latitude due to both increased ozone amounts and the longer pathlength through the atmosphere.

Bener (1960) found a linear relationship on clear days between the logarithm of intensity of UV radiation at the earth's surface and the total amount of ozone. Using this relation (shown in Fig. 2.4), an increase in ozone amount from 0.2 to 0.3 cm corresponds, at 300 nm, to a decrease in the intensity of UV radiation at the surface by a

---

<sup>+</sup> milli-atmosphere-centimetre. The total ozone amount is expressed as the depth of the ozone in a vertical atmospheric column if condensed to standard temperature and pressure.

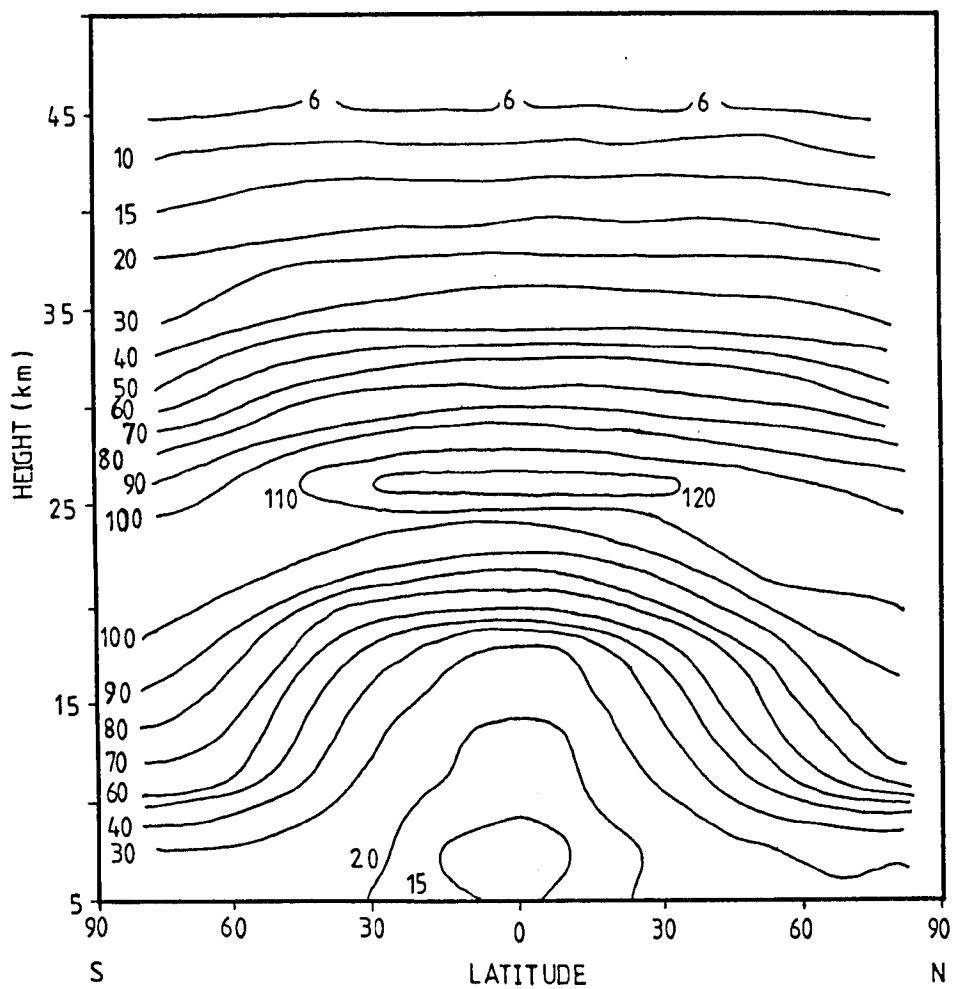


Fig. 2.3 Vertical ozone distribution ( $\mu$  mb).

Partial pressure of mean vertical ozone with latitude, based on 8,500 measurements from 1956-1966. (WMO, 1979).

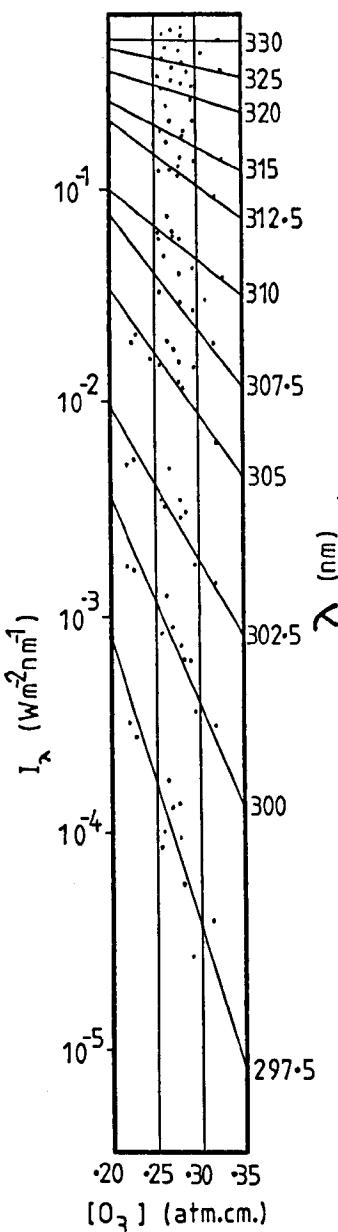


Fig. 2.4 The measured intensities of UV global radiation as a function of ozone amount for a zenith angle of  $45^\circ$ .

Similar figures were constructed for other zenith angles.

factor of 8 to 16, depending on the solar altitude. The influence of ozone decreases at longer wavelengths, with little effect for  $\lambda > 330$  nm. A similar trend was observed for diffuse UV radiation: an increase in ozone amount from 0.2 to 0.3 cm decreased diffuse UV by a factor between 3.5 and 16 for  $\lambda = 300$  nm and solar altitudes between 20 and 50°. The UV incident at the earth's surface is therefore very sensitive to the amount of ozone in the atmosphere, particularly at the short wavelength end of the spectrum. However, other meteorological factors also influence the UVB reaching the earth and ozone values can be used to predict UVB irradiance only on clear days (Klein and Goldberg, 1978).

#### Tropospheric Attenuation of UV Radiation

Another factor responsible for UV attenuation in the atmosphere is Rayleigh scattering. This is scattering by gaseous molecules in the atmosphere: Brownian motion of the molecules causes minute fluctuations of density in the atmosphere which result in corresponding variations in refractive index. As attenuation is inversely proportional to the fourth power of the wavelength, its importance increases rapidly as wavelength decreases.

The energy of the incoming beam is not absorbed but is scattered in all directions. The intensity of the scattered light is a maximum in the forward and backward directions and a minimum at right angles to the incident beam. Direct radiation from the sun is therefore attenuated, some of it being scattered back into space, while a further component reaches the earth as diffuse radiation. This sky radiation

penetrating diffusely in all directions is of environmental importance as even in the shade there is exposure to UV radiation. Fig. 2.5 shows the annual variation of the ratio of the vertical component of the direct beam (B) to diffuse (D) radiation for  $300 < \lambda < 320$  nm, as measured by Bener (1963) at an altitude of 1590 m a.s.l.; Klein and Goldberg (1978), measuring UVB in 5 nm bands from 285-320 nm at three different latitudes, reported that 40% of UVB at the earth's surface is contained in the direct beam and 60% is diffuse radiation even on relatively clear days.

In a Rayleigh atmosphere, ozone absorption and Rayleigh scattering are equally important at  $\lambda \approx 310$  nm. Ozone absorption is the dominant attenuator below 310 nm and Rayleigh scattering dominates at longer wavelengths. However, in practice the atmosphere generally contains many fine suspended particles: aerosols, cloud and pollution which vary considerably with atmospheric conditions and also attenuate UV radiation. The overall effect of these transient atmospheric constituents is very difficult to quantify.

When the radius of scattering particles in the atmosphere is between  $0.1 \lambda$  and  $25 \lambda$  for the wavelength of light considered, the Rayleigh scattering theory is no longer applicable, and the more complicated theory of Mie scattering must be used (Van de Hulst, 1957). The scattering by spherical particles depends on the interaction of reflected, refracted and diffracted light waves and is a function of size and refractive index of the particles, and the wavelength of the incident light. At larger particle sizes the

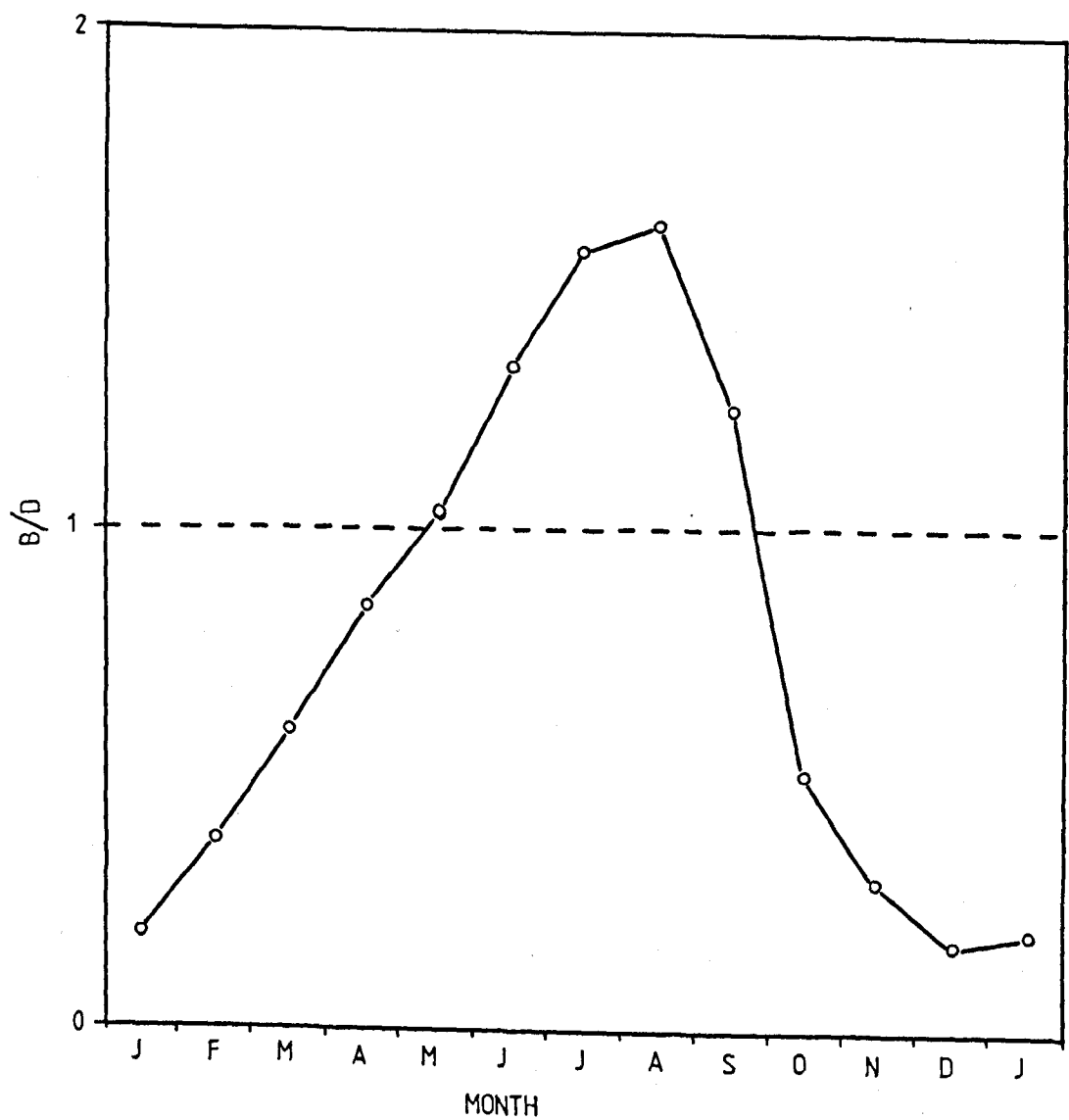


Fig. 2.5 The annual variation of  $B/D$  at noon, Benner (1963).

scattering is increasingly in a forward direction (the Mie effect). At particle radii  $> 25 \lambda$  geometrical optics can be used to assess the scattering effect. Any computation of scattering in a non-Rayleigh atmosphere must therefore be based on an assumed distribution of particle size and composition, the total scattering effect involving integrals over both wavelength and particle radius.

The effect of cloud depends to a large extent on the type and spatial distribution of the cloud. Bener (1964) in measurements at Davos for  $\lambda = 330$  nm found evidence for both increases and decreases in UV radiation depending on cloud pattern. Broken cloud with high scattering properties can increase the diffuse radiation while not blocking the direct radiation and hence increase the total radiation flux. On the other hand closed layers of thick dark cloud strongly reduce the intensity of sky radiation and the overall flux. Each combination of cloud height, density and type may therefore have a different effect on the attenuation of the incident radiation. Klein and Goldberg (1978) found that the daily average of UVB at Panama ( $9^{\circ}$  N) was correlated with the change between wet and dry season rather than daylength or ozone amount. Spinhirne and Green (1978) calculated that cloud effects on received UV radiation depend on cloud reflectivity and transmissivity, the albedo of the underlying surface, and the height and thickness of the cloud. The relative importance of these variables changes with wavelength and the associated ozone absorption.

Measurements taken in Los Angeles (Nader, 1969) for the UV waveband 300-380 nm (mainly UVA) under a range of smog conditions

showed that UV attenuation varied with smog intensity. Transmission through the smog layer (containing the pollutants CO, HC, O<sub>3</sub>, NO<sub>2</sub>, NO, NO<sub>x</sub> and SO<sub>2</sub>) was 87% on a clear day, falling to 65% for a moderately heavy smog day. The outgoing radiation measured above the smog layer was found to increase by a factor of 2 in heavy smog, and also tended to increase exponentially with elevation through the smog layer. This high scattering of a polluted atmosphere increases the ratio of diffuse to direct UV radiation, but the overall net effect is to decrease the total UV flux at the ground.

On reaching the ground, some UV radiation is reflected back into the atmosphere where further reflection can enhance the amount of diffuse radiation incident at the surface. The degree of this augmentation depends on the surface albedo (~ 3% for soils and vegetation, 85% for snow (Bener, 1960)) and the particular scattering properties of the overlying air. These factors govern how much of the incoming radiation is made available at each 'boundary' to undergo further reflection and scattering, and possibly return to the surface as diffuse radiation.

The other factors governing the amount of UV radiation received on a horizontal surface are the solar zenith angle and the solar declination. These also affect the ratios of diffuse and direct radiation which make up the global UV radiation. When the sun is overhead the diffuse and direct components are approximately equal, but the diffuse radiation becomes the major component as the sun falls towards the horizon. At high solar altitudes the short wavelength limit of the spectrum of natural UV radiation is near 290 nm,

but this shifts towards longer wavelengths for lower solar altitudes (Table 2.1). The diurnal variation of UV radiation intensity is most rapid at times of low sun i.e. in the early morning and late afternoon. Towards longer wavelengths the intensity increases less rapidly with solar altitude.

Table 2.1 The short wavelength limit (in nm) of the solar spectrum as a function of zenith angle in various seasons in Switzerland (Robinson, 1966).

| Season      | Zenith angle |     |     |     |     |     |
|-------------|--------------|-----|-----|-----|-----|-----|
|             | 30°          | 40° | 50° | 60° | 70° | 80° |
| Spring      | 298          | 298 | 302 | 304 | 308 | 316 |
| Summer      | 298          | 299 | 301 | 306 | 310 | 319 |
| Autumn      | -            | -   | 300 | 302 | 305 | 312 |
| Winter      | -            | -   | -   | 307 | 308 | 314 |
| Year (mean) | 298          | 299 | 302 | 304 | 308 | 316 |

### Solar UV Radiation Measurements and Models

The most comprehensive measurements of solar UV radiation in the literature are those made by Bener (1960, 1963, 1964) at Davos Platz in Switzerland. He used a recording spectrometer with spectral resolution  $\pm 0.2$  nm to measure global and diffuse UV radiation in the spectral region 295-380 nm over a three year period from 1958-1961. His measurements reveal the interaction between some of the factors affecting UV radiation at the ground. The annual variation of both

diffuse and global UV is partly determined by the declination of the sun and further influenced by the annual trend of atmospheric ozone and ground reflection.

The extraterrestrial UV intensity increases from January to April with increasing solar altitude, but the ozone amount also increases during this time (Fig. 2.1), counteracting the effect of changing zenith angle. During April to May the ground reflection at Davos changes to its summer value (decreasing) and ozone amount reaches its maximum in April, both factors acting to decrease the incident UV radiation. From May to July the ozone amount diminishes and this has the effect of extending the UV radiation intensity maximum to July although the solar altitude is a maximum in June. Ozone then decreases to its minimum value in October, thus counteracting the decreasing solar altitude during this period. Ground reflection increases in November with a change to the winter albedo value increasing the potential diffuse radiation, while ozone amount changes little. From November to January the ozone increases, shifting the annual UV radiation minimum from December to January for short wavelengths. At longer wavelengths the solar altitude prevails with a minimum in December.

This annual variation of UV radiation receipt cannot necessarily be extended to regions at different latitudes or altitudes and with different annual albedo changes. The interplay of factors governing surface irradiation is such that calculations of UV exposure are based on a set of idealisations (e.g. cloud free, aerosol free atmospheres,

simplified scattering models, mean ozone amounts, constant extra-terrestrial radiation) and the models may be 1, 2 or 3 dimensional. A brief discussion of some of these factors, and the way they are dealt with as modelling progresses, is given by Green and Schippnick (1982). The models are often fitted to Bener's measurements as the most comprehensive data base available (Green, et al., 1974; Mo and Green, 1974; Green, et al., 1980) but this procedure must be treated with caution. Measurements of global, diffuse and UV radiation (310-340 nm) were made at 3 heights in the Northern Alps (Reiter, et al., 1982) and the dependence of the radiation on altitude investigated. This work showed an increase of 27% (December) to 52% (June) in incident UV with increasing height from 0.7 to 3 km a.s.l. This emphasises the need for care when applying Bener's relationships (made at 1590 m a.s.l) to less elevated sites. A discussion of the models already mentioned and the development of more elaborate calculations is given by Nachtewy and Rundel (1982).

Other workers have measured UV radiation at various locations with different types of instrument. Collins (1973) reports UV measurements made in Australia with standard meteorological pyranometers and broadband glass filters. Goldberg and Klein (1974) report the development of a scanning radiometer for monitoring the spectral distribution of daylight which was adapted to monitor wavelengths below 330 nm. A discussion of the inherent problems of interference filters used for this purpose is given in the report. The Robertson-Berger meter which records the integrated erythemally

effective radiation measured in 'sunburn units' has been used in Australia (Barton and Robertson, 1975) and similar instruments have been used elsewhere e.g. at 9 locations in the U.S. (Scotto and Fears, 1977) and in Dundee (Frain-Bell, 1979). The Building Research Establishment used a detector that they developed (Harris, 1973) to measure solar UV radiation at three wavelengths: 315 nm, 350 nm and 400 nm at three sites in Southern England (Smith, 1975). This, and the Robertson-Berger type instruments, all work on the principle of a phosphorescent material re-emitting energy absorbed from UVB radiation, with suitable filters used to define the waveband measured.

Models of erythermal dose have been compared with the 'sunburn' measurements for Australia (Barton and Paltridge, 1979) but do not give the incident UVB radiation in absolute energy units. More recent models intended to give a general guide to UVB radiation at a given time and place are being tested on measurements made at various locations (Gerstl, et al., 1983; Rundel, 1985). As more data become available and the influence of the different UVB attenuating factors is better understood the models should become more reliable. However, at present a picture of the available natural UVB at a given location under a variety of meteorological conditions is accurately attainable only by measurement.

### 3. VITAMIN D

#### Introduction

The body has two sources of vitamin D: cutaneous synthesis under exposure to UVB radiation, and diet. Deficiency of the vitamin can lead to the malformed and weak bones of the diseases rickets and osteomalacia. In Britain, rickets was common in infants and toddlers until the beginning of World War II (Plate 3.1) but since the 1940's and the fortification of some foodstuffs with vitamin D, rickets has not been common among British children. Osteomalacia remains a problem in the elderly: many elderly people may be confined indoors due to general ill health, and with a diet low in vitamin D they can be at risk. In Britain dietary vitamin D is insufficient to prevent plasma  $25(\text{OH})\text{D}$  falling below  $3 \text{ ng ml}^{-1}$ , the level of clinical deficiency, in many of the elderly (Lawson, 1981).

Another section of the population susceptible to rickets is the Asian community, whose lifestyle and diet does not favour vitamin D production or oral intake. In many cities with a significant population of immigrants from the Indian sub-continent, adolescent rickets is a major public health problem (Taylor, 1984), especially in Scotland and Northern England.

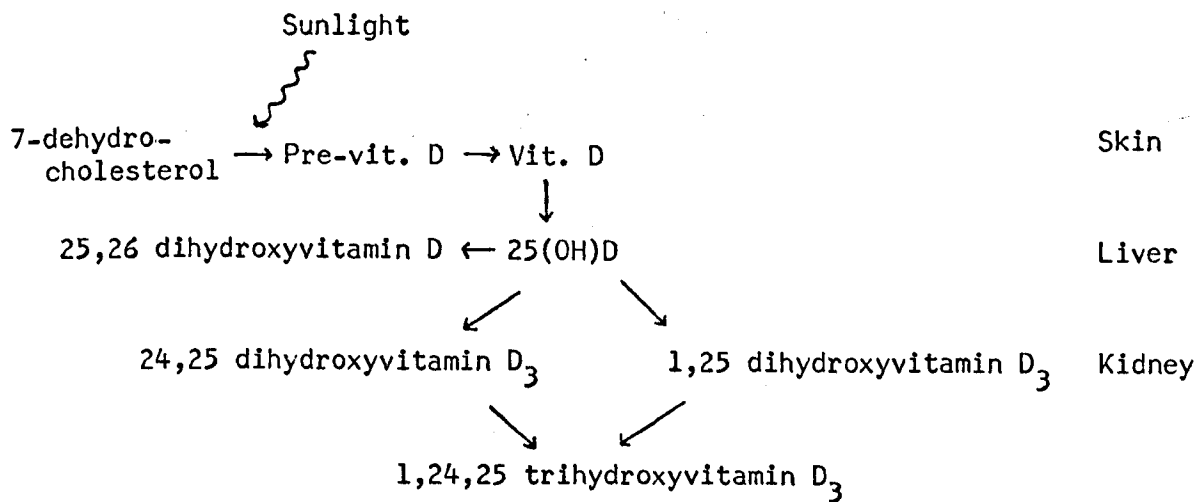
#### Formation and Metabolism

The active form of vitamin D is the metabolite 1,25-dihydroxy-vitamin D ( $1,25-(\text{OH})_2\text{D}_3$ ) and this has three main functions in animals: to control calcium homeostasis; to regulate growth and development of bone; to regulate phosphorous metabolism.

Plate 3.1   Rachitic children in the 1920's  
(Taylor, 1984).

Cutaneous synthesis of the vitamin is dependent on the wavelengths of the incident light and on temperature. In the skin the action of UV light on 7-dehydrocholesterol forms pre-vitamin D. From pre-vitamin D the formation of vitamin D is a heat dependent reaction. At skin temperature any pre-vitamin D formed is likely to be converted to vitamin D. The vitamin is converted to its 25-hydroxy-derivative  $25(OH)D$  in the liver, and this circulating metabolite can be measured by radio-stereo-assay, thus providing a precise index of vitamin D status. Synthesis of the  $(1,25-(OH)_2D_3)$  metabolite then takes place in the kidney (Fig. 3.1).

Fig. 3.1 Formation and metabolism of vitamin D (Hay, 1982)



The metabolic pathway of the vitamin absorbed from the intestinal tract is different from that formed in the skin. Oral doses of the vitamin are absorbed from the blood stream with dietary fat which is quickly cleared by the liver. There deactivation takes place or the vitamin is secreted into bile or back into the blood stream as

25(OH)D . There is no storage. By contrast cholecalciferol in skin diffuses slowly into the bloodstream where it is associated with a specific binding protein. Slow penetration to, and uptake by, the liver results in a slower rate of conversion<sup>to</sup> 25(OH)D<sub>3</sub>, and protects against hepatic deactivation of the vitamin.

A limiting concentration of 50-80 ng ml<sup>-1</sup> for plasma 25(OH)D<sub>3</sub> has been found by Stanbury, et al. (1980) who postulated a feedback mechanism between 25(OH)D<sub>3</sub> circulating in the blood and a cutaneous binding protein for the vitamin. The circulating 25(OH)D<sub>3</sub> is redistributed to tissues including the skin. There it will bind preferentially with the cutaneous binding protein, reducing its capacity to accept cholecalciferol. At the limiting plasma concentration uptake of cholecalciferol from skin to blood is blocked and any further photosynthesised cholecalciferol remains in the skin until use of the circulating 25(OH)D<sub>3</sub> releases the cutaneous binding protein for further transfer. The cholecalciferol stored in the skin is then available for withdrawal long after exposure to UVB radiation has ceased.

#### The Relative Importance of UVB Irradiation and Diet

The body's use of vitamin D available from its two sources suggests that skin synthesis of the vitamin is more effective than oral doses. In support of this Poskitt, et al. (1979) working with healthy children and adults, and Lawson, et al. (1979) working with the elderly, both found that the most important source of vitamin D for long term healthy status was that due to the action of UV light on the skin. When vitamin D was given orally at twice the

recommended daily intake (Poskitt, et al. (1979), plasma concentration of  $25(\text{OH})\text{D}_3$  was only slightly increased, suggesting that the average British intake of  $2.6 \mu\text{g day}^{-1}$  (MAFF, 1980) may be an ineffective source of vitamin D.

Studies in Denmark and Britain showed no correlation between dietary vitamin D intake and  $25(\text{OH})\text{D}$  levels in healthy adults (Lester, et al. 1980) although the mean  $25(\text{OH})\text{D}$  levels were higher in Danish subjects, many of whom took regular vitamin D supplements. Another study in Denmark (Lund and Sørensen, 1979) illustrated the positive correlation between plasma  $25(\text{OH})\text{D}$  levels and sunshine exposure in subjects of all ages who did not take regular vitamin supplements. Subjects taking regular vitamin D supplements ( $\sim 5 \mu\text{g day}^{-1}$ ) maintained a higher  $25(\text{OH})\text{D}$  plasma level throughout the year, and did not show any marked seasonal variation.

It has been found, however, that prolonged oral doses of vitamin D can be harmful (DHSS, 1980). The minimum daily requirement for health is estimated at 2.5-10  $\mu\text{g}$  (Fraser, 1983) for adults and children. Intakes of over  $2000 \mu\text{g day}^{-1}$  are known to be exceedingly toxic, and there is some evidence that daily doses of 25-100  $\mu\text{g}$  can also be harmful (Fraser, 1980; Reinhold, et al. 1981) causing nausea, thirst, abdominal pain and dehydration, often some weeks after the treatment, though symptoms may appear sooner. Prolonged effects can include damage to the kidneys and bone structure. However it is only in an attempt to prevent or cure the diseases of vitamin D deficiency that such an oral overdose is likely to be taken.

Classical rickets is seldom found in British children today. The fortification of National Dried Milk and margarine in the 1940's did much to reduce the incidence of this disease, which was a common sight in spring although rare in autumn. This seasonal appearance of D-deficient symptoms suggests that summer sunshine was the major source of vitamin D, but that exposure was insufficient to maintain a healthy status throughout the year. As early as 1890 Palm recommended that children in heavily polluted industrial areas where rickets was most prevalent should be taken to areas with cleaner air and more sun, and that the public as a whole should be more appreciative of the effect of sunshine on health. Today, with a general increase in the standard of living, cleaner city air and more leisure during which to enjoy exposure to sunshine, natural UVB radiation is still the main source of vitamin D.

Stamp and Round (1974) measuring plasma  $25(\text{OH})\text{D}_3$  in healthy white subjects over a two year period found a marked seasonal variation. High values in autumn declined during winter and then rose again from March to July, approaching previous autumn values by August. No significant correlation was found between plasma  $25(\text{OH})\text{D}_3$  and dietary vitamin D intake and it would seem that vitamin D status declines when the dose of UV radiation falls. Seasonal variation of plasma  $25(\text{OH})\text{D}$  levels has also been observed by, amongst others, Poskitt, et al. (1979), Beadle, et al. (1980), Devgun, et al. (1981a) and Lamberg-Allardt (1984). To remain above deficiency status when there is little UVB radiation (during the winter months) sufficient reservoirs must have been stored in the body tissues during the summer months to

maintain healthy values until the following spring. Devgun, et al. (1983) showed that the plasma 25(OH)D levels changed with variations in the natural UVB radiation during a given year, and also that differences in plasma 25(OH)D levels from year to year are associated with annual differences in the levels of UVB radiation.

### Vitamin D Deficiency in the Community

Sections of the population who do not receive the necessary exposure to UVB radiation during the summer may be susceptible to rickets and osteomalacia. The two communities most at risk in Britain today are the elderly and adolescent Asians. A review of the influence of vitamin D levels on bone health in the elderly is given by Parfitt, et al. (1982). The development of rickets in children is described by Fraser (1980).

#### The elderly

Vitamin D levels in the elderly are low compared with those of younger people even for healthy subjects (Stamp and Round, 1974; Corless, et al., 1979; Lawson, 1981; Omdahl, et al., 1982). A range of plasma 25(OH)D concentrations from  $8-36 \text{ ng ml}^{-1}$  was found in Bristol office workers (Beadle, et al., 1980), and similarly in children in the West Midlands (Poskitt, et al., 1979), while the seasonal variation in healthy elderly people throughout Britain was reported as  $8.6 - 14.1 \text{ ng ml}^{-1}$  by Lester, et al. (1977) and  $10-19 \text{ ng ml}^{-1}$  by Dattani, et al. (1984).

Reasons for the decrease of plasma 25(OH)D levels with age are not fully understood. Davie and Lawson (1980) found that the

response to ultraviolet irradiation by lamps was similar in both the young and elderly. Devgun, et al. (1981b) finding similar results suggested that low levels of plasma 25(OH)D in the elderly may be partly due to reduced levels of 7-dehydrocholesterol or reduced amounts of enzymatic synthesis of the metabolites in the skin, liver and kidneys. Lund and Sørensen (1979) suggested less effective skin synthesis or hepatic hydroxylation in the elderly although Davie and Lawson (1980) do not consider impaired 25-hydroxylation to be responsible. They suggest that the skin as it ages may require more ultraviolet power to synthesise vitamin D - the lamps used in their study were more powerful and contained spectral components at shorter wavelengths than natural UVB radiation. The effect of low plasma 25(OH)D levels in the elderly is exacerbated by the decrease with age of the ability of the kidney to convert 25(OH)D to its active metabolite, 25-hydroxyvitamin D (Tsai, et al., 1984). This implies that the elderly require a higher concentration of 25(OH)D to achieve the same level of the active form of the vitamin as younger individuals (Olson, 1985).

Despite the general low levels of plasma 25(OH)D in the elderly, a seasonal variation is still observed when there is exposure to sunlight. Lester, et al. (1977) and Poskitt, et al. (1979) working with elderly subjects in Britain both found that vitamin D status improved with exposure to summer sunshine. However, Nayal, et al. (1978) found a correlation between dietary vitamin D intake and plasma 25(OH)D levels, but no correlation with sunlight for patients in a geriatric unit. They suggest that these subjects had very little

sunlight exposure, and as yearly exposure was estimated from the patients memory its accuracy is questionable. Toss, et al. (1980) observed higher concentrations of 25(OH)D in healthy elderly subjects than those in institutions, as a result of greater outdoor exposure and/or better diet. Lamberg-Allardt (1984) working in Finland with long-stay geriatrics, residents of old people's homes, healthy elderly and young adults observed seasonal variations of plasma 25(OH)D levels in all four groups, with the smallest variation for the long-stay geriatrics who were only outside for brief periods in summer. This group of patients also had the lowest vitamin D levels at all times, and did show a correlation between dietary vitamin D intake and 25(OH)D levels. Lamberg-Allardt concluded that this correlation indicated that in Finland there is not enough sunlight to ensure a satisfactory vitamin D status when exposure is very brief, and long-stay geriatrics require more dietary vitamin D to maintain a healthy status. Where more environmental UVB radiation is available and longer exposure possible this may not be necessary.

#### Asian immigrants

The deficiency of Asian children is due to the combination of a number of factors (Stamp, 1975; Fraser, 1983). Their diet, low in fortified margarine (the most regular source of vitamin D in the British diet), liver and oily fish, also relies heavily on chappatis. A number of studies have shown that diets high in fibre and phytic acid (as chappati flour is) restrict the efficiency of the vitamin D - calcium metabolism, although the precise means by which this occurs is not fully understood (Reinhold, et al., 1981; Robertson, et al., 1981).

Batchelor and Compston (1983) found some evidence that the rate of turnover of 25(OH)D is higher on a high fibre diet than on a low fibre diet. Asian children may therefore require a greater intake of vitamin D to compensate for that lost in faeces. However, Offerman and Manhold (1979) found signs of vitamin D deficiency among Turkish immigrants in Germany who do not consume chappati flour suggesting that the Asian diet is a contributory but not a decisive factor in immigrant rickets. They consider the low sunshine exposure of northern industrial cities to be the important aetiological factor.

A further contributory factor is the pigmentation of the skin. It has been shown (Clemens, et al., 1982) that melanin pigment acts as a barrier to the cutaneous synthesis of vitamin D under low UVB light levels such as those experienced in the UK. This, together with the lack of exposure to that UV radiation which is available (due to change of climate (Stamp, 1975)) may be partially responsible for the rickets of adolescent Asians. At higher levels of irradiation (representative of the tropics and 42° N), Holick, et al. (1981) found that pigmentation was limiting over short exposure periods but with sufficient exposure time the same vitamin D levels were reached with skin of European, Asian and African types. Linhares, et al. (1984) reported high levels of 25(OH)D in both healthy and poorly nourished Brazilian children, indicating that where there is sufficient UVB exposure in relation to pigmentation, diet is not an important source of vitamin D.

Methods of combatting deficiency

To reduce the incidence of rickets the vitamin D status of the section of population most at risk must be increased. Additional fortification of basic foodstuffs is not a viable solution as this increases the dietary vitamin D intake of the whole population, which may bring already healthy people within the range of harmful vitamin doses. It is also likely that the people at risk, elderly and Asians, would benefit least as they consume less of the basic foodstuffs likely to be fortified.

Alternative methods are to give vitamin D supplements to those at risk or to increase exposure to UVB so that sufficient vitamin D is naturally synthesised in the skin. The latter could be achieved by UV lamp treatment, by the development of UV transmitting 'glass' for use in hospitals and homes for the elderly, or by educating people to the need for more exposure to natural sunlight.

UV lamp treatment given as a weekly dose in controlled UV chambers was found to be a safe and efficient way of preventing vitamin D deficiency in the elderly (Toss, et al., 1982). However it was very time consuming for ward staff and oral vitamin D supplementation was more convenient. Commercially-available sun lamps tested for their ability to promote vitamin D synthesis (Devgun, et al., 1981b) proved effective but also caused other adverse skin reactions (erythema) over the exposure time required. Such lamps are therefore unsuitable as a routine domestic method for maintaining vitamin D levels. Certain types of lighting in homes for the elderly and hospitals have also been suggested, but studies with Vita-Lite fluorescent tubes (Devgun, et al., 1980) showed no positive effects on the levels of plasma 25(OH)D for patients exposed to these lights at normal lighting levels for one year.

The transmissivity of glass in the ultraviolet part of the spectrum is minimal. At a wavelength of 300 nm the extinction coefficient,  $\alpha$ , for any type of glass is  $\alpha = \ln(I_0/I) > 240 \text{ m}^{-1}$ , so for glass 5 mm thick transmission  $I/I_0 < \exp(-240 \times 0.005) \approx 0.3$ . Even for the most UV transparent glass the amount of transmitted light would be small under the low levels of irradiation by solar UVB. Ordinary window glass does not transmit light of wavelengths less than 334 nm and hence removes all active wavelengths for vitamin D synthesis (Hess, et al., 1922). Truly UVB transmitting windows would have to be made of quartz although other materials have potential in this respect: clear teflon (1 mm) is being tested for use in a UVB transmitting greenhouse (Biggs, 1982).

Vitamin D supplements may be a convenient solution for patients at risk in institutions, but they are difficult and expensive to administer regularly to other potential sufferers in the community. As Goel, et al. (1981) said "The long term answer to rickets in Asian children is health education to Western diet and way of life". If way of life implies more sunshine exposure this statement applies to all sufferers.

The summer months provide the opportunity for adequate natural UV exposure, and as the half-life of  $25(\text{OH})\text{D}_3$  is over two weeks (Davie, et al., 1982) additional exposure every weekend for example, will have a cumulative effect on plasma  $25(\text{OH})\text{D}_3$  concentrations, helping to maintain a healthy level throughout the winter months.

The length of time which constitutes an 'adequate natural exposure' depends upon the spectral properties of the incident solar radiation and is therefore a function of both time and place (Chapter 2).

This is because all photobiological responses to irradiation with ultraviolet and visible light show a dependence on the energy of the incident photons. The response has a maximum at a fairly well defined photon energy and a limited range over which the biologically important molecules are able to absorb the appropriate photons. To measure the biologically effective radiation for a given reaction it is necessary to know the effective range of wavelengths and the shape of the action spectrum.

#### The Vitamin D Action Spectrum

The action spectrum of UV radiation for cutaneous synthesis of vitamin D in man has not been accurately quantified. The formation of pre-vitamin D has been investigated by a number of workers. Early investigations by Knudsen and Benford (1938) assessed the effectiveness of six different wavelengths in curing rachitic rats. The rats were irradiated with a monochromator, then killed 11 days after the end of the treatment period, and the degree of healing judged by X-ray of the bones. The most effective wavelength for the conversion of 7-dehydrocholesterol to pre-vitamin D, was 280.4 nm, with a secondary peak in the action spectrum at 296.7 nm (Fig. 3.2). 313 nm was the longest wavelength showing any healing effect. When ergosterol solution (ergosterol and 7-dehydrocholesterol are collectively known as pro-vitamin D) was irradiated with UV light it showed a similar absorption curve although a much lower dose of UV radiation was needed to produce pre-vitamin D. This was thought to be due to the absorption of the incident radiation by skin.

KEY :

- (a) Knudsen and Benford: The efficiency to produce healing in rachitic rats (w.r.t. 297 nm).
- (b) Kobayashi and Yasumara: Relative yield of potential vitamin D<sub>2</sub> in ergosterol solution (w.r.t. 295 nm)
- (c) Abillon and Mermet-Bouvier: Relative maximum previtamin D<sub>2</sub> production in ergosterol solution (w.r.t. 295 nm).

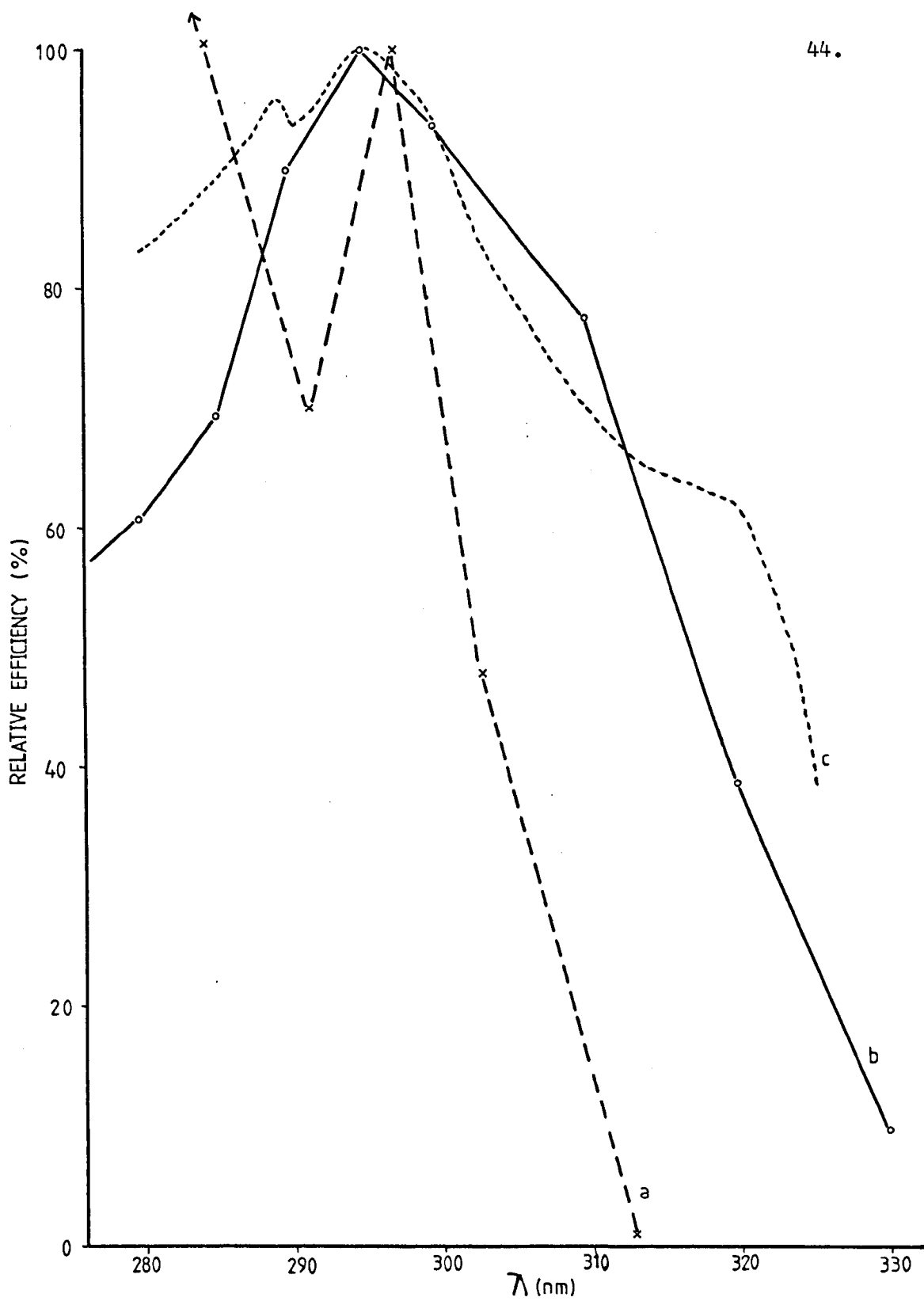


Fig. 3.2 The relative efficiency of different wavelengths in producing vitamin D.

It was further observed that large amounts of energy of any wavelength appeared to destroy vitamin D; the healing effect increased with increasing dosage, but not as much as would be expected. The shorter wavelengths, below 296.7 nm, seemed to have a greater destructive action than light of longer wavelength. Later studies (Kobayashi and Yasumara, 1973) confirmed this observation.

More recently Abillon and Mermet-Bouvier (1973) and Kobayashi and Yasumara (1973) investigated the action spectrum of vitamin D synthesis by illuminating ergosterol solution with various wavelengths of UV light. Abillon and Mermet-Bouvier used wavelengths in the range 240-320 nm to irradiate ergosterol at low temperatures (so that the pre-vitamin D formed by irradiation was not then converted to vitamin D), and found that the most effective wavelength for pre-vitamin D production was 295 nm (Fig. 3.2).

Kobayashi and Yasumara irradiated ergosterol solution with a range of wavelengths at a fixed quantum energy of  $40 \text{ J cm}^{-2}$  and measured the formation of potential vitamin D (the sum of pre-vitamin D and vitamin D). Their action spectrum peaked at 295 nm (Fig. 3.2). The quantity of UV radiation required was also investigated. At a wavelength of 295 nm irradiances of  $21\text{-}64 \text{ J cm}^{-2}$  were most effective. Higher irradiation decreased the yield, supporting the earlier results of Knudsen and Benford.

The three action spectra shown in Fig. 3.2 for vitamin D synthesis by ultraviolet light indicate the uncertainty that still exists in quantifying the importance of irradiation by different wavelengths in vivo. The healing of rachitic rats was assessed only at 6 discrete wavelengths by Knudsen and Benford, but may be more

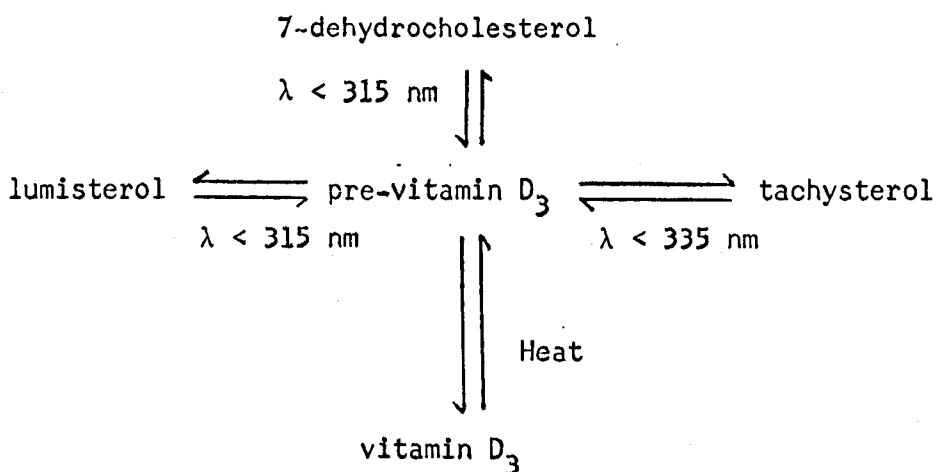
representative of the effectiveness of UV light in vivo than the later work of Kobayashi and Yasumara and Abillon and Mermet-Bouvier working with ergosterol solution.

Pre-vitamin D<sub>3</sub> formed by the action of UVB light on the skin is converted to vitamin D<sub>3</sub> in a temperature dependent reaction. This process seems to be more rapid <sup>in vivo than</sup> in vitro at a temperature of 37 ± 1° C (Holick, et al., 1980), probably due to the vitamin D<sub>3</sub> being removed into the circulation by the vitamin D binding protein. Because the vitamin D<sub>3</sub> is removed as it is formed, a true equilibrium between D<sub>3</sub> and pre-D<sub>3</sub> never occurs (as it does in vitro), and all pre-D<sub>3</sub> is essentially converted to D<sub>3</sub>. The translocation of the vitamin D<sub>3</sub> into the circulation ensures that small quantities of pre-D<sub>3</sub> are efficiently converted to vitamin D<sub>3</sub> by shifting the reaction pre-D<sub>3</sub> → D<sub>3</sub> to the right at a time when equilibrium is being approached. The skin therefore acts as a reservoir for the storage of pre-D<sub>3</sub> and can continually synthesise and release vitamin D<sub>3</sub> for up to three days after a single exposure to sunlight (Holick, et al., 1980). Work done on ergosterol solution measures the effectiveness of UVB radiation to convert 7-dehydrocholesterol to previtamin D, but takes no account of any feedback mechanism which may affect further reactions in vivo.

Another discrepancy between conditions in laboratory experiments and in the natural environment is the quality of the radiation used. All three action spectra were determined using monochromatic radiation to illuminate skin or solution. Solar radiation is not monochromatic and there may be synergistic interactions between the responses to different wavelength combinations.

Pre-vitamin D<sub>3</sub> can be converted to vitamin D<sub>3</sub> (a heat dependent reaction) or to two other isomers (tachysterol and lumisterol) by photoreaction (Fig. 3.3) (MacLaughlin, et al., 1982; Olson, 1984).

Fig. 3.3 Possible reactions between pre-vitamin D<sub>3</sub> and its isomers (MacLaughlin, et al., 1982).



The rate at which any of the photoreactions takes place is equivalent to the product of the quantum yield for the reaction and the number of relevant photons available to, and absorbed by, the isomer. The number of absorbed photons is determined by the spectral properties of the irradiating source and the absorption cross-section of the isomer.

7-dehydrocholesterol and lumisterol have negligible absorption at wavelengths longer than 315 nm, whereas pre-vitamin D<sub>3</sub> will react to wavelengths up to 325 nm and tachysterol to 335 nm. As the solar spectral irradiance increases by 6 orders of magnitude from 290-320 nm the isomer photoreaction is driven from tachysterol to pre-vitamin D<sub>3</sub>.

to lumisterol under solar irradiation. MacLaughlin, et al. (1982) observed a build up of lumisterol in organic solution under simulated solar radiation and concluded that the spectral power distribution of sunlight has a dramatic effect on the cutaneous photosynthesis of pre-vitamin D<sub>3</sub> and its isomers.

Work in vivo on human skin presents more practical and ethical problems than work with rats or solutions, but some attempts have been made to measure the vitamin D action spectrum in vivo.

Davie, et al. (1982) used the data of Kobayashi and Yasumara to calculate the cholecalciferol synthesis in skin in vivo per dose of UV light. They used a Hanovia 7A lamp to irradiate a known area of skin with UV light for a set time each day. The power at each incident wavelength was expressed as a proportion of the most efficient wavelength (295 nm) to give the total power at this wavelength, and the effective incident energy was thus found. Plasma concentrations of 25(OH)D<sub>3</sub> and cholecalciferol were measured, and two methods were used to calculate cholecalciferol synthesis.

The first method employed the steady state equation: the relationship between dose and plasma concentration at the plateau level (after an initial exposure to UV light a plateau region in plasma 25(OH)D<sub>3</sub> concentration is reached; Lawson and Davie (1979)). This gave cholecalciferol synthesis in the skin as  $0.0015 \pm 0.0008 \text{ nmol mJ}^{-1}$ . A second method calculated the oral dosage required to yield the same plasma 25(OH)D<sub>3</sub> concentration as the UV radiation. This gave skin synthesis of cholecalciferol equivalent to  $0.0024 \pm 0.0018 \text{ nmol mJ}^{-1}$ .

At first sight this study appears to have quantified the vitamin D production in skin per dose of UV light. However the vitamin D action

spectrum used to calculate the results may not be truly representative of the action spectrum in vivo, as already discussed. Also a Hanovia 7A lamp does not have the same spectral output as the sun, thereby introducing the type of inconsistencies highlighted by MacLaughlin, et al. (1982).

Clearly more work is needed to quantify the action of environmentally available ultraviolet light on human skin.

#### 4. MATERIALS AND METHODS - CLIMATOLOGY

UVB solar radiation incident on a horizontal surface was measured at the meteorological site, Sutton Bonington ( $52^{\circ} 50'N$ ,  $1^{\circ} 15'W$ ) from January 1983 to March 1985. The site (Plate 4.1) is 50 m a.s.l. surrounded by flat farmland with some buildings about 100 m to the north which obscure approximately 1/165 (0.6%) of the sky's hemisphere. The underlying surface is short grass with a reflection coefficient of about 3% in the UVB band (Bener, 1960).

Two commercial instruments were used to measure the UVB radiation. A scanning spectroradiometer (LICOR) measured the spectral distribution on selected days with little or no cloud. For regular long-term recording a vacuum photodiode tube (International Light) was mounted on the meteorological site to measure the broad-band UVB irradiance.

##### The LICOR LI1800 Portable Spectroradiometer

The LICOR LI1800 portable spectroradiometer (Plate 4.2) scans the wavelength range 300-1100 nm and therefore responds to virtually all the UVB radiation received at the earth's surface. At a latitude of  $53^{\circ}$  N, the amount of radiation of wavelength less than 300 nm is insignificant as even in midsummer the intensity of radiation drops by 4 orders of magnitude between 300 nm and 290 nm (Gerstl, *et al.*, 1983). At other times of year the proportional reduction in irradiance is even more pronounced and there is no measurable radiation at wavelengths less than 300 nm at the winter solstice.



Plate 4.1 The meteorological site, Sutton Bonington.



Plate 4.2 The LICOR LI1800 portable spectroradiometer.

The spectroradiometer has three major optical components (Fig. 4.1): a filter wheel, a monochromator and a silicon photodetector. Light enters the instrument through a diffusing cosine-corrected receptor and then passes through one of the filters on the automatically-controlled filter wheel. There are seven filters on the wheel, reducing the possibility of stray light reaching the detector by intercepting wavelengths outside the spectral region being measured. One of the slots in the filter wheel is blocked by a black surface which acts as a dark reference and is checked before and after each scan.

The filtered radiation enters the monochromator through a rectangular slit 0.5 mm wide and falls onto a holographic grating. The grating reflects and diffracts the incident light so that component wavelengths are projected towards the exit slit at slightly different angles. As the grating rotates and the angle between the entrance slit and the face of the grating changes, the wavelength of light passing through the exit slit also changes. Other wavelengths of light are absorbed by the black interior of the monochromator.

The width of the exit slit determines the spectral width of the waveband and the amount of radiation reaching the detector and hence determines the balance between resolution and signal to noise ratio. This model has a 0.5 mm exit slit which gives a waveband with a half-power bandwidth of 6 nm and a noise equivalent irradiance (NEI) of  $7 \times 10^{-4} \text{ W m}^{-2} \text{ nm}^{-1}$  at 300 nm (Manufacturer's data, Appendix A1).

Light from the monochromator falls onto a silicon photovoltaic detector and the resulting signal is electronically processed and passed to a microprocessor. The silicon detector gives the instrument

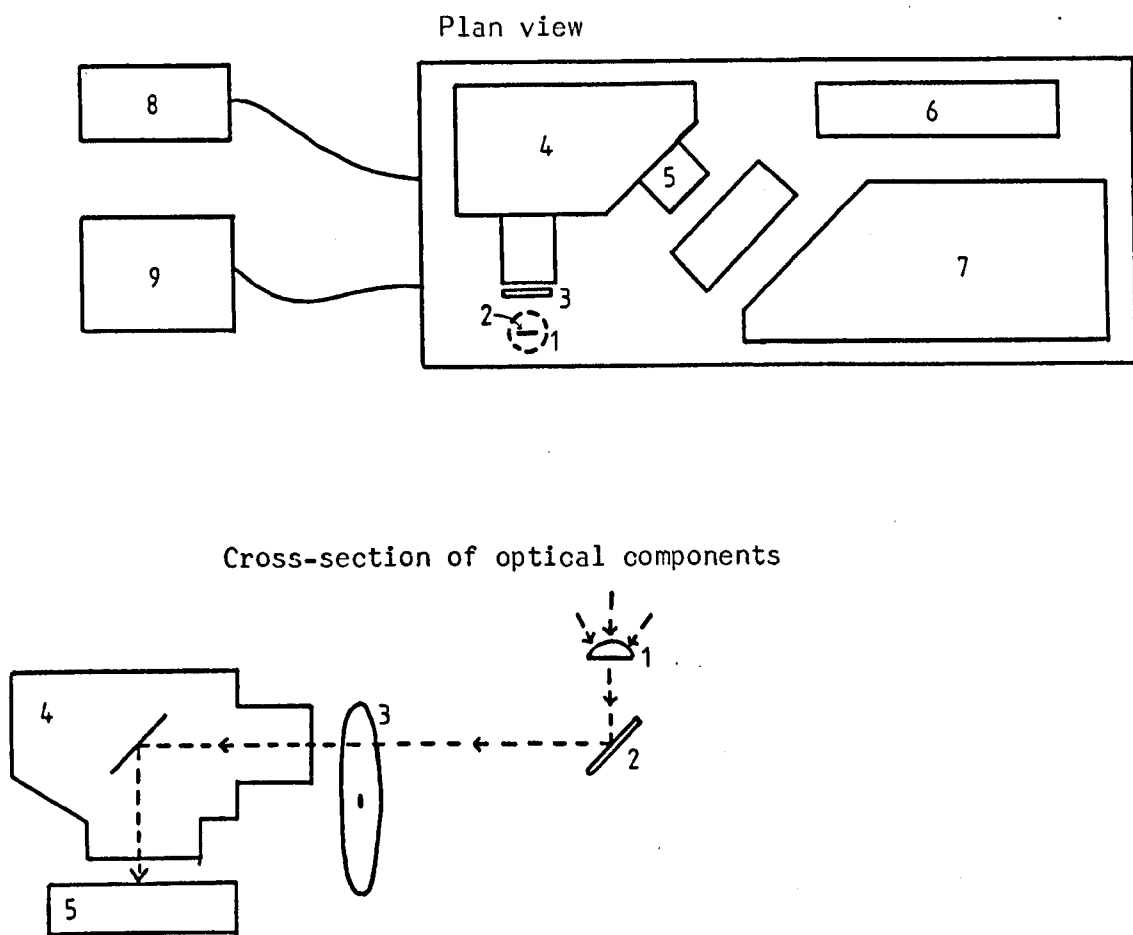


Fig. 4.1 Diagram of LII800 scanning spectroradiometer

- KEY:
- 1. Diffusing cosine corrected head
  - 2. Silvered mirror
  - 3. Filter wheel
  - 4. Holographic grating monochromator
  - 5. Silicon photovoltaic detector and autoranging amplifier
  - 6. Rechargeable battery
  - 7. Microcomputer
  - 8. Hand held terminal
  - 9. Printer/plotter or RS232 interface to PET

a low response to temperature and good long-term stability. It is mechanically rugged and does not fatigue.

The LI1800 was initially calibrated by the manufacturer to National Bureau of Standards (NBS) standards. The calibration accuracy at 300 nm was given as  $\pm 10\%$  (Appendix A1).

The spectroradiometer is operated through a hand-held terminal. Data is stored in the instrument in RAM of 32K bytes capacity, equivalent to about 20 full scans (300-1100 nm) at 2 nm wavelength intervals. Power for operation can be supplied either from the mains or by the instrument's rechargeable internal Ni-Cad batteries. Further details of the instrument's specifications are given in Appendix A1.

The data stored in the memory of the LI1800 could be relayed to a Gulton Microplot 44T plotter either before or after simple data manipulation (e.g. integration of wavebands - see Appendix A1 for list of LI1800 functions). For more detailed analysis of the spectra the scans were transferred to, and processed by, a more powerful machine. An RS232 interface enabled scans from the LI1800 to be transferred to a PET computer where they were compressed and stored on disc.

While the LI1800 is easily portable, its limited memory space meant that even at a rate of one full scan per half-hour the memory would hold only about one day's data. This was sufficient for gathering detailed spectral information on selected days, but for regular long-term measurement of the UVB waveband another instrument was needed.

The properties required of an instrument for long-term field measurement of the solar UVB radiation are:

- a) Spectral selectivity. The steep fall in intensity of the solar spectrum below 300 nm provides its own selectivity at the short wavelength end of the UVB waveband, but at the long wavelength edge it is important that the instrument should be "solar-blind" with a sharp cut-off at the end of the band of interest. As the incident radiation at longer wavelengths is very much greater than in the UVB, any 'tail' to the spectral response spectrum of the instrument will result in large errors (Fig. 4.2).
- b) Sensitivity. The amount of UVB radiation (300-316 nm) to be detected is very small, of the order of  $10^{-2} - 10 \text{ W m}^{-2}$  (winter and summer noonday values respectively). The instrument must be able to measure changes in irradiance over the full range of daily and annual cycles and has therefore to be capable of detecting fluxes of radiation over several orders of magnitude.
- c) Angular response. The irradiance of a horizontal surface is the integral of the components of radiation from each zone of sky weighted according to the cosine of the zenith angle (Fig. 4.3). An instrument with a cosine-weighted response simplifies the analysis of measurements.
- d) Stability. The calibration of the instrument should not depend on time, temperature, humidity or other variable factors so that operation under all weather conditions is possible. There should be no zero drift.
- e) The instrument should be robust and weather resistant.
- f) Ideally the relation between the incident irradiance and the detector signal should be linear to allow for simple integration with time.

KEY :

- a) Solar spectrum measured on 18 June 1983 at 1155 (LH scale)
- b) Relative response of a hypothetical instrument with 'tail' for  $\lambda > 316$  nm (RH scale)
- c) (a) x (b) (LH scale)

The spectral response of the instrument is proportional to the area under curve (c). Area under curve for  $\lambda > 316$  nm is ~ 30% of total signal, although the instrument sensitivity is < 0.1 of its peak value above 316 nm.

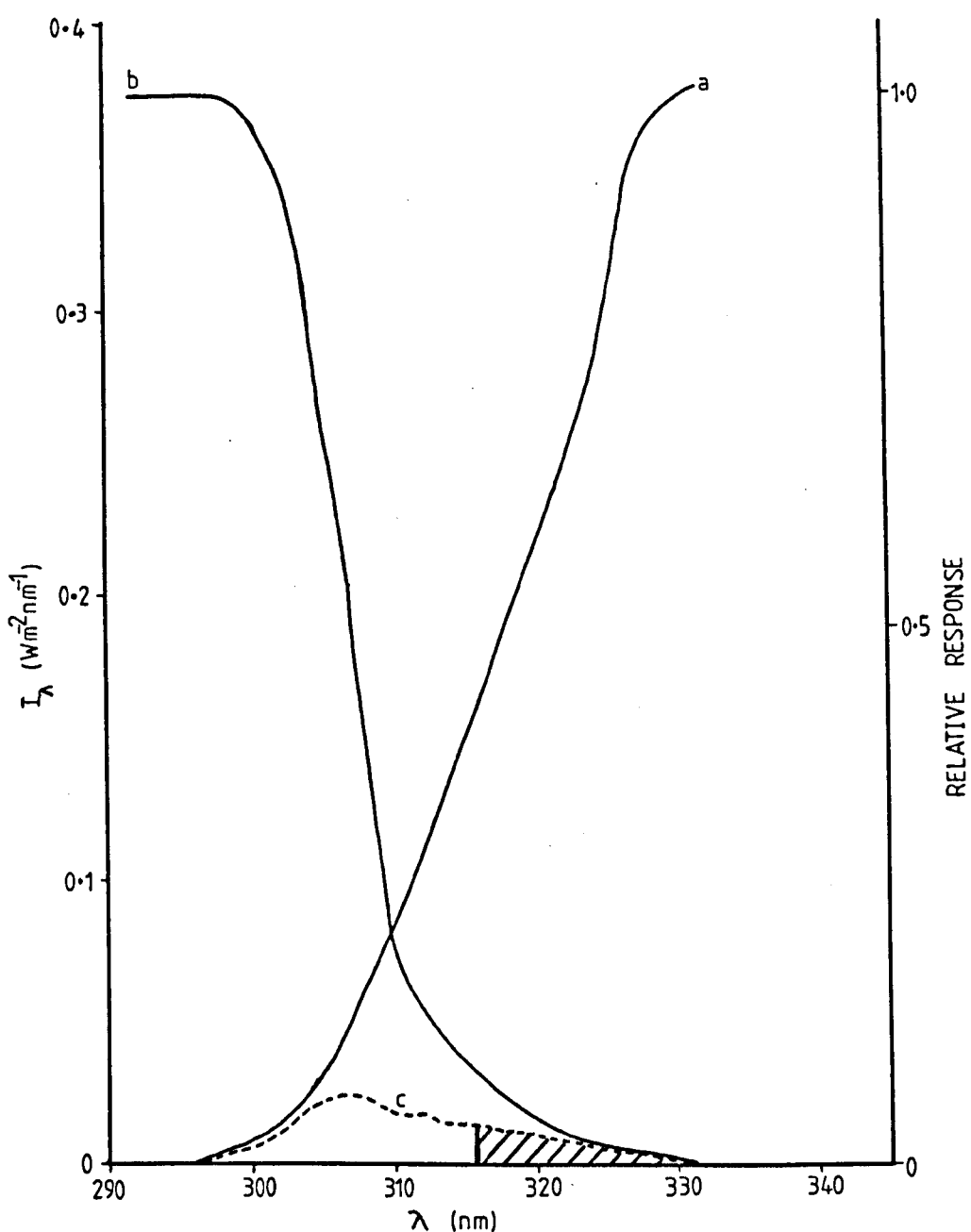
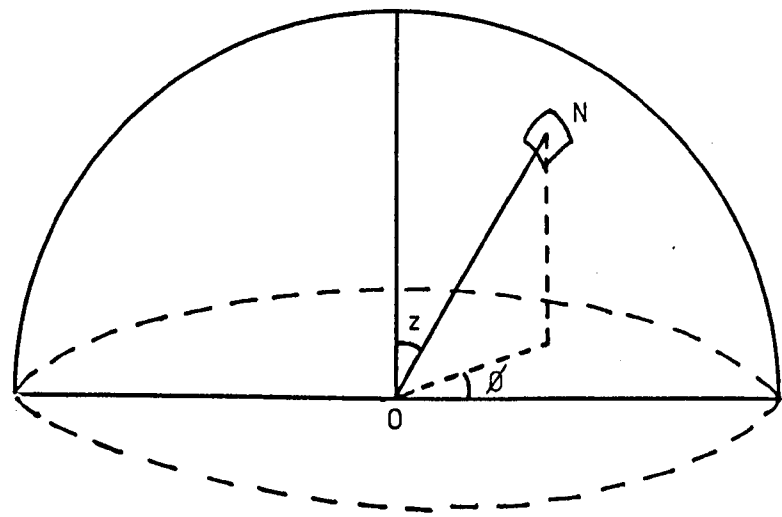


Fig. 4.2 The influence of a long wavelength 'tail' on the response of an instrument measuring solar UVB radiation.

Fig. 4.3 Irradiance of a horizontal surface.



**z** Zenith angle

**φ** Azimuth angle

**N** Radiation from small zone of sky

Irradiance at a point O is given by

$$I = \int_0^{2\pi} d\phi \int_0^{2\pi} N \cos z dz$$

Non-linearity is not a serious problem for point measurements, but very clever electronics are needed to undo the curvature of response if the signal from a non-linear instrument is to be integrated.

- g) Measuring and recording devices of minimum sophistication and requiring little maintenance are desirable for long term use.

A commercial instrument (International Light, SEE 240) satisfied the criteria a, b, c and f. It was tested for stability and robustness and performed well. A calibration was made using the LII800 as a reference and the output from the instrument recorded in two ways.

#### The SEE 240 Vacuum Photodiode

The SEE 240/UVB/W/Probe is the sensor designed for a phototherapy radiometer system supplied by International Light Ltd (Appendix A2). As the sensor was the only part of the system really suited to the project, this alone was purchased and a more suitable device was built to record its output (Appendix B).

The SEE 240 is a solar-blind vacuum photodiode. This means that the excitation of the detector is quantum limited and it will only respond to photons with energy above a certain threshold ( $\lambda < 340$  nm). The lack of response to longer wavelengths is not therefore dependent on blocking by filters, which are never perfectly black.

The UVB filter has a response spectrum matched to the erythemal action spectrum of human skin (Fig. 4.4) and similar to that of vitamin D synthesis (as far as it is known). The combination response of vacuum photodiode and UVB filter covers the waveband 270-315 nm.

A quartz W "wide-eye" diffuser gives the instrument a cosine angular response, weighting the incident radiation by the cosine of the zenith angle before it reaches the detector.

KEY :

- a) Relative response of SEE 240/UVB/W (published)
- b) Erythemal action spectrum (Paltridge and Barton, 1978)
- c) Vitamin D action spectrum (Knudsen and Benford, 1938)

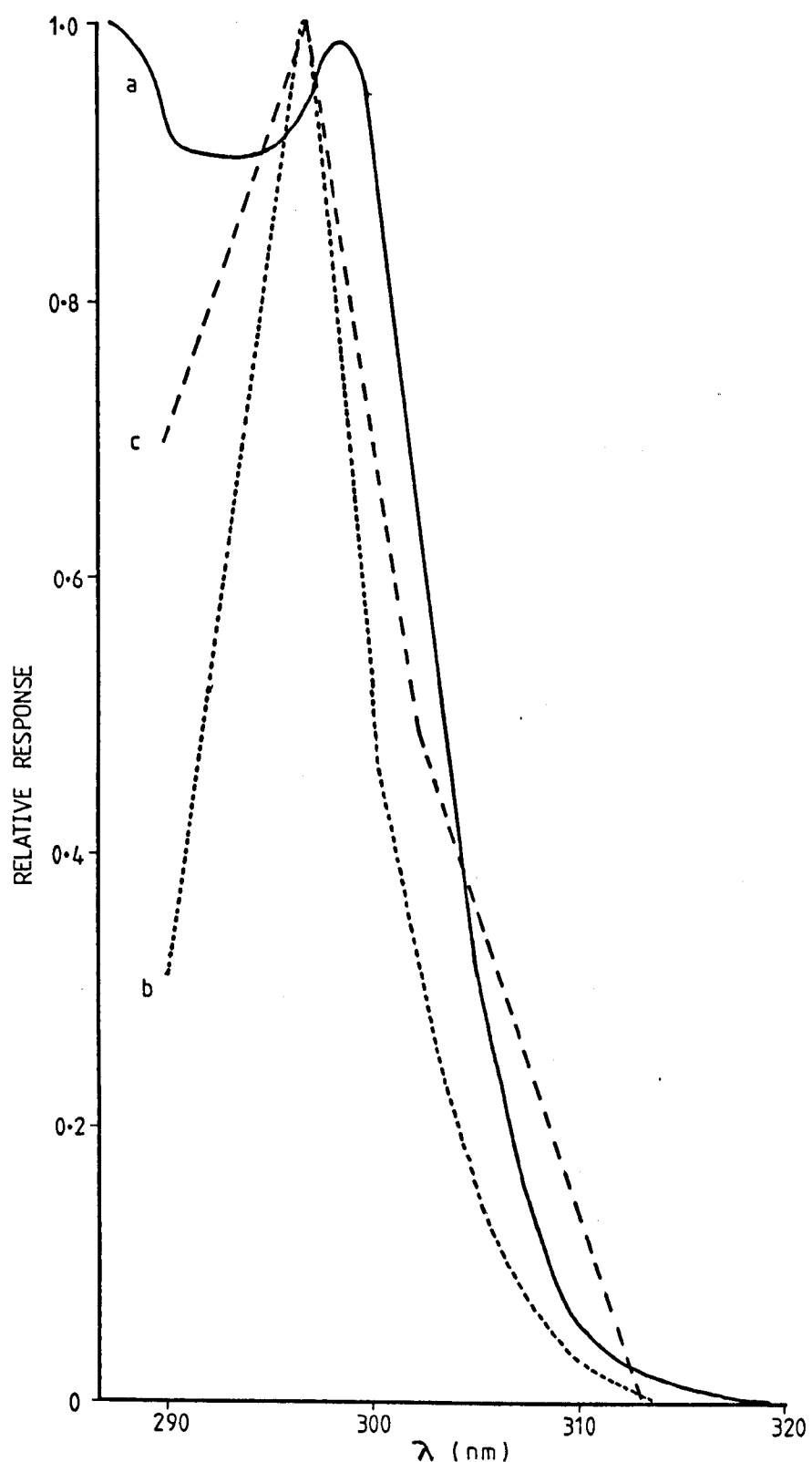


Fig. 4.4 The response spectrum of the SEE 240/UVB/W sensor and the action spectra of human erythema and vitamin D synthesis.

The unit was supplied with a calibration at 290 nm peak irradiance and a 'typical' response curve. This calibration was unsuitable because it was referenced to a peak wavelength outside the range of solar radiation to be measured, and the calibration light source used was completely different to the solar spectrum. In order to make use of this calibration the output spectrum of the calibration lamp, the solar spectrum, and the response spectrum of the instrument would have to be known to a very high degree of accuracy. The SEE 240 was therefore recalibrated under natural solar radiation, the conditions for which it was to be used.

#### Testing of the SEE 240

To check that the response of the units to be used was representative of this type of detector, their relative response was measured with particular emphasis on the long wavelength cut-off.

In the laboratory of Glen Creston (Appendix A1) the output from the SEE 240 was compared with the output from a silicon detector of known sensitivity. A SPEX microprocessor-controlled spectrometer was used to scan the output of a Xenon arc lamp over the wavelength range 270-330 nm. With a spectrometer bandwidth of 1 nm there was insufficient energy to give a reproducible output from the SEE 240. Increasing the bandwidth to 5 nm gave the relative response spectrum, normalised to 290 nm, in Fig. 4.5.

The output from the sensor is proportional to the product of this response spectrum and the spectrum of the incident light source integrated over all wavelengths. As such it is a biologically active

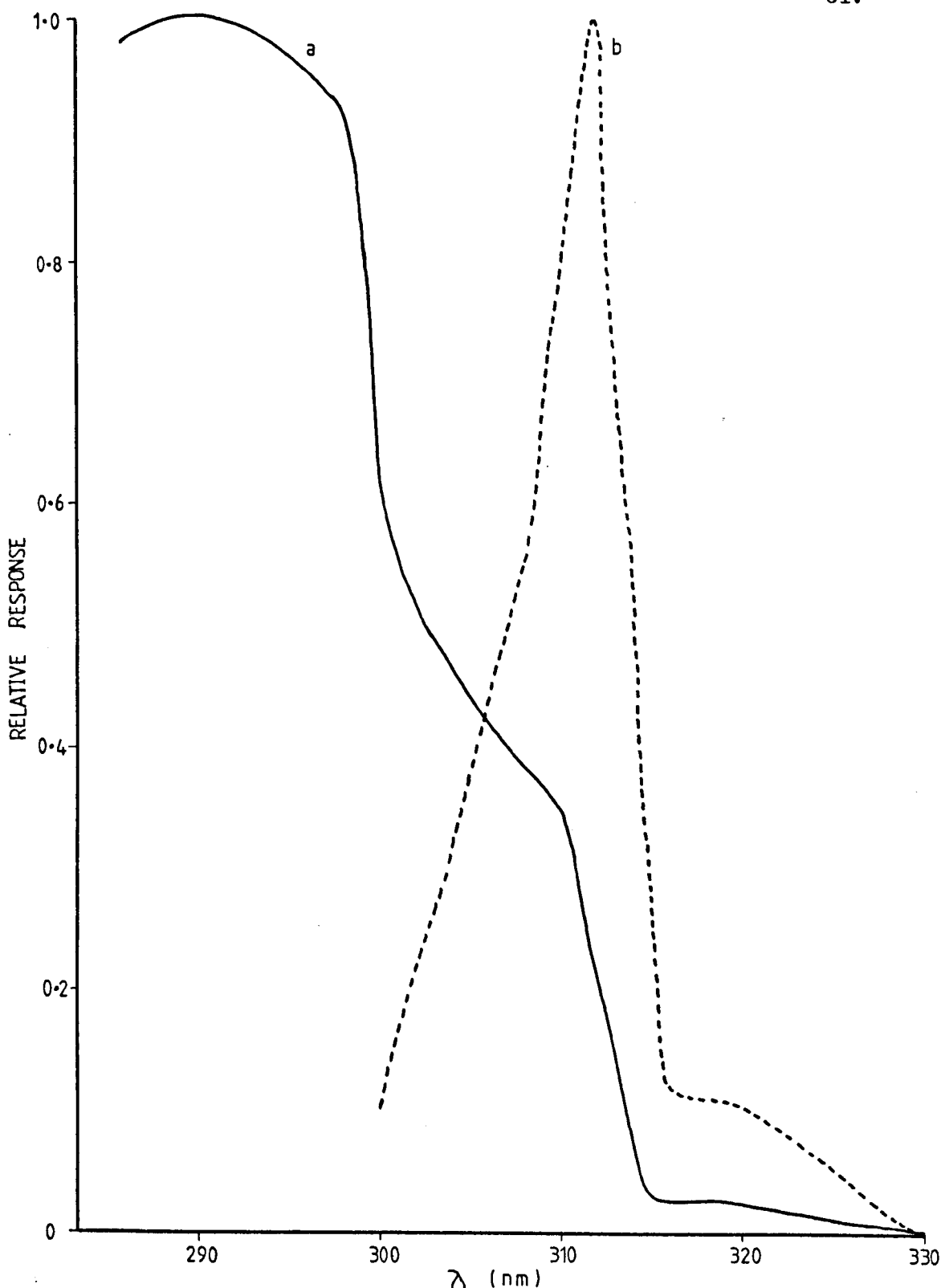


Fig. 4.5 The measured relative response spectrum of the SEE 240/UVB/W sensor, and the response when multiplied by the solar spectrum.

- KEY :
- (a) Relative response of SEE 240/UVB/W
  - (b) (a)  $\times$  solar spectrum measured on 29 June at 1100.

energy flux that is measured - for this instrument the equivalent flux at 290 nm of erythemally effective radiation - rather than a physical unit of radiation ( $\text{W m}^{-2}$ ).

In order to measure UVB radiation in absolute units the SEE 240 was calibrated against the LI1800 spectroradiometer. Firstly, solar spectra measured with the spectroradiometer at hourly intervals on a clear day (15 April 1983) were multiplied at each wavelength by the corresponding relative response of the SEE 240, as measured at Glen Creston. The resulting spectra, proportional to the sensor output, indicated:

- i) the magnitude of the fraction of the SEE 240 signal due to  $\lambda > 316 \text{ nm}$ ;
- ii) the best waveband with which to match the output of the SEE 240.

At noon the contribution to the sensor signal at  $\lambda = 318 \text{ nm}$  was only 12% of the peak contribution from  $\lambda = 312 \text{ nm}$ . The integrated spectrum showed that only 6% of the signal was accounted for by wavelengths greater than 316 nm. At 0900 the corresponding fraction was 8%.

The error introduced by the 'tail' of the SEE 240 response spectrum was small enough to make calibration against the 300-316 nm waveband feasible. This band corresponds to the waveband for vitamin D synthesis and a number of other important photobiological responses.

To ensure that this was the best waveband over which to calibrate the instrument, the output from the sensor was measured at the same time as scans of the UVB radiation were made with the LI1800, with both instruments mounted on the meteorological site. The millivolt

output from the SEE 240 was then plotted against three candidate wavebands from the LI1800 and correlation coefficients were calculated:

300-314 nm ,  $r = 0.992$

300-316 nm ,  $r = 0.996$

300-318 nm ,  $r = 0.988$

Readings were taken throughout a clear day, 26 April 1983 so that a range of incident radiation values was covered.

All three sets of data gave good straight lines, as shown by the correlation coefficients,  $r$ , and therefore the waveband 300-316 nm was selected for calibration as it was of most biological interest.

Having ascertained the optimal waveband for calibration of the SEE 240 the sensor was mounted on the meteorological site and calibrated in situ. As the instrument was to be exposed to the English climate it was first tested for temperature sensitivity and resistance to moisture.

The temperature stability of the SEE 240 was tested by mounting both the SEE 240 and the LI1800 beneath a 500W Thorn 'Sun 500' Tungsten Halogen lamp in a controlled environment room. The output from the sunlamp should be stable after an initial warming period, but to check this a scan was made with the LI1800 every time a measurement was taken, the LI1800 temperature correction was applied, and the integrated 300-316 nm waveband was taken as the light incident at that time on the SEE 240. The values were normalised to the value at  $T = 17^{\circ}\text{C}$  and the voltage output from the SEE 240 corrected to account for changing lamp output.

The controlled environment room was set at a range of temperatures between  $0^{\circ}\text{C}$  and  $30^{\circ}\text{C}$ . At each temperature the instruments were

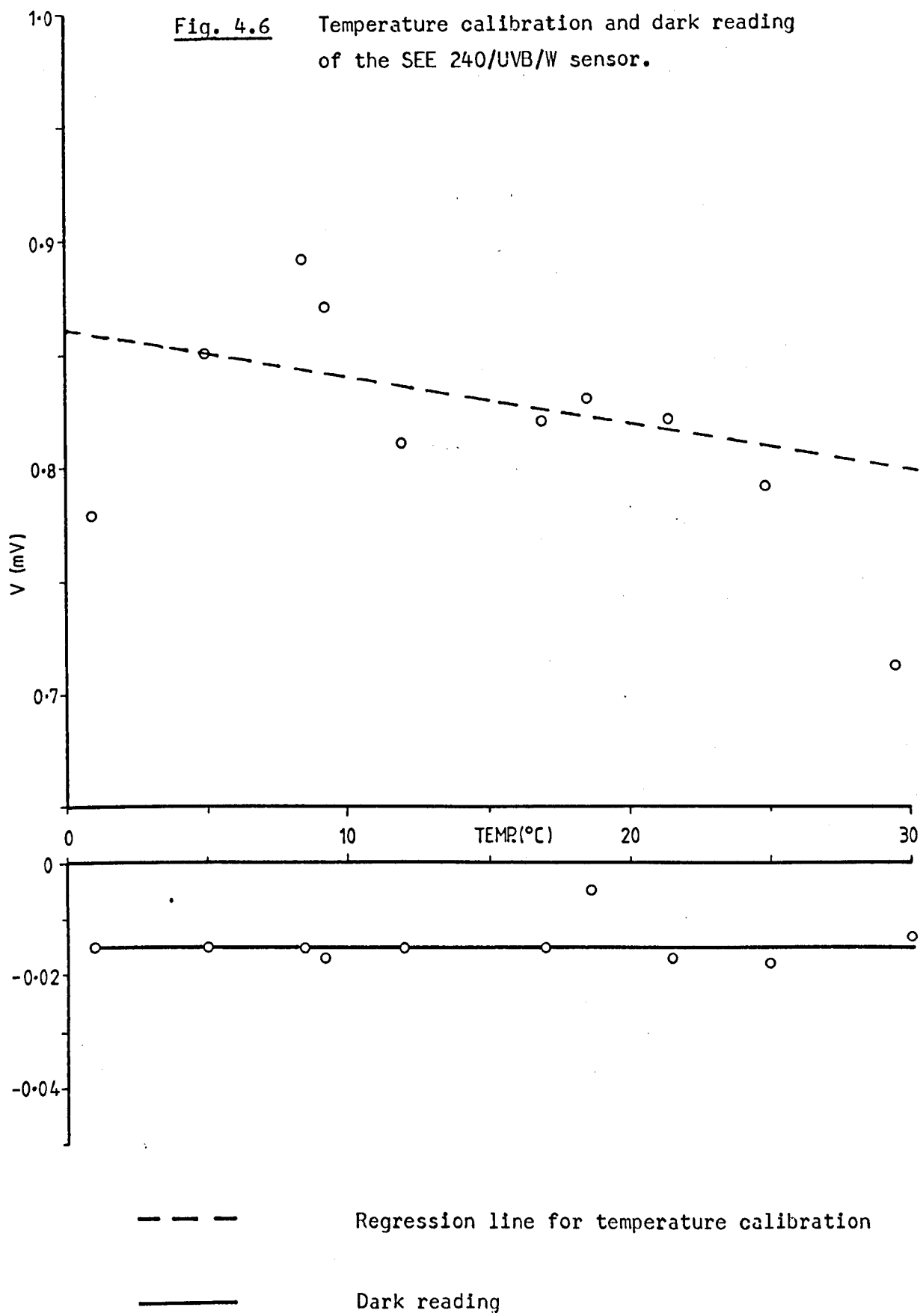
given one hour to equilibrate to room temperature before measurements were taken. The millivolt output of the SEE 240 was then recorded as a simultaneous scan with the LI1800 was made. Following this the SEE 240 was covered with a black velvet cloth and a dark reading taken at each temperature (Fig. 4.6).

There is no evidence of any temperature dependence in the dark reading, although there is some scatter of the points. The mean dark reading was  $-15.2 \mu\text{V}$  and the standard error of the mean was  $\pm 7\%$ . In a signal in the millivolt range (for solar radiation) this would give an error in the signal of 0.1%.

The graph of SEE 240 output V against temperature T (Fig. 4.6) showed a great deal of scatter. A linear regression fitted to the data gave the relationship  $V = -(3.136 \times 10^{-3}) T + 0.8629$  with T in  $^{\circ}\text{C}$  and V in mV. The standard error of the slope was  $1.6 \times 10^{-3} \text{ mV } ^{\circ}\text{C}^{-1}$ .

Because of the scatter a t-test was performed on the data to test for the absence of any temperature dependence. The 92% confidence limit for zero slope obtained from the t-test is too small to state with any certainty that the output of the SEE 240 has no temperature dependence, but given the scatter of observations there is still a statistical possibility that the instrument's performance is independent of temperature.

Taking the temperature dependence given by the regression analysis, the error over the temperature range 0 to  $30^{\circ}\text{C}$  would be 0.1 mV. The signal due to solar radiation is typically of the order 1-20 mV. Taking a signal of 20 mV at  $30^{\circ}\text{C}$  and 1 mV at  $0^{\circ}\text{C}$  and applying the temperature correction with  $15^{\circ}\text{C}$  as the standard temperature shows that



what is measured as a 20 mV signal difference would be 19.9 mV, an error of  $\pm 0.5\%$ . Considering the size of possible errors incurred by assuming that the SEE 240 is temperature stable, it was not considered necessary to build any temperature correction device into the circuitry of the recording devices.

Any instrument mounted outdoors must be able to withstand the range of weather conditions encountered in the regime where it is sited. In England, moisture can be a problem as rain is frequent throughout the year. The SEE 240 was to be mounted in a protective cover, but the light-receiving surface could not be protected in any way and it was tested to ensure that water lying on the flat surface did not penetrate the instrument. At the same time the effect of water droplets on the transmission of UV at the outer surface of the instrument was investigated.

The SEE 240 was mounted beneath a 500 W sunlamp as in the temperature experiment and water droplets of various size and distribution were placed on top of the instrument with a pipette. Neither a sheet of water nor any combination of discrete drops had any significant effect on the sensor signal. The transmission of water in the UVB is  $\sim 80\% \text{ m}^{-1}$  at 300 nm for clear water (Halldal, 1979).

To test the impermeability of the SEE 240 it was left overnight with a pool of water on the upper surface. The following day it was inspected for leakage but there was no evidence of any water in the sensor.

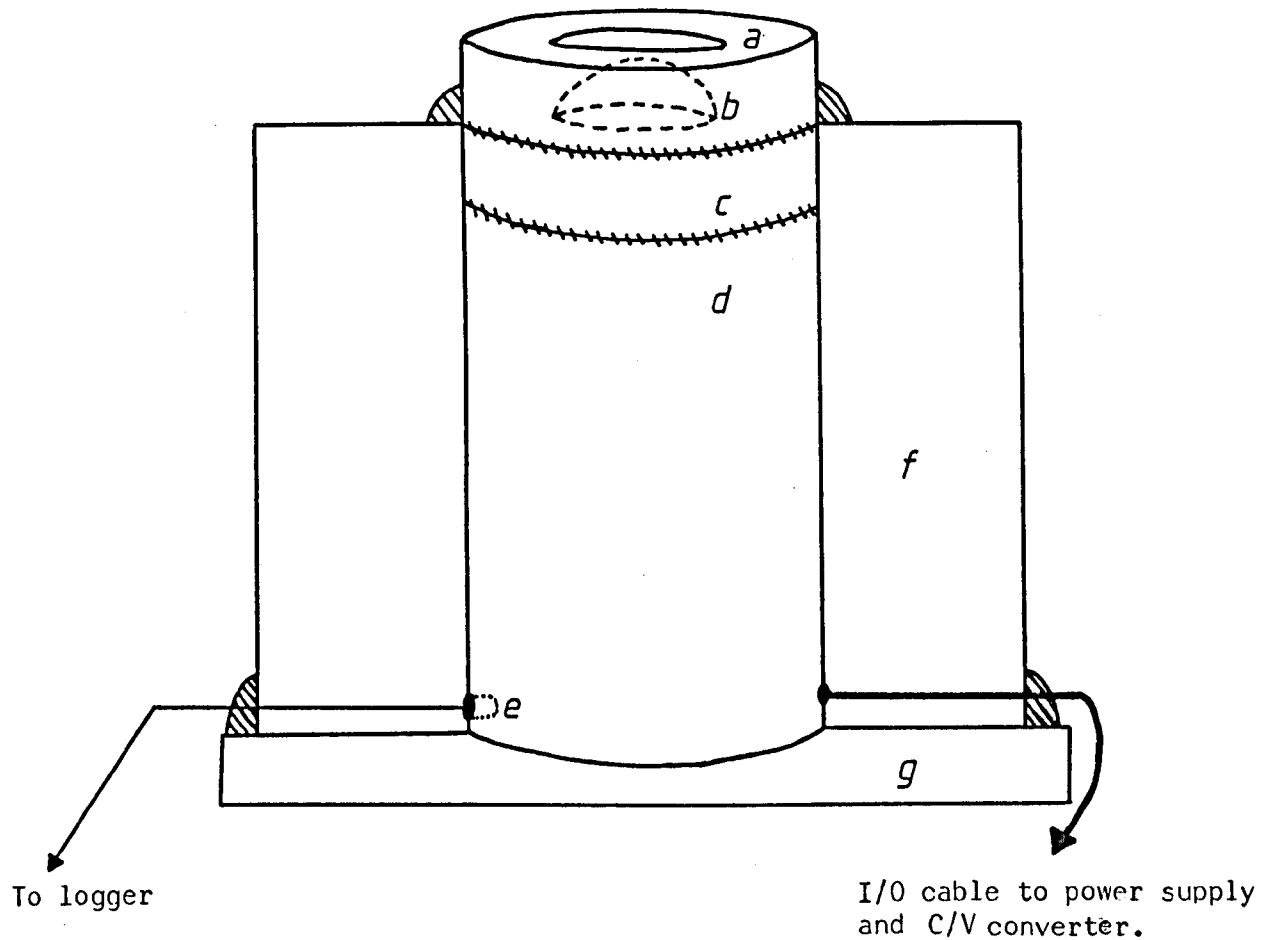
However, during the temperature experiment condensation had been noticed on the cosine diffuser, beneath the upper surface, when the

temperature fell to 4°C after being 20°C. Moist air in the instrument cooling below its dewpoint was responsible for this. Air was most likely to enter the instrument where the cosine diffuser screwed onto the main body of the vacuum photodiode (Fig. 4.7) and this was sealed with silicone rubber compound.

To prepare the SEE 240 for mounting in the field the cosine diffuser and the filter were unscrewed from the vacuum photodiode tube and all three components placed in a cold room at - 20°C for a number of hours. The complete unit was then reassembled, smearing the screw threads between components and sealing the joints with silicone rubber compound. This process sealed very dry air into the instrument and in the absence of leaks minimised the risk of condensation in the range of temperatures likely to be encountered in the English East Midlands. These precautions proved adequate and no condensation was observed at any time during field operation.

To reduce temperature variation and increase the thermal response time the whole photodiode tube was encased in a block of polystyrene with the surface of the sensor 0.5 cm above the surface of the polystyrene. A thermocouple was mounted in a small hole in the base of the instrument to measure the instrument temperature.

All interfaces were liberally coated with silicone rubber compound. Thus protected against sudden temperature changes and inclement weather, the SEE 240 was mounted on the meteorological site alongside a Kipp solarimeter measuring broadband solar irradiance. The polystyrene block was mounted on a wooden base, and once the SEE 240 had been levelled this was screwed into place on a table.



- a Flat upper surface of detector
- b Diffusing cosine head immediately beneath upper surface
- c UVB phototherapy filter
- d Vacuum photodiode tube
- e Thermocouple
- f Polystyrene block
- g Wooden base
- ||| Silicone rubber compound

Fig. 4.7 Diagram of the SEE 240 mounted for field use.

The power supply and current/voltage converter (Appendix B1) for the instrument were housed in a wooden box under the table. The output from the C/V converter went to a junction box on the table leg, and from there by subterranean cable to a Solartron data logger in the meteorological site hut. From the junction box, the signal was also sent to a printing dose timer (Appendix B2) housed in the box beneath the table (Fig. 4.8).

#### Calibration

The SEE 240 was ready for calibration. The Solartron data logger recorded the millivolt signal from the sensor as a spot sample at specified time intervals. The LI1800 was mounted on another table on the meteorological site and its clock synchronised with the data logger. Spectroradiometer scans of the UVB (300-316 nm) radiation were taken every 10 minutes at the same time as the logger sampled the signal from the SEE 240. The first measurements were collected on 19 June 1983, a clear day, from 0820 to 1900 GMT.

When the signal from the sensor was plotted against the integrated 300-316 nm waveband measured by the LI1800, the points fell on two lines, one set taken during the morning and one set in the afternoon. The difference was most noticeable near noon. The levelling of both instruments was checked and found to be correct. The following day measurements were taken only in the afternoon, and when added to the previous day's data followed the afternoon line (Fig. 4.9).

The cause of this discrepancy was first thought to be due to an imperfection of one or other of the cosine receptors, although in this

KEY :

- Signal cable
- Thermocouple wire
- a SEE 240/UVB/W
- b Kipp solarimeter
- c Junction box
- d Wooden box
- e Thermocouple junctions
  - i) ambient air temperature
  - ii) sensor temperature
- f Thermocouple reference junction, 1 m depth
- g To data logger
- h Mains
- j Mains filter
- k Power supply and C/V converter
- m Dose timer
- n Calculator
- p  $\pm 7.5$  V
- r - 12 V to SEE 240
- s Current signal from SEE 240
- t Signal (mV)
- u Print signal

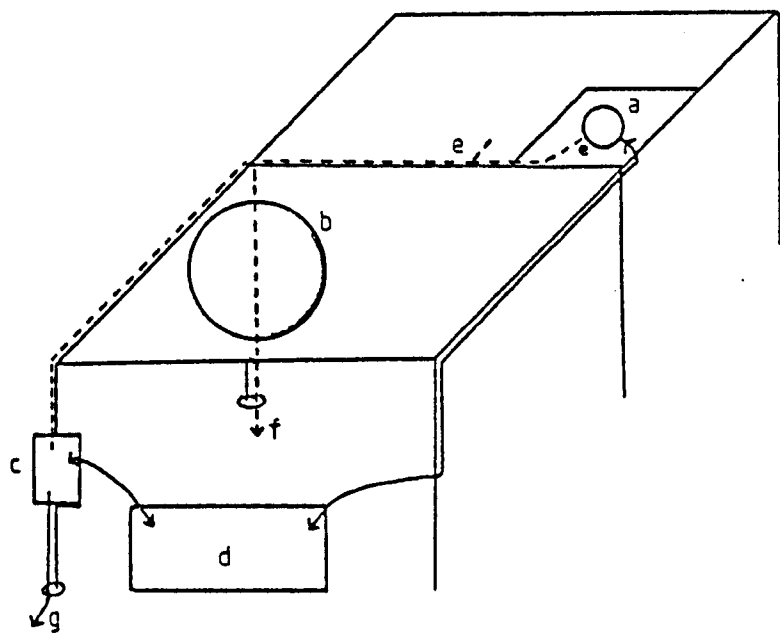
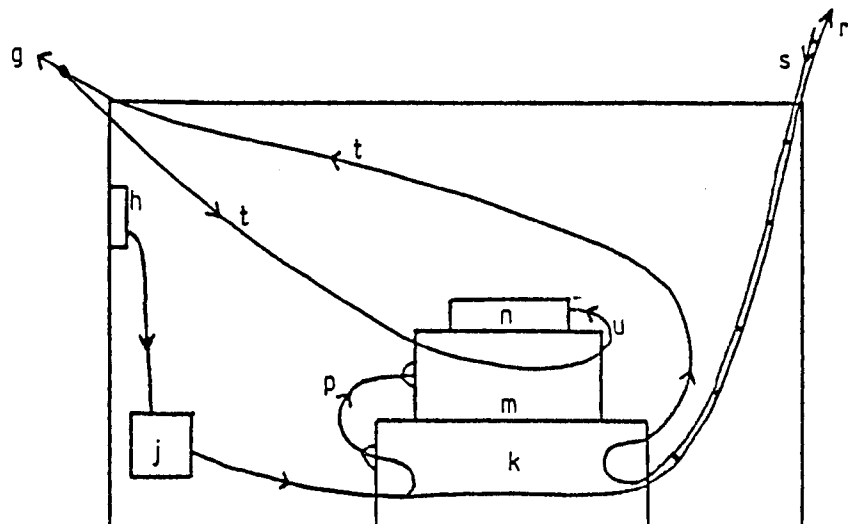


Fig. 4.8      Diagram of meteorological site connection  
for the SEE 240.



Signal collection and processing in the field:  
the wooden box.

KEY :

- \* 19 June 1983 morning
- o 19 June 1983 afternoon
- ♦ 20 June 1983 afternoon
- † 21 June 1983 morning
- 21 June 1983 afternoon - LII1800 turned through 180°
- 25 June 1983 afternoon - LII1800 turned through 180°

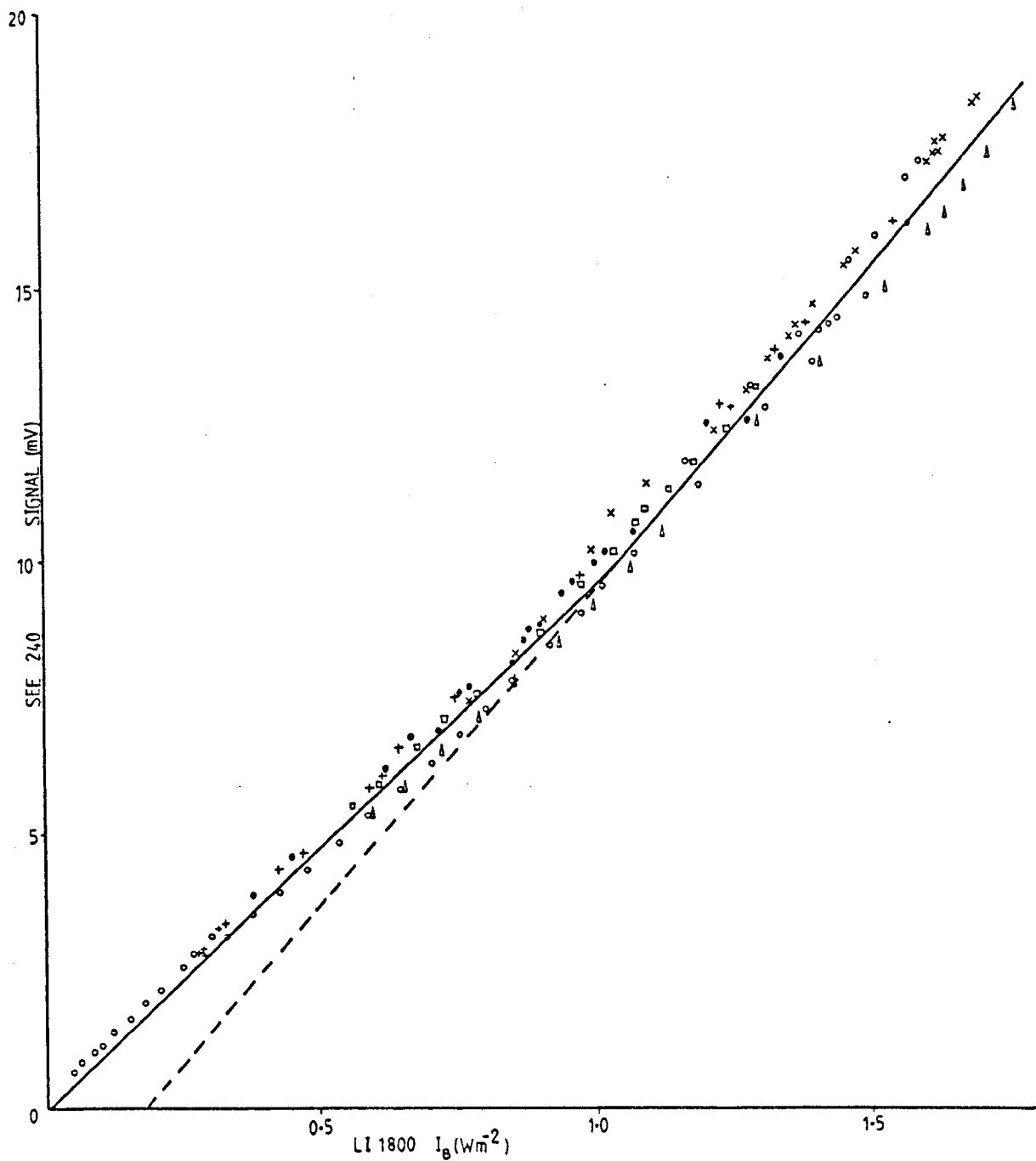


Fig. 4.9 Calibration graph: signal from SEE 240 vs integrated 300-316 nm waveband from LII1800.

case the error should decrease with increasing solar elevation instead of increasing.

To ascertain which system was at fault further measurements were taken on another two days. On 21 June, a day with a complete cover of grey stratus cloud, readings were taken throughout the morning. The LI1800 was turned through  $180^{\circ}$  and more measurements taken during the afternoon. Both sets of data fell on the morning line.

The afternoon of 25 June was clear and with the LI1800 orientated as for the afternoon of the 21st the plotted points again fell on the morning line.

This suggested that the LI1800 was at fault. Because the discrepancy was still in evidence under diffuse radiation conditions, and did not decrease with increasing solar elevation, it was deduced that the fault was not the cosine response of the diffuser, but an azimuth error (see error section). The maximum difference between morning and afternoon values was  $< 8\%$  ( $1.3 \text{W.m}^{-2}$  for a signal of  $16.5 \text{W.m}^{-2}$ ), giving a maximum error from the calibration line of  $< 4\%$ . This was taken to be the azimuth error of the spectroradiometer. Despite the fact that the two sets of points can be separated according to LI1800 orientation with respect to the sun, the two sets were considered close enough to be treated as homogenous for calibration.

The resultant calibration curve (Fig. 4.9) could be approximated to two straight lines, meeting when the signal from the SEE 240 was 10 mV. The two lines were

$$V < 10 \text{ mV} , V = (9.43 \pm 0.29)I_B \quad r = 0.995 \quad (4.1)$$

$$V > 10 \text{ mV} , V = (11.6 \pm 0.22)I_B - (2.2 \pm 0.32) \quad r = 0.984 \quad (4.2)$$

where  $V$  (mV) is signal at logger,  $I_B$  is integrated radiation from  $300\text{-}316 \text{ nm in } \text{W m}^{-2}$  from the LI1800. Taking 2 standard errors either side of the mean gave an error of  $\pm 6\%$  for line 1, and  $\pm 8\%$  for line 2. The calibration error was therefore taken as  $\pm 8\%$ . This includes the error resulting from the azimuthal response variation in the LI1800.

With the SEE 240 calibrated and mounted on the meteorological site regular recording of the solar UVB radiation began in June 1983. The signal from the SEE 240 was recorded as a spot sample on the data logger every 5 minutes during the day. At night, hourly spot samples were taken. Also recorded on the logger were the total (300-3000 nm) global and diffuse radiation from the two Kipp solarimeters on the meteorological site, and the sensor temperature and ambient air temperature from two copper-constantan thermocouples with reference junctions in the soil at a depth of 1 m.

The punched tape output from the data logger was read into files on the mainframe computer and the raw data converted from millivolts to the appropriate units by a Fortran 77 program.

The UVB radiation was also recorded by a printing dose timer. The integrator was specially designed to accept the signal from the SEE 240 and used a Casio CP10 printing calculator to record the time after which a set dose of radiation had been received. Details of

the circuitry are given in Appendix B2. On range scale 3 the time was printed whenever a dose of  $0.028 \text{ J cm}^{-2}$  was accumulated. Changing range changed the dose rate for printing by a factor of 2 for each range so that the integrator could be set to be more sensitive in winter when there is little UVB radiation and less sensitive in summer when dose rates are high.

This method of recording the incident UVB radiation made it easy to calculate the total UVB dose available during any period of the day. When considering photobiological responses to radiation this measurement is more important than the instantaneous value of irradiance at a given time, as recorded on the logger. A standard integrator (recording total radiation received over a specified time interval) misses some of the structure of the irradiation pattern, giving no indication of the range of radiation values incident during the time period of integration. The dose timer reveals more details of the irradiation and the amount of information is weighted towards the more important times of day: when the incident radiation is high (around midday) prints are frequent; during times of low irradiance and at night when there is little radiation of biological significance or interest there are few if any prints. For a climatological rather than a biological record, the printout from the dose timer can be inverted to calculate the average UVB radiation in  $\text{W m}^{-2}$  incident during the time between two prints. It can thus be used to give a smoothed version of the daily variation in UVB radiation. Again the information is more detailed than for a standard integrator, at least during the middle of the day, although more work is involved in extracting the data.

The SEE 240 with the printing dose timer was also used to calibrate the polysulphone badges used as personal exposure meters (Chapter 7).

All three means of recording the UVB radiation, the LI1800, the SEE 240 on the logger and the SEE 240 on the dose timer were periodically compared to test for drift in calibration. The results of two such checks are shown in Fig. 4.10 for 21 November and 21 July 1983.

#### Diffuse UVB Radiation Measurement

##### Broadband measurements

In 1984, a second SEE 240 unit was purchased. The peak irradiance response calibration of the second sensor showed it to be less sensitive than the first by a factor of  $\sim 8$ . A second power supply and printing dose timer were built and the ranges on the latter altered to give the same print times when the two SEE 240 sensors were mounted side by side on the meteorological site (see later section). Calibrated thus against the first sensor, the second was taken to Nottingham General Hospital to record the UVB radiation on a hospital terrace (Chapter 8). At the end of this trial the sensor was returned to Sutton Bonington and mounted under a shade ring on the meteorological site. The diffuse UVB radiation was recorded on the data logger with the other radiation measurements from July 1984 to March 1985.

##### Shade-ring correction

A shade-ring is designed to shade a sensor from the direct solar beam throughout the day. It is positioned according to season and

KEY :

- ◊ SEE 240 at logger (to  $\pm$  0.005  
due to analysis program)
- SEE 240 at printing integrator
- \* LII800

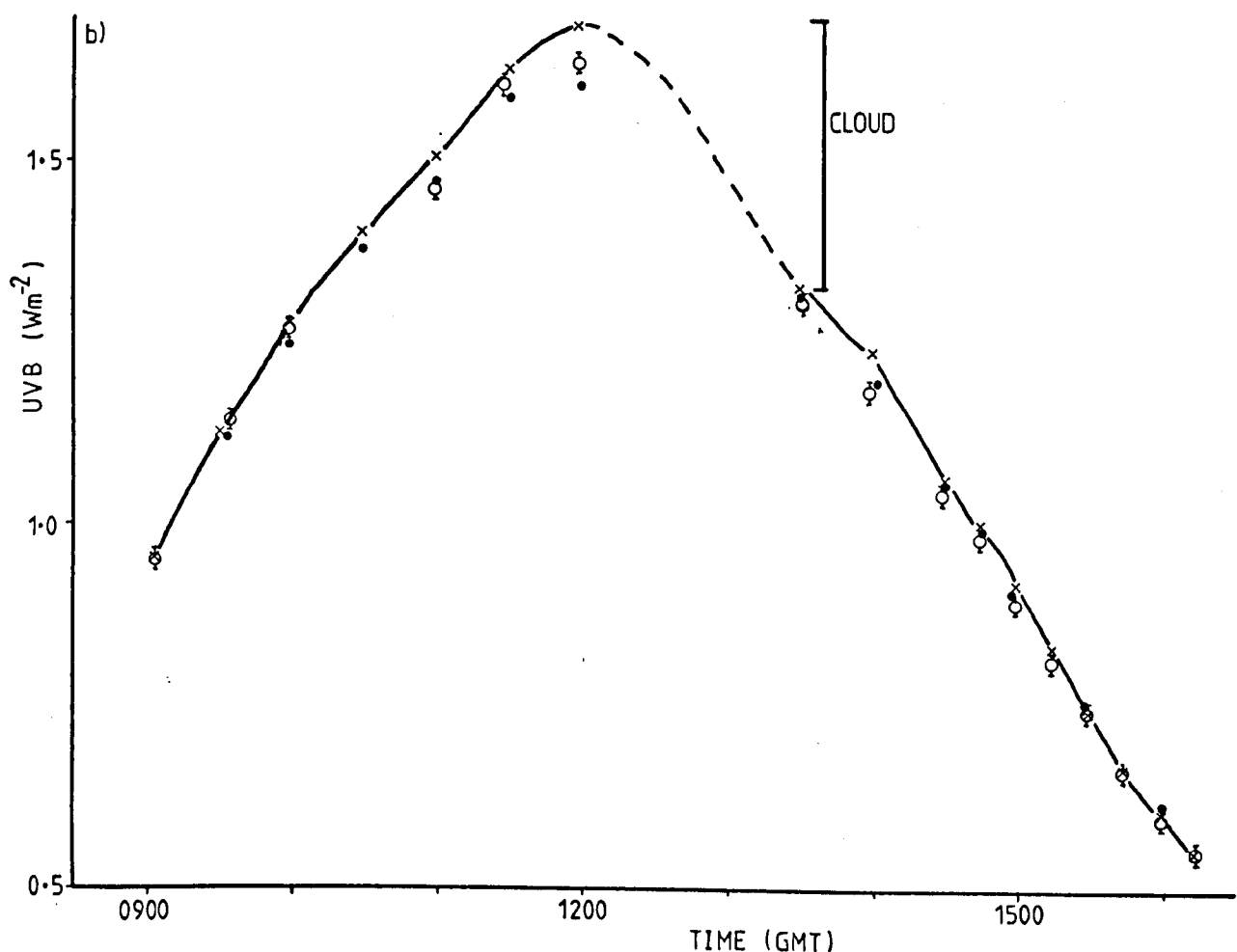
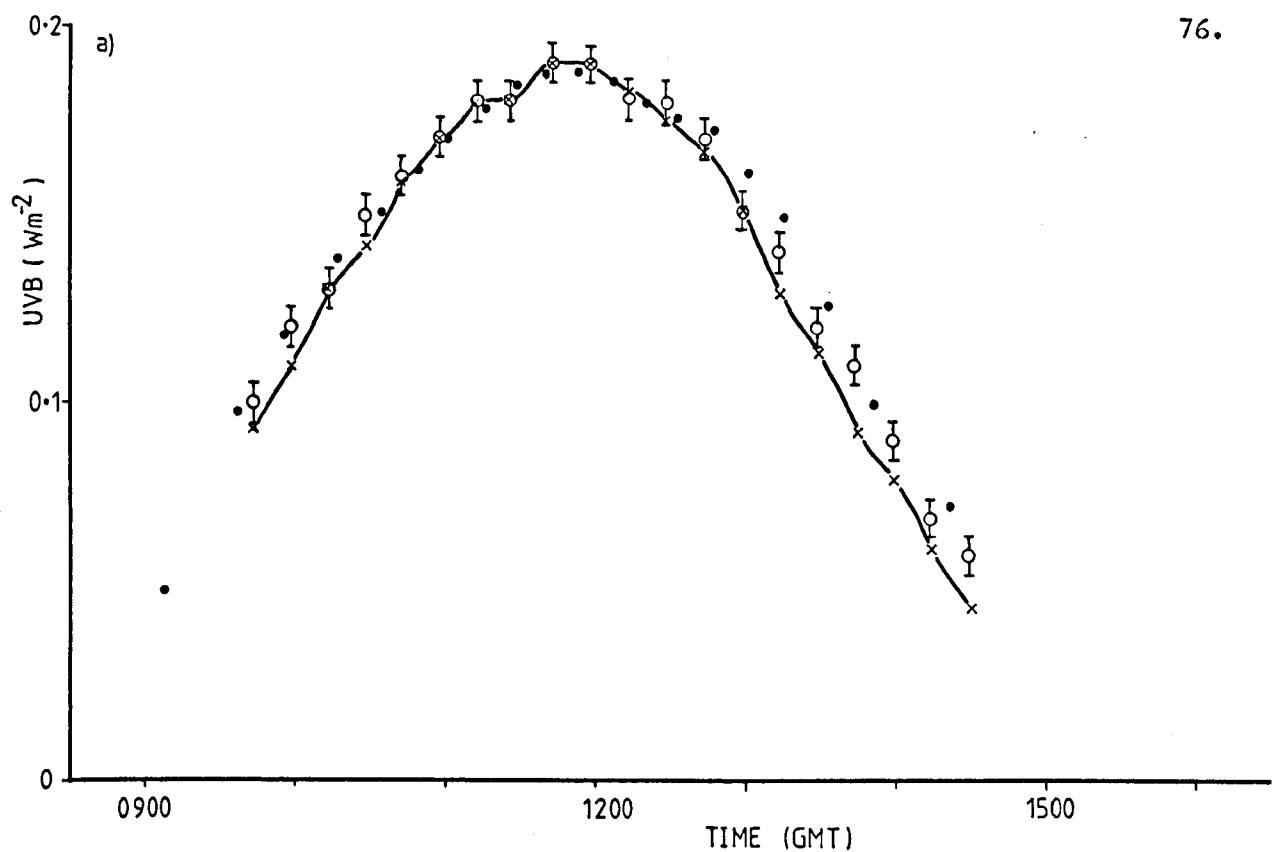


Fig. 4.10 Inter-sensor calibration checks for 2 clear days  
a) 21 November 1983, b) 21 July 1983.

latitude so that as the sun moves through the sky one part of the ring always obscures the sensor from the direct beam. While the requisite  $10^{\circ}$  diameter cone of circumsolar radiation is prevented from reaching the detector, the rest of the ring cuts out some of the diffuse radiation from the surrounding sky. To compensate for this a small shade-ring correction should be applied. This correction depends on sky conditions as well as season and location. Shade ring corrections for the total solar waveband have been well documented for Sutton Bonington (Steven and Unsworth, 1980; Steven, 1984) but corrections may not be the same for the UVB waveband because of the different effects of atmospheric scattering with wavelength. At UV wavelengths Rayleigh scattering accounts for virtually all the sky radiation, whereas Mie scattering becomes more important at longer wavelengths (Chapter 2).

To investigate the shade-ring correction needed for the UVB band, a series of measurements were taken in clear sky conditions. The sensor signal was recorded on a millivoltmeter in the following sequence:

1. With the ring in place.
2. With a blackened disc (diameter 15.5 cm) held at a distance of 90 cm from the sensor so as to obscure the  $10^{\circ}$  circumsolar radiation only.
3. With no shade.
4. With the disc as in 2.
5. With the ring as in 1.

The five readings were taken in rapid succession and the incident radiation assumed constant over the time ( $\sim 2$  min.) needed to take a set of measurements. The shade ring correction was then calculated as

$$\text{Correction} = \left[ 1 - \frac{D_{\text{disc}} - D_{\text{ring}}}{D_{\text{disc}}} \right]^{-1} = \frac{D_{\text{disc}}}{D_{\text{ring}}} \quad (4.3)$$

The shade-ring corrections measured on 11 clear days are shown in Fig. 4.11, together with the geometric ring correction (Drummond, 1956) - the correction under isotropic radiation conditions calculated for Sutton Bonington (Steven and Unsworth, 1980). The higher correction factors calculated from measurements give an indication of the anisotropy of UVB sky radiation (Chapter 6). The 11 clear day corrections plotted are mean values for each day.

The shade-ring correction applied to the diffuse UVB measurements made with the SEE 240 was taken to be the geometric correction plus 0.01. This gave a seasonal variation in shade-ring correction of 1.02 to 1.14.

#### Spectral measurements

Spectral measurements of diffuse radiation were made with the LI1800 spectroradiometer on clear days throughout 1983 and 1984. A blackened disc was held so as to obscure a  $10^{\circ}$  diameter cone of circum-solar radiation and two scans were made in rapid succession, one with and one without the disc. Assuming that the incident radiation was constant during the time taken for the scans ( $\sim 2$  minutes), this gave spectral measurements of diffuse and global radiation under the same conditions.

#### Errors of Measurement - LI1800 Portable Spectroradiometer

All measurements of UVB radiation in this work are traceable by intercalibration, back to the LI1800 spectroradiometer and it is therefore of vital importance to assess the accuracy of this instrument.

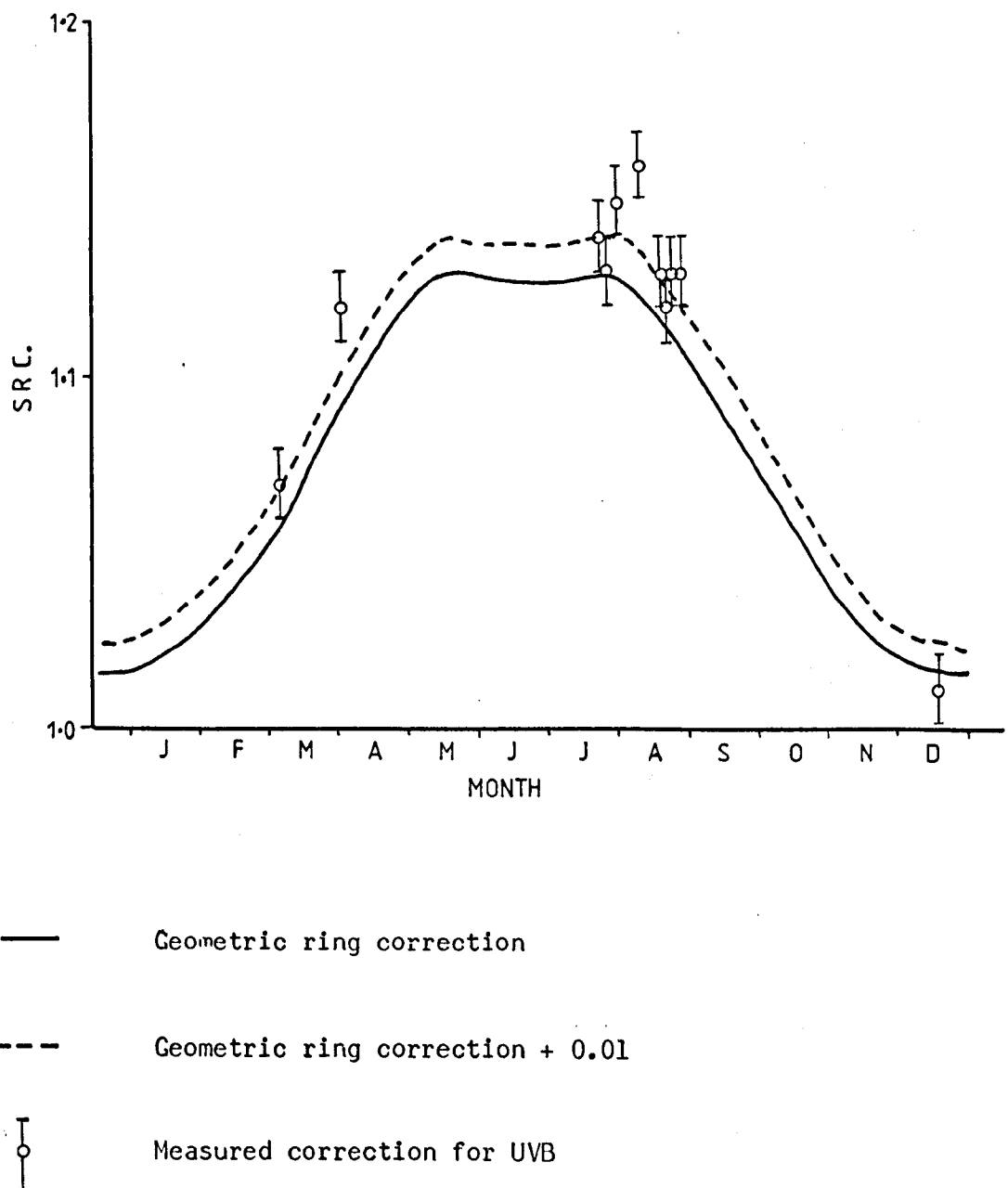


Fig. 4.11 Seasonal variation of shade-ring corrections at Sutton Bonington.

The LI1800 was delivered with a factory calibration obtained with a lamp calibrated to  $\pm 5\%$  by the National Bureau of Standards. The instrument's calibration against this 1000 W Tungsten/Halogen lamp was given as  $\pm 10\%$  at 300 nm.

Maximum accuracy in spectroradiometry can be obtained by using a standard source to calibrate an instrument that is as similar as possible to the test source in size, shape, spectral power distribution, intensity, polar distribution of radiation and polarisation of radiation. When the sun is the test source it is not possible to closely match all these criteria and the best approximation possible in terms of spectral power and intensity is used.

Disregarding for a moment the above potential sources of systematic error, the calibration is still limited in its accuracy by the reliability of the standard source used. A secondary standard source has been calibrated by comparison with a national primary standard, in this case NBS. There is variation even between primary standards kept by different national standards laboratories. An international inter-comparison of spectral irradiance measurements from 300-800 nm on Tungsten/Halogen lamps was organised by the Commission International d'Eclairage in 1974. The results showed that the difference in standards between NBS and NPL was never more than 2% (1% at 300 nm) but other national laboratories showed greater deviation (Moore, 1980).

Added to this international variability is the uncertainty of the relation of the lamp used as a secondary standard to the primary standard. Ideally any calibration laboratory should have at least three standards of any one type so that performance drift with time or sudden changes due to damage can be pinpointed by cross-checking between standards.

The absolute calibration specification for LICOR standards is  $\pm 5\%$  traceable to NBS and checked by National Research Council of Canada (NRC). The error is quoted as more typically  $\pm 3\%$ .

Taking the standard source used for calibration as correct while recognising the inherent uncertainty in this assumption, it is the spectroradiometer itself which must then be inspected for sources of error. The input optics of the instrument take the incident radiation into the monochromator and should ensure that the radiation from each source follows the same optical path. As monochromators are often non-uniform with respect to angle and position of light on the entrance slit, direct irradiance of the monochromator slit should be avoided unless size, shape and location of the sources can be guaranteed identical.

The input optics of the LI1800 consist of a diffusing cosine head, mirror, and filter wheel. The spatial error (cosine response) can be tested by rotating the instrument about an axis placed across the centre of the measuring surface. The output signal from the sensor is measured as the angle of incidence of a collimated light source is changed. The cosine error at angle  $\theta$  is the percentage difference of  $I/I_0$  compared to  $\cos \theta$ , where  $I$  is the sensor output at an angle  $\theta$  and  $I_0$  is the output at normal incidence. This process is repeated for several azimuth angles. For global (sun and sky) radiation at a zenith angle of  $60^\circ$ , the cosine error is  $\pm 2\%$ .

The azimuth error is the change in the sensor output as the sensor is rotated about the axis at a constant angle of incident radiation. The azimuth error of the LI1800 became apparent when calibrating the SEE 240. The maximum azimuth error was observed at zenith angles of  $\sim 30^\circ$  when the error was  $\pm 4\%$ .

The monochromator is responsible for the wavelength accuracy and stray light performance of the instrument. The wavelength accuracy of the holographic grating monochromator in the LI1800 is quoted as  $\pm 2$  nm with a repeatability of  $\pm 0.5$  nm. In July 1984 the absolute wavelength accuracy was checked with the spectral lines of a low pressure mercury arc lamp at Glen Creston and found to be correct to  $\pm 0.5$  nm.

Stray radiation at wavelengths other than that being measured is of considerable importance when measuring the solar UVB radiation as the incident radiation intensity falls so rapidly over this region of the spectrum. The filter wheel limits the waveband of light entering the monochromator, and with the 0.5 mm entrance and exit slits the bandwidth of the monochromator is given as 6 nm.

#### The effective UVB response spectrum

Spectral data from the LI1800 is recorded at discrete wavelengths, but because the bandpass function of the monochromator has a finite width, radiation from wavelengths other than that designated will contribute to the measured signal producing errors. The magnitude of these errors is estimated below.

The shape of the bandpass function for the monochromator was not known. It was therefore taken to have a normal distribution about the peak wavelength,  $\lambda_0$ , with half-power point at  $\lambda_0 \pm 3$  nm according to the manufacturer's data. The response  $R$  of the instrument to radiation at a given wavelength  $\lambda$  for irradiance measured at a band centred on  $\lambda_0$  is then

$$R(\lambda)/R(\lambda_0) = \exp \left\{ - (0.77)(\lambda - \lambda_0)^2 \right\} \quad (4.4)$$

This relative response was multiplied by the incident radiation  $S_\lambda$  at the earth's surface for each 1 nm wavelength in the range  $(\lambda_0 - 9 \text{ nm}) < \lambda < (\lambda_0 + 9 \text{ nm})$  and for  $\lambda_0$  in the range 300-320 nm.

The solar spectrum at the earth's surface was taken from the UVB Handbook (Gerstl, et al., 1983) initially for a latitude of 50°N, zenith angle = 50° and ozone amount  $[O_3] = 327 \text{ matm cm}$  with clear skies and no aerosol; a set of conditions representative of Sutton Bonington.

The effective response of the LI1800 (at a nominated  $\lambda_0$ ) for each wavelength was given by

$$\text{Effective Response} = \text{Relative Response} \times I_\lambda \quad (4.5)$$

and is shown in Fig. 4.12.

The consequence of measuring over a finite bandwidth when the measured irradiance increases sharply with increasing wavelength is to shift the wavelength of peak response from  $\lambda_0$  towards longer wavelengths. A nominal  $\lambda_0$  of 300 nm is therefore in practice measuring a narrow waveband with a peak at 303 nm. This shift of the peak wavelength is greatest at the shortest wavelengths. For  $\lambda_0 = 310 \text{ nm}$  the shifted peak  $\lambda_p$  is 311 nm, while at  $\lambda_0 = 320 \text{ nm}$  there is no change in the peak wavelength.

As the calculations for effective response were made only at discrete wavelengths (every 1 nm) and the resulting effective response spectra were not symmetrical, the integrated area under each curve was calculated and the median wavelength  $\lambda_{\frac{1}{2}}$  was found. The UVB Handbook was then used to estimate what the 'true' irradiance at  $\lambda_0$  would be if the value measured at  $\lambda_0$  by the spectroradiometer was equivalent to the radiation incident at  $\lambda_{\frac{1}{2}}$ . The results of this procedure are given in Table 4.1.

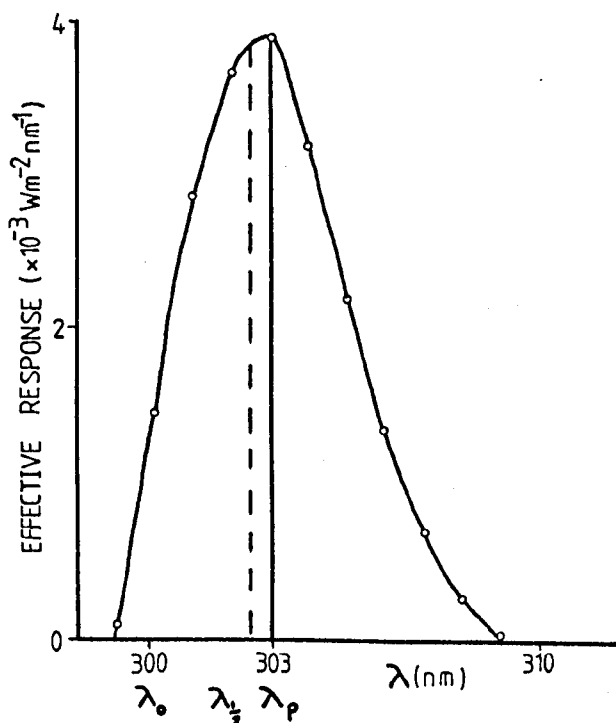


Fig. 4.12 The effective response of the LI1800 at  $\lambda_0 = 300 \text{ nm}$ .

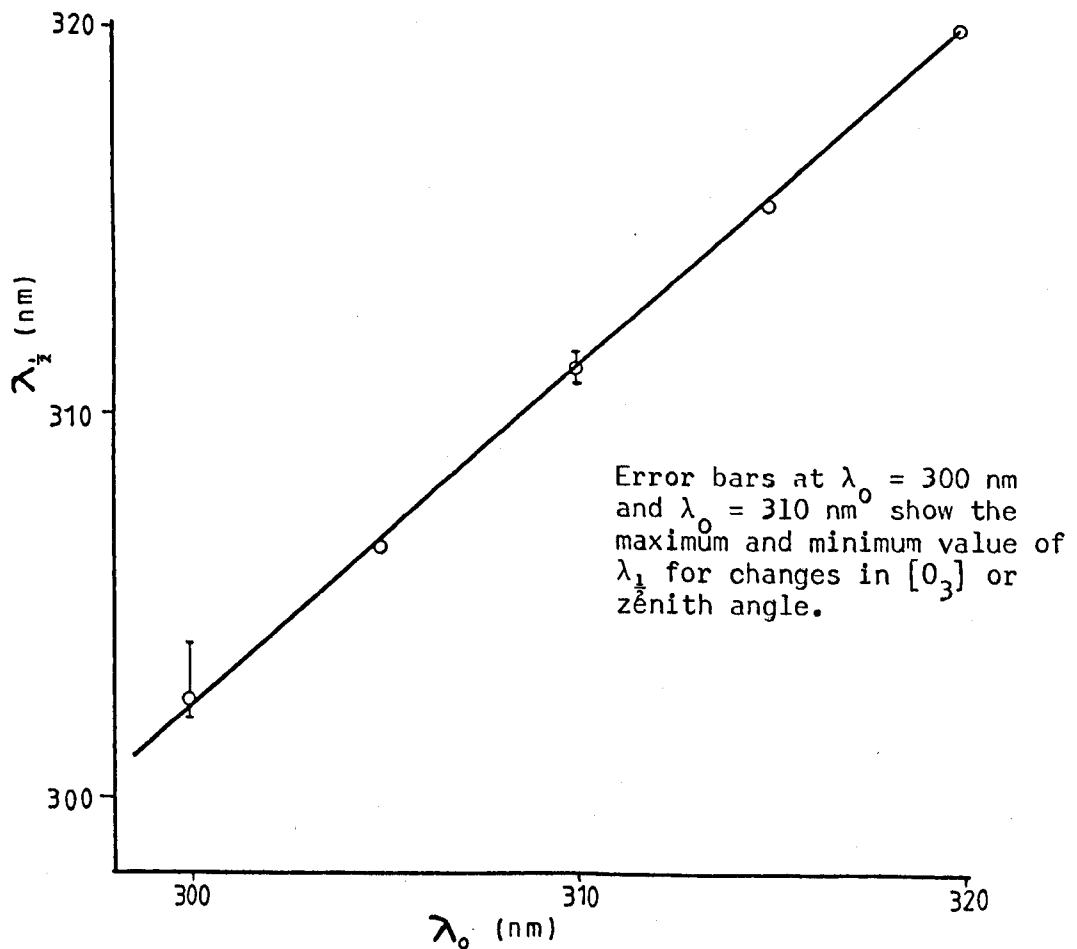


Fig. 4.13  $\lambda_{\frac{1}{2}}$  vs  $\lambda_0$  for latitude  $50^\circ$ ,  $[O_3] = 327 \text{ matm cm}$ ,  $z = 50^\circ$ .

Table 4.1 Ratio of measured to 'true' irradiance at 5 wavelengths.

| $\lambda_o$ (nm) | $\lambda_p$ (nm) | $\lambda_{\frac{1}{2}}$ (nm) | $I_{\lambda_{\frac{1}{2}}} : I_{\lambda_o}$ |
|------------------|------------------|------------------------------|---|
| 300              | 303              | 302.5                        | 4.3   |
| 305              | 307              | 306.5                        | 1.7   |
| 310              | 311              | 311.2                        | 1.3   |
| 315              | 316              | 315.3                        | 1.04  |
| 320              | 320              | 320                          | 1   |

The shape of the solar UVB spectrum changes with changing zenith angle and fluctuating ozone amount (Chapter 2). A decrease in ozone and a smaller zenith angle both shift the limit of the spectrum and the steepest decline in irradiance towards shorter wavelengths.

To estimate the effect of these changes on the above analysis the calculations were repeated at 300 nm and 310 nm for a) zenith angles of  $30^\circ$  and  $70^\circ$  with ozone amount (327 matm cm) and latitude ( $50^\circ$ ) as before; b) ozone amounts of 294 matm cm (10% depletion) and 261 matm cm (20% depletion) at zenith angle =  $50^\circ$  and latitude  $50^\circ$ . The results are given in Table 4.2.

As zenith angle or ozone amount increases, the proportion of light from longer wavelengths measured at  $\lambda_o$  also increases (i.e.  $I_{\lambda_{\frac{1}{2}}} : I_{\lambda_o}$  increases). Effects of both types of change are more pronounced at shorter wavelengths and give erroneously high values for the irradiation at a given wavelength.

**Table 4.2** Effect of a) zenith angle and  
b) ozone amount on  $I_{\lambda_{\frac{1}{2}}} : I_{\lambda_0}$

| For $\lambda_0 = 300 \text{ nm}$ |             |                         |   | For $\lambda_0 = 310 \text{ nm}$ |             |                         |   |
|----------------------------------|-------------|-------------------------|---|----------------------------------|-------------|-------------------------|---|
| a) Zenith angle                  | $\lambda_p$ | $\lambda_{\frac{1}{2}}$ | $I_{\lambda_{\frac{1}{2}}} : I_{\lambda_0}$ |                                  | $\lambda_p$ | $\lambda_{\frac{1}{2}}$ | $I_{\lambda_{\frac{1}{2}}} : I_{\lambda_0}$ |
| 30°                              | 302/303     | 302.2                   | 2.6   |                                  | 311         | 310.9                   | 1.15  |
| 50°                              | 303         | 302.5                   | 4.1   |                                  | 311         | 311.2                   | 1.3   |
| 70°                              | 305         | 304.1                   | 21*   | 311/312                          | 311.6       |                         | 1.6   |
| <hr/>                            |             |                         |   |                                  |             |                         |   |
| b) [O <sub>3</sub> ] matm cm     |             |                         |   |                                  |             |                         |   |
| 327                              | 303         | 302.5                   | 4.3   | 311                              | 311.2       |                         | 1.3   |
| 294                              | 303         | 302.5                   | 3.8   | 311                              | 311.1       |                         | 1.23  |
| 261                              | 302         | 302.3                   | 2.9   | 311                              | 311         |                         | 1.17  |

\* Any measurements made would be below the noise equivalent irradiance of the LI1800 and therefore unreliable.

For spectral data, if the irradiance measured at 300 nm is taken as the 'true' irradiance at  $\lambda_{\frac{1}{2}} = 302.5 \text{ nm}$  then the uncertainty in the median wavelength  $\lambda_{\frac{1}{2}}$  is  $\pm 0.2 \text{ nm}$  for the range of zenith angles  $30^\circ < z < 70^\circ$  at latitude =  $50^\circ$ . A change in ozone amount of  $\pm 20\%$  would give the same variation in  $\lambda_{\frac{1}{2}}$ . However taking  $\lambda_{\frac{1}{2}} = 302.5 \text{ nm}$  as the measured wavelength for all zenith angles and ozone amounts would give a maximum error in  $I_{\lambda_{\frac{1}{2}}}$  of  $\pm 12\%$  at 300 nm. As wavelength increases the factor  $(\lambda_{\frac{1}{2}} - \lambda_0)$  decreases with a corresponding reduction in the error of  $\lambda_{\frac{1}{2}}$ .

The spectral 'shift' required from median to measured wavelengths is given in Table 4.3. The figures were taken from a graph of  $\lambda_{\frac{1}{2}}$  vs  $\lambda_0$  (Fig. 4.13) as the calculations based on the UVB Handbook could only be made at 5 nm intervals.

Table 4.3 Median and measured wavelengths for LI1800.

| $\lambda_0$ (nm) | $\lambda_{\frac{1}{2}}$ (nm) | $\lambda_0$ (nm) | $\lambda_{\frac{1}{2}}$ (nm) |
|------------------|------------------------------|------------------|------------------------------|
| 300              | 302.5                        | 310              | 311.1                        |
| 301              | 303.2                        | 311              | 311.9                        |
| 302              | 304.0                        | 312              | 312.8                        |
| 303              | 304.8                        | 313              | 313.6                        |
| 304              | 305.7                        | 314              | 314.5                        |
| 305              | 306.5                        | 315              | 315.4                        |
| 306              | 307.4                        | 316              | 316.2                        |
| 307              | 308.3                        | 317              | 317.1                        |
| 308              | 309.2                        | 318              | 318.1                        |
| 309              | 310.2                        | 319              | 319.0                        |

While this spectral shift is vitally important when considering measurements at individual wavelengths, it has very little influence on broader band measurements. The principal waveband studied in this thesis is 300-316 nm. This, measured with the spectroradiometer, is effectively 302.5-316.2 nm. However the amount of radiation in the waveband 300-302.5 nm is approximately 1.5% of the total 300-316 nm band while the radiation in the band 316-316.2 nm is approximately 3%

of the UVB band (calculated from the area under the spectral curve). As the two errors act in opposite directions (- (300 → 302.5), + (316 → 316.2)) they give an overall error of only + 1.5%.

#### The total error

The typical calibration error of the LI1800 quoted by LICOR as  $\pm 10\%$  at 300 nm is a combination of all sources of error other than long term stability and temperature coefficient (personal communication). However, a more detailed error analysis was required for measurements taken in the UVB waveband and is presented here both for spectral measurements and for the broadband (300–316 nm) measurements. In both cases the sources of error can be divided into two categories: systematic and random.

##### a) Spectral measurements

Errors for spectral measurements are given assuming that the spectral drift calculated in the previous section has been applied i.e. the radiation measured at  $\lambda_0$  is assigned to the wavelength  $\lambda_{\frac{1}{2}}$ .

##### Systematic errors

Absolute error from standards  $\pm 3\%$  (Manufacturer's data)

Long term stability  $\pm 10\%$  (Appendix A)

As the long term stability of the absolute error (consistency of LICOR calibrations) appears to be within the 10% stability of the instrument (Appendix A), the total systematic error is taken to be  $\pm 10\%$ .

##### Random Errors

|               |           |                       |              |
|---------------|-----------|-----------------------|--------------|
| Cosine error  | $\pm 2\%$ | (Manufacturer's data) | $\} \pm 6\%$ |
| Azimuth error | $\pm 4\%$ | (measured)            |              |

Temperature error  $\pm 1\%$  (Manufacturer's data) over  $20^{\circ}\text{C}$  temperature range.

Residual spectral shift error due to changing ozone and zenith angle (calculated: Table 4.4)

Table 4.4 Random errors associated with LI1800 measurements.

|                              |         |         |         |       |
|------------------------------|---------|---------|---------|-------|
| $\lambda_0$ (nm)             | 300     | 305     | 310     | 315   |
| $\lambda_{\frac{1}{2}}$ (nm) | 302.5   | 306.5   | 311.2   | 315.3 |
| Error<br>(Spectral)          | ± 12.5% | ± 12%   | ± 10%   | ± 7%  |
| Total random<br>error        | ± 14%   | ± 13.5% | ± 11.5% | ± 9%  |

Combining the cosine and azimuth error, all other random errors are independent, and were therefore combined as the square root of the sum of the squares to give the total random error at different wavelengths shown in Table 4.4.

b) Broadband (300-316 nm) measurements

Systematic errors

|                               |              |
|-------------------------------|--------------|
| Absolute error from standards | ± 3%         |
| Long term stability           | ± 10%        |
| Spectral error                | ± 1.5%       |
| Total                         | ± 10% + 1.5% |

Random errors

|                   |      |   |      |
|-------------------|------|---|------|
| Cosine error      | ± 2% | } | ± 6% |
| Azimuth error     | ± 4% |   |      |
| Temperature error | ± 1% |   |      |
| Total             | ± 6% |   |      |

For both spectral and broadband measurements it is the random errors which are important when discussing the relationships between data obtained from the spectroradiometer and other meteorological variables. The random errors indicate the degree of confidence that can be placed on trends, whether daily or annual, in the UVB climatology. The systematic error acts in the same way in all measurements and affects only the magnitude of constants in any given relationship, not the form of the relation. It is therefore important when comparing these measurements with other work, whether measured or modelled, but is not of great concern in seeking a pattern of UVB irradiance.

#### Spectral sharpening

Mention has already been made of errors in spectral measurements from the LI1800 resulting from the instrument's bandpass function combined with the steep change of irradiance with wavelength in the UVB. Calculations were made to reassign the measured irradiation at a designated wavelength  $\lambda_0$  to the wavelength of greatest significance  $\lambda_i$  at each sampling interval. The alternative way of tackling this problem is to estimate the 'true' irradiance at  $\lambda_0$  given the spectrum at a range of  $\lambda_i$ 's and the bandpass function.

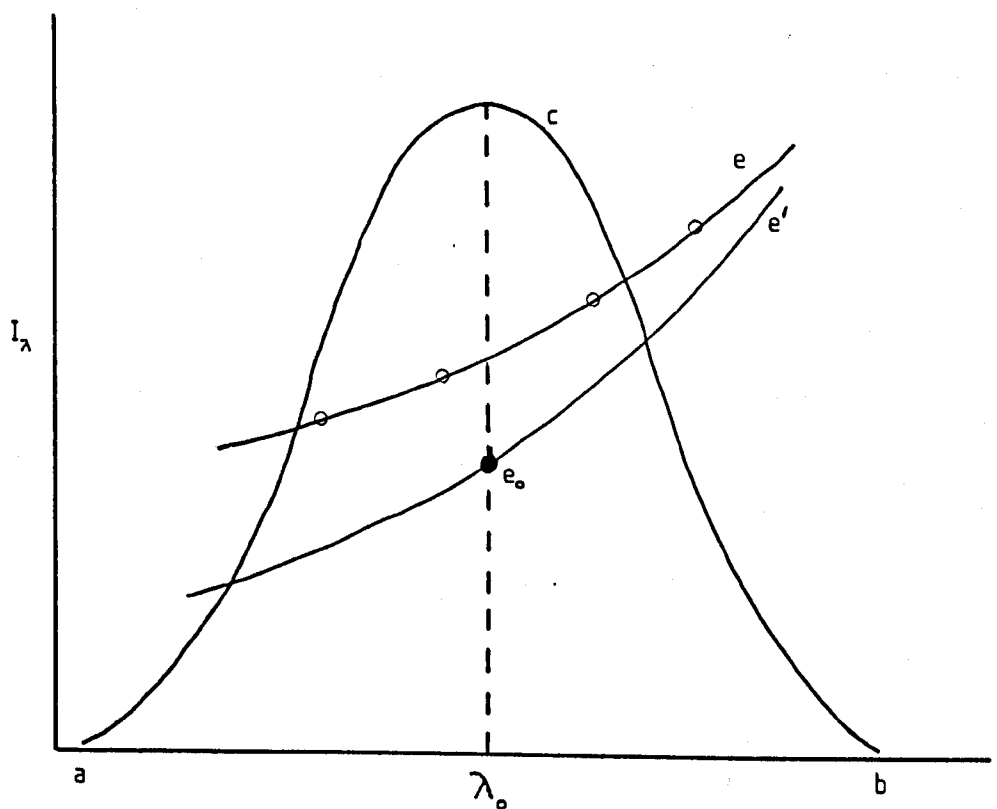
Let  $e$  be the spectrum as measured at the designated wavelengths, and  $e'$  be the 'true' spectrum at those wavelengths, with  $c$  the bandpass function of the instrument (Fig. 4.14).

$e_0$ , the measured irradiance at wavelength  $\lambda_0$  is given by

$$e_0 = \int e'c' d\lambda \approx \sum_a e'_i c'_i \quad (4.6)$$

where  $c'_i$  is the value of the bandpass function  $c_i$  at  $\lambda_i$  normalised

Fig. 4.14 The quantities involved in the calculation of 'true' irradiance at a wavelength  $\lambda_0$ .



e Measured spectrum

e' True spectrum

c Bandpass function of instrument with limits a and b.

by dividing by the total area under the bandpass  $q$ . Therefore  $c' = c/q$ . Hoover (1937) showed that  $e'_0$  can be calculated by iteration using

$$e'_0 = e_0^2 / \sum e_i c'_i = q e_0^2 / \sum e_i c_i \quad (4.7)$$

where  $e$  is used for  $e_0$  to start the iteration, and  $e'_0$  is used for each successive iteration.

Equation 4.7 enables calculation of  $e'_0$  for a range of values of  $\lambda_0$ , giving a new curve closer to the 'true' curve. If the process is repeated using the new values of  $e'_0$  in place of  $e_0$  until there is little change in the final curve upon further repetition of the calculation then a good approximation to  $e'$  has been reached.

Following this analysis for the spectroradiometer, the bandpass function  $c$  was assigned the normal distribution given in the previous section (eqn 4.4) with the limits  $a$  and  $b$  of  $\lambda_0 \pm 9$  nm, the wavelengths at which sensitivity has dropped to  $10^{-3}$  of peak value.

Successive iterations of the procedure for the waveband 300-320 nm shifted the measured curve in the expected direction, reducing the measured irradiances most at the shortest wavelengths (Fig. 4.15). However, the calculations also introduced perturbations from a smooth spectral curve, the deviations increasing at each iteration and preventing convergence of the successively calculated spectra towards a final solution.

The perturbations in Fig. 4.15 are often found in inverse problems and indicate that the true spectrum is not uniquely determined by the data. In order to solve the problem it is necessary to assume some model for the spectrum which has fewer free parameters than eqn 4.7.

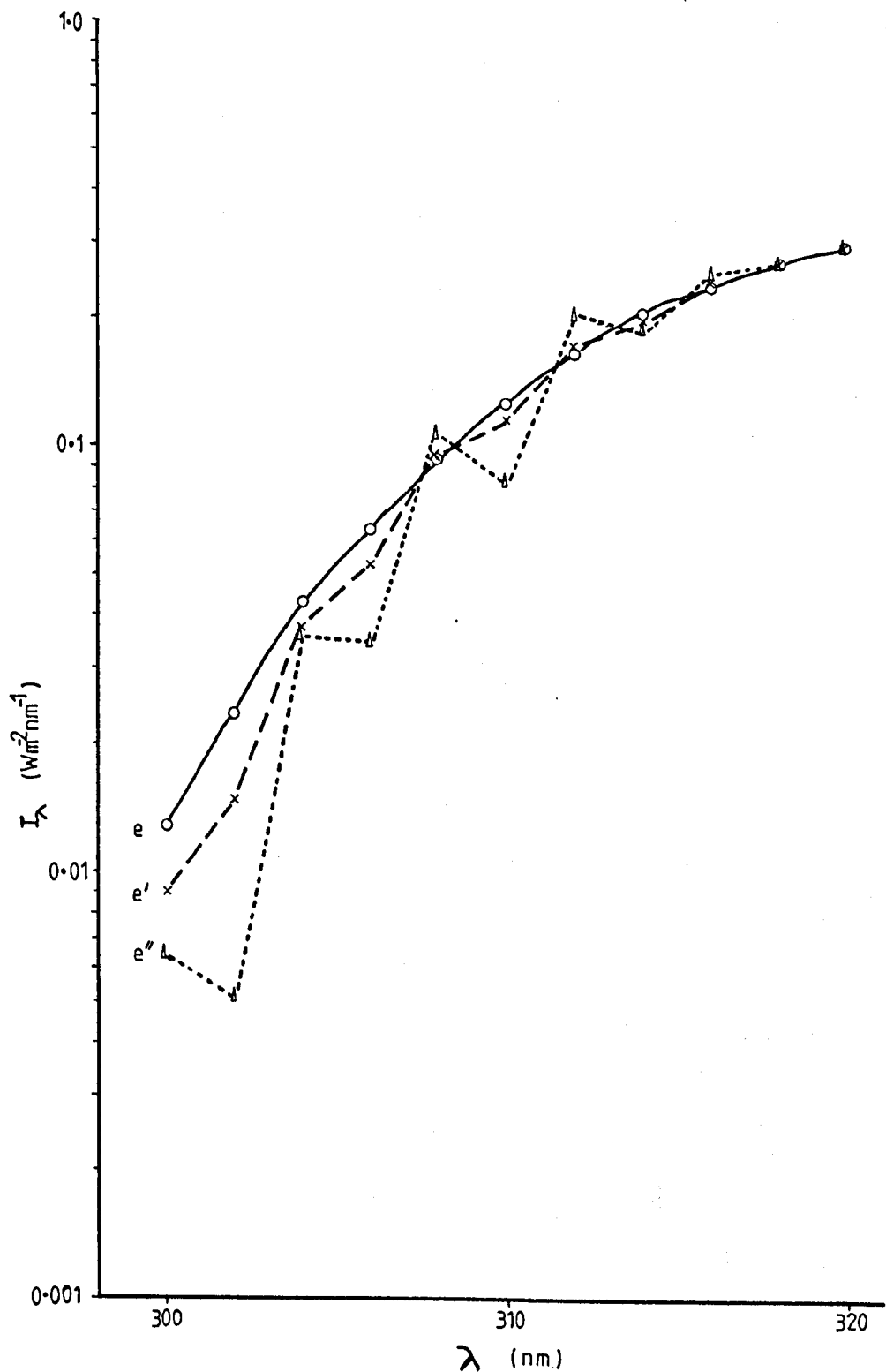


**Fig. 4.15** The measured spectrum (e) on 28 July 1983 at 1150 and the corrected spectra after 2(e') and 4(e'') iterations of Hoover's analysis.

The final solution was therefore assumed to be a smooth curve approximated by a fourth order polynomial

$$e' = \exp (a_0 + a_1\lambda + a_2\lambda^2 + a_3\lambda^3 + a_4\lambda^4) \quad (4.8)$$

The function  $c'$  takes the form (see previous section)

$$c' = A \exp (-B(\lambda - \lambda_0)^2) \quad (4.9)$$

and from eqn 4.6 values of  $e$  are approximated by  $\hat{e}_0$  where

$$\hat{e}_0 = \sum \exp (a_0 + a_1\lambda + a_2\lambda^2 + a_3\lambda^3 + a_4\lambda^4) A \exp (-B(\lambda - \lambda_0)^2) \Delta\lambda \quad (4.10)$$

An equation of this form exists for each measurement wavelength, and as there are more equations than polynomial coefficients,  $a_i$ , the problem of finding the values  $a_i$  is overdetermined.

Irradiances in this part of the spectrum vary over several orders of magnitude, and it therefore seems reasonable to assume that measurement errors are smaller at smaller readings. If the error is a constant fraction of the data value at each wavelength then a uniform variance over all data values can be obtained by log-transforming the data. The coefficients in eqn 4.10 are therefore to be determined in the least squares sense by minimising  $\sum (\ln e_i - \ln \hat{e}_0)^2$  (Menke, 1984).

An example of the corrected spectrum for 1515 on 11 July is shown in Fig. 4.16 together with the original measured spectrum and the spectrum obtained by the spectral shift.

The inversion technique gives equal weighting to errors of the log-transformed measurements at all wavelengths, a more valid assumption than applying a single absolute error to the full spectrum.

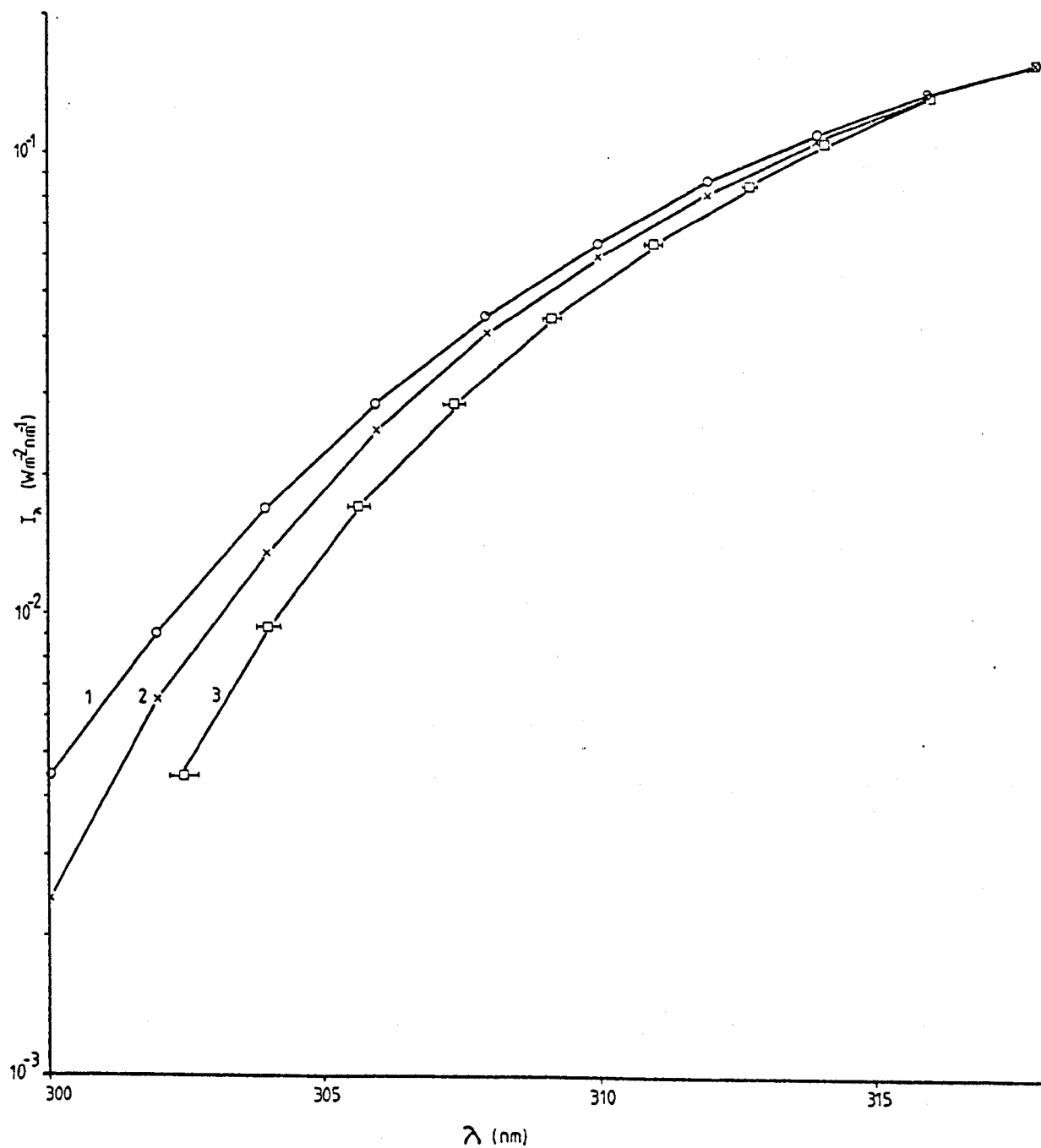


Fig. 4.16 LiI800 spectra: 1 measured, 2 with spectral correction, 3 with spectral shift.

However, relative errors of measurement at the shortest wavelengths are probably larger than those at larger wavelengths so more weight may be given to the short wavelength measurements than is justified when calculating the polynomial coefficients. At low levels of irradiance this could result in corrected spectra unrepresentative of the shape of the solar spectrum.

The spectral shift is based upon the model of a Rayleigh atmosphere, which becomes increasingly uncertain as wavelength decreases. The error bars (Fig. 4.16) show the uncertainty resulting from assuming single ozone amount and zenith angle conditions.

Each method of improving the measured spectrum is employed in different circumstances in Chapter 5, the justification for each choice being given in the appropriate place.

#### SEE 240 UVB/W Vacuum Photodiode

The SEE 240 vacuum photodiode was calibrated against the LI1800 spectroradiometer and the errors attached to measurements from this instrument are therefore related to those of the broadband LI1800 measurements.

##### Random errors

|                   |             |                     |
|-------------------|-------------|---------------------|
| Calibration error | $\pm 6\%$   | (calibration graph) |
| Temperature error | $\pm 0.5\%$ | (measured)          |
| Total             | $\pm 6\%$   |                     |

##### Systematic errors

The SEE 240 has been assumed (Appendix A) to have good long term stability, but it is nonetheless susceptible to the uncertainty in the spectroradiometer calibration to which it is directly

related. Once again this error does not affect trends in the radiation regime, only the absolute magnitude of the values which must all be transformed in the same way. The systematic error for the SEE 240 is therefore  $\pm 10\% + 1.5\%$ .

No mention has been made of the recording devices for the SEE 240, as distinct from the sensor. The calibration was performed with the SEE 240 output read from the logger and the dose timer (Appendix B) also connected so that the sensor was calibrated exactly as used. Any error due to the logger is therefore incorporated in the calibration error. The zero reading of the logger is automatically recorded every time a scan is made and subtracted from each channel reading during the analysis of the data files. Zero drift of the logger should therefore not introduce any additional error. The dose timer was more susceptible to change but any deviation in performance was immediately apparent and the fault remedied, the faulty data being discarded.

During the winter months of 1983/4 the dark current offset ( $\sim 0.3$  mV) at the dose timer disappeared when it was very cold at night. This anomaly was eventually traced to a thermostatic heater in the meteorological site hut. If the heater was on continuously to maintain the temperature in the hut to above  $10^{\circ}\text{C}$  the power used drew a very small voltage from the external equipment by way of the common mains supply. This did not appear to offset the logger or the SEE 240 itself, but only the dose timer. When the weather was warmer and the heater was switching on and off the offset was affected less, often by a negligible amount.

Periods during which the offset disappeared were marked by the absence of overnight prints caused by integration of the dark current.

Data recorded on the dose timer during such periods was discarded.

Frequent intercalibration of recording methods showed that except for sudden, rapidly apparent faults the dose timer was very stable.

When calculating the incident UVB from the prints<sup>of</sup> the dose timer the slope of the SEE 240 calibration curve applicable to each time interval was used i.e. if time period  $> 266$  s the calibration for  $V < 10$  mV was applied. A fluctuating input signal to the dose timer, for example on a day with broken cloud cover, may result in signals both greater and less than 10 mV contributing to the integrated total that produces a print. However, if most of the incident radiation was in one or other of the calibration regions, then it was deemed reasonable to apply the relevant calibration over the corresponding time period. Radiation under changing conditions that gave a time period close to 266 s indicates approximately equal contributions from both sides of the 10 mV demarcation point, but as the difference between calibrations is small close to 10 mV, the time period criterion for choosing a calibration constant was maintained. The error incurred by using the wrong section of the calibration curve is 4% at 8 mV and 12 mV. Outside the 8-12 mV signal range, the assigning of one or other calibration constant to the dose timer output is considered to produce little error, and the error in dose timer UVB estimates due to the calibration of the SEE 240 is taken to be  $\pm 5\%$ .

Changes in the print period for a 10 mV input did not drift by more than 6 s between recalibrations, giving an additional error due to the dose timer of  $6/266 \times 100 = \pm 2\%$ .

The total random error of the dose timer measurements is therefore  $(6^2 + 5^2 + 2^2)^{\frac{1}{2}} = \pm 8\%$ . The systematic error is the same as that for the SEE 240 and LI1800 broadband measurements.

#### Intercalibration of the two SEE 240 sensors

To check the relative sensitivities of the two SEE 240 instruments an IL700 radiometer, designed for use with these sensors, was borrowed and the output of the two photodiodes measured in rapid succession throughout a clear day. A linear regression of the output of sensor II on sensor I showed that sensor I was 8.18 times more sensitive than sensor II. The correlation coefficient of the data points was 0.999.

A power supply, C/V converter and printing dose timer were built for the second vacuum photodiode, to the same design as before. By using a different input to one of the frequency dividers of the integrating circuit each range on dose timer II was stepped up by a factor of 8 (Appendix B2).

The complete outfit II (sensor and recorder) was mounted next to outfit I on the meteorological site and the two were run together for a number of days. Using these data, the program to convert print period to average UVB radiation during the period was modified for sensor II so that the difference in sensitivity not accounted for by the integrator was compensated for in the analysis and plots of average radiation vs mid-time interval for the two sensors were the same, to within  $\pm 1\%$ .

In July 1984 the second vacuum photodiode was used for diffuse radiation measurements at Sutton Bonington. The instrument was

mounted on the meteorological site under a Kipp shade ring. The output was to be recorded on the logger as spot samples along with the global UVB and total solar radiation. Because of the decreased sensitivity of the second sensor it was not possible to simultaneously record the diffuse UVB on a dose timer and the logger. The offset reading caused by the dual wiring to run both recorders (Appendix B2) became very large compared with the output from the shaded, less sensitive instrument.

An intercalibration of the two sensors was made from their millivolt outputs recorded on the data logger, with the shade ring removed so that both were measuring the global UVB radiation. The calibration gave

$$UV_{II} = 0.154 (UV_I) + (2.74 \times 10^{-3})$$

with a correlation coefficient  $r = 0.997$ .

This conversion factor was applied to the calibration for SEE 240 I from mV to  $W\text{ m}^{-2}$ , and written in to the analysis program to be used on the logger output from SEE 240 II. The two sensors were run together (i.e. without a shade ring) for a further few days and the logger outputs analysed and checked. The measured radiation from the two sensors, after processing, agreed to  $\pm 0.01 W\text{ m}^{-2}$ . This error was most likely due to rounding errors within the analysis. Except near sunrise and sunset and in mid-winter this error is small ( $\sim 1\%$  for mid-morning in spring or autumn).

The random errors in diffuse radiation measurements from SEE 240 II are thus  $\pm 8\%$  (as SEE 240 I)  $\pm 1\%$  (intercalibration),

giving an error of  $\pm 9\%$  for the analysed logger records. The subsequent application of the shade ring correction introduces a further uncertainty. Taking the shade ring correction to be (geometric correction  $+ 0.01$ ) could, from the few measurements available, add an error of  $\pm 2\%$  to the corrected diffuse radiation values, which then have a total random error of  $\pm 9\%$ .

The systematic error, as with all calibrations reverting back to the LI1800, is  $\pm 10\% + 1.5\%$ ,

The climatology of solar UVB radiation at Sutton Bonington measured in the reported manner is discussed in Chapters 5 and 6. A further device for monitoring individual exposure to UVB is described in Chapter 7.

## 5. RESULTS AND DISCUSSION - THE UVB SPECTRUM

### Introduction

The solar radiation incident on the earth's surface at a given location is a function both of time, governing the pathlength of radiation through the atmosphere, and of the concentration of attenuating atmospheric constituents encountered by the radiation along that path.

Pathlength follows daily and annual cycles, and can be calculated for any position on the globe at any time. By contrast, atmospheric attenuation changes constantly but irregularly as concentrations of aerosol, ozone and water vapour fluctuate. Furthermore these changes are not uniform across the full solar spectrum: ozone is the dominant absorber of ultraviolet radiation but is irrelevant to the infra-red spectrum where water vapour plays a major role. Additional complexity is introduced by the appearance of cloud in its many shapes and forms. For analysis, the system is usually simplified as far as possible. The modeller begins with a Rayleigh atmosphere; the measurer, lacking this ideal situation, starts with the radiation regime on a cloudless day.

Spectral measurements made on clear days are examined first (Chapter 5), before considering the full UVB band (300-316 nm) under scrutiny and its relation to other solar wavebands (Chapter 6). The range of meteorological conditions at Sutton Bonington is then introduced in a study of the UVB climatology in all weathers and its association with more routine and accessible radiation measurements.

The partitioning of global radiation into its direct and diffuse components is important when considering the illumination of variously oriented surfaces, and diffuse UVB measurements are presented together with all-weather values for solar UVB incident on vertical surfaces.

Exposure of individuals within the UVB environment at Sutton Bonington is described in Chapter 7.

#### The UVB Spectrum Throughout the Year

##### Spectral correction technique

The data presented in this section was measured with the LI1800 spectroradiometer under clear sky conditions and has been corrected by means of the spectral shift (Chapter 4). This correction was chosen in order to utilise as much of the limited clear sky data as possible. At large zenith angles radiation measurements at the shortest wavelengths are unreliable and can result in misinterpretation of the whole spectrum as the mathematical procedure of spectral sharpening attempts to fit a solution to all data points. By applying the spectral shift, measurements at longer wavelengths may still be used while excluding doubtful values below the NEI of the LI1800. Spectra measured at large zenith angles are needed if a complete picture of daily and annual trends in the UVB spectrum is to be given. As the changing form of irradiance rather than its absolute value is important in this respect the spectral shift was considered most appropriate of the two correction techniques.

##### Clear-day climatology

The shape of the UVB spectrum changes considerably throughout the year as the interplay between zenith angle and ozone cycles has a wavelength-dependent influence in this steeply declining region of solar spectral irradiance.

Figure 5.1 shows two spectra measured at noon on clear days in June and December. Extrapolation of the December curve below the noise equivalent irradiance of the LI1800 shows that the incident radiation at 302.5 nm increases by two orders of magnitude from December to June, while at 316.2 nm the corresponding increase is only one order of magnitude. This in turn means that in June the incident radiation at 316.2 nm is ten times that at 302.5 nm, but in December irradiance at the two wavelengths differs by a factor of 100. The annual change in radiation levels at 3 wavelengths is shown in Fig. 5.2 for clear days at noon, with values taken from spectroradiometer measurements made during 1983 and 1984.

The asymmetry about the summer solstice is apparent at all three wavelengths (302.5 nm, 309.2 nm and 316.2 nm) and demonstrates the effect of the phase difference between the annual cycles of ozone and solar declination. The points in Fig. 5.2 have been plotted with no regard to the ozone amount on individual days, which may have been anomalous for the time of year. This possible anomaly and day-to-day changes of other atmospheric variables accounts for some of the scatter of the data, but the general annual trend remains consistent at each wavelength.

The noonday sun becomes progressively higher in the sky from January to June and radiation at the earth's surface is expected to increase as the geometrical pathlength through the atmosphere decreases. However, from January to April/May ozone amount increases (Chapter 6, Fig. 6.9, ozone data supplied by the Meteorological Office, Bracknell) offsetting the change in geometry to a certain extent. From late spring the amount of ozone decreases and for a couple of months

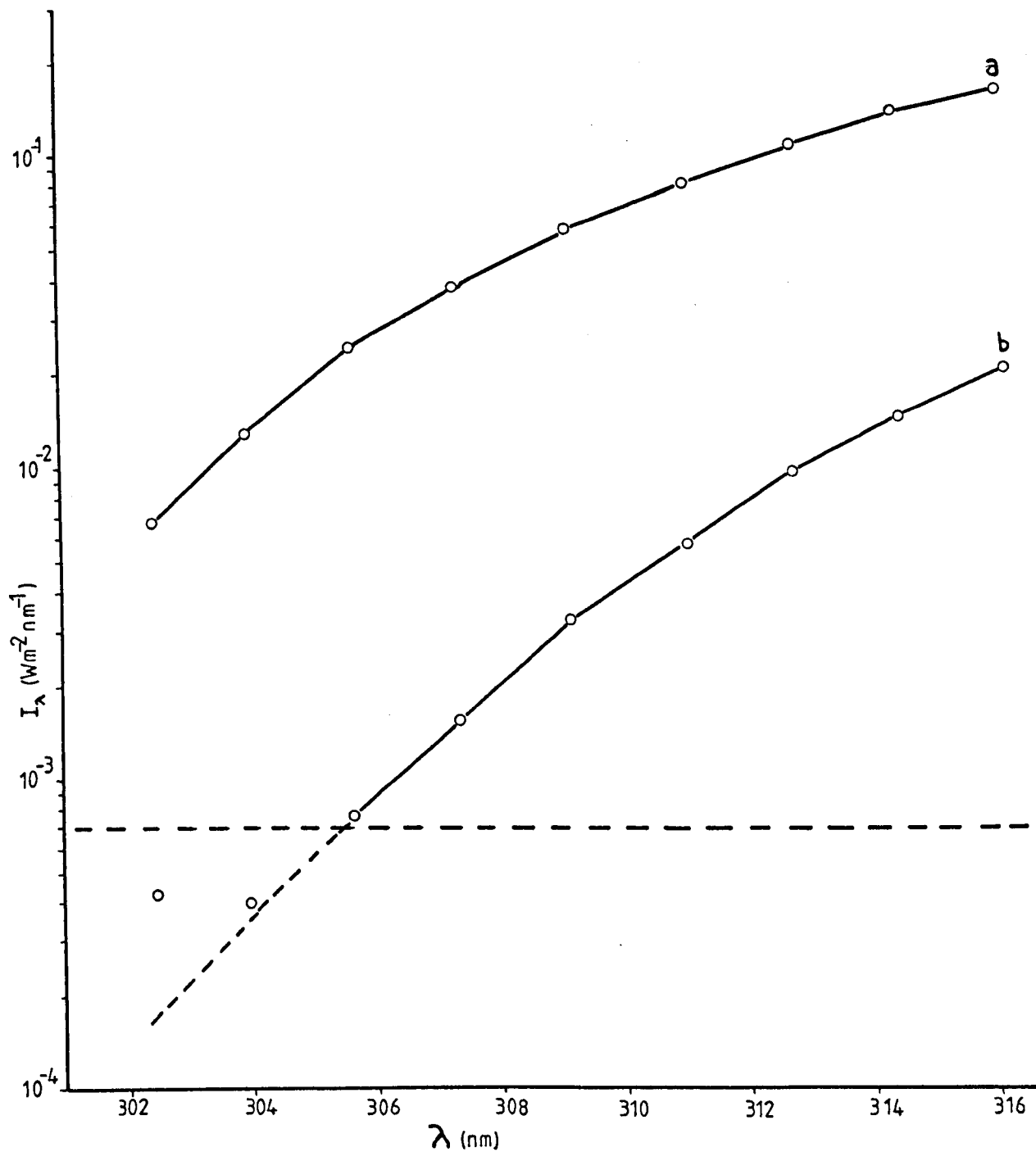
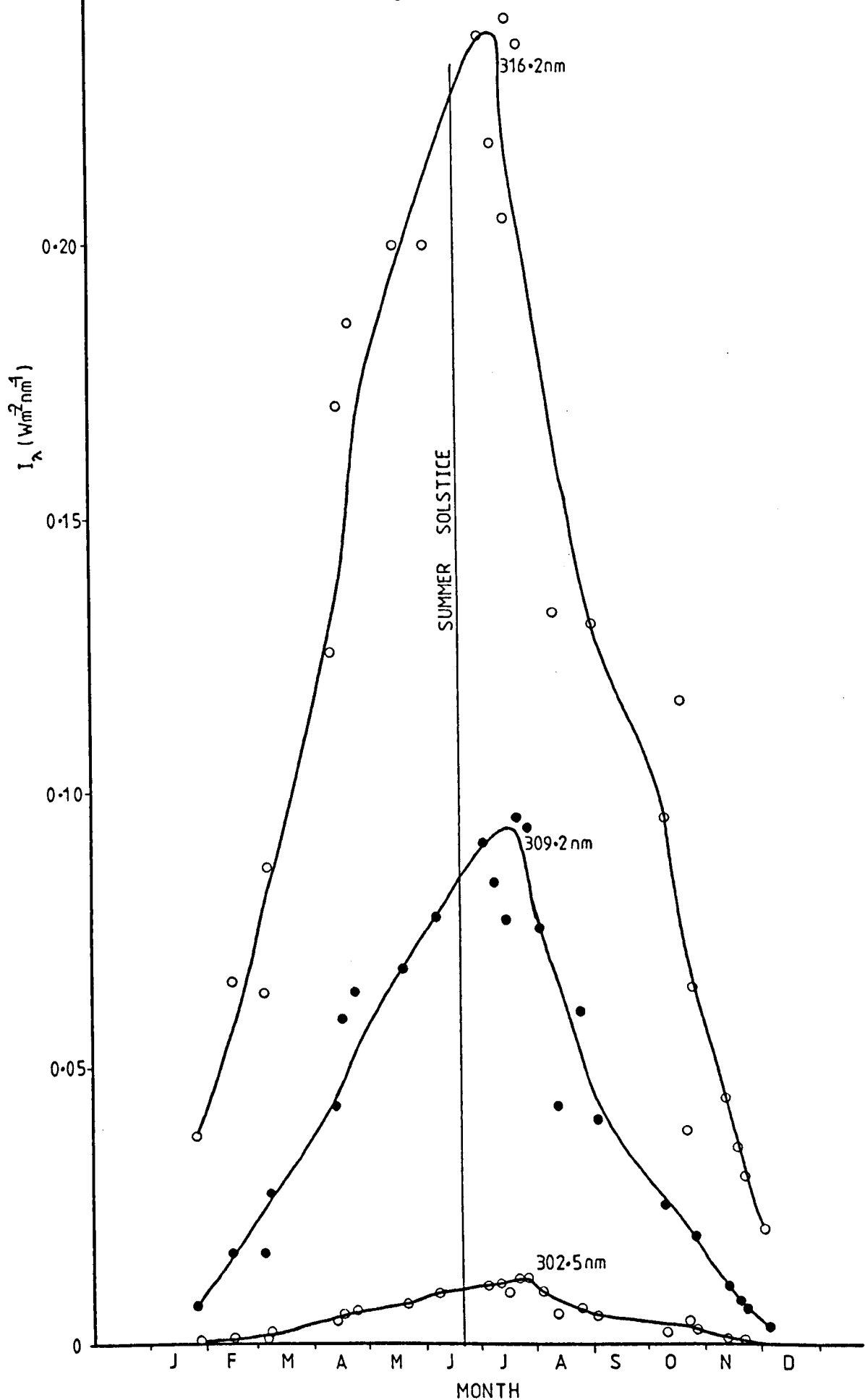


Fig. 5.1 The UVB spectrum at noon on clear days in  
 (a) June and (b) December.

Fig. 5.2 Spectral irradiance values at noon on clear days  
for 3 wavelengths.



acts in the same direction as the shortening of the geometrical pathlength, whose rate of change decreases as the maximum declination is approached. The change from opposition to reinforcement of the two cycles during this first half of the year serves to transform the irradiance curve from a cosine curve to something approaching a straight line.

Once the summer solstice has been passed, increasing mean zenith angle decreases the incident radiation, but this trend is offset in the UVB by the decreasing amount of ozone. Close to the extremes of the solar cycle when rate of change of zenith angle is small the reduction in absorbing ozone becomes the most prominent of the two effects and this dominating influence is clearly seen as a shift of the time of maximum UVB irradiance from June to July. This shift is apparent at all three wavelengths, with the suggestion that at 302.5 nm, where the ozone absorption coefficient is greatest, the peak radiation level is delayed further into July than at longer wavelengths. This July radiation peak was also observed by Bener (1963) at Davos in Switzerland.

For the next three months decreasing ozone amount and increasing pathlength again work in opposition, the magnitude of the ozone changes, which can vary from year to year, determining the precise nature of the UVB trend during these months. In November, ozone amount reaches a minimum and thereafter the ozone and zenith angle cycles work in tandem to decrease UVB until the winter solstice. No data are available for the period from early December to late January and it is not possible to say whether the UVB minimum is displaced from the date

of the winter solstice in the same way that the maximum is extended to July. A shift in the annual minimum intensity of global UVB radiation was observed by Bener (1963) for wavelengths shorter than 310 nm while at longer wavelengths the minimum was found in December.

The irregular annual radiation intensity curves illustrate the influence of ozone on irradiances at UVB wavelengths. To investigate the effect of changing zenith angle alone, the diurnal changes of irradiance were considered, assuming the amount of ozone to be constant throughout the day.

Figure 5.3a-c illustrate the measured changes in radiation intensity at three wavelengths for three clear days during the year. The curves show that as wavelength becomes shorter the effect of zenith angle on irradiance increases. This is clearly seen in Fig. 5.3b and c for days in April and July as irradiance values decline more steeply either side of noon at 302.5 nm than at the longer wavelengths. For the February day illustrated (Fig. 5.3a) the changing wavelength dependence on zenith angle is less obvious. However, the irradiance levels at 302.5 nm were below the noise equivalent irradiance of the spectroradiometer for much of the day and are therefore unreliable.

The spectral ozone absorption coefficient is largely responsible for the differences in zenith angle dependence across the UVB waveband. Zenith angle determines the pathlength of radiation through the atmosphere, and hence the pathlength through the ozone layer. At the shorter wavelengths where the ozone absorption coefficient is greatest ( $k_{302.5} \approx 6 k_{316}$ ) Smithsonian Institute (1951) the response

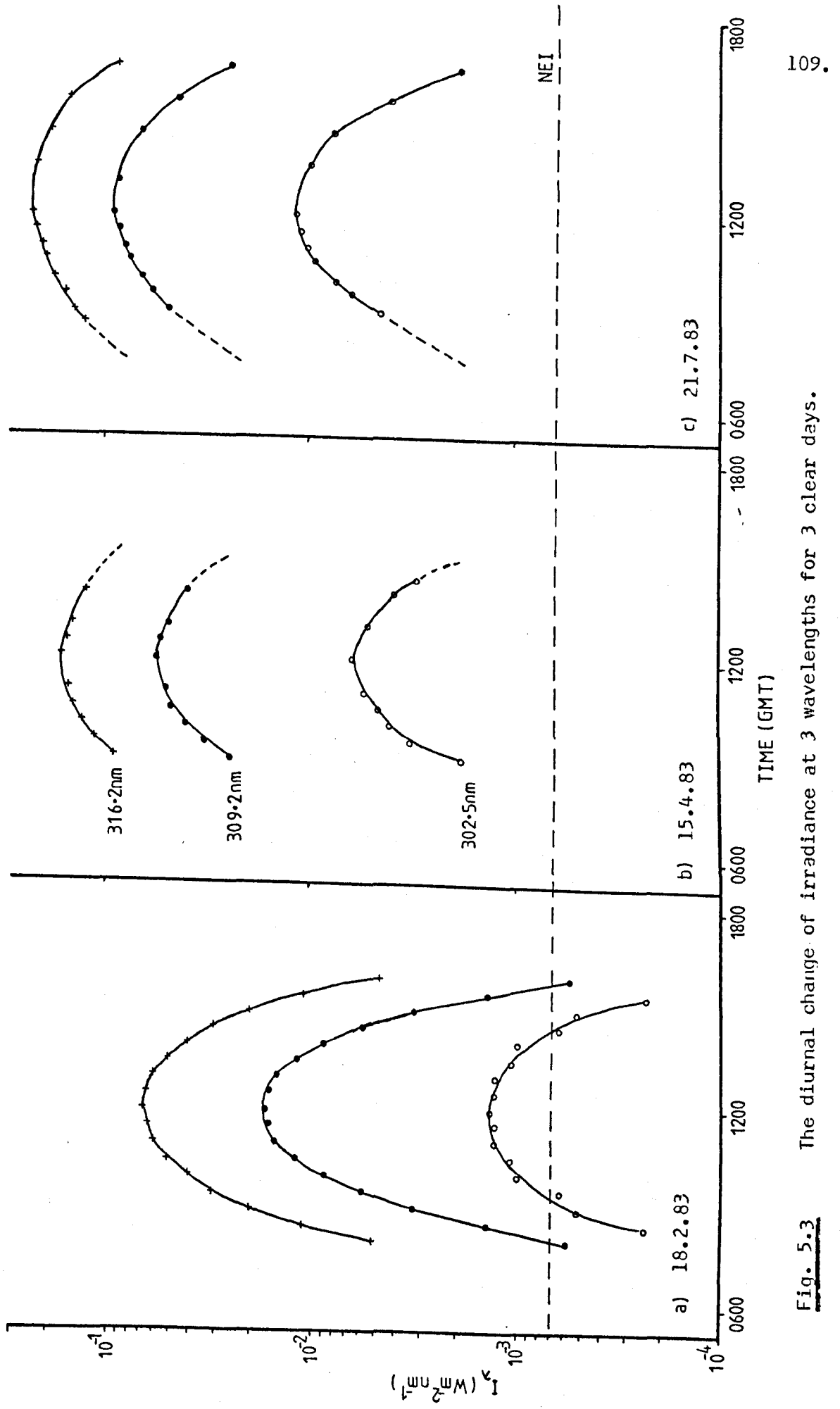


**Fig. 5.3** The diurnal change of irradiance at 3 wavelengths for 3 clear days.

of radiation levels to changing pathlength is therefore most pronounced. Added to this, as Rayleigh scattering in the atmosphere below the ozone layer is proportional to  $\lambda^{-4}$ , any lengthening of the radiation path will attenuate the shortest wavelengths most, although for the UVB waveband absorption by ozone is the dominating factor.

Having described the major influences on the daily and annual clear-day spectral irradiances observed at Sutton Bonington, the dependence of UVB irradiance on ozone amount and atmospheric pathlength are now examined in more detail.

#### Spectral Attenuation in the Atmosphere

When considering the atmospheric attenuation of UVB radiation the atmosphere may be treated as three layers: an upper stratospheric layer where attenuation is by ozone absorption only; a middle layer in the troposphere where Rayleigh scattering takes place; and a layer closer to the ground within which attenuation by aerosol occurs. For a horizontal plane at the earth's surface the direct beam irradiance  $B_\lambda$  is given by

$$B_\lambda = I_{\lambda_0} \exp (-k_\lambda [O_3]\mu - bm - cm) \quad (5.1)$$

where  $I_{\lambda_0}$  is the extraterrestrial radiation at wavelength  $\lambda$  on a plane parallel to the earth's surface,  $k_\lambda$  is the ozone absorption coefficient at wavelength  $\lambda$ ,  $[O_3]$  is the equivalent depth of the ozone layer,  $b$  is the Rayleigh scattering coefficient,  $c$  is an attenuation coefficient for aerosol and other absorbers,  $m$  is air mass number ( $\approx \sec z$  where  $z$  is solar zenith angle) and  $\mu$  is ozone pathlength ( $\mu \approx m$  for small  $z$ ).

Neglecting multiple scattering, the diffuse irradiance  $D_\lambda$  on a horizontal surface at the earth may be expressed as a proportion of the radiation scattered out of the solar beam in each layer, and calculated from

$$D_\lambda = I_{\lambda_0} \exp(-k[O_3]\mu) \left\{ f_r (1 - \exp(-bm)) + f_a \exp(-bm) (1 - \exp(-cm)) \right\} \quad (5.2)$$

where  $f_r$  is the fraction of radiation attenuated by Rayleigh scattering that is returned to the surface and  $f_a$  is the analogous fraction for attenuation by aerosol (Brinkman and MacGregor, 1983).

The global irradiance  $I_\lambda$  is then given by

$$\begin{aligned} I_\lambda &= B_\lambda + D_\lambda \\ &= I_{\lambda_0} \exp(-k[O_3]\mu - bm - cm) g(m) \end{aligned} \quad (5.3)$$

$$\text{where } g(m) = 1 + f_r \exp(bm + cm) + (f_r - f_a) \exp(cm) - f_a \quad (5.4)$$

The function  $g(m)$  is the ratio of global to direct beam irradiance at wavelength  $\lambda$ , and may be expressed in terms of diffuse radiation as

$$g(m) = (1 - D_\lambda/I_\lambda)^{-1} \quad (5.5)$$

For measurements made on clear days, the Rayleigh and aerosol attenuation coefficients were assumed to be constant, and for solar UVB radiation  $I_\lambda = I_\lambda([O_3], m)$ .

Plotting  $\ln I_\lambda$  against  $\mu (\approx m)$  for different clear days and at different wavelengths gave a series of straight lines (Fig. 5.4).

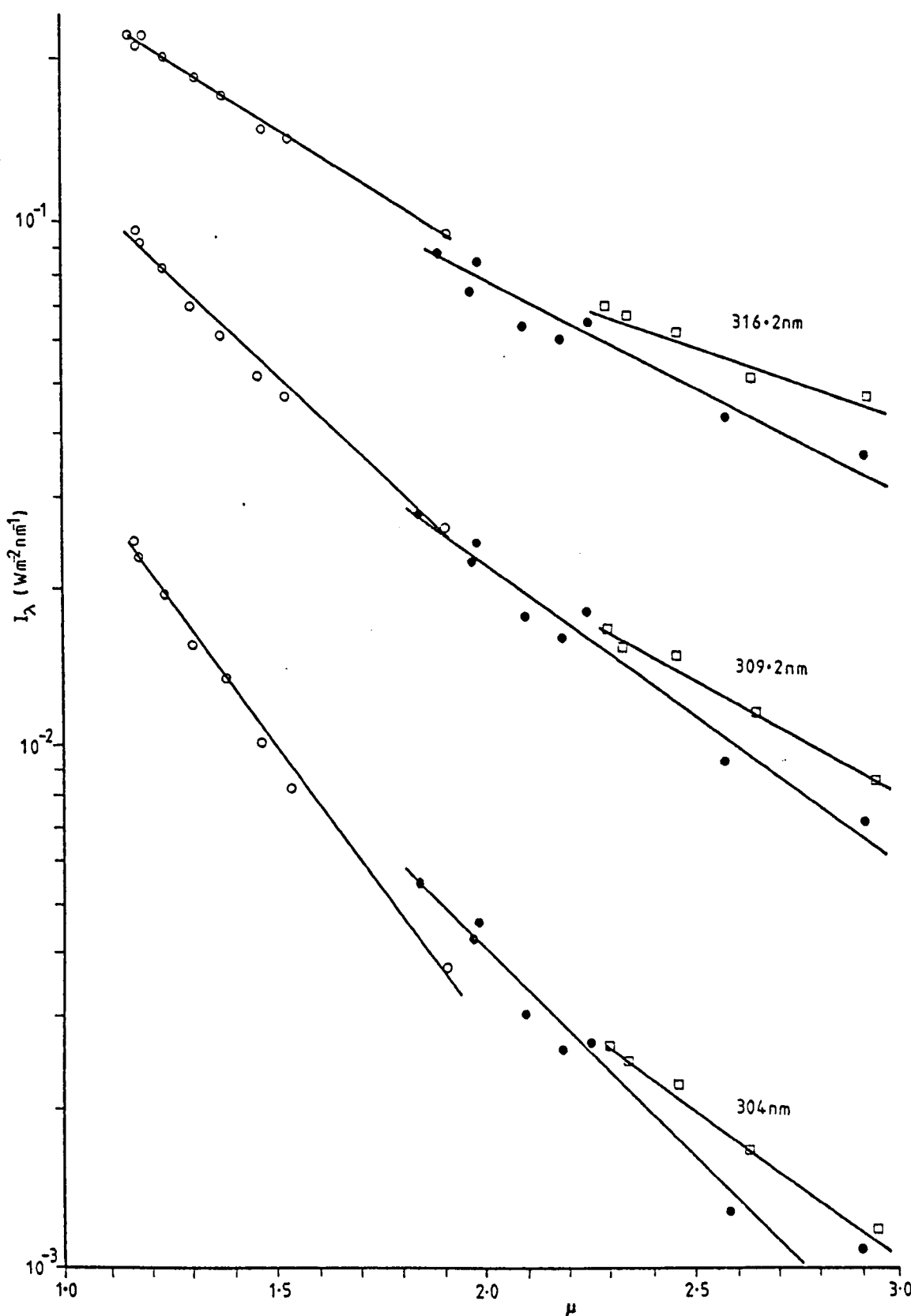


Fig. 5.4  $\ln I_\lambda$  vs  $\mu$  at 3 wavelengths for 3 clear days.

○ 21 July 1983 [ $O_3$ ] = 307 matm cm, • 8 March 1983

[ $O_3$ ] = 271 matm cm, □ 18 February 1983 [ $O_3$ ] =

315 matm cm.

By differentiating eqn 5.3, the slopes of these lines should be

$$\partial \ln I_\lambda / \partial \mu = -k[O_3] - b - c + \partial \ln g / \partial \mu \quad (5.6)$$

In preliminary analysis (Webb and Steven, 1984)  $g$  appeared (from limited data) to be a weak function of  $m$  and  $\partial \ln g / \partial \mu$  was assumed constant.

Diffuse radiation terms should not be associated with ozone absorption which occurs above the main scattering layers of the atmosphere. Under such conditions a plot of  $\partial \ln I_\lambda / \partial \mu$  against ozone concentration  $[O_3]$  should give a line of gradient  $-k_\lambda$ . Daily ozone measurements supplied by the Meteorological Office at Bracknell were used to plot  $-\partial \ln I_\lambda / \partial \mu$  against ozone amount  $[O_3]$  for 3 wavelengths (Fig. 5.5).

The gradients of the lines in Fig. 5.5 are compared in Table 5.1 with the ozone absorption coefficient  $k_\lambda$  taken from Smithsonian Meteorological Tables.

Table 5.1  $k_\lambda$  and the corresponding values of  $\partial^2 \ln I_\lambda / \partial \mu \partial [O_3]$

| Wavelength (nm) | $k_\lambda$ (atm cm <sup>-1</sup> ) | Gradient (atm cm <sup>-1</sup> ) |
|-----------------|-------------------------------------|----------------------------------|
| 304.0           | 4.93                                | 10.0 $\pm$ 4                     |
| 309.2           | 2.70                                | 12.2 $\pm$ 3.4                   |
| 316.2           | 0.995                               | 9.1 $\pm$ 2.1                    |

The gradients ( $G \pm$  standard error) are for wavelengths designated by the spectral shift applied to the measurements made with the spectroradiometer.

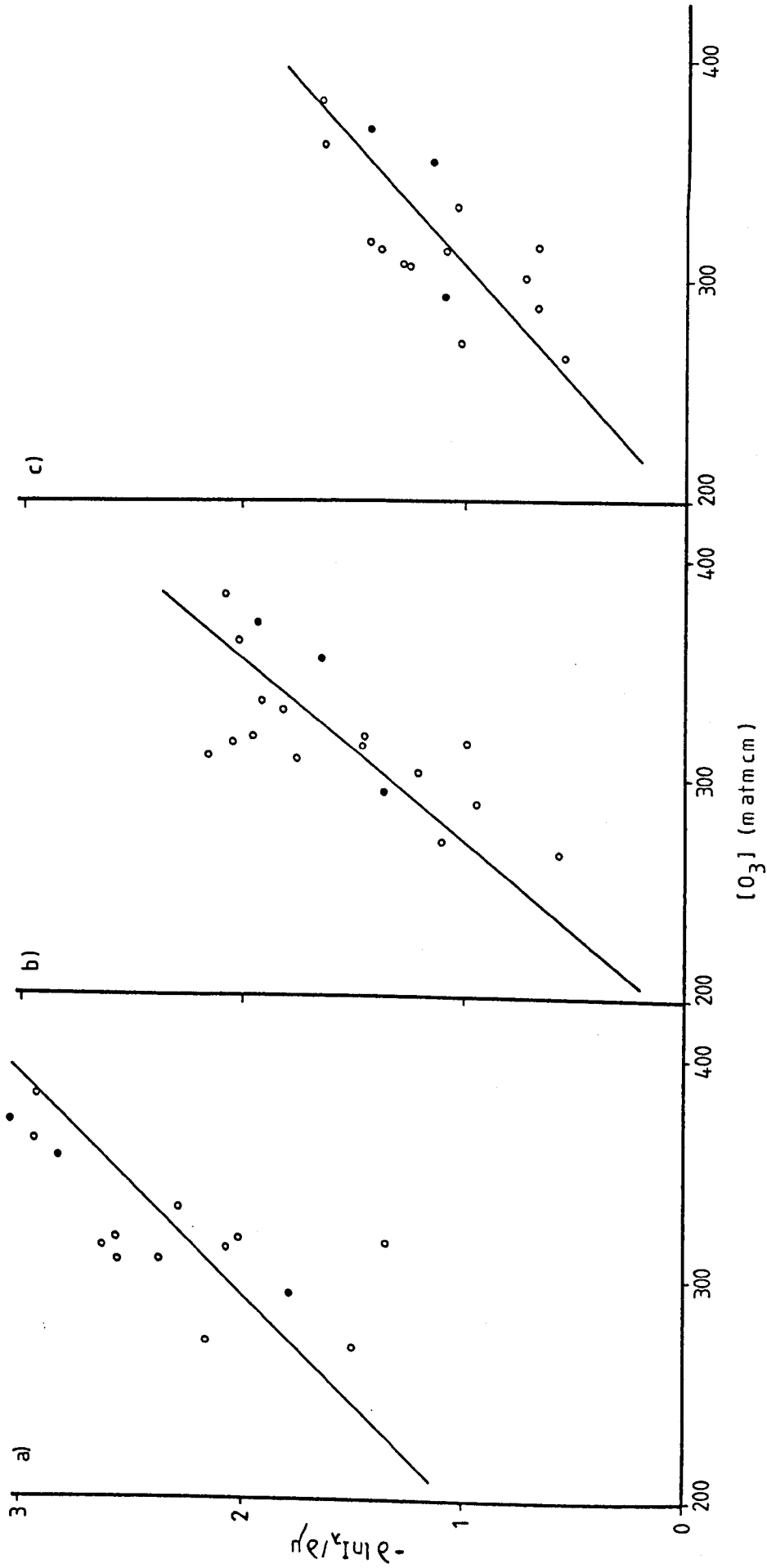


Fig. 5.5 -  $-d \ln I_\lambda / d\lambda$  vs ozone concentration  $[O_3]$  at 3 wavelengths: a) 304 nm, b) 309.2 nm, c) 316.2 nm.

- Benner's data at a) 305 nm, b) 310 nm, c) 315 nm.

Measurement and theory clearly do not agree. At 304 nm the accepted ozone absorption coefficient and  $G$  differ by a factor of two. Considering the assumptions made of clear-day tropospheric uniformity, and the uncertainty in the final gradient, this margin of error is acceptable. At longer wavelengths the discrepancy between  $k_\lambda$  and  $G$  increases to a factor of 6 at 309 nm and a factor of 10 at 316 nm. Furthermore the expected decrease in  $G$  towards longer wavelengths is not apparent.

To determine whether theory or practice was at fault, recourse to Bener's measurements (1960) was made.

Bener followed a similar analysis for his clear-day data, but in reverse order, differentiating  $\ln I_\lambda$  with respect to ozone at various zenith angles, and then plotting  $\partial \ln I_\lambda / \partial [O_3]$  against  $k_\lambda$  at each zenith angle. A plausible dependence between gradient and  $k$  was found for wavelengths less than  $\lambda^*$  (where  $315 \text{ nm} < \lambda^* < 330 \text{ nm}$ ) for zenith angles of between  $40$  and  $75^\circ$ .

Bener's work made use of far more measurements than were made for Sutton Bonington and his form of analysis could not be attempted for comparison. However some of Bener's figures were taken and treated in the same way as those presented here. The data from Bener (1960) are in the form of mean values of spectral intensity,  $I_\lambda$ , at a stated zenith angle and ozone amount (average for days of measurement) and albedo. At Davos, albedo changes considerably from winter (snow) to summer (vegetation). Three ozone amounts occurred at more than one zenith angle, enabling  $\partial \ln I_\lambda / \partial \mu$  to be calculated for  $\lambda = 305, 310, 315 \text{ nm}$ . At two of these ozone amounts all measurements had the same

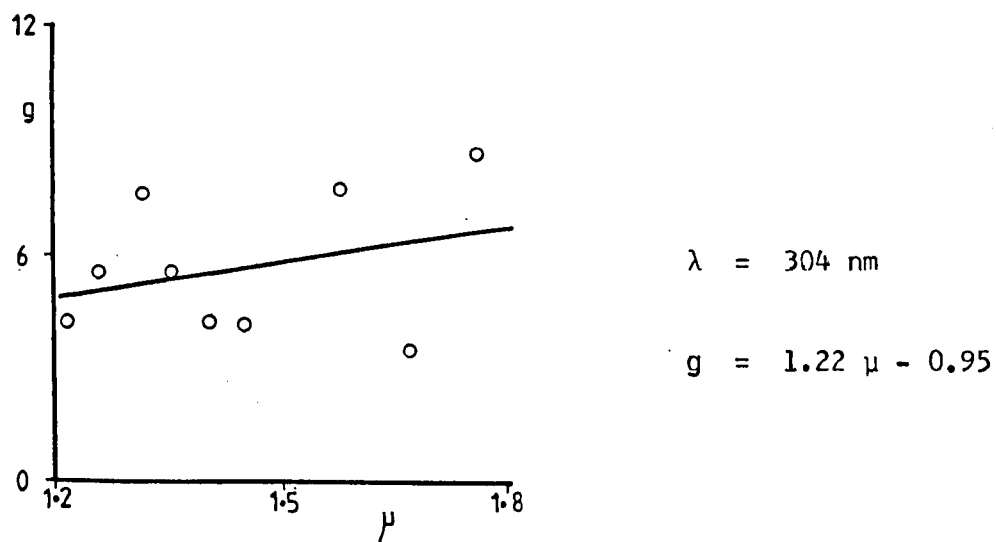
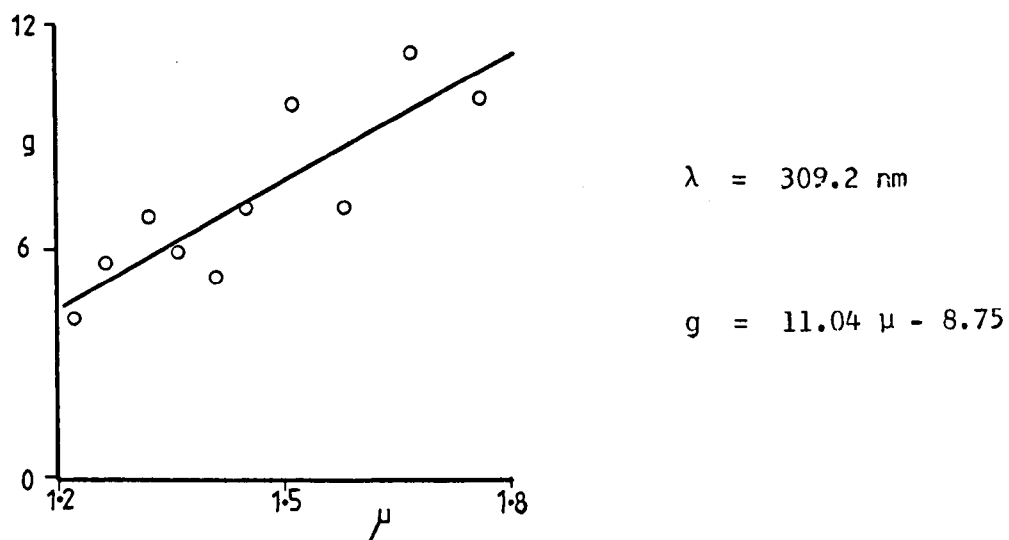
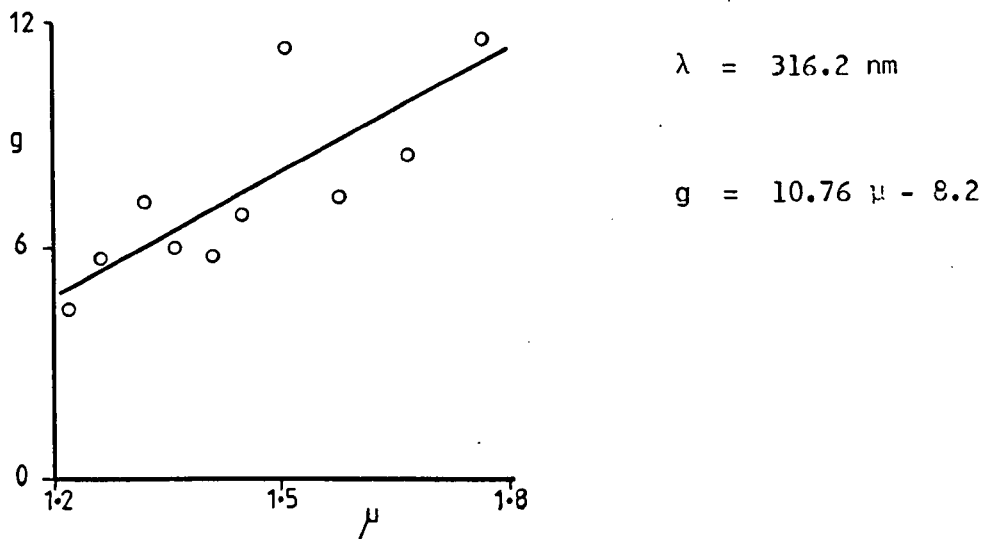
albedo. For the third amount only two measurements were available, one in summer and one in winter, resulting in a gradient smaller than might otherwise be expected.  $\partial \ln I_\lambda / \partial \mu$  from Bener's data are also plotted in Fig. 5.5 against their respective amounts of ozone and matched to the closest Sutton Bonington wavelength: 305 to 304 nm, 310 to 309.2 nm, 315 to 316.2 nm.

Despite the approximations of the comparison, the Davos data analysed according to eqns 5.3 to 5.6 appear consistent with the measurements made at Sutton Bonington, suggesting the need for a re-appraisal of the theoretical background.

The grossest assumption made in deriving the experimental values of  $k_\lambda$  was that  $\partial \ln g / \partial \mu$  remained constant from day to day. Diffuse spectral scans taken immediately after the global measurements were available for nine clear days in 1983 and 1984 and in sufficient number to allow the change of  $g$  with  $\mu$  to be investigated. The best relationship between the two quantities proved to be one of direct proportionality at 309.2 and 316.2 nm. At 304 nm there was no significant correlation between  $g$  and  $\mu$ . The plots of  $g$  against  $\mu$  are shown in Fig. 5.6 for three wavelengths on 11 July 1983. The slopes ( $\pm$  standard errors) are given in Table 5.2.

Table 5.2      Slopes of  $g$  vs  $\mu$  for  
                  3 wavelengths

| Wavelength (nm) | Slope          |
|-----------------|----------------|
| 304             | $1.2 \pm 1.8$  |
| 309.2           | $11.9 \pm 2.3$ |
| 316.2           | $10.7 \pm 2.9$ |

Fig. 5.6 g vs  $\mu$  at 3 wavelengths for 11 July 1983

$\partial g/\partial \mu$  varies considerably over the nine days for which it could be calculated (Table 5.3) and assuming it to be constant must have created error in the early analysis.

Attempts to fit the measured data to theory by including  $g$  in the analysis failed to significantly improve the experimentally derived values of  $k_\lambda$ . More work is needed in this area to thoroughly investigate the discrepancy between theory, laboratory and field measurements of the ozone absorption coefficient.

#### Comparison with UVB Model

##### The model

Spectral data obtained with the LI1800 spectroradiometer were compared with the calculations of UV-B irradiances given by Gerstl, Zardecki and Wiser in their UV-B Handbook Vol I (1983). This Handbook gives the expected fluxes of UV-B radiation for conditions of a clear standard atmosphere, including the effects of all orders of Rayleigh and Mie scattering plus molecular absorption. Values of incident radiation on a horizontal surface are given for seven wavelengths 290 (5) 320 nm at 8 northern latitudes 0 (10) 70° for 39 solar zenith angles 0 (2) 76° and 5 assumed ozone depletions 0 (5) 20% from measured summer and winter ozone profiles.

Spectral measurements made at Sutton Bonington were matched to values in the handbook using the following criteria:

- i) All measurements were made on 'clear' days.
- ii) Sutton Bonington is at latitude 52° 50' N and was therefore compared with calculations for 50° N.

Table 5.3  $\partial \ln I_\lambda / \partial \mu$  for clear days, and  $\partial g / \partial \mu$  where available.

| Date            | $[O_3]$ (atm cm) | $-\partial \ln I_{304} / \partial \mu$ | $-\partial \ln I_{309.2} / \partial \mu$ | $-\partial \ln I_{316.2} / \partial \mu$ | $(\partial g / \partial \mu)_{309.2}$  | $(\partial g / \partial \mu)_{316.2}$ |
|-----------------|------------------|--|--|--|--|---------------------------------------|
| 18. 2.83        | 0.315            | 1.35                                   | 0.99                                     | 0.67                                     |  |                                       |
| 8. 3.83         | 0.271            | 2.16                                   | 1.10                                     | 1.02                                     |  |                                       |
| 15. 4.83        | 0.333            | 2.32                                   | 1.92                                     | 1.31                                     |  |                                       |
| 11. 7.83        | 0.317            | 2.57                                   | 1.96                                     | 1.43                                     | 11.04                                  | 10.8                                  |
| 12. 7.83        | 0.314            | 2.63                                   | 2.05                                     | 1.38                                     | 13.1                                   | 10.5                                  |
| 15. 7.83        | 0.308            | 2.37                                   | 2.17                                     | 1.28                                     | 9.5                                    | 7.2                                   |
| 21. 7.83        | 0.307            | 2.56                                   | 1.76                                     | 1.25                                     | 4.3                                    | 3.8                                   |
| 26. 8.83        | 0.313            | 2.07                                   | 1.43                                     | 1.09                                     | 6.2                                    | 4.7                                   |
| 24.10.83        | 0.288            | 1.50                                   | 0.93                                     | 0.67                                     | 5.4                                    | 5.1                                   |
| 14.11.83        | 0.265            | -                                      | 0.57                                     | 0.55                                     | 5.4                                    | 9.4                                   |
| 6.12.83         | 0.301            | -                                      | 1.11                                     | 0.73                                     |  |                                       |
| 25. 4.84        | 0.361            | 2.94                                   | 2.03                                     | 1.64                                     | 6.2                                    | 5.5                                   |
| 1. 8.84         | 0.381            | 2.93                                   | 2.08                                     | 1.65                                     | 3.7                                    | 3.9                                   |
| 2. 9.84         | 0.317            | 2.10                                   | 1.46                                     | 1.14                                     |  |                                       |
|                 |                  |  | $-\partial \ln I_{305} / \partial \mu$   | $-\partial \ln I_{310} / \partial \mu$   | $-\partial \ln I_{315} / \partial \mu$ |                                       |
| Bener's<br>Data |                  |  |  |  |  |                                       |
|                 | 0.293            | 1.78                                   | 1.37                                     | 1.09                                     |  |                                       |
|                 | 0.354            | 2.83                                   | 1.65                                     | 1.15                                     |  |                                       |
|                 | 0.369            | 3.05                                   | 1.95                                     | 1.43                                     |  |                                       |

- iii) Zenith angles at the time of measurement were to within  $\pm 0.5^\circ$  of the tabulated zenith angles.
- iv) Ozone amount (as measured at Bracknell) was matched to one of the ozone scenarios to  $\pm 2 \text{ matm cm}$  ( $\pm < 0.75\%$ ).
- v) Comparisons were made at wavelengths of 300, 310 and 320 nm.

#### Correction of measurements

The measured spectra were corrected for the bandpass function of the LI1800 using the spectral sharpening techniques described in Chapter 4. For comparison purposes this method of correction was preferred to that of a wavelength shift (Chapter 4) because it is independent of any model used to estimate the wavelength shift. It also retains the measurement at  $\lambda = 300 \text{ nm}$  which is lost in applying the change of wavelength correction but is most in need of validation.

#### Results

Measured spectra were matched to the UVB model at three wavelengths: at 300 nm and 310 nm comparison was made with the corrected LI1800 scans, at 320 nm comparison was with the original uncorrected irradiance measurement. 37 clear day spectra met the criteria for zenith angle and ozone amount stated earlier for model comparison. The irradiance values taken from tables in the UVB Handbook were matched to their respective measured spectra and the model irradiances plotted against the measured irradiances for each of the three wavelengths, as shown in Fig. 5.7a-c. The slopes and intercepts of each line, with their standard errors, are given in Table 5.4.

All intercepts lie within 2 standard errors of zero, and are not significantly different from zero at the  $p = 0.05$  level.

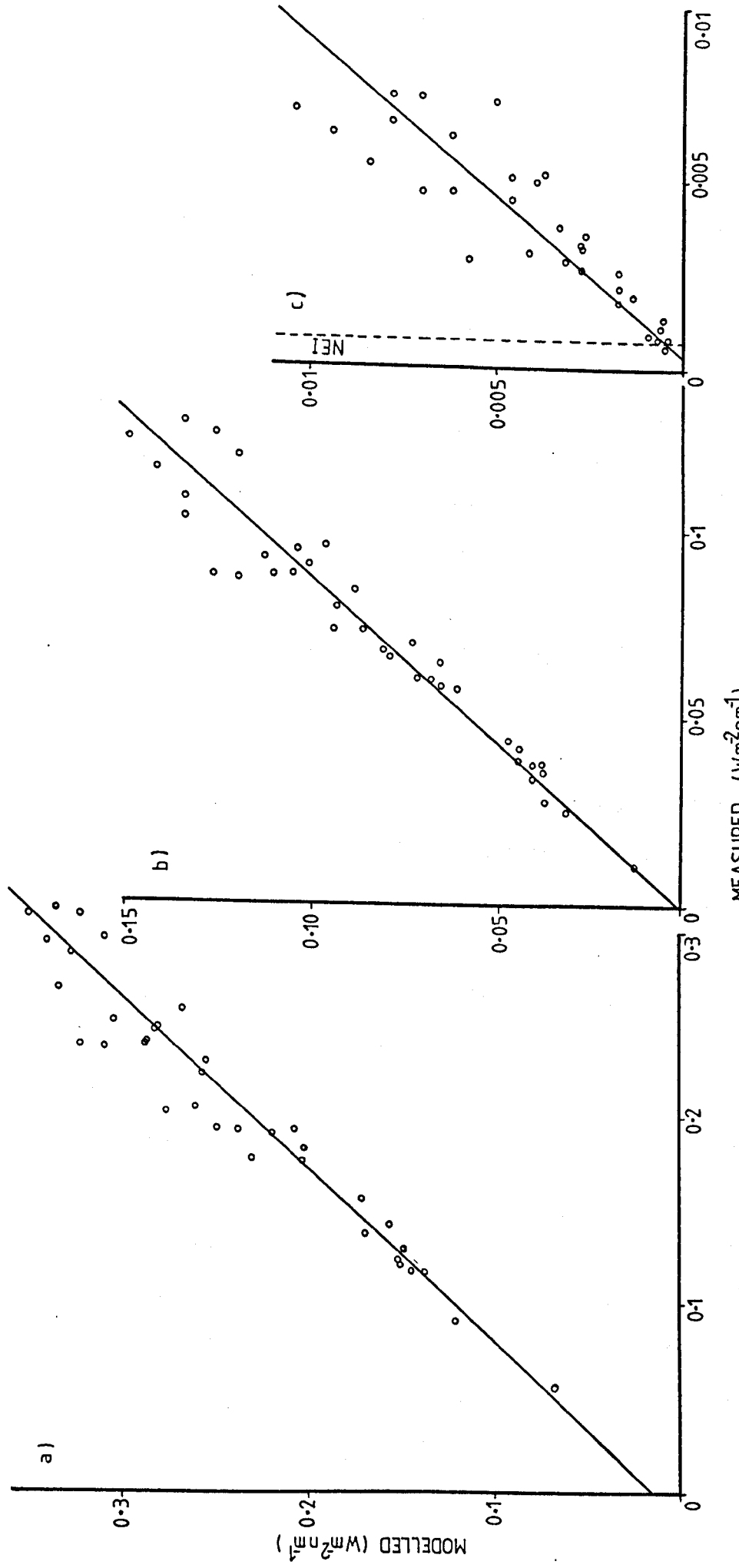


Fig. 5.7 Modelled vs measured irradiances at 3 wavelengths: a) 320 nm, b) 310 nm, c) 300 nm.

Table 5.4 Slopes and intercepts of modelled vs measured irradiance plots.

| Wavelength (nm) | Slope           | Intercept ( $\text{W m}^{-2} \text{ nm}^{-1}$ ) |
|-----------------|-----------------|---|
| 300             | 1.21 $\pm$ 0.09 | (4.0 $\pm$ 3.6) $\times 10^{-4}$                |
| 310             | 1.13 $\pm$ 0.05 | (1.3 $\pm$ 4.0) $\times 10^{-3}$                |
| 320             | 1.09 $\pm$ 0.05 | 0.016 $\pm$ 0.01                                |

The slope of each line gives the ratio of modelled to measured irradiance for each of the three wavelengths. The modelled irradiances are always greater than those measured, with the discrepancy decreasing at longer wavelengths. The difference may be partly explained by recourse to the criteria under which models and measurements were paired.

- i) A clear day at Sutton Bonington is never truly clear in the modeller's terms. There will always be some atmospheric aerosol which will increase attenuation and hence decrease irradiance measured at the ground.
- ii) Sutton Bonington is almost  $3^{\circ}$  latitude further north than the model location and so receives less extraterrestrial solar radiation during the central part of the day.
- iii) Radiation received on a horizontal surface is a function of zenith angle. Zenith angles were matched to  $\pm 0.5^{\circ}$ , giving a maximum errors in  $\cos z$  of  $\pm 0.5\%$  at  $z = 30^{\circ}$  and  $\pm 1.5\%$  at  $z = 60^{\circ}$ .
- iv) The matching procedure for ozone amount can also lead to errors as ozone is the major absorber in the UVB. The effect of any ozone mismatch is negligible at 320 nm, but at a wavelength of 300 nm where ozone is a major absorber any difference may lead to model-

measurement divergence, particularly when coupled with differences in zenith angle which govern the pathlength of the radiation through the ozone layer.

The differences in the first two criteria between the ideal and the real world will both result in an overestimation of model irradiances when compared with Sutton Bonington. The latter two differences may create either over or underestimation if acting alone, and this accounts for some of the scatter seen in Fig. 5.7a-c, complicated by the possible interactions of all four factors. The spread of the data in Fig. 5.7c is greater than in a and b, the standard error of the slope being 7% at 300 nm while it is 4% at 310 nm and 320 nm. At 300 nm the measured radiation is more susceptible to error. As already mentioned, this wavelength is the most sensitive of the three to the amount of ozone in the atmosphere, and in addition is most affected by the spectroradiometer's bandpass function and hence by the spectral correction technique employed. Some of the low irradiances are also at or below the noise equivalent irradiance of the LI1800 and may therefore contain a significant element of noise in the signal.

Considering the sources of error inherent in the method of comparison, agreement between modelled and actual UVB radiation levels is good.

It must be remembered that the systematic error in spectral measurements i.e. the error in the absolute magnitude of all measured irradiances is  $\pm 10\%$ , increasing the error on each slope in Table 5.4 by  $\pm 10\%$ . For reasons given in Appendix A the original calibration of the spectroradiometer is assumed correct, and all measurements used in this comparison were made using the original calibration. As theory

dictates that for this model calculated irradiances should be higher than those measured, one of two suppositions may be inferred. Firstly, if the model is approximately correct then the choice of original calibration is also reasonable. Using the latter (Glen Creston) calibration the measured values would be about 30% less than those produced by the model. The systematic reductions of the measured irradiances are due to latitude, which by extrapolation from the Handbook would be  $\sim 6\%$  for  $3^{\circ}$  latitude at 300 nm and  $\sim 3\%$  at 310 nm, and atmospheric aerosol. It is unlikely that on a nominally clear day aerosol would reduce UVB radiation by  $\sim 25\%$ . Secondly, if the original calibration is in error by  $\pm 10\%$  of the given value, then the model is either underestimating or overestimating UVB irradiances at the earth's surface.

The natural inclination is to follow the first line of reasoning, but there is insufficient evidence to discard the possibility of the second argument.

## 6. THE UVB WAVEBAND (300 - 316 nm)

### Introduction

The spectral properties of the UVB waveband have been discussed for clear sky conditions, and a study of the total radiation incident over the whole UVB waveband (300 - 316 nm) begins in the same way.

### Clear-Day Climatology

When considering the biological effects of UVB radiation it is important to know the level of environmentally available UV light. The annual and diurnal trends of UVB radiation on clear days at Sutton Bonington are shown in Figs 6.1 and 6.2, indicating the maximum level of natural UVB available at any time.

The annual change in UVB radiation at noon (Fig. 6.1) is given independently of any day-to-day variations in ozone or atmospheric aerosol, and with ozone amounts ranging from 278 to 423 matm cm for days from May to July this explains some of the spread of irradiances measured in these months. In general the annual ozone cycle and the changing sun angle combine to give the slightly asymmetrical curve shown with respect to the solar cycle. The shift of the time of maximum UVB radiation from June to July is not evident for the full UVB band as it is for the individual wavelengths (Fig. 5.2). This may be due in part to the additional data available for the full UVB band (4 days in June compared with one for the spectral plots) providing two high June irradiances and necessitating greater smoothing of the final curve. No data are available for the period from early December to late January but by extrapolation the minimum UVB should

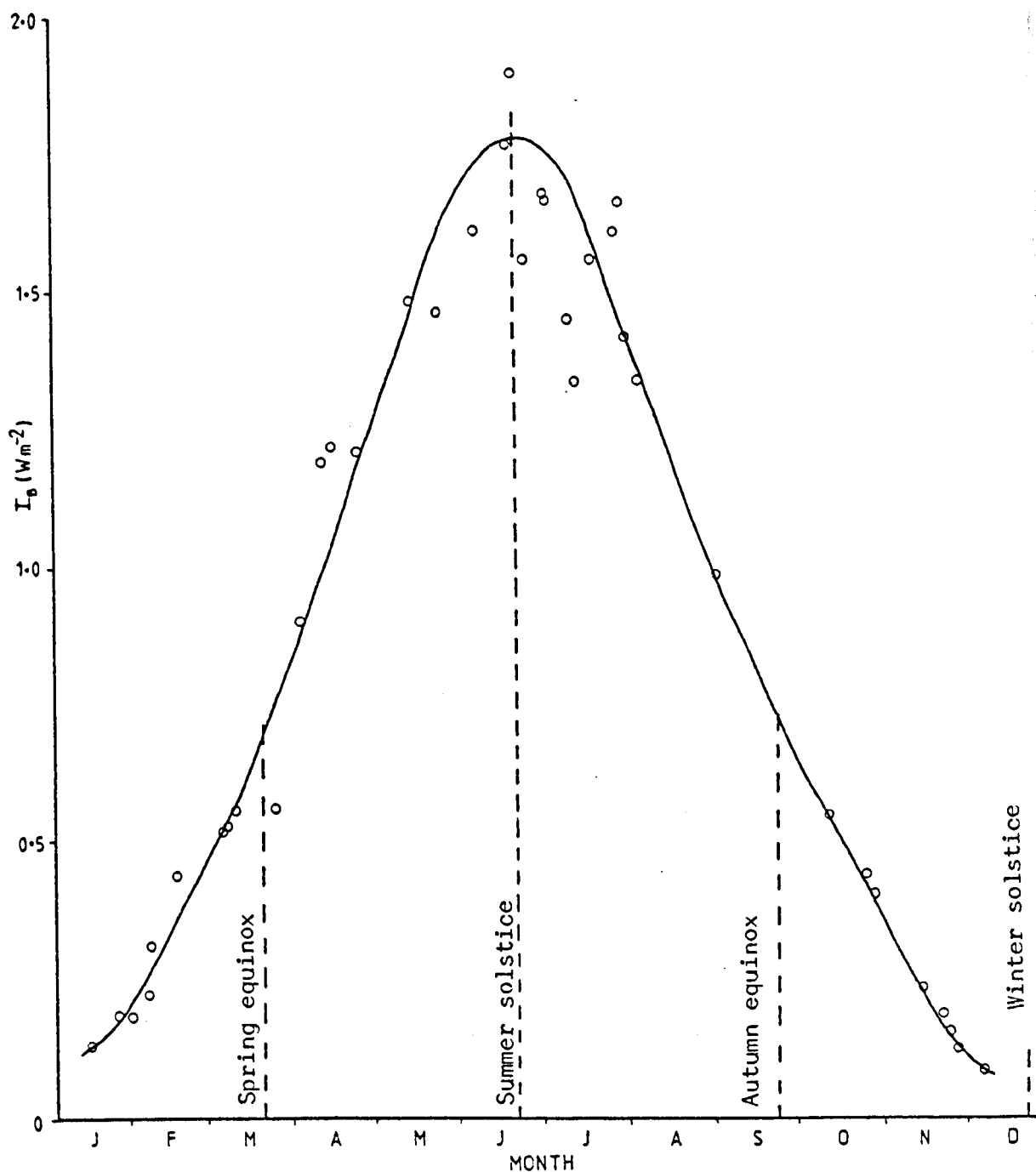
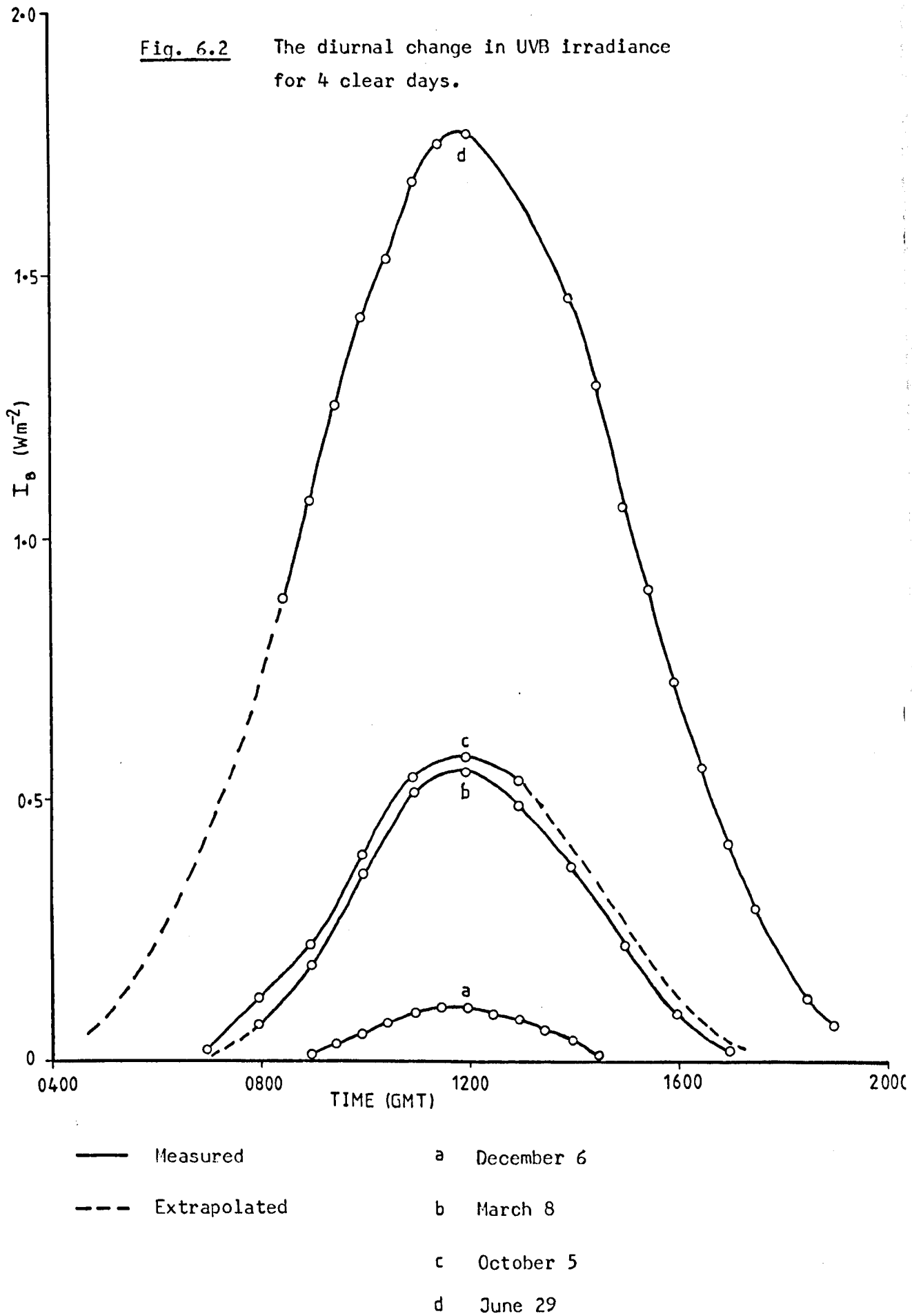


Fig. 6.1 UVB irradiance at noon on clear days in 1983 and 1984. The points are measured values, the curve was fitted by eye.



be at the time of the winter solstice. The extremes of noon irradiance are  $0.09 \text{ W m}^{-2}$  minimum and  $1.78 \text{ W m}^{-2}$  maximum, a 20-fold increase from winter to summer.

The influence of ozone is more apparent in Fig. 6.2, depicting the diurnal cycle of UVB radiation on clear days throughout the year. In March (curve b), ozone amount is greater than in October (curve c). Although both dates were 14 days from the equinox so that the solar path across the hemisphere was the same, the UVB irradiance in March is lower than that in October. The difference in ozone amount for the two days shown was 11% whereas the monthly mean difference of ozone for March and September (at the equinoxes) is 6%.

Just as solar daylength changes with time of year so does UVB daylength\*. The UVB day for clear conditions is shortest at the winter solstice, from ~0900 to 1500, then increasing to ~11 hours (0630 to 1730) at the equinoxes and reaching a maximum of ~16 hours (0400 - 2000) at midsummer. UVB daylength is shorter than that of total daylight hours as increasing pathlength through a clear atmosphere has the greatest attenuating affect at short wavelengths, a phenomenon easily observed by the red sky of sunset.

The lengthening UVB day compounded by increasing irradiance from December to June means that the total daily UVB radiation available in the natural environment changes by a factor of ~40 throughout the year. For the two clear days, December 6 and June 29, of Fig. 6.2 the daily incident UVB increases from  $1.3 \text{ kJ m}^{-2}$  to  $46.4 \text{ kJ m}^{-2}$ , a factor of 36. In March/October the total irradiance for a clear day is ~ $10.8 \text{ kJ m}^{-2}$

---

\* defined as the hours for which there is a measureable ( $> 5 \times 10^{-3} \text{ W m}^{-2}$ ) UVB component in the solar irradiance.

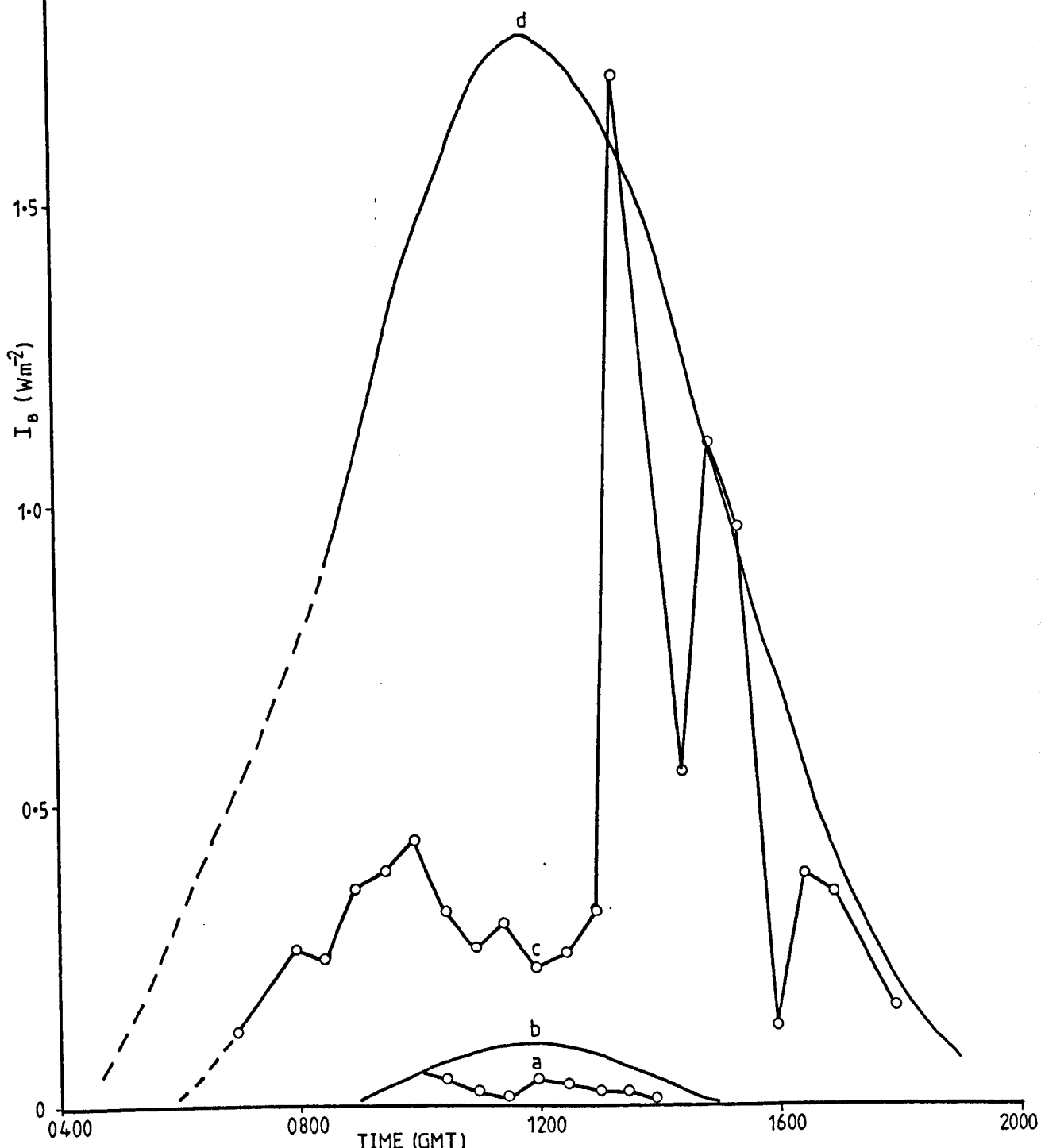
### The influence of cloud

These figures for clear skies represent the maximum UVB received as a function of time of year. Under less ideal atmospheric conditions the amount of UVB reaching the ground may be severely reduced. The influence of cloud as the major transient attenuator is difficult to quantify as it depends on cloud type, height, thickness and amount. In Fig. 6.3 the diurnal irradiance curves for June and December are reproduced from Fig. 6.2 and two cloudy days for the same time of year are shown for comparison. The cloudy days were as near as possible in time to the clear day comparison and were days, or part days, when the cloud cover was 8 octas of uniform grey stratus as classified by a ground-based observer. Even on generally overcast days the cloud conditions fluctuated as demonstrated by the irregular curves a and c. Thickening or darkening of cloud is seen as a reduction in incident UVB when the extraterrestrial radiation was increasing. Increasing UVB with increasing zenith angle suggests a lessening of cloud cover.

In winter, cloud can reduce UVB irradiance to almost imperceptible levels (e.g.  $0.1 \text{ W m}^{-2}$  at 1130 on December 9), and with the associated cold weather attire, exposure of individuals is likely to be negligible. The total daily UVB represented by curve a is 35% of the clear day total of curve b.

In June the percentage decrease in total UVB due to cloud is even greater. Comparing the totally overcast hours of June 25 (curve c to noon) with the same hours for June 29 (curve d) gives a reduction to 22% of the clear sky irradiance. Although it is not possible to

Fig. 6.3 The effect of cloud on UVB irradiance  
in June and December.



a December 9, clear

b December 6, clear

c June 25, cloudy

d June 29, clear

compare the characteristics of the cloud on the two overcast days, a greater reduction in UVB intensity may be expected in June for identical cloud cover. With the low sun angle and long atmospheric pathlength of December most of the UVB ( $\sim 90\%$ ) reaching the earth's surface is in the form of diffuse radiation, even on a clear day. By contrast a clear day in June has diffuse radiation accounting for only  $\sim 50\%$  of the global radiation. As direct beam radiation is more severely attenuated by cloud than diffuse, the reduction in irradiance should be greatest in June.

During the afternoon of June 25 there were two periods with breaks in the cloud, one at  $\sim 1330$  and the other from 1500 to 1530. At these times, with the sun clear of cloud, levels of UVB radiation exceeded those of clear sky conditions for June 29. For the prolonged break in the clouds the irradiance levels for the two days are very similar and the difference may be a feature of day to day changes in ozone or aerosol, for which no data are available. The single elevated spot reading at 1330 suggests that the direct solar beam traversed a smaller cloud free area. It is likely that cloud in the vicinity of the sun, but not obscuring it, increased diffuse radiation by forward scattering from the cloud while not attenuating the direct beam. This phenomenon was also observed by Bener (1964) and may be the cause of the rather high irradiance at 1330 compared with the clear-day value for the same time. The increased flux of full band global solar irradiance when isolated clouds are present in an otherwise clear sky is a commonly observed phenomenon. Over the complete solar waveband the clear sky irradiance may be exceeded by 5-10% in conditions of broken cloud cover (Monteith, 1973).

### UVB and Its Relation to Broadband Measurements

The UVB radiation was compared with the broadband visible (300-700 nm) and full (300-3000 nm) solar radiation in a search for relations which might enable the UVB irradiance to be predicted from routine meteorological records. Full solar radiation is measured at all climatological and some meteorological sites, and visible radiation records are kept at some of the larger meteorological stations.

#### Visible radiation on clear days

On clear days the LI1800 spectroradiometer was used to scan the waveband 300-700 nm at 2 nm intervals, and the resulting spectra were integrated over the two wavebands  $I_B = 300-316 \text{ nm}$  and  $I_V = 300-700 \text{ nm}$ . The ratio of the global radiation incident in the two wavebands,  $I_B/I_V$ , was plotted as a function of  $\cos z$  for each day (Fig. 6.4) giving a set of straight lines of the form

$$I_B/I_V = x + y \cos z \quad (6.1)$$

The gradients and intercepts of the lines for sixteen clear or partly clear days in 1983 and 1984 are shown in Table 6.1, as calculated by linear regression analysis.

All gradients lie between 4 and  $4.5 \times 10^{-3}$ , with the majority between 4 and  $4.3 \times 10^{-3}$ . The mean and standard deviation of all gradients is  $(4.19 \pm 0.15) \times 10^{-3}$ . On one day (August 3, 1983) the plotted points showed far greater scatter than at other dates. Excluding this day the mean gradient becomes  $(4.16 \pm 0.14) \times 10^{-3}$ .

The intercept of the lines at  $\cos z = 0$  ( $z = 90^\circ$ ) shows more variability, suggesting dependence on factors additional to those controlling the gradient.

Fig. 6.4

The changing ratio of UVB to visible radiation with zenith angle for 2 clear days: a) 8 March 1983, b) 28 July 1983.

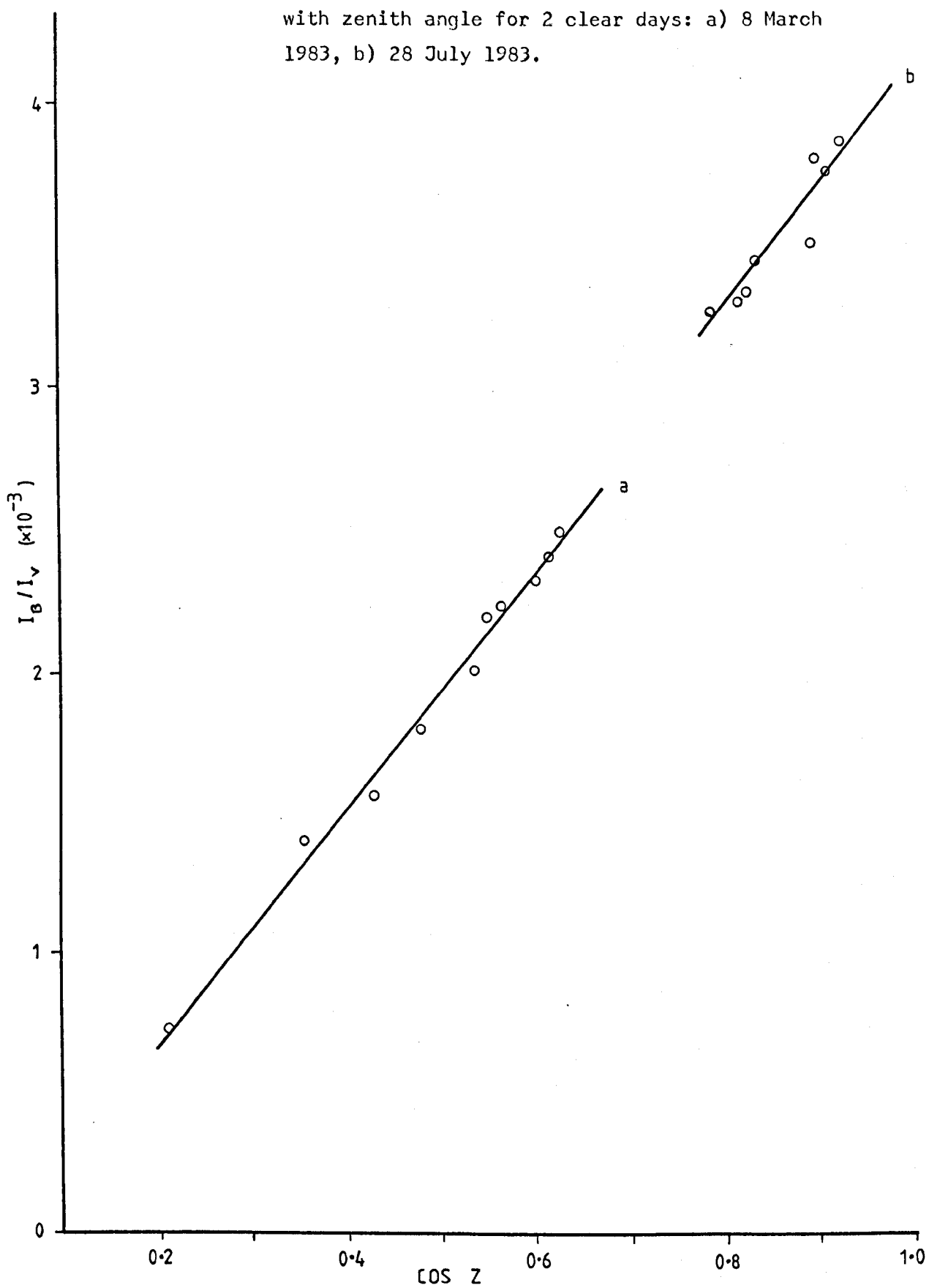


Table 6.1 Gradients and intercepts for  $I_B/I_V$  vs  $\cos z$   
on clear days

| Date        | Gradient ( $\times 10^{-3}$ ) | Intercept ( $\times 10^{-3}$ ) |
|-------------|-------------------------------|--------------------------------|
| <b>1983</b> |                               |                                |
| 18. 2       | 4.30                          | 0.56                           |
| 8. 3        | 4.20                          | 0.26                           |
| 5. 7        | 4.00                          | 0.05                           |
| 11. 7       | 4.00                          | 0.40                           |
| 15. 7       | 4.00                          | 0.33                           |
| 21. 7       | 4.24                          | 0.44                           |
| 28. 7       | 4.20                          | 0.30                           |
| 3. 8        | 4.49 *                        | 0.10                           |
| 26. 8       | 4.42                          | - 0.02                         |
| 24.10       | 4.12                          | 0.39                           |
| 14.11       | 4.14                          | 0.43                           |
| <b>1984</b> |                               |                                |
| 9. 2        | 4.11                          | 0.35                           |
| 25. 4       | 4.11                          | 0.11                           |
| 1. 8        | 4.00                          | 0.53                           |
| 29. 8       | 4.28                          | 0.84                           |
| 2. 9        | 4.35                          | - 0.06                         |
| <b>1985</b> |                               |                                |
| 6. 3        | 4.05                          | - 0.54                         |

\* Scattered data

To investigate the factors to which constant slope and changing intercept can be attributed, the analysis of Brinkman and McGregor (1983) was applied to the UVB and visible wavebands.

### General theory

Unsworth and Monteith (1972) established the relationship

$$S_p = S_{p_0} \exp (-m\tau) \quad (6.2)$$

where  $S_p$  is irradiance over the whole solar spectrum measured normal to the spectral beam,  $S_{p_0}$  is the corresponding value for a dust free atmosphere with the same quantities of ozone and water vapour,  $m$  is airmass,  $\tau$  is an integral aerosol turbidity.

Brinkman and McGregor (1983) expressed the amount of radiation  $\Delta I$  removed from the direct solar beam by aerosol scattering and absorption as

$$\Delta I = (1 - \exp (-m\tau)) S_{p_0} \quad (6.3)$$

A proportion  $\alpha$  of  $\Delta I$  will be scattered, with  $\beta(z)$  (an amount dependent on zenith angle) being scattered downwards.

When the total irradiance  $I$  on a horizontal surface is measured the angular distribution of downward scattered radiation gives rise to a weighting factor equal to the average cosine of the incidence angles,  $\overline{\cos i}$ . Both  $\beta(z)$  and  $\overline{\cos i}$  are a result of the angular relationship between the scattering phase function of the aerosol and the solar zenith angle.

$\alpha$ ,  $\beta(z)$  and  $\overline{\cos i}$  cannot be separately determined from diffuse irradiation measurements alone, and they are combined in a single parameter,  $P(z)$ . The diffuse irradiance at the ground  $D$  is then given by

$$D(z, \tau) = R(z) + P(z) (1 - \exp (-m\tau)) S_{p_0} \quad (6.4)$$

where  $R(z)$  is a component due to Rayleigh scattering. For simplification,  $P(z)$  is assumed independent of aerosol density. This is valid for single scattering, but for multiple scattering  $P(z)$  is a function of  $\tau$ . However for low turbidities when multiple scattering is negligible it is reasonable to assume that  $P$  is independent of  $\tau$ .

The effects of surface albedo are neglected because the proportion of ground-reflected irradiance which is subsequently back-scattered is negligible in the UVB region.

Both  $B(z)$  and  $\cos i$ , and thus  $P$ , decrease with increasing zenith angle. Following Unsworth and Monteith (1972) and McCartney (1975), the ratio of diffuse to global radiation is taken as

$$D/I = e + d\tau \quad (6.5)$$

where  $e$  and  $d$  are constants.  $e$  is associated with Rayleigh scattering ( $\tau = 0$ ) and is only valid for small turbidities.

The global irradiance is the sum of direct ( $B$ ) and diffuse ( $D$ ) components on a horizontal surface, where the direct component is  $B = S_p \cos z$ . The ratio of diffuse to global radiation can therefore also be expressed as

$$D/I = (D/S_p \cos z)(1 + D/S_p \cos z)^{-1} \quad (6.6)$$

From eqns 6.4 and 6.2

$$D/S_p \cos z = \exp(m\tau) \sec z (r + P) - P \sec z \quad (6.7)$$

$$\text{where } r = R/S_{p_0} \quad (6.8)$$

Expanding eqn 6.6 in a McLaurin series to 2nd order, expanding the exponential in eqn 6.7 and then dropping all terms higher than second order (after Brinkman and McGregor, 1983) gives

$$D/I \approx r \sec z + (r - 2rP \sec z + P)\tau_m \sec z \quad (6.9)$$

Comparing coefficients with eqn 6.5 gives

$$P \approx (d \cos z/m - r)/(1 - 2r \sec z) \quad (6.10)$$

Data collected by Brinkman and McGregor and analysed in this way agreed with the findings of Unsworth and Monteith (1972) and of McCartney (1975).

#### Spectral measurements

The spectral dependence of aerosol scattering is complicated by the fact that aerosol particles vary in both size and chemical composition. In general the degree of spectral dependence is a function of the width of the particle distribution; ~~the broader~~ the distribution the more neutral is the scattering (Diermendjian, 1969). For natural continental aerosols the scattering has an approximately linear variation with wavelength (Brinkman and McGregor, 1983).

For any spectral band, a spectral turbidity  $\tau_\lambda$  can be defined by

$$S_{p\lambda} = S_{p_0\lambda} \exp (-m\tau_\lambda) \quad (6.11)$$

the terms of eqn 6.11 are defined in the same way as those for eqn 6.3 for the spectral band or wavelength designated by  $\lambda$ .

#### Application to ultraviolet and visible radiation

$$\text{In general, } I = B + D \quad (6.12)$$

$$B = B_0 \exp \left\{ -k[O_3]^m - \tau_R^m - \tau_a^m \right\} \cos z \quad (6.13)$$

$$D = B_0 \exp \left\{ -k[O_3]m \right\} (1 - \exp (-m\tau_a)) P + R \quad (6.14)$$

where  $I$  is global irradiance on a horizontal surface,  $B$  is direct beam irradiance on a horizontal surface,  $D$  is diffuse irradiance on a horizontal surface,  $B_0$  is extraterrestrial irradiance. Absorption by ozone is considered to take place above the scattering layer, and turbidity has been split into two components due to Rayleigh ( $\tau_R$ ) and aerosol ( $\tau_a$ ) scattering.

On clear days, Rayleigh scattering is much more effective than aerosol scattering, especially in the ultraviolet waveband, so  $\tau_R$  and  $\tau_a$  were combined and assumed to be approximately a constant,  $\tau$ . The component of diffuse radiation due to Rayleigh scattering,  $R$  can be expressed in the same way as aerosol scattering with a parameter  $P_R$ . Assuming  $\tau (= \tau_R + \tau_a)$  is constant,  $P$  is also assumed constant and under clear skies refers mainly to the Rayleigh scattered radiation in a downward direction.

From eqns 6.12 to 6.14 comes

$$I_B = I_{B_0} \exp (-k[O_3]m) \left[ \exp (-\tau_m) \cos z + \left\{ 1 - \exp (-\tau_m) \right\} P \right] \quad (6.15)$$

$$I_V = I_{V_0} \left[ \exp (-\tau'm) \cos z + \left\{ 1 - \exp (-\tau'm) \right\} P' \right] \quad (6.16)$$

where  $I_B$  is global UVB irradiance,  $I_{B_0}$  is extraterrestrial UVB irradiance,  $I_V$  is global irradiance in the visible band (300-700 nm),  $I_{V_0}$  is extraterrestrial irradiance in the visible band,  $\tau$  is a turbidity coefficient for the UVB waveband,  $\tau'$  is a turbidity coefficient for the visible waveband and  $P$ ,  $P'$  are fractions of downward scattered radiation in the UVB and visible wavebands.

There is no ozone dependence in eqn 6.16 as absorption by ozone is negligible over the full visible waveband.

The ratio of irradiance in the two wavebands is given by

$$\frac{I_B}{I_V} = \left( \frac{I_{B_0}}{I_{V_0}} \right) \exp(-k[O_3]m) \left[ P + \exp(-\tau m) \{ \cos z - P \} \right] / \left[ P' + \exp(-\tau'm) \{ \cos z - P' \} \right] \quad (6.17)$$

The parameter  $P(z)$  incorporates several factors:  $\alpha$ , the proportion of  $\Delta I$  scattered,  $\beta(z)$ , the fraction scattered downwards,  $\overline{\cos i}$ , average angle of incident radiation. For Rayleigh scattering, the dominant mechanism on clear days,  $\beta(z) = 0.5$  for all wavelengths.

In the ultraviolet and visible bands the ratio of  $\alpha$ 's, the proportion of scattered radiation in each waveband, is a constant, with  $\alpha$  expected to be close to unity in the ultraviolet.

Assume that  $\overline{\cos i}$  is the same for all wavelengths

$$P(z) = f(\alpha, \beta(z), \overline{\cos i}) = f(\overline{\cos i}) = f(\cos z) \quad (6.18)$$

implying that the ratio  $P/P'$  is a constant.

Let  $C = \cos z$  and  $\gamma = (I_{B_0}/I_{V_0})P/(I_{V_0}P') = \text{constant}$ . Then eqn 6.17 can be written

$$\frac{I_B}{I_V} = \gamma \exp(-k[O_3]m) \left[ 1 + \left( \frac{C - P}{P} \right) \exp(-\tau m) \right] \left[ 1 + \left( \frac{C - P'}{P'} \right) \exp(-\tau'm) \right]^{-1} \quad (6.19)$$

Consider the magnitude of the term  $(\frac{C - P}{P}) \exp(-\tau m) = x$ . Brinkman and McGregor in the Sahara found values of  $P$  for the full solar

waveband, ranging from 0.13 to 0.26 depending on background aerosol for  $z = 60^\circ$ . Calculating values of  $P$  for Unsworth and Monteith's (1972) data they found  $P = 0.33$  at a zenith angle of  $45^\circ$ . McCartney, applying the same analysis to his data for English aerosol, found that despite the different chemical composition of English and Saharan aerosols, values of  $P$  were approximately the same. At Sutton Bonington, with  $\tau$  typically of the order 0.25 (Unsworth and Monteith, 1972),  $x < 1$  and expanding eqn 6.19 as  $(1 + x)^{-1} = 1 - x + x^2 - x^3 \dots (-1 < x < 1)$  and dropping terms of order 2 or more gives

$$\frac{I_B}{I_V} \approx \gamma \exp(-k[O_3]m) \left[ 1 - \exp(-\tau m) + \exp(-\tau' m) + \frac{C}{P} \exp(-\tau m) - \frac{C}{P'} \exp(-\tau' m) \right] \quad (6.20)$$

Expanding the exponential terms in eqn 6.20 and discarding terms of order 2 and above ( $k[O_3]m \sim 0.5$   $m < 1$  for  $m < 2$ ,  $z < 60^\circ$ ) and expanding gives

$$\begin{aligned} \frac{I_B}{I_V} \approx \gamma \left[ 1 - k[O_3]m + (\tau - \tau')m + \frac{C}{P}(1 - \tau m) - \frac{C}{P'}(1 - \tau' m) - k[O_3](\tau - \tau')m^2 - \frac{C}{P}k[O_3]m + \frac{C}{P}k[O_3]\tau m^2 + \frac{C}{P'}k[O_3]m - \frac{C}{P'}k[O_3]\tau' m^2 \right] \end{aligned} \quad (6.21)$$

Since  $\tau \ll \tau'$  and  $k[O_3](\frac{C}{P}\tau - \frac{C}{P'}\tau') \ll 1$

$$\begin{aligned} \frac{I_B}{I_V} \approx \gamma \left[ 1 - k[O_3]m + (\tau + \tau')m + \frac{C}{P}\tau' m - \frac{C}{P}\tau m - \frac{C}{P}k[O_3]m + \frac{C}{P'}k[O_3]m + \frac{C}{P} - \frac{C}{P'} \right] \end{aligned} \quad (6.22)$$

Putting  $m = (\cos z)^{-1}$  and  $C = \cos z$  gives

$$\frac{I_B}{I_V} \approx \gamma \left[ 1 - k[O_3]m + (\tau + \tau')m + \frac{\tau'}{P'} - \frac{\tau}{P} - \frac{k[O_3]}{P} + \frac{k[O_3]}{P'} + \left( \frac{1}{P} - \frac{1}{P'} \right) \cos z \right] \quad (6.23)$$

Comparing coefficients of eqns 6.1 and 6.23

$$x \approx \gamma \left[ 1 - k[O_3]m + (\tau - \tau')m + \frac{\tau'}{P'} - \frac{\tau}{P} + k[O_3] \left( \frac{1}{P'} - \frac{1}{P} \right) \right] \quad (6.24)$$

$$y \approx \gamma \left( \frac{1}{P} - \frac{1}{P'} \right) \quad (6.25)$$

In clear (Rayleigh) conditions the  $\cos i$  and  $\beta(z)$  dependence of  $P$  and  $P'$  are the same. The difference between  $P$  and  $P'$  is attributable to different values of  $\alpha$  for the two wavebands, but in each case  $\alpha$  is a constant therefore  $P$  and  $P'$  are constants, as is  $y$ . When scattering is not purely Rayleigh deviations from the constant value occur. The consistency of slope in eqn 6.1 for clear days is therefore explained by this analysis: small departures from a uniform slope are expected because even on a clear day a perfect Rayleigh atmosphere is not expected.

The intercept of each line  $x$  is dependent on airmass, ozone amount and the two spectral turbidities, all of which change from day to day giving a range of values for  $x$ .

#### Full solar radiation on clear days

In a continuation of the analysis discussed for visible radiation, the ratio  $I_B/I_F$  was plotted against  $\cos z$  for clear days, where  $I_F$  is the full solar radiation (300-3000 nm) measured with a standard meteorological pyranometer.

A linear relationship was again evident on each day, although with a greater degree of scatter (see Fig. 6.5). However, the slopes of the lines covered a wide range, from  $1.08$  to  $4.02 \times 10^{-3}$ , and the intercepts were again variable.

Attenuation of infra-red radiation by water vapour becomes a complicating factor when working with the total solar waveband. Even on a clear day differing amounts of water vapour will result in different values for  $\alpha$  and hence  $P$  for a waveband with an infra-red component and  $y = (I_{B_0} P / I_{F_0} P') (\frac{1}{P} - \frac{1}{P_1})$  is no longer a constant.

#### Daily Totals of UVB and Fullband Solar Radiation

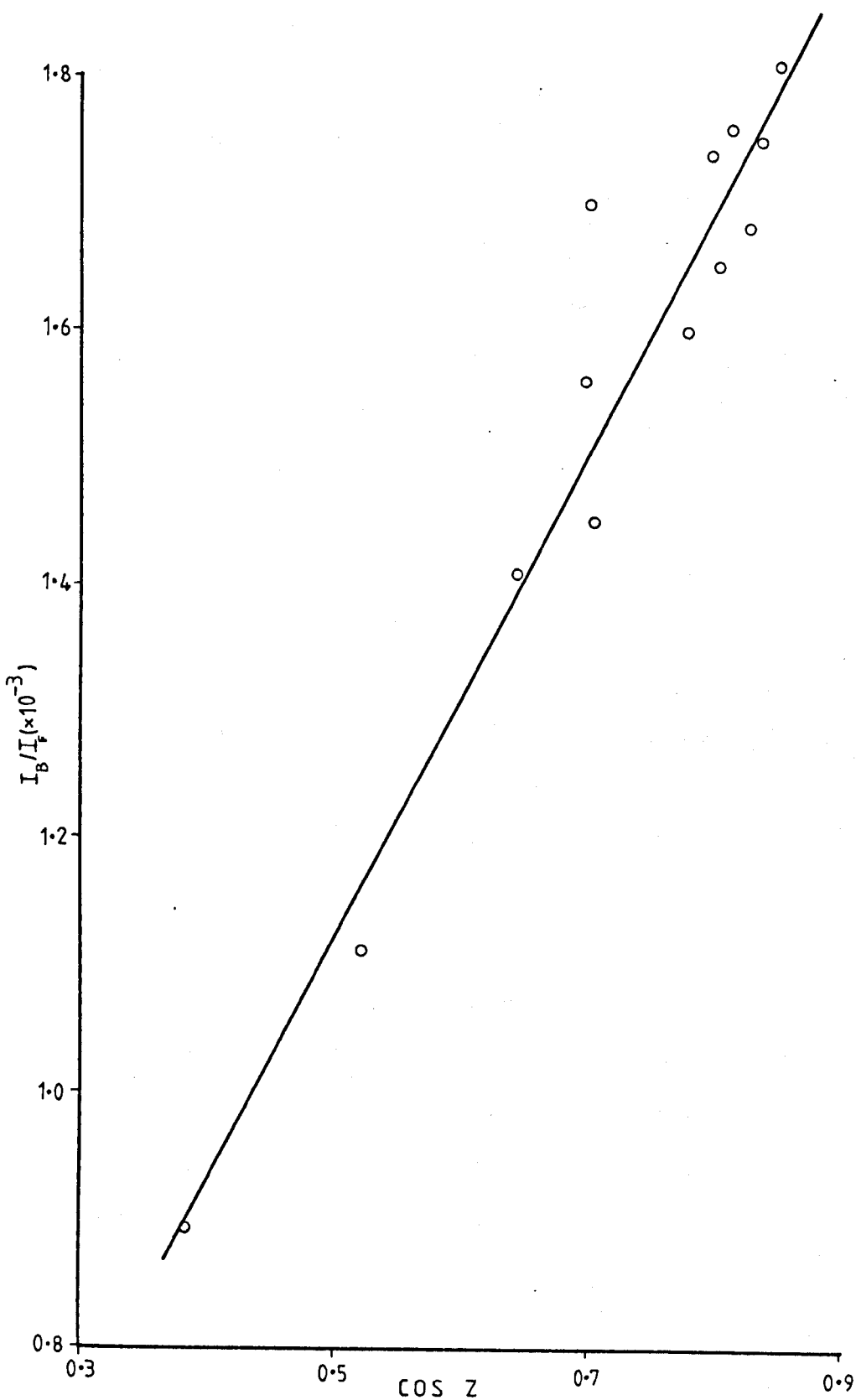
The correlation between UVB and broader-band radiation discussed thus far enable the UVB irradiation to be estimated on clear days, given information about ozone amount, aerosol and a broad band radiation measurement. The visible band provides the simplest relation with which to work. However such a set of data is rarely available, and the above parameters are regularly recorded at few national meteorological stations around the world.

Much more common are measurements of the full solar waveband, usually reported as daily totals of radiation. Therefore in order to provide a guide to the UVB climate from routinely-made meteorological observations a link between the daily integrated UVB and full solar radiation was sought.

Such integrated values of UVB are also the most relevant when considering the impact of UVB irradiation on biological systems. Most organisms must be able to cope with an extensive range of

Fig. 6.5

The changing ratio of UVB to full-band radiation with zenith angle on a clear day: 15 July 1983.



instantaneous radiation fluxes because of the large diurnal and annual trends, and it is the total accumulated dose over a given period of time which may be of more significance for the photo-biological reaction under consideration.

Maintaining the policy of beginning analysis in clear sky conditions the daily totals of UVB radiation  $\Sigma I_B$  were plotted against the daily totals of the broad band (300-3000 nm) solar radiation  $\Sigma I_F$  for clear days in 1983 and 1984 (Fig. 6.6). No account of ozone amount or any other atmospheric constituent has been made.

On clear days, zenith angle appears to be the major determinant of the ratio of the daily integrals of UVB and full solar radiation. Other factors affecting the two wave bands by day-to-day fluctuation (ozone, aerosol and water vapour) have a smaller influence than the annual zenith angle cycle, as shown by Fig. 6.6 where no account of atmospheric variables is taken.

An analogous dependence of waveband ratios on solar zenith angle has also been shown to hold on individual clear days for both the visible and full solar radiation with UVB.

This analogy was extended to all weather conditions as follows.

The daily integrated UVB ( $\Sigma I_B$ ) values were plotted against the integrated full solar waveband ( $\Sigma I_F$ ) for each month from June 1983 to November 1984. A linear regression analysis applied to each monthly curve (Fig. 6.7) gave the slopes, intercepts and their standard errors shown in Table 6.2 for the fitted lines

$$\Sigma I_B = \rho \Sigma I_F + n \quad (6.26)$$

Fig. 6.6 UVB and full solar waveband daily radiation totals for clear days in 1983 and 1984.

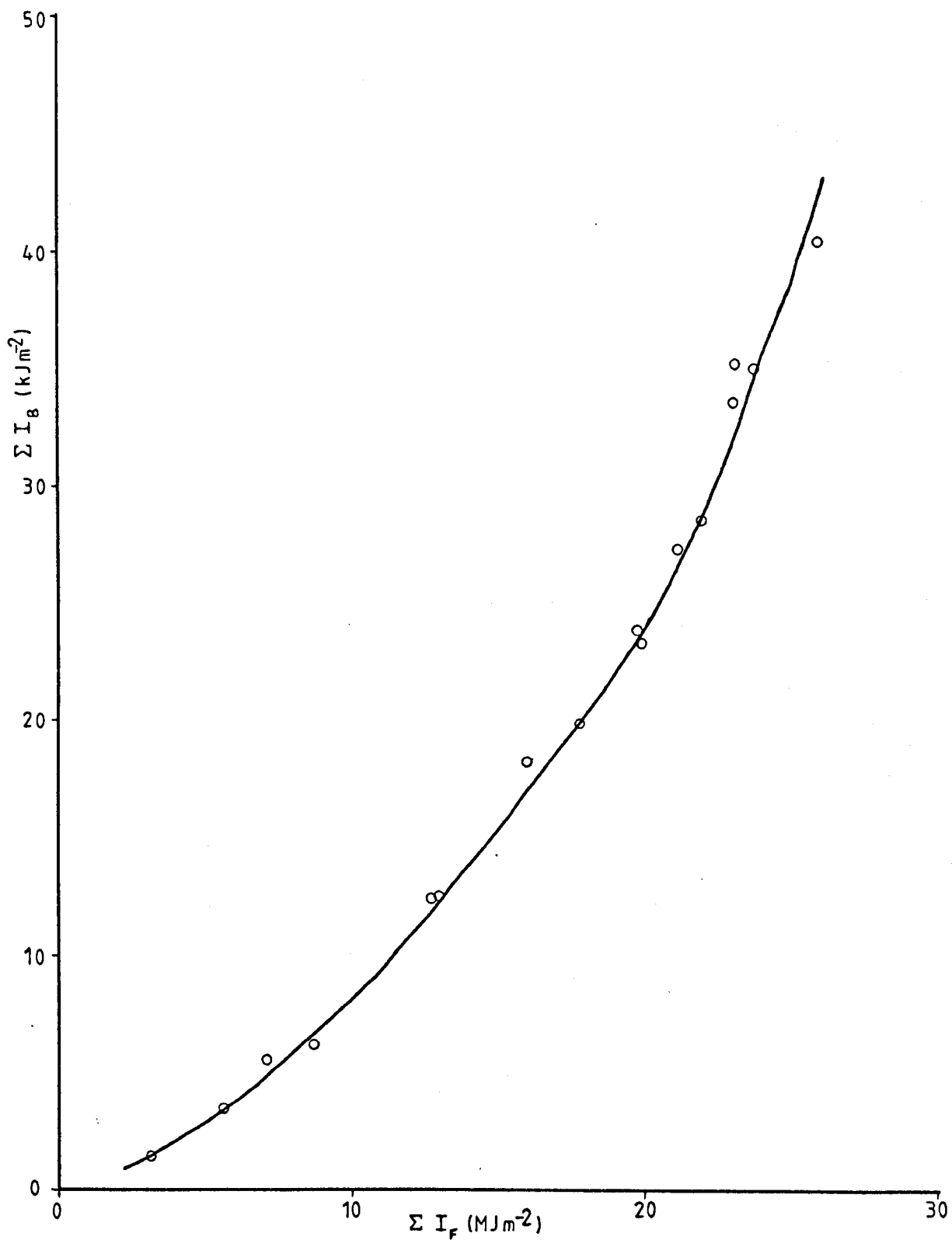
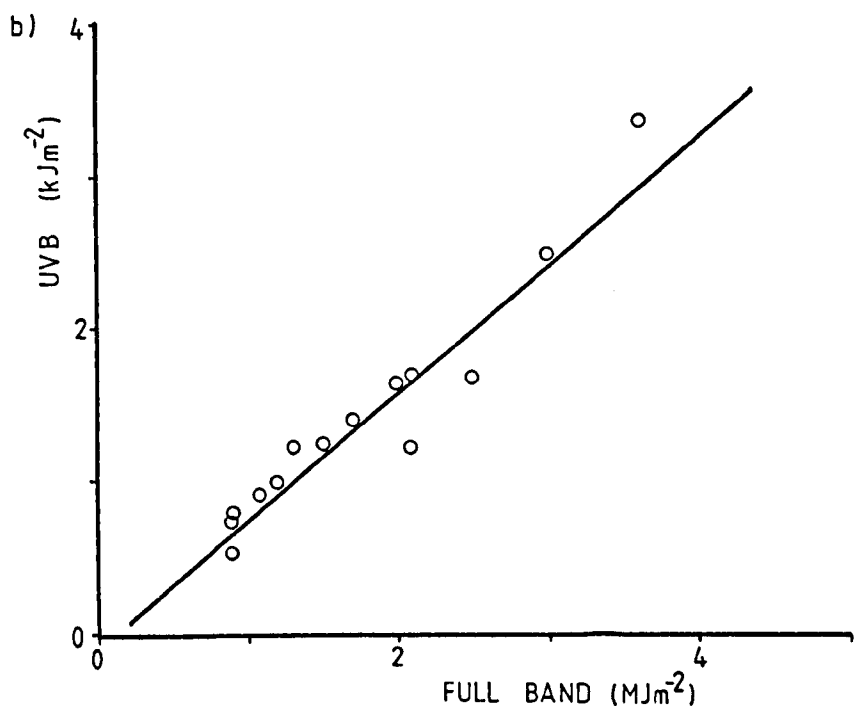
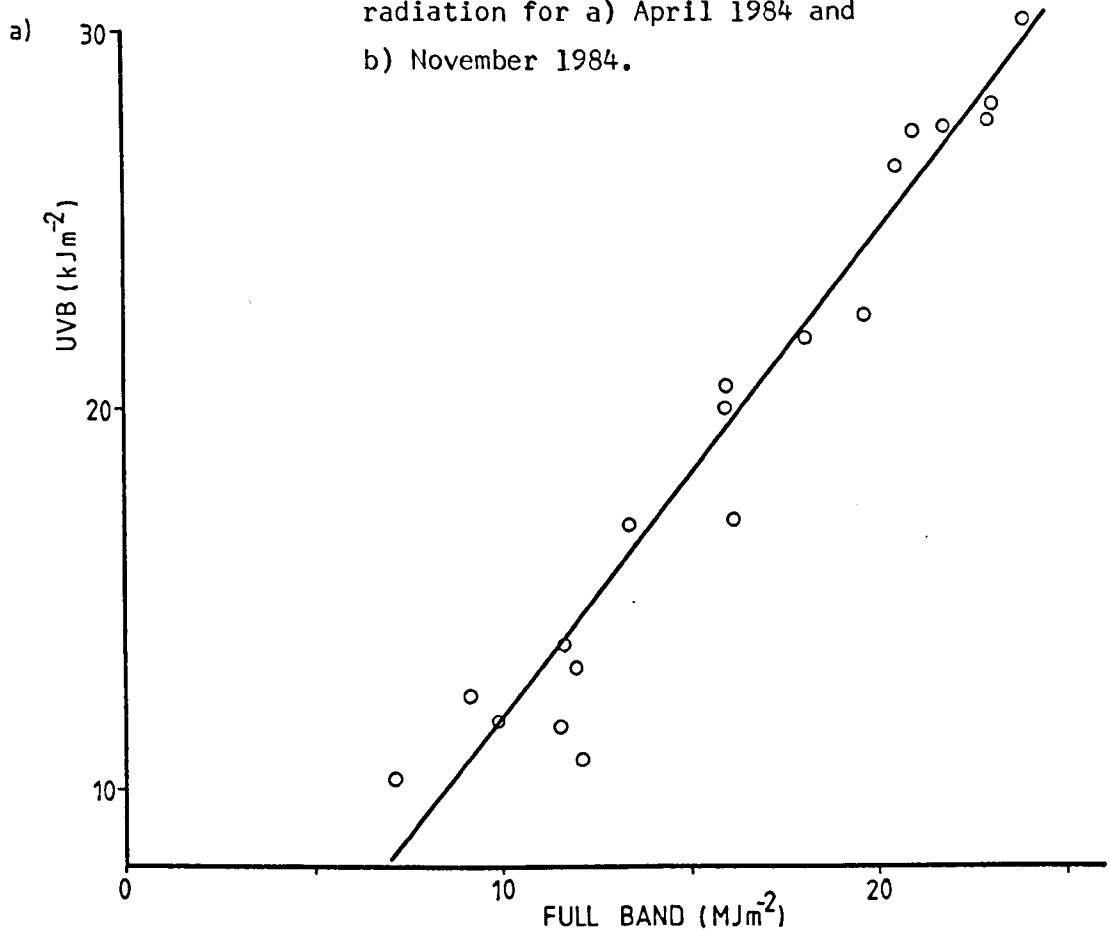


Fig. 6.7

Daily totals of UVB and fullband radiation for a) April 1984 and b) November 1984.



As  $\Sigma I_B$  must be zero when  $\Sigma I_F$  is zero, the intercept  $\eta$  might be expected to be zero (or negative). This is not the case, but for all months except January, March and July 1984 and October 1983, the value of  $\eta$  is less than twice its standard error, and may therefore be considered to be not significantly different from zero. As Sutton Bonington is too far south of the Arctic circle for conditions approaching zero daylight there are no measurements close to complete darkness, and the relative behaviour of the two wavebands under these conditions is uncertain. The values of  $\eta$  are therefore assumed to be zero, and eqn 6.26 becomes

$$\Sigma I_B = \rho \Sigma I_F \quad (6.27)$$

$\rho$  represents the ratio of daily UVB to daily fullband solar radiation under all meteorological conditions for each month.

To represent the zenith angle associated with each value of  $\rho$  the zenith angle at noon (Sivkov, 1971) on the 15th day of each month ( $Z_m$ ) was calculated.

The monthly values of  $\rho$  are different for the two years 1983 and 1984, although the pattern of decreasing  $\rho$  with increasing  $Z_m$  is similar. Of the other variables likely to affect  $\rho$ , data was available only for ozone concentration. In 1983 the amount of atmospheric ozone was consistently ~ 10% lower than for the corresponding month in 1984 (Table 6.3). The 1983 values of  $\rho$  were therefore corrected to the 1984 ozone levels by multiplying by the correction factor  $C_o$  where

$$C_o = \exp(-k[O_3^4 - O_3^3] \cdot m_m) \quad (6.28)$$

**Table 6.2**  $\rho$  and  $\eta$  for each month of 1983 and 1984

| Month     | $\rho$ ( $\times 10^{-3}$ ) |                 |                | $\eta$ ( $\text{kJ m}^{-2}$ ) |                  |
|-----------|-----------------------------|-----------------|----------------|-------------------------------|------------------|
|           | 1984                        | 1983            | Corrected 1983 | 1984                          | 1983             |
| January   | 0.39 $\pm$ 0.05             |                 |                | 0.52 $\pm$ 0.14               |                  |
| February  | 0.73 $\pm$ 0.07             |                 |                | 0.61 $\pm$ 0.38               |                  |
| March     | 0.85 $\pm$ 0.05             |                 |                | 1.23 $\pm$ 0.34               |                  |
| April     | 1.25 $\pm$ 0.10             |                 |                | -0.60 $\pm$ 1.71              |                  |
| May       | 1.28 $\pm$ 0.05             |                 |                | 1.30 $\pm$ 0.74               |                  |
| June      | 1.35 $\pm$ 0.08             | 1.55 $\pm$ 0.11 | 1.38           | 2.03 $\pm$ 1.40               | 1.40 $\pm$ 2.14  |
| July      | 1.22 $\pm$ 0.09             | 1.50 $\pm$ 0.11 | 1.30           | 4.07 $\pm$ 1.82               | -0.72 $\pm$ 2.17 |
| August    | 1.24 $\pm$ 0.16             | 1.33 $\pm$ 0.13 | 1.16           | 1.01 $\pm$ 2.59               | 0.70 $\pm$ 2.35  |
| September | 1.09 $\pm$ 0.12             | 1.13 $\pm$ 0.05 | 0.93           | 1.92 $\pm$ 1.00               | 1.64 $\pm$ 0.62  |
| October   | 0.87 $\pm$ 0.14             | 0.87 $\pm$ 0.10 | 0.58           | -0.18 $\pm$ 1.05              | 2.07 $\pm$ 0.70  |
| November  | 0.87 $\pm$ 0.08             | 0.81 $\pm$ 0.12 | 0.48           | -0.12 $\pm$ 0.15              | 0.31 $\pm$ 0.26  |
| December  | 0.47 $\pm$ 0.04             |                 | 0.28           | 0.19 $\pm$ 0.09               |                  |

Table 6.3 Monthly mean ozone values used to correct 1983  $\rho$  values, and monthly mean  $\cos z_m$ .

| Month     | $\cos z_m$ | $[O_3]$ (matm cm) |      |
|-----------|------------|-------------------|------|
|           |            | 1983              | 1984 |
| January   | 0.278      | 297               | 366  |
| February  | 0.411      | 327               | 342  |
| March     | 0.588      | 333               | 373  |
| April     | 0.740      | 411               | 366  |
| May       | 0.833      | 393               | 421  |
| June      | 0.869      | 341               | 370  |
| July      | 0.847      | 321               | 355  |
| August    | 0.769      | 324               | 354  |
| September | 0.633      | 300               | 333  |
| October   | 0.465      | 291               | 335  |
| November  | 0.311      | 273               | 319  |
| December  | 0.240      | 299               | 334  |

where  $O_3^3$  and  $O_3^4$  are monthly mean ozone amounts for 1983 and 1984.  $m_m$  is  $\sec z_m$  and  $k$  is mean ozone absorption coefficient for the waveband 300-316 nm =  $3.546 \text{ (atm cm)}^{-1}$ .

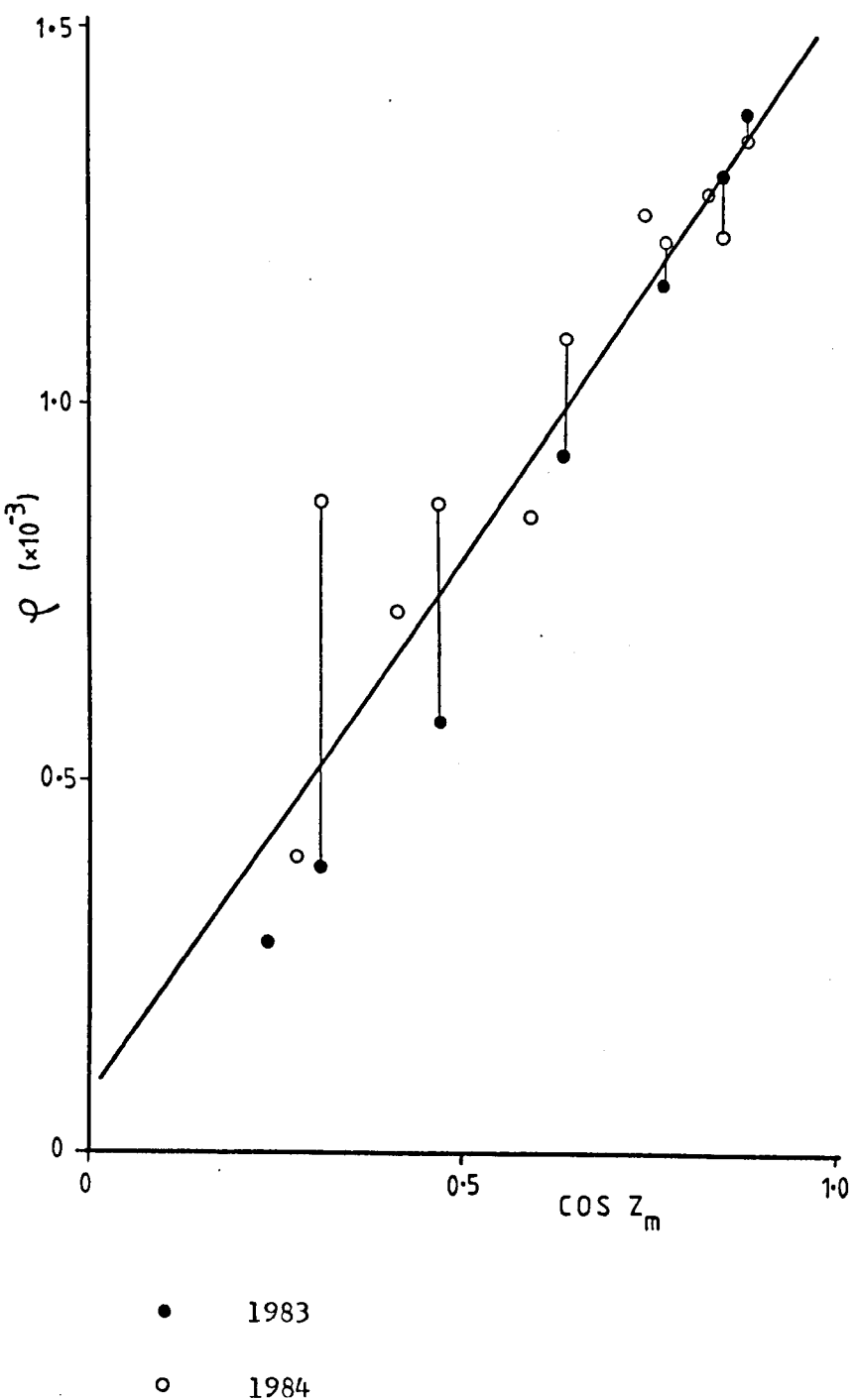
The corrected figures for  $\rho$  are given in Table 6.2 and are plotted against  $\cos z_m$  in Fig. 6.8 together with values of  $\rho$  for 1984.

A line fitted to these data gave the relation

$$\rho = \frac{\Sigma I_B}{\Sigma I_F} = (1.45 \times 10^{-3}) \cos z_m + 8 \times 10^{-5}, \quad (6.29)$$

$r = 0.94$

Fig. 6.8  $\rho$  vs  $\cos z_m$  for months in 1983 and 1984.



Some of the scatter about this line can be attributed to the annual ozone cycle, which is not synchronised with the zenith angle cycle. Fig. 6.9 shows that the maximum and minimum ozone amounts occur one month before the highest and lowest values of  $\cos z_m$ . As maximum amount of ozone implies minimum UVB while maximum  $\cos z_m$  gives maximum irradiation the two cycles work in opposition as well as being out of phase. In order to remove the ozone dependency from the relationship between  $\rho$  and  $\cos z_m$ , the values for  $\rho$  were normalised to an arbitrary ozone amount of 350 matm cm using a correction factor  $C_m$  similar to  $C_0$  (eqn 6.28) with

$$C_m = \exp(-\bar{k}[0.350 - O_3] m_m) \quad (6.30)$$

where  $O_3$  is the mean amount of ozone for any given month.

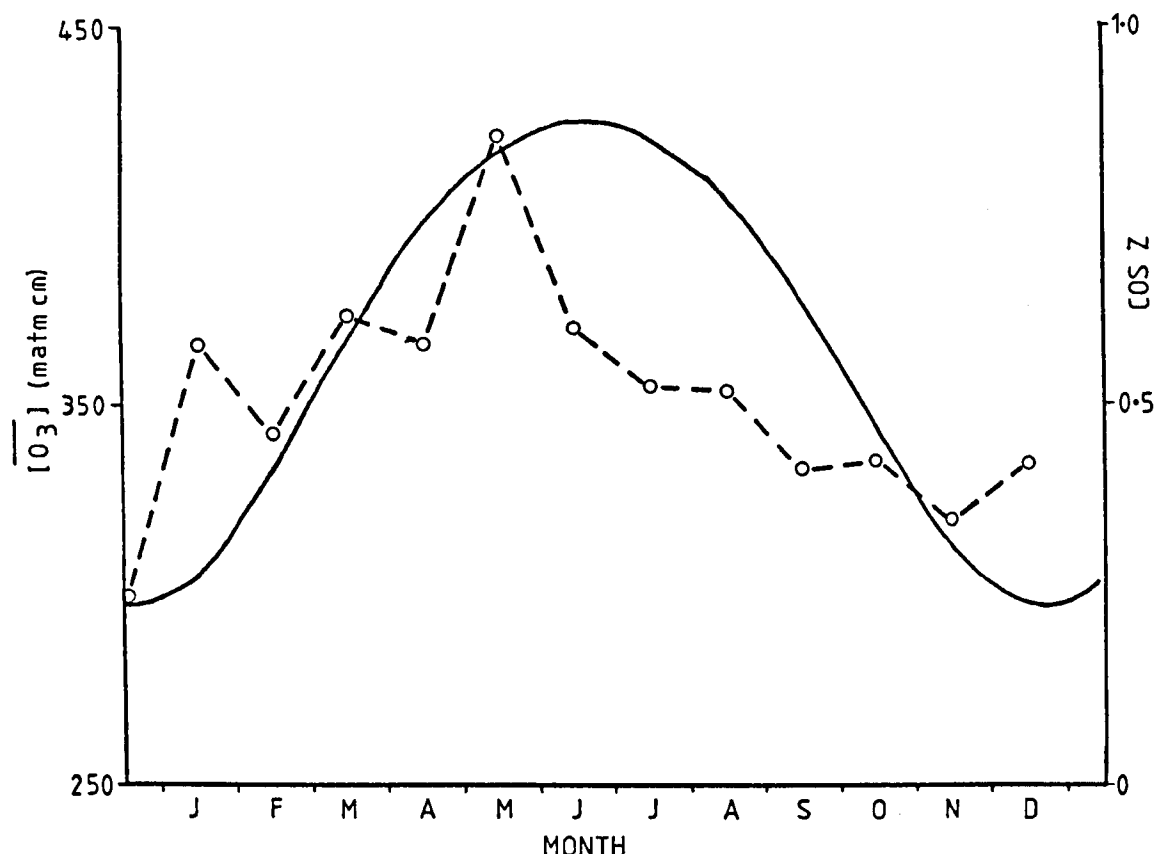
Normalised values  $\rho_n$  are plotted against  $\cos z_m$  in Fig. 6.10 for 1984. The fitted line for these points is given by

$$\rho_n = (\Sigma I_B / \Sigma I_F)_n = (1.62 \times 10^{-3}) \cos z_m - 2 \times 10^{-5}, \quad (6.31)$$

$$r = 0.97$$

Equation 6.31 enables the daily integrated UVB radiation to be estimated from standard meteorological measurements of the daily integrated full solar radiation. Given the date and latitude at which observations were made  $\cos z_m$  can be calculated for any location. With no additional information the error of the estimate of  $\Sigma I_B$  is potentially large, and is due mainly to the magnitude of the departure in ozone amount from the standard value of 350 matm cm. In Britain the annual range of ozone amounts is 300 to 400 matm cm, giving a

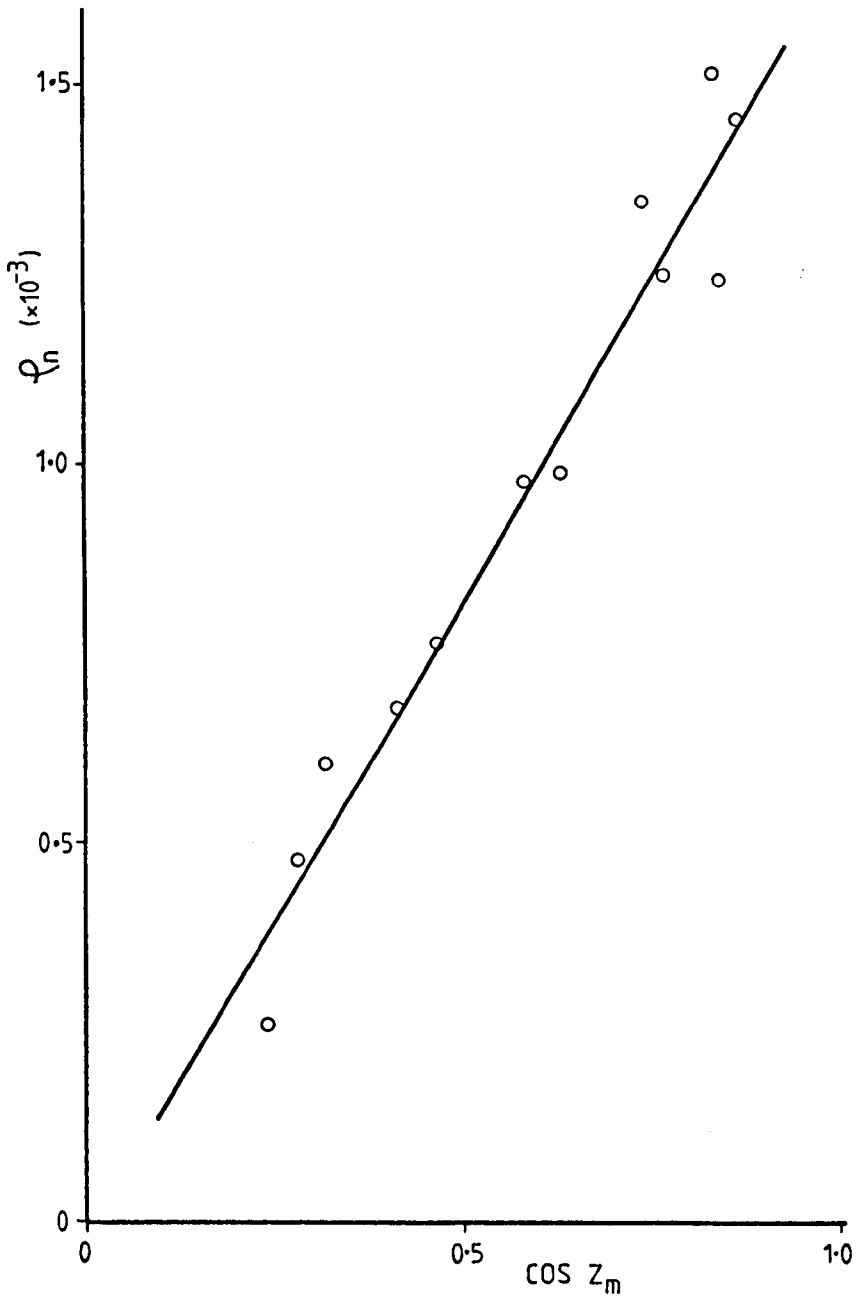
Fig. 6.9 Annual cycles of monthly mean ozone amount and  $\cos z$ .



— Annual  $\cos z$  cycle.

-- Annual cycle of monthly mean ozone amounts (1984 values).

Fig. 6.10 Normalised  $\rho$  values vs  $\cos z_m$  for 1984.



maximum error (for 50 matm cm departure in December) of 23%. A similar change in ozone in June results in a 12% error. However, if a figure for the amount of atmospheric ozone is available, either as a climatological value for the monthly mean or a daily value, then the resulting  $\Sigma I_B$  from eqn 6.31 can be corrected by means of eqn 6.30, and the error of the estimate is reduced to that of the error in eqn 6.31.

The standard errors of the slope and intercept in eqn 6.31 are 0.12 and 0.077 respectively, giving

$$\rho_n = (1.62 \pm 0.12) \times 10^{-3} \cos z_m - (0.02 \pm 0.077) \times 10^{-3} \quad (6.32)$$

The intercept is not significantly different from zero ( $P < 0.01$ ) and therefore

$$\Sigma I_B = (1.62 \pm 0.12) \times 10^{-3} \Sigma I_F \cos z_m / C_m \quad (6.33)$$

allowing the daily integrated total of UVB radiation to be estimated from routine meteorological measurements of daily full solar waveband radiation totals and ozone amount.

#### Diffuse UVB Radiation

The diffuse UVB radiation was recorded regularly from July 1984 to March 1985 using a SEE 240 vacuum photodiode mounted under a standard UK Meteorological Office shade-ring of width 5 cm and radius 25.4 cm. Diffuse spectral scans were also made with the LI1800 spectroradiometer on selected clear days in 1983 and 1984 using a blackened disc (diameter 15.5 cm, held 90 cm from the sensor) to occlude a  $10^{\circ}$  circumsolar region of the sky. The discrepancy between the two systems,

with the geometric plus empirical shade-ring correction applied to the SEE 240 values (Chapter 4), was  $\pm 4\%$ . Results presented use data from both measuring devices. Diffuse irradiance readings for the full solar waveband (300-3000 nm) were taken from a Kipp solarimeter fitted with a shade-ring and similarly corrected.

The ratio of diffuse to global radiation

The concept of a 3-layer atmospheric model [ a) stratospheric ozone absorption; b) tropospheric Rayleigh scattering; c) boundary layer aerosol (Mie) scattering] introduced in Chapter 5.3 is used again in the consideration of diffuse radiation.

The ratio of diffuse to global radiation is an indication of the amount of scattering from the direct beam that has taken place along the path of the radiation through the atmosphere. As ozone absorption takes place well above the tropospheric scattering layers the diffuse to global UVB ratio  $(D/I)_B$ , should be independent of ozone amount. The factors affecting this ratio are then scattering in the atmosphere and the pathlength of the radiation.

Dispersal of light from the direct beam takes place mainly in the troposphere, by Rayleigh scattering. As Rayleigh scattering is proportional to  $\lambda^{-4}$  the fraction of diffuse radiation in the UVB waveband is consequently much greater than in the full solar waveband. Secondary scattering by aerosol occurs in the lower troposphere and is much less dependent on wavelength (Mie scattering). Table 6.4 shows the ratio  $(D/I)$  for clear conditions at 1200 GMT throughout the year for the UVB and full solar wavebands.

Table 6.4 Annual variation of  $(D/I)_B$  and  $(D/I)_F$  at 1200 GMT on clear days.

| Date     | $(D/I)_B$          | $(D/I)_F$ |
|----------|--------------------|-----------|
| 9. 2.84  | 0.89               | 0.21      |
| 12. 2.85 | 0.94*              | 0.51      |
| 25. 4.84 | 0.63               | 0.27      |
| 12. 7.83 | 0.74               | 0.29      |
| 15. 7.83 | 0.81               | 0.36      |
| 21. 7.83 | 0.61               | 0.29      |
| 24. 7.84 | 0.60 ( $\pm$ 2%)*  | 0.26      |
| 28. 7.83 | 0.63               | 0.32      |
| 1. 8.84  | 0.60*              | 0.26      |
| 5. 8.83  | 0.58               | 0.20      |
| 25. 8.83 | 0.76               | 0.55      |
| 24.10.83 | 0.71               | 0.23      |
| 14.11.83 | 0.90               | 0.23      |
| 23.11.83 | 0.93               | 0.27      |
| 18.12.84 | 1.00 ( $\pm$ 20%)* | 0.40      |

$(D/I)_B$  measured with LI1800 spectroradiometer

\* Values from SEE 240 also available and consistent with LI1800.

The range of clear-day noon  $(D/I)$  values for the UVB is 0.58 to 1.00, compared with 0.2 to 0.55 for the full solar waveband. The lowest value of  $(D/I)_B$  recorded was 0.56 at 1440 on 20 June 1983, so at the latitude of Sutton Bonington the UVB radiation is always at least 50% diffuse.

The general trend of  $(D/I)_B$  throughout the year follows the expected pattern, with the ratio decreasing in the summer when pathlength is short and increasing in winter when the scattering pathlength traversed is longer. However there is no clear relationship between  $(D/I)_B$  and zenith angle, and anomalies occur at both wavebands (e.g. 25 April 1984 and 15 July 1983).

Further illustration of the lack of close correlation between pathlength and  $(D/I)_B$  is given in Fig. 6.11. This shows the daily variation of  $(D/I)_B$  for two clear days at the same time of year when the sun follows the same path across the celestial hemisphere. Both plots show an asymmetry about noon but to different extents, and  $(D/I)_B$  at a given time (zenith angle) differs by  $\pm 0.05$  ( $\sim 8\%$ ) from day to day.

The deviations of  $(D/I)$  from any systematic relationship with zenith angle imply a further fluctuating influence on the degree of scattering that takes place in the atmosphere. This may be attributed to the lower layers of the troposphere and the aerosol contained therein.

All measurements of  $(D/I)$  were made under 'clear' sky conditions but a visually cloudless sky gives no indication of the aerosol content of the air mass. When considering the absolute levels of UVB irradiation, aerosol content was largely disregarded as being of negligible influence in comparison with the absorption by ozone. However, when considering  $(D/I)$  which is independent of ozone absorption, aerosol can no longer be neglected.

No additional measurements of atmospheric turbidity were made and it is not possible to give any quantitative discussion of the effect of

Fig. 6.11 Daily variation of  $(D/I)_B$  with zenith angle for 2 clear days.

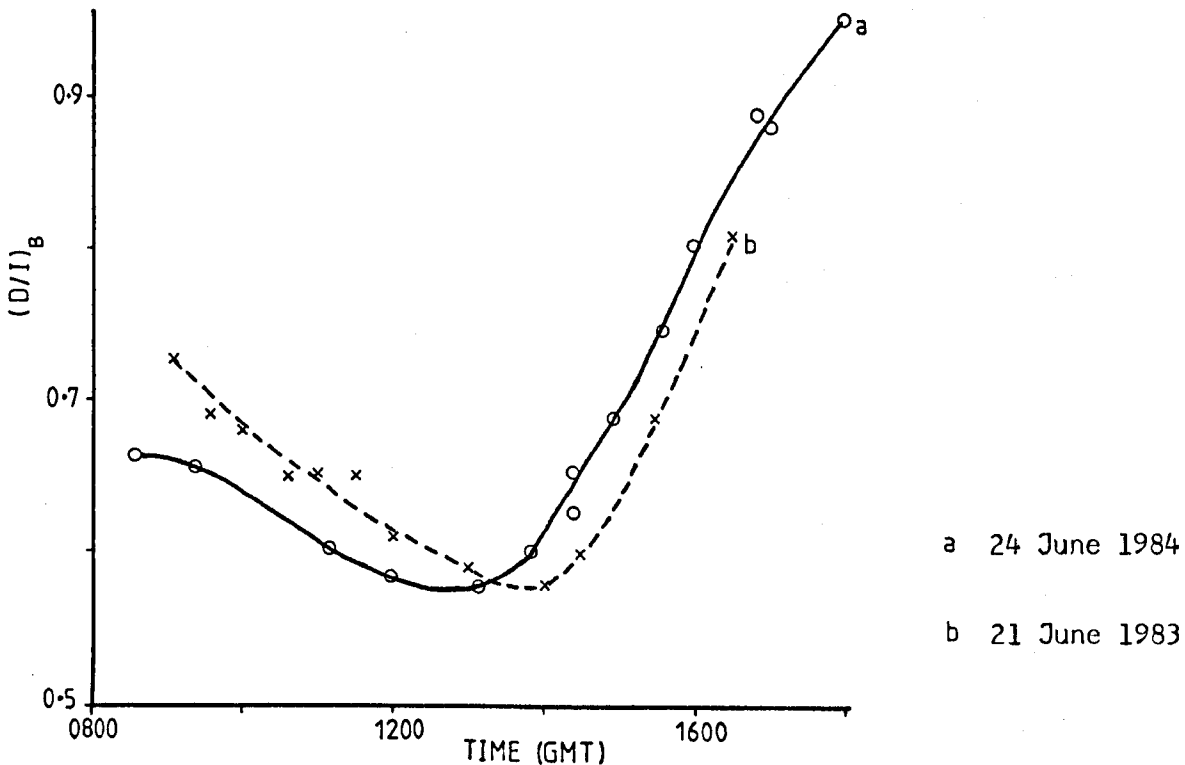
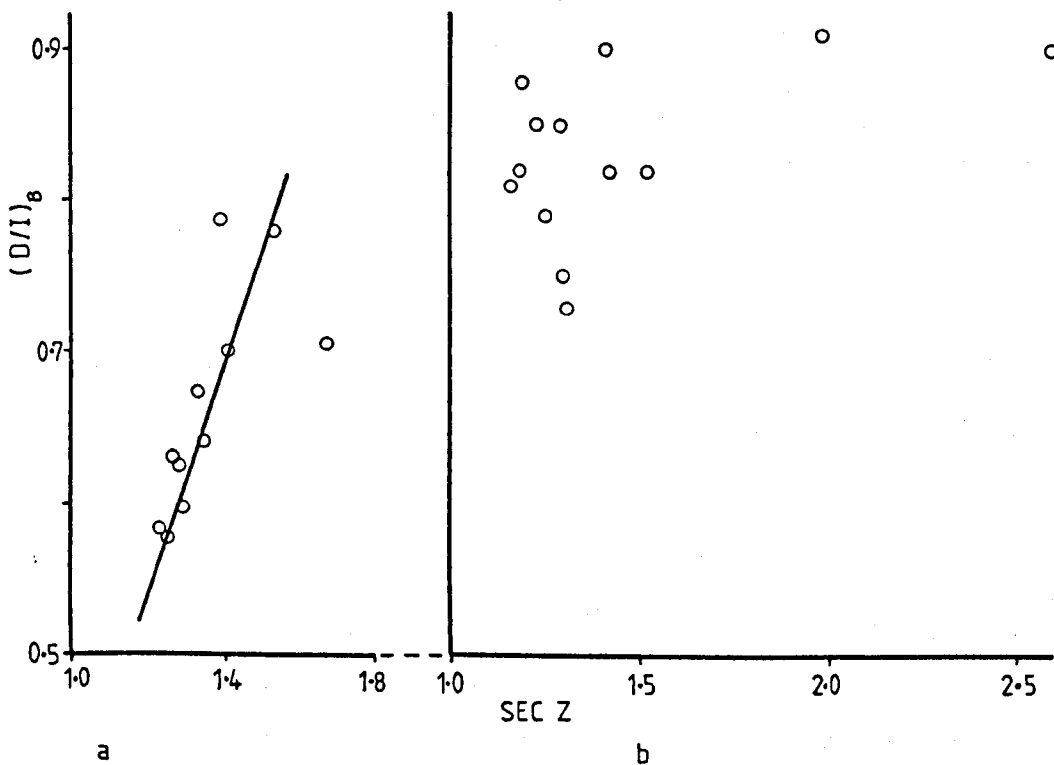


Fig. 6.12  $(D/I)_B$  vs  $\sec z$  for 2 days with  
a) low turbidity and b) high turbidity.



aerosol on the scattering of UVB radiation. The changing turbidity affects different wavebands to varying degrees, depending on the wavelength of radiation and the size distribution and nature of the aerosol particles. This can be seen from Table 6.4 where changes from month to month in  $(D/I)_F$  differ quite markedly in degree if not in general direction from the corresponding changes in  $(D/I)_B$ .

The relative strength of the two scattering processes, Rayleigh and Mie also vary with wavelength and the type of aerosol. On days with low and constant turbidity the relationship between  $(D/I)$  and pathlength is stronger than on days with high or varying turbidity as the dominant Rayleigh scattering has a constant attenuating coefficient. Fig. 6.12 illustrates this with a plot of  $(D/I)_B$  against  $\sec z$  for two days: a) August 1983, a day with low  $(D/I)$  values for the time of year, implying low turbidity; b) July 1983, a day with anomalously high  $(D/I)$  values, indicating high turbidity. The linearity of plot a) contrasts well with the scatter of plot b). The behaviour of the quantity  $(D/I)_F$  is again similar only in the general trend of its dependence on  $\sec z$  because of the different balance between Rayleigh and aerosol scattering for the full 300-3000 nm waveband. In particular the infra-red component of the full solar waveband is affected by water vapour absorption, a further atmospheric variable which introduces additional deviation from a simple proportionality between  $(D/I)_F$  and  $\sec z$ .

The aerosol scattering will also have a dependence on zenith angle and as turbidity can be assessed, in the absence of other measurements, by  $(D/I)_F$  (Unsworth and Monteith, 1972), a relation was sought between  $(D/I)_B$  and  $(D/I)_F$  on individual days, and then for limited ranges of zenith angle.

Data for individual days showed no consistent relation between  $(D/I)_B$  and  $(D/I)_F$ . There was a clear linearity between the two quantities on certain dates, while at other times no such relation could be inferred (Fig. 6.13). This analysis supports the preliminary findings of Webb and Steven (1984) who report a similar inconsistency for daily plots of  $(D/I)_B$  and  $(D/I)_V$ , the visible waveband ratio. The interplay of changing zenith angle and fluctuating aerosol components, and the effect of this on the two wavebands considered, might explain the deviation of results both within and between days.

To remove some of the zenith angle dependence of the atmospheric scattering  $(D/I)_B$  was plotted against  $(D/I)_F$  over 3 limited ranges of sun angle with values of  $\cos z$  in the ranges 0.55 to 0.65, 0.65 to 0.75 and 0.75 to 0.85. Fig. 6.14 shows only a weak relation between the diffuse to global radiation ratios in the two wavebands. To remove further zenith angle dependence more measurements are needed than are available.

The transient nature of atmospheric aerosol and its wavelength-dependent scattering function, combined with the zenith angle dependence of scattering, means that further study is required before estimates of diffuse UVB radiation can be attempted from routine measurements of full band diffuse radiation. A first consideration might be the removal of the zenith angle dependence from the atmospheric scattering process by gathering sufficient data to enable plots similar to Fig. 6.14 to be made at single values of  $\cos z$ . Some measure of aerosol type and content would then give scope for further analysis.

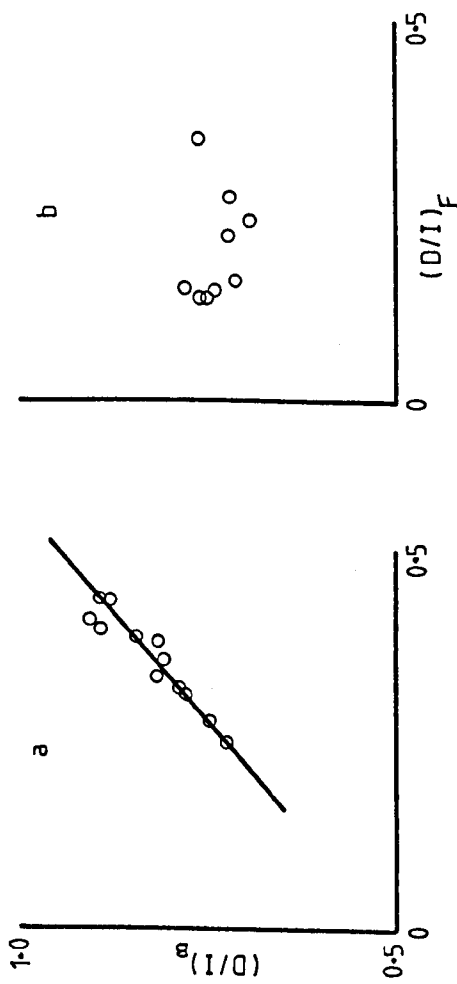


Fig. 6.13  $(D/I)_B$  vs  $(D/I)_F$  for 2 clear days.

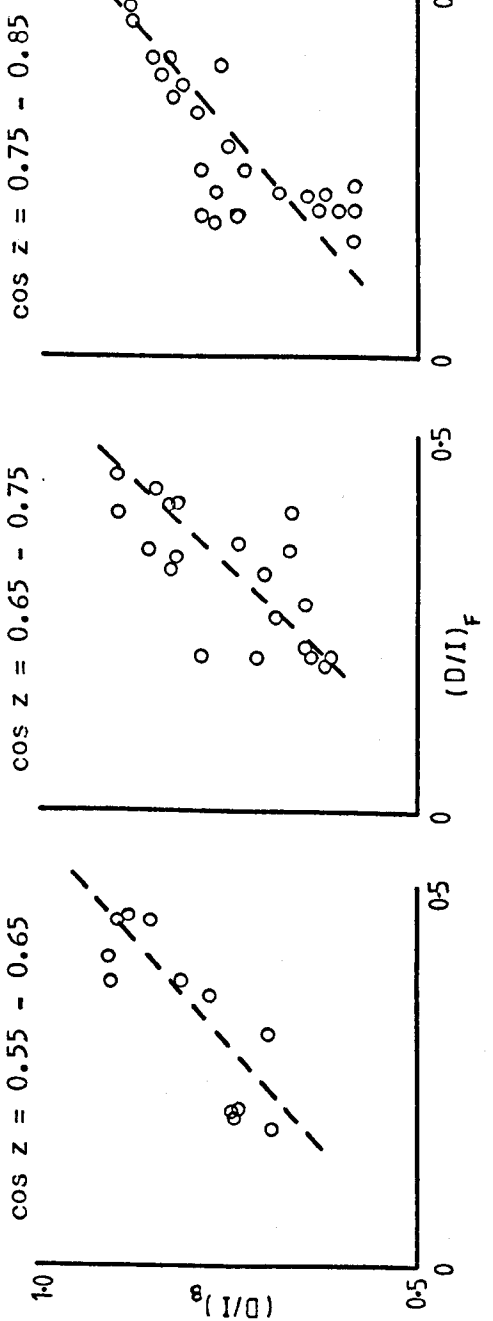


Fig. 6.14  $(D/I)_B$  vs  $(D/I)_F$  for 3 limited ranges of sun angle.

### Anisotropy of UVB radiation

Diffuse radiation is often assumed to have an isotropic angular distribution across the sky, but in general there is a brighter region of sky towards the sun. The distribution of diffuse radiation under clear sky conditions is determined by solar zenith angle and atmospheric turbidity (Steven, 1977). Steven (1984) showed that shade-ring measurements may be used to estimate the anisotropy of diffuse radiation and hence avoid the errors that can be introduced by an isotropic assumption when calculating the illumination of oriented surfaces.

Steven and Unsworth (1980) showed that the shade-ring correction SRC can be expressed as

$$\text{SRC} = \frac{D_{\text{disc}}}{D_{\text{ring}}} = \left(1 - \frac{D_s}{D_{\text{disc}}}\right)^{-1} = \left(1 - q \frac{D_{s_0}}{D_{\text{disc}}}\right)^{-1} \quad (6.34)$$

where  $D_{\text{disc}}$  is the true diffuse irradiance from the sky, measured using a shading disc,  $D_{\text{ring}}$  is diffuse irradiance measured with the shade-ring in place,  $D_s$  is component of diffuse irradiance occluded by the ring,  $D_{s_0}$  is  $D_s$  under isotropic conditions and  $q$  is an anisotropic factor  $D_s/D_{s_0}$ , the ratio of the true value of occluded radiation to its theoretical value under an isotropic sky.

The isotropic component of eqn 6.34 is a function only of time, position and shade-ring dimensions, and may be written

$$\frac{D_{s_0}}{D_{\text{disc}}} = 2\omega r^{-1} \pi^{-1} \cos^3 \delta f'$$

where  $f' = t_o \sin \lambda \sin \delta + \sin t_o \cos \lambda \cos \delta$ ,  $\lambda$  is latitude,

$\delta$  is solar declination,  $t_0$  is hour angle (radians) of sunrise/sunset from solar noon,  $w$  is ring width and  $r$  is ring radius.

Steven (1984) modelled the radiance distribution of solar radiation from clear skies as a background radiance plus a circumsolar component to show that

$$\frac{D_s}{D_{s_0}} = 1 - C_* \xi_*^! + C_* f' \quad (6.35)$$

The anisotropy factor  $q$  is then a function of three parameters.  $f'$  is a geometric term describing the relative positions of shade-ring and sensor;  $C_*$  expresses the relative strength of the circumsolar component of radiation;  $\xi_*^!$  is a measure of the angular width of the circumsolar region and appears because a finite slice of the circumsolar region is occluded by the shade-ring. The smaller  $\xi_*^!$  the larger the fraction of the total solid angle of this brighter region that is occluded.

By plotting  $D_s/D_{s_0}$  against  $1/f'$  it is possible to obtain values for  $C_*$  and  $\xi_*^!$ .

$D_s/D_{s_0}$  can be calculated from shade-ring correction measurements if the geometric ring correction  $g_r$  (for isotropic conditions) is known.

$$g_r = (1 - D_{s_0}/D_{disc})^{-1} \quad (6.36)$$

and combining this with eqn 6.34 gives

$$\frac{D_s}{D_{s_0}} \approx (1 - (SRC)^{-1})/(1 - g_r^{-1}) \quad (6.37)$$

Using values of  $g_r$  calculated by Steven for Sutton Bonington, and values of SRC measured for solar UVB radiation,  $D_s/D_{s_0}$  and  $1/f'$  were calculated for 10 clear days.

A plot of  $D_s/D_{s_0}$  against  $1/f'$  is shown in Fig. 6.15. The error bars indicate the uncertainty in  $D_s/D_{s_0}$  resulting from the uncertainty in the SRC values, which were mean values for the day,  $\overline{\text{SRC}} \pm 0.01$ . For  $z < 75^\circ$  the SRC may be taken as constant during the day (LeBaron, et al., 1980; Steven and Unsworth, 1980).

The equation of the line is

$$D_s/D_{s_0} = 0.36/f' + 0.72 \quad (6.38)$$

giving the relative strength of the circumsolar region  $C_*$  as 0.36, and the angular width of this region  $\xi_*$  as 0.78 radians. This compares with values of 1.10 and 0.60 radians for the full solar waveband at  $50^\circ$  latitude as calculated by Steven (1984).

Anisotropy in the UVB waveband is almost entirely due to the anisotropy of Rayleigh scattering, whereas a large mean component of Mie scattering by aerosol is included in the broadband results.

Mie scattering is generally stronger (hence a larger  $C_*$ ) and more concentrated in the forward direction (hence a smaller  $\xi_*$ ), giving a stronger but narrower circumsolar region for broadband radiation compared with that for the Rayleigh scattered UVB.

#### Illumination of Vertical Surfaces

##### General theory

The irradiance of inclined surfaces is important in assessing the radiation received by an object in many practical exposure studies.

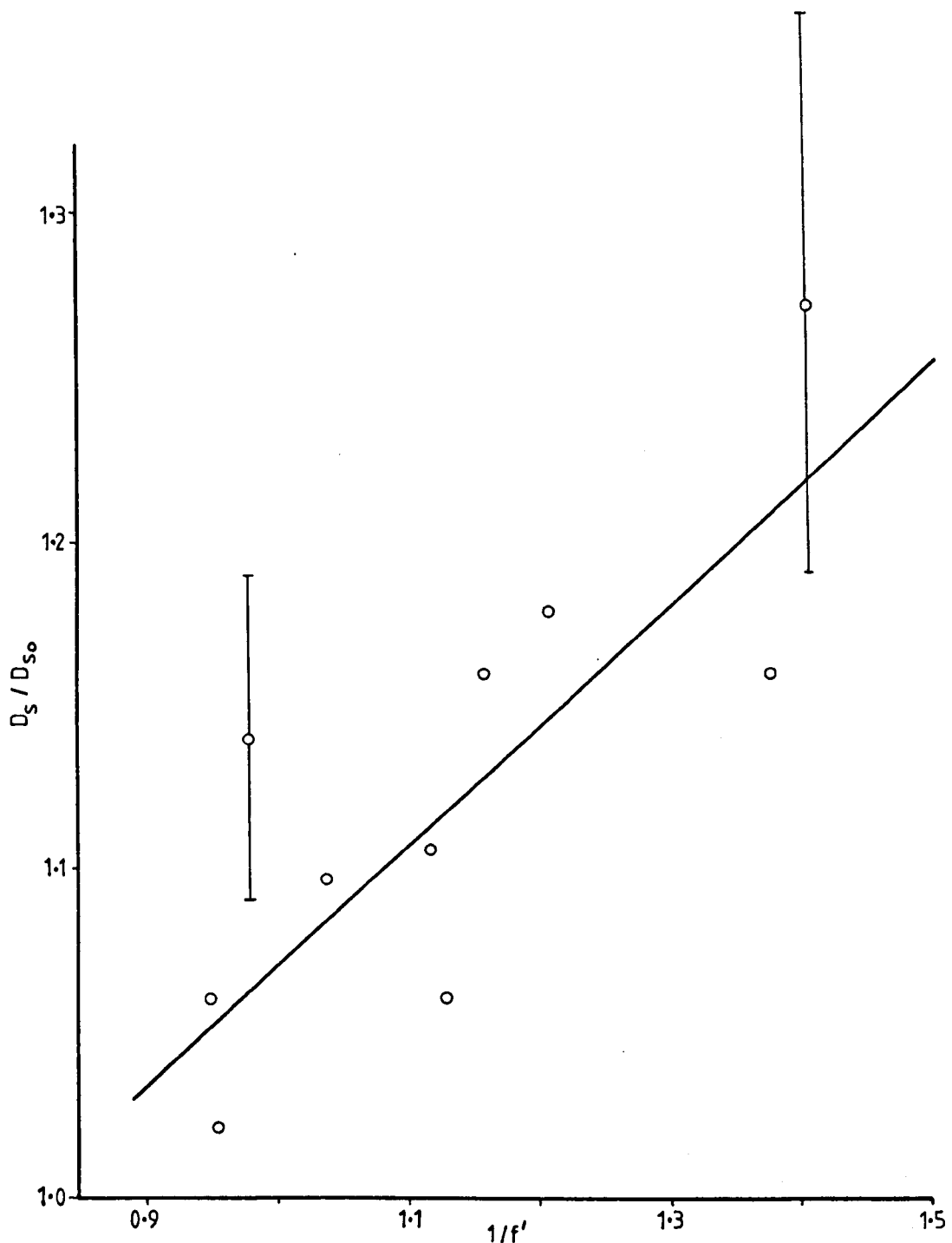


Fig. 6.15  $(D_s / D_{s_0})$  vs  $1/f'$  for 10 clear days.

The error bars are a result of the uncertainty in the SRC.

The component of direct beam irradiance incident on a sloping surface (Fig. 6.16) is given by

$$B_i = B' [\cos z \cos i + \sin z \sin i \cos (\phi - \phi_n)] \quad (6.39)$$

where  $B_i$  is the direct beam radiation flux on the sloping surface,  $B'$  is the direct beam solar radiation on a surface normal to the sun's rays,  $i$  is the angle of slope from the horizontal,  $\phi$  is azimuth angle of sun,  $\phi_n$  is azimuth angle of the normal to the slope and  $z$  is zenith angle. For a vertical surface eqn 6.39 simplifies to

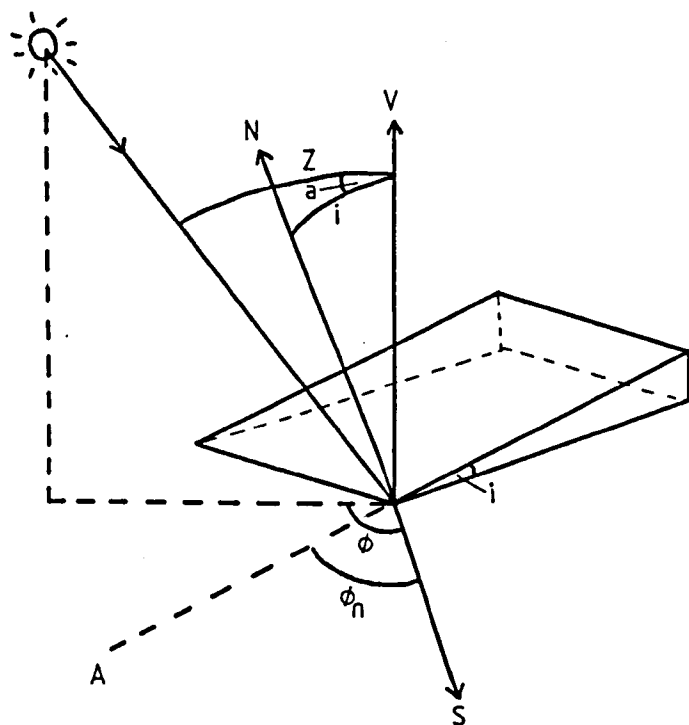
$$B_L = B' \sin z \cos (\phi - \phi_n) \quad (6.40)$$

where  $B_L$  is direct beam radiation flux on a vertical surface.

The daily and annual changes in direct beam illumination of a vertical surface are a function of  $\phi_n$ . A south facing wall ( $\phi_n = 0$ ) always receives maximum intensity at solar noon, and (at  $53^{\circ}$  N) is shaded from the direct beam only during early morning and late evening in the summer months, when sunrise and sunset are in the NE and NW quadrants of the hemisphere (Fig. 2.1). By contrast a north facing wall ( $\phi_n = 180^{\circ}$ ) receives direct beam illumination only at the times when the south facing wall is in shade. East and west facing slopes ( $\phi_n = \pm 90^{\circ}$ ) have no direct beam irradiance in the afternoon and morning respectively. The time of maximum intensity varies on these faces throughout the year: the beam is nearest normal to the surface early or late in the day respectively, but the rays are most intense at noon.

The total radiation intercepted by a vertical surface is the sum of direct and diffuse radiation components. Diffuse radiation is far less susceptible to the direction of the receiving slope but due to the

Fig. 6.16 Diagram of direct beam irradiance on a sloping surface.



S South

N Normal to slope

V Vertical

Z Solar zenith angle

A Azimuth of normal

a  $\phi - \phi_n$

i Angle of slope from horizontal

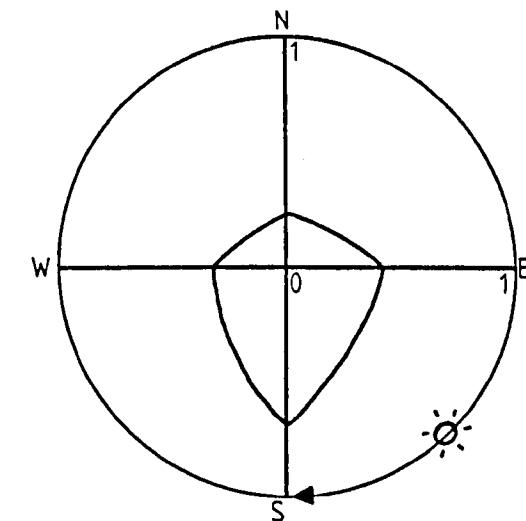
anisotropy of the scattered radiation the greatest irradiance is still expected on south facing slopes with least on north facing walls, east and west slopes being intermediate and dependent on time of day.

Applying these general principles to UVB radiation the directional dependence of diffuse radiation assumes a greater importance than for total solar radiation as at least 50% of UVB radiation is always diffuse. At low angles (in winter, near sunrise and sunset) over 90% of UVB is diffuse. This means that illumination of a north facing slope will be almost entirely by diffuse radiation at all times of year as the only direct beam irradiation would be early and late in the day during the winter months, at which times there is virtually no direct beam UVB.

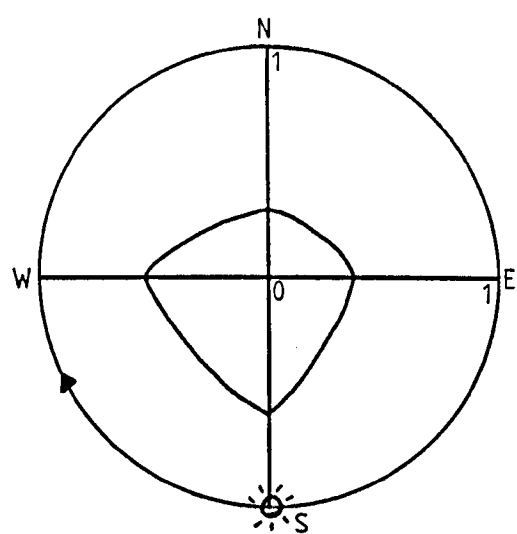
#### Daily UVB irradiance of vertical surfaces

Measurements of the UVB radiation incident on vertical surfaces were made using polysulphone film badges (Chapter 7). Four badges were mounted on a vertical pole 0.5 m above the ground and orientated to face north, south, east and west. Badges were exposed in this manner over the same periods of time for which badges were exposed horizontally on the meteorological site i) on 13 days from August to October 1983 during initial calibration of the polysulphone film; ii) on weekdays during the January and June exposure trials at Sutton Bonington in 1984 (Chapter 7), giving 9 sets of badges which had been exposed over a period of 5 days each.

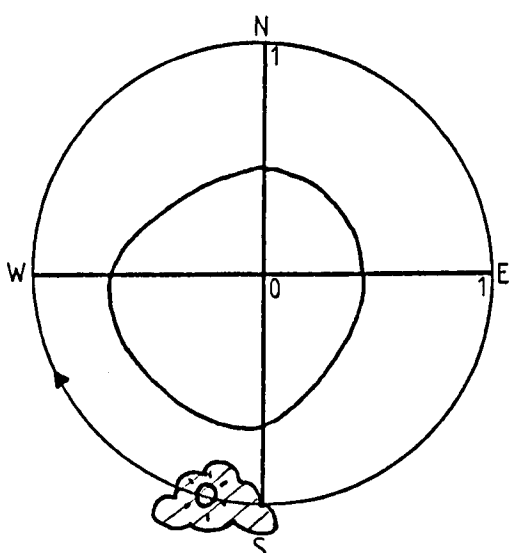
The total incident UVB on vertical surfaces facing N, S, E and W is shown in Fig. 6.17, normalised to the irradiation on a horizontal



a) 18 Aug. 1983, 1000 → 1150



b) 18 Aug. 1983, 1203 → 1515



c) 20 Oct. 1983, 1300 → 1545

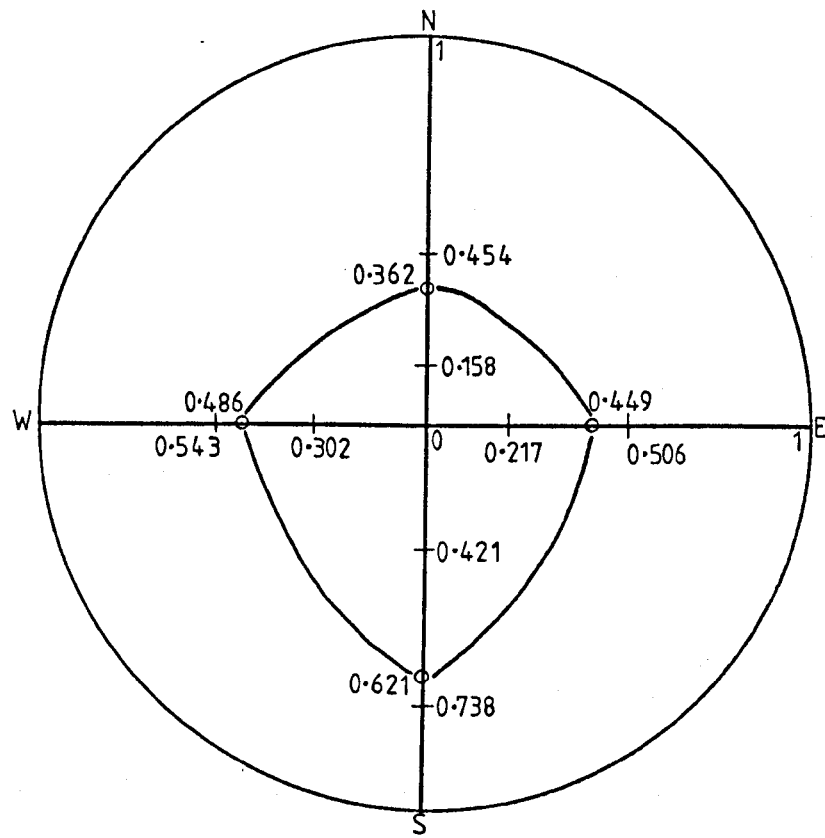
Fig. 6.17 The irradiation of vertical surfaces  
normalised to the corresponding horizontal irradiance.

surface. The diagrams show the incident radiation for the morning and afternoon of 18 August 1983, a largely clear day (there were a few transient clouds during the period), and the afternoon of 20 October 1983, when cloud cover was 8 octas of grey stratus. Figs 6.17a and b illustrate the influence of the direct beam on the irradiation of vertical surfaces. In the morning the east facing slope received more radiation than the west facing surface, while the reverse was true in the afternoon. During both periods illumination of the south facing slope was greatest, always receiving a component of the direct UVB radiation, while the north facing surface received only diffuse radiation and recorded the lowest irradiance levels.

Fig. 6.17c reveals the anisotropy of UVB radiation under cloudy conditions. The north and east surfaces received the same amount of radiation during the exposure period, as did the south and west surfaces. However, the N/E exposure was 67% of the S/W exposure, indicating a brighter region of the hemisphere in the vicinity of the sun, despite the apparently uniform sky observed by a ground-based observer.

All other measurements of vertical irradiation made from August to October 1983 were under changing sky conditions and as such are used only to show the mean and range of normalised exposures received by the variously oriented surfaces (Fig. 6.18). Exposure times varied from 2 hours in the morning or afternoon to 6 hours throughout the day. Some of the irradiances for east and west slopes therefore cover periods with only diffuse incident radiation whereas others include periods with a component of direct irradiation

Fig. 6.18 Mean and range of normalised vertical irradiances for part-day exposures.



Instantaneous and short term values of vertical irradiances depend very much on the conditions at the time of measurement: the state of the sky and the position of the sun with respect to each surface. A more generalised view of the degree of radiation received by oriented surfaces is obtained from measurements made over longer periods of time.

#### Weekly UVB irradiance of vertical surfaces

During the Sutton Bonington exposure trials vertically-mounted badges were exposed for periods of 5 days, from Monday to Friday, being covered only when it rained. The normalised exposure values thus obtained represent the average irradiation of each surface for all times of day and under all sky conditions experienced during each week.

Table 6.5 shows the horizontal exposure, the normalised vertical exposures and the average vertical exposure for two weeks in January and seven weeks in May/June.

Disregarding for a moment the last weeks of January and June, the proportion of horizontal UVB radiation received on vertical surfaces is more consistent from week to week than from day to day as a result of the time/condition averaging. As might be expected the southern face receives most radiation and the northern face least, with east and west taking intermediate values dependent on the relative amounts of sun and cloud conditions before and after midday. The average value of  $V/H$ , or the value which may be applied to a vertical surface randomly oriented over a period of time, is about 0.5 for each week with a range of 0.45 to 0.56.

Table 6.5 Weekly irradiances on horizontal and vertical surfaces.

| Date      | Horizontal irradiance<br>(J cm <sup>-2</sup> ) | V/H   |       |       | Average |         |  |
|-----------|--|-------|-------|-------|---------|---------|--|
|           |  | S     | N     | E     | W       | V/H     |  |
| Jan. 9-13 | 0.567 ( $\pm$ 6%)                              | 0.766 | 0.364 | 0.471 | 0.364   | 0.491   |  |
| 23-27     | 0.660  | 0.785 | 0.653 | 0.549 | 0.549   | 0.634 * |  |
| May 14-18 | 3.95   | 0.686 | 0.418 | 0.559 | 0.545   | 0.552   |  |
| 21-25     | 4.63   | 0.581 | 0.371 | 0.403 | 0.540   | 0.473   |  |
| /Ju 28- 1 | 4.34   | 0.552 | 0.362 | 0.493 | 0.475   | 0.471   |  |
| June 4- 8 | 4.56   | 0.511 | 0.351 | 0.453 | 0.489   | 0.451   |  |
| 11-15     | 5.49   | 0.622 | 0.449 | 0.544 | 0.622   | 0.559   |  |
| 18-22     | 5.73   | 0.677 | 0.408 | 0.469 | 0.527   | 0.520   |  |
| 25-29     | 10.99  | 0.367 | 0.259 | 0.291 | 0.338   | 0.314 + |  |

\* The ground was snow-covered throughout the week giving an increased albedo.

+ The horizontal badge was outside the range of linear film response.

During the week 23-27 January the ground was snow-covered and there were long periods with clear skies on three out of the four days for which badges were exposed. At this time of year very little of the UVB radiation is in the direct beam, but high values of V/H at all points of the compass reveal the effect of increased reflection of light from the snow surface. The incident radiation recorded on the north facing slope is higher than on the eastern and western faces for this week. The elevated V/H value may be the result of a faulty badge or could represent some form of directional reflection from the snow covered ground.

The horizontal badges for 25-29 June were exposed beyond the range of the linear response of polysulphone film to irradiation, and the unreliable value for radiation on a horizontal surface renders all the V/H ratios equally unreliable in magnitude if not in relation to each other.

The most significant relationship found from these measurements (in view of the application discussed in Chapter 8) is that Randomly orientated vertical irradiance is approximately  $0.5 \times$  Horizontal irradiance.

This chapter has explored the broadband features of solar UVB radiation and its relation to other routinely recorded environmental variables. These general measurements have been applied to a specific cause: personal exposure within the natural environment and its influence on vitamin D status (Chapters 7 and 8).

## 7. POLYSULPHONE FILM

### Introduction

The measurements of UVB radiation described in the previous chapter give a climatological account of the radiation incident on a horizontal surface; the available UVB in the natural environment. The efficacy of this radiation for the initiation of cutaneous vitamin D synthesis is largely dependent on individual behaviour patterns governing personal exposure. A population will contain a wide range of individual exposures, the study of which requires an unobtrusive, low maintenance method of monitoring UVB exposure that is cheap and simple enough to be used in large numbers. Personal dosimeter badges of polysulphone film appeared to fulfil these criteria.

### Polysulphone Film

The polymer polysulphone was recognised as a possible UV radiation monitor by Davis, et al (1976) who describe the preparation of the film and their tests of its applicability for personal dosimetry. Since then polysulphone film badges have been used by a number of workers to monitor the exposure to natural UV radiation of different populations - for example: Corless, et al (1979) studied elderly patients in hospital and residential homes; Diffey, et al (1982a) monitored holidaymakers during sun-seeking activities, and Holman, et al (1983) investigated the UV radiation received at various anatomical sites by volunteers in different occupations and engaged upon a variety of outdoor recreational activities. Polysulphone film badges have also been used under artificial sources of UVB: Corless, et al (1978) measured the irradiation of geriatric patients

undergoing UV lamp treatment; Young, et al (1982) tested the film badges on the cages of animals undergoing UV radiation treatment and found them applicable to long-term monitoring of irradiation.

Polysulphone film of thickness 40  $\mu\text{m}$  has a response spectrum similar to that of the vitamin D action spectrum (Fig. 7.1). On exposure to ultraviolet radiation the film degrades and loses tensile properties, while the initial absorption band in the near ultraviolet extends towards the visible. The degree of degradation can be assessed by measuring the change in absorbance of the film at a wavelength of 330 nm ( $\Delta A_{330}$ ). The change in absorbance is proportional to the dose of UV radiation that the badge has received. For monochromatic irradiation at a wavelength of 297 nm the UV dose  $T_p$  in  $\text{J cm}^{-2}$  is related to the change in absorbance by the equation

$$T_p = 4.3 (\Delta A_{330})^{1.38} \quad (7.1)$$

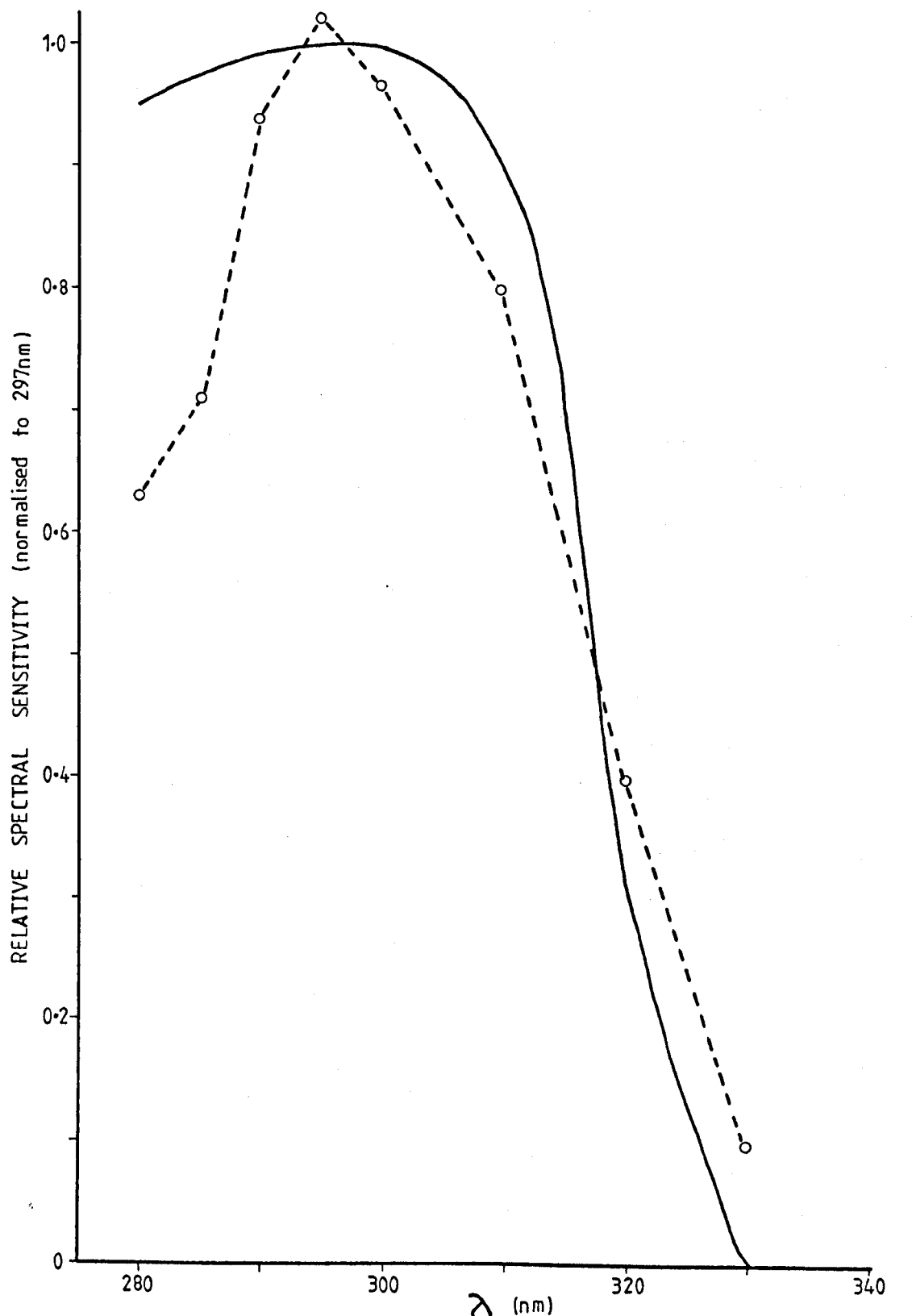
(Diffey, et al 1982b).

To use this equation to convert badge degradation to biologically active UV dose received, the wavelength response of the polysulphone film would have to match exactly the action spectrum of the biological response being studied. As polysulphone film responds to wavelengths up to 330 nm, the UV dose calculated from eqn 7.1,  $T_p$ , would have to be corrected to give an effective biological dose at 297 nm  $T_B$ . This correction is made by the equation

$$T_B = K T_p \quad (7.2)$$

where  $K$  is a dimensionless factor that compensates for the difference

Fig. 7.1 The response spectrum of 40  $\mu\text{m}$  polysulphone film.



— Polysulphone film

— Vitamin D action spectrum (Kobayashi and Yasumura, 1973).

between the wavelength response of polysulphone and the biological action spectrum. The value of  $K$  depends on the spectral distribution of the irradiating source, and can be calculated from

$$K = \frac{\int I(\lambda) R_b(\lambda) d\lambda}{\int I(\lambda) A(\lambda) d\lambda} \quad (7.3)$$

where  $I(\lambda)$  is the relative spectral distribution of incident radiation,  $R_b(\lambda)$  is the biological action spectrum relative to the response at 297 nm and  $A(\lambda)$  is the response spectrum of polysulphone in terms of  $\Delta A_{330}$ , relative to the absorbance change at 297 nm.

Using eqn 7.2 to estimate the dose of vitamin D effective radiation received by a badge-wearer poses two problems. Firstly the action spectrum for vitamin D synthesis  $R_b(\lambda)$  in eqn 7.3, is not known accurately enough. Secondly, with solar radiation as the UV source the spectral distribution  $I(\lambda)$  is continually changing. Furthermore, exposure data related in such a way to a specific application cannot easily be applied to other response spectra in the same wavelength range unless both action spectra are accurately known so that a correction factor analogous to  $K$  can be calculated.

In view of these difficulties it was decided that an independent calibration of polysulphone film should be made using solar radiation as the UV source, giving the dose in absolute units ( $J \text{ cm}^{-2}$ ) over the waveband 300-316 nm recorded by the SEE 240 sensor. 316 nm corresponds to the half-power point of the polysulphone film response and 300 nm to the short wavelength cut-off of solar irradiance.

Calibration

The polysulphone film was mounted between two pieces of card-board to give a badge 1.6 cm x 3.2 cm with a window of film 0.6 cm x 2 cm (Plate 7.1). The badge dimensions were designed to fit into the cuvette holder of the Perkin-Elmer double beam spectrophotometer

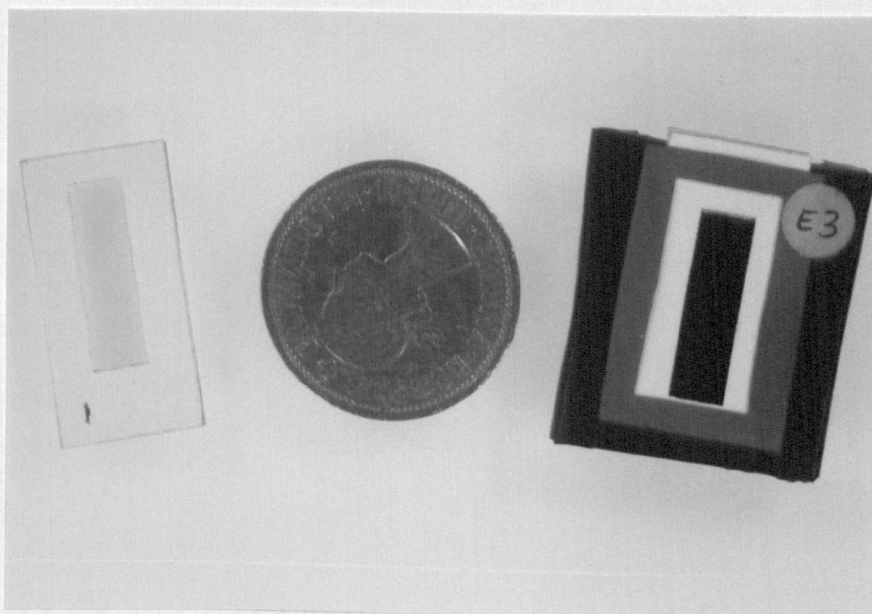


Plate 7.1 Polysulphone film badge, 10 pence piece, and badge mounted in holder.

(Model No. 124) used for absorbance measurements. The cardboard badges were then mounted in more robust holders. These were made of perspex which was covered with black velvet to provide a matt black background for the film, and hence avoid errors due to UV radiation reflected from the holder. The front of the badge holder was made of darkened celluloid film with a window cut in it to expose the polysulphone badge (Plate 7.1).

For calibration, badge holders were fixed horizontally to the table on the meteorological site where the SEE 240 UVB sensor was mounted. The badges could then be slipped in and out of the holders, and once in place were exposed to the same radiation field as the SEE 240.

The badges record the integrated UV dose received during the exposure time and were therefore calibrated against the integrated output from the SEE 240 sensor, as recorded by the printing dose-timer (Chapter 4).

Throughout the period May to August 1983, badges were exposed, in batches of four, for varying lengths of time from 30 mins to 12 hours under differing sky conditions. To avoid timing errors the badges were placed in their holders as the dose-timer print mechanism was activated, and removed at a subsequent time printing. The total dose  $T_B$  received by the badges in the waveband 300-316 nm was then calculated from the number of prints activated over the intervening time period. The absorbance at 330 nm was measured for each badge before and after exposure to UV radiation, and the change in absorbance  $\Delta A_{330}$  calculated. A log-log plot of  $T_B$  against  $\Delta A_{330}$  gave a linear relation represented by the equation.

$$T_B = 7.65 (\Delta A_{330})^{1.65} \quad (7.4)$$

Eqns 7.1 and 7.4 are of the same form

$$T = \alpha (\Delta A_{330})^\beta \quad (7.5)$$

but take different values for  $\alpha$  and  $\beta$  as the correction factor  $K$  (eqn 7.3) has been incorporated directly into the calibration in eqn 7.4 to give  $T_B$  rather than  $T_p$ .

The value of  $K$ , and hence  $\alpha$  and  $\beta$ , depends upon the relative spectral distribution of the irradiating source  $I(\lambda)$  and the response of the polysulphone film  $A(\lambda)$ .  $I(\lambda)$  changes throughout the year for solar radiation resulting in different values of  $\alpha$  and  $\beta$  for summer and winter.  $A(\lambda)$  can also change between batches of polysulphone film. Tate (1979) reported that batches of 40  $\mu\text{m}$  polysulphone film ranged in thickness from 0.36  $\mu\text{m}$  to 0.44  $\mu\text{m}$ , the thickness affecting the degree of absorbance change on exposure to UV radiation.

For the calibration shown in Fig. 7.2 a single batch of film was used (constant  $A(\lambda)$ ) and errors due to changing  $I(\lambda)$  from May to August are included in the calibration.

Eqn 7.2 shows that polysulphone film can be directly calibrated against the solar 300-316 nm waveband. However, because of the dependence of  $\alpha$  and  $\beta$  on  $I(\lambda)$  and  $A(\lambda)$  each batch of film used in future work was calibrated for the incident solar UVB at the time of use (Table 7.1).

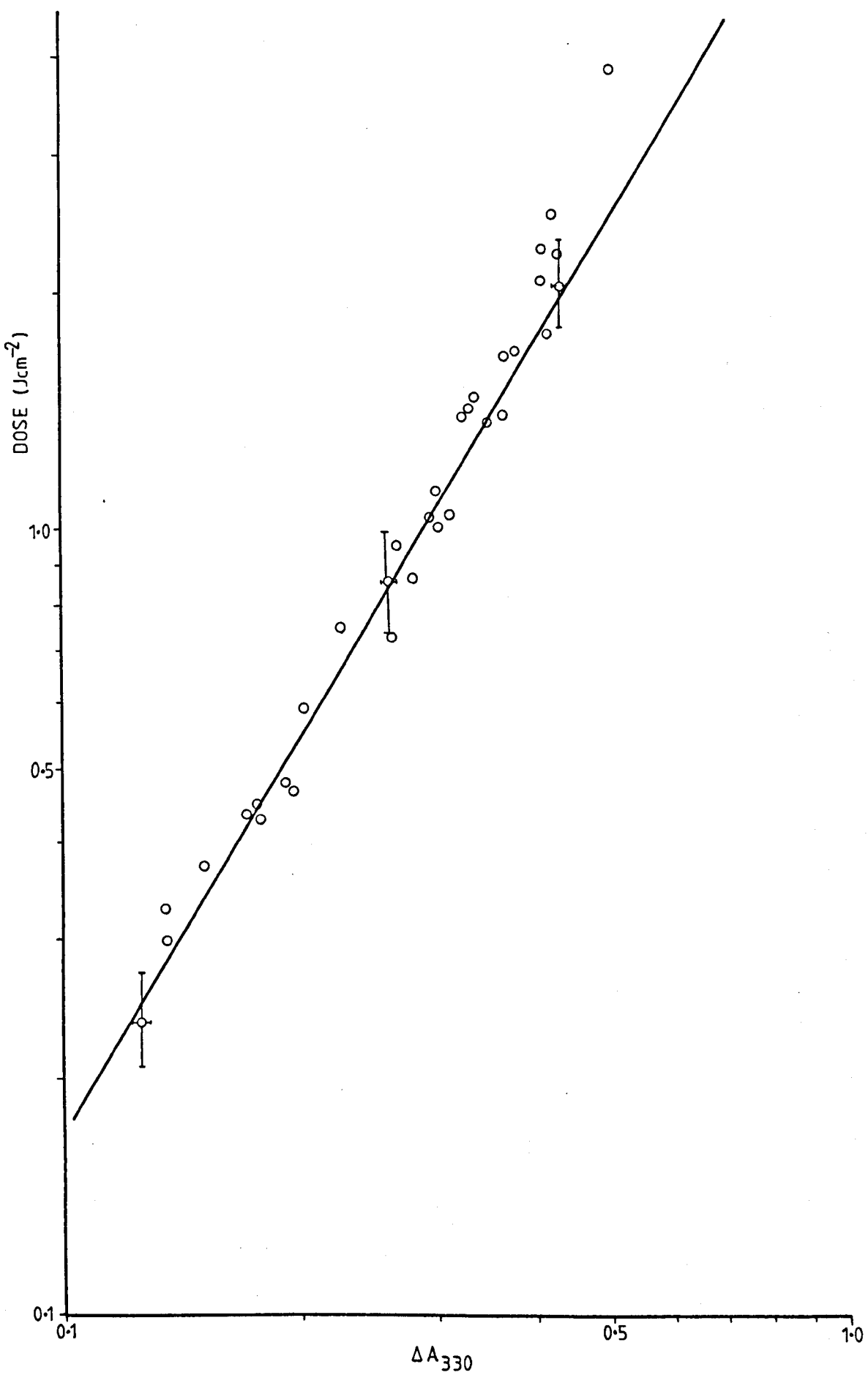
Table 7.1 Values of  $\alpha$  and  $\beta$  for different batches of polysulphone film used in summer and winter.

| Film batch | Date                | $\alpha$ | $\beta$ |
|------------|---------------------|----------|---------|
| 1          | May - Aug 1983      | 7.65     | 1.65    |
| 1          | Oct 1983 - Jan 1984 | 10.50    | 1.65    |
| 2          | March 1984          | 10.50    | 1.65    |
| 3          | May 1984            | 10.50    | 1.62    |
| 4          | June 1984           | 12.42    | 1.86    |
| 5          | June - Aug 1984     | 31.80    | 2.49    |

Batches 1 and 2 were ordered together, as were Batches 3 and 4.

Fig. 7.2

Polysulphone film badge calibration.



At absorbance changes greater than  $\Delta A_{330} = 0.4$  departure of points from the calibration line increased. Tate (1979) also found that when doses of UV radiation gave values of  $\Delta A_{330}$  above 0.4, the degree of degradation of the polysulphone film was less than predicted by the calibration.

The set of badges which deviated most from the calibration ( $\Delta A_{330} = 0.51$ ) were exposed from 0800 to 1930 on 4 July 1983, a clear day. It was considered unlikely that any badge used as a personal dosimeter would receive such a high dose, and for lower doses the badges are suitable for monitoring individual exposure to solar UVB radiation.

For individual badges the uncertainty in the value of  $\Delta A_{330}$  due to the accuracy of reading the spectrophotometer scale was 0.005. Badges were exposed in groups of four, with a fifth badge kept in the dark as a control and as a check against changes in spectrophotometer output. Values of  $\Delta A_{330}$  were found to be repeatable for the exposed badges, variation within a set being attributable to the uncertainty of  $\Delta A_{330}$ . Occasionally a single badge differed from the rest of the set by 50% or more. Such unexplained deviations were discarded from the analysis.

The error in the values of UVB dose calculated from the printing dose-timer is  $\pm 8\%$  random (Chapter 4).

The above sources of error are incorporated in the calibration graph (Fig. 7.2, error bars are shown at three points) for which the standard errors of the slope and intercept are 0.1 and 0.14 respectively

$$\alpha = 7.65 \pm 0.14 \text{ and } \beta = 1.65 \pm 0.1.$$

Taking two standard errors on either side of the calculated values gives a maximum error in UVB dose due to the calibration of  $\pm 10\%$ , for high values of  $\Delta A_{330}$  this error is less.

The polysulphone film calibration was tested for additivity by exposing different sets of badges for consecutive periods of time, and one set of badges for the total time period. The calculated dose of the fully exposed badges was always within 3% of the sum of the doses of the consecutively exposed badges. The badges therefore provide an accurate time integral of UVB radiation.

As with all the measuring techniques which have calibrations traceable to the LI1800 there is a systematic uncertainty in the absolute values of irradiance levels of  $\pm 10\% + 1.5\%$ .

#### Stability of the film

The polysulphone film was tested for stability during storage by a series of  $\Delta A_{330}$  measurements both before and after exposure to UVB radiation. The effect of surface contamination on the performance of the film was also investigated.

Storage at room temperature for 12 weeks before irradiation had no effect on the initial absorbance or subsequent performance of the film. After exposure to UVB radiation storage of the film for periods of up to one week showed no significant change in the final absorbance measurement, although Tate (1979) reported a 5% increase in absorbance after storage of irradiated film for one week in the dark.

Tate (1979) also found that extreme storage temperatures of  $-20^{\circ}\text{C}$  and  $50^{\circ}\text{C}$  had no effect on the absorbance of film either before or after

irradiation. He further showed that irradiation at temperatures between - 4°C and 53°C had no significant effect on the performance of the film. The film used for the project described here was exposed at environmental temperatures well within the temperature range investigated by Tate. As the calibration was performed under a variety of environmental conditions additional temperature tests were not considered necessary.

Badges used as personal dosimeters are liable to contamination from fingering or exposure to dusty or smoky atmospheres. To investigate the effect of such surface contamination on the performance of the badges, sets of badges were deliberately fingered to different extents either during or after exposure. Further badges were shaken in a bag with dust particles at different stages of their exposure. After the final absorbance reading of the treated badges, the polysulphone film was cleaned with ethanol and cotton wool and a further absorbance measurement taken.

Light fingering and small amounts of dust had no significant effect on the performance or final absorbance of the polysulphone film. Where greasy fingerprints or large dust particles covered the film the final absorbance was high. If contamination took place after exposure the final absorbance was unaffected provided the film was cleaned before taking the measurement. Heavy contamination of the film during exposure reduced the performance of the film slightly by preventing UVB radiation falling on the dirty areas of film. The departure of marked badges from the film calibration depended on the degree of contamination and the proportion of the exposure time during which the badge was contaminated.

Badges worn by a heavy smoker were measured for final absorbance both before and after cleaning and did not appear to be adversely affected by a smoky atmosphere.

From these results and those of Tate (1979), who also tested the effect of dust and grease on polysulphone film, only badges showing visible signs of contamination or denting were discarded from experimental analysis.

The results of wetting badges depended on the subsequent treatment of the badge. Water droplets wiped off the polysulphone film had no adverse effect on badge performance. If the droplets were allowed to dry and left smears or a deposit on the film the result was similar to that of dust or grease contamination. Wetting the whole badge with clean water did not affect the performance of the film, but if the badge bent or wrinkled as it dried the absorbance readings were affected and the badge had to be discarded. Badges which remained flat in their holders while being washed in an NHS laundry (Chapter 8) appeared to hold their calibration. Such badges were not however used in the analysis.

In summary, polysulphone film badges proved to be stable and robust enough to be used as personal dosimeters, and gave a good calibration against the solar UVB radiation under standard meteorological site conditions. To test the practicalities of using them in uncontrolled environments a small personal exposure trial was conducted in January 1984.

## Polysulphone Personal Exposure Trial

### Materials and method

Polysulphone film badges were worn by a group of 31 volunteers for a three week period from 9 - 29 January 1984. The volunteers were staff and students at Nottingham University, 21 based at Sutton Bonington and 10 at the main campus in Nottingham. They were asked to wear film badges on their lapel during working hours (0900 to 1700 GMT) and to record on hourly exposure grids the proportion of time spent out of doors. Occupations ranged from computer staff spending virtually all the time indoors to gardeners working outside much of the time, weather permitting.

Badges were also exposed on the meteorological site for the same time periods and with similar exposure grids (these badges were not exposed during rain). The meteorological site badges were placed a) horizontally and b) mounted vertically on a pole with badges facing north, south, east and west. These badges provided a measure of the total UVB radiation available in the environment during exposure periods, both on a horizontal surface and on vertical faces more representative of the position of the lapel badges and of the exposure of skin areas on the hands and faces of volunteers.

Each volunteer was provided with two badges per week, one to be worn from Monday to Friday and the second for use at the weekend. Casualties among the weekend badges were high as many were forgotten or lost and these have therefore been excluded from the statistical analysis, but where available have been used for comparison of occupational and leisure exposure patterns.

One set of badges was stored unexposed during each period as a check against changes due to other causes. During the second week (16 - 22 January) of the trial the control badges showed a negative change in absorbance. This was later found to be due to a fault in the spectrophotometer during the pre-exposure absorbance measurements, so the results for this week were excluded from the analysis.

The exposure grids, used to assess time spent out of doors, were marked for each hour of the day on a scale of 0 to 3 as shown in Table 7.2.

Table 7.2 Exposure grid scores

| Score | Time outdoors (min) |
|-------|---------------------|
| 0     | 0                   |
| 1     | 1 - 29              |
| 2     | 30 - 59             |
| 3     | 60                  |

Throughout the three week trial period the UVB incident on a horizontal surface (the SEE 240 sensor) was recorded as a spot sample on the data logger every five minutes, giving a continuous record of the 'available' UVB radiation even when the meteorological site badges were covered because of rain.

During the two weeks for which badges were analysed, Week 1 (9 - 13 January) and Week 3 (23 - 27 January) the weather conditions were very different. Week 1 was mild but fully overcast on three days, the 10th, 11th and 13th, with rain the afternoon of the 11th and all

day on the 13th, when the meteorological site badges were covered.

The 9th and 12th were days with intermittent sunny periods.

Week 3 was cold and there was snow covering the ground throughout the week, giving an increase in the surface albedo. Snow was falling on the 23rd and the meteorological site badges were not exposed. The following three days were generally clear and sunny after a misty early morning with low temperatures. On the 27th there was fog as the thaw began and snow cover became increasingly patchy. The changing personal weather affected ~~exposure~~ patterns and also had a bearing on the amount of indoor lighting, a further factor for consideration when analysing the badges. Polysulphone film responds to light of wavelengths up to 330 nm and artificial lights (generally fluorescent tubes) have a small spectral component in the 316-330 nm waveband, although there is no natural light indoors in the UVB band of interest because the transmission of window glass is negligible in this band.

To assess the effect of this unwanted radiation on the badge readings the LI1800 spectroradiometer was used to scan the waveband 300-330 nm in a typical laboratory with the lights on and then off. A further scan was taken outdoors in hazy sunshine for comparison. Three volunteers spent time in growth cabinets with different types of artificial lighting, and spectral scans were also taken in these cabinets. Table 7.3 shows the amount of radiation in different wavebands under various lighting regimes.

The spectral details of laboratory lighting are shown in Fig. 7.3. With the lights off there is no significant radiation at wavelengths less than 330 nm, the spectral plot shown is attributable to instrumental

Table 7.3 UVB radiation under different lighting conditions.

| Lighting conditions      | $\frac{316}{300} \sum I_\lambda (\text{W m}^{-2})$ | $\frac{330}{300} \sum I_\lambda (\text{W m}^{-2})$ |
|--------------------------|--|--|
| Laboratory, lights off   | $2.23 \times 10^{-4}$                              | $9.59 \times 10^{-4}$                              |
| Laboratory, lights on    | $1.00 \times 10^{-3}$                              | $1.26 \times 10^{-3}$                              |
| Growth room, sodium lamp | $3.58 \times 10^{-3}$                              | $1.06 \times 10^{-1}$                              |
| Glasshouse, mixed light  | $6.25 \times 10^{-3}$                              | $6.76 \times 10^{-3}$                              |
| Solar radiation (Feb)    | $1.2 \times 10^{-1}$                               |  |

noise. With the lights on there is some indication of a very small spectral component from 300-316 nm, although being two orders of magnitude lower than a winter value for solar radiation its relevance to vitamin D synthesis is negligible. Of more concern is the contribution from light at wavelengths above 316 nm, affecting the badge measurements but not the vitamin D metabolism. As shown in Fig. 7.3 and Table 7.3 such error is minimal compared with outdoor exposure for any length of time. However the badges of workers who remained indoors all the time were used to establish a baseline against which to assess other badges, so as to eliminate as far as possible the effects of artificial lighting.

### Results

The outdoor exposure  $E (\text{J cm}^{-2})$  received by each volunteer was calculated from the information on the exposure grid and the record of incident UVB radiation from the data logger.

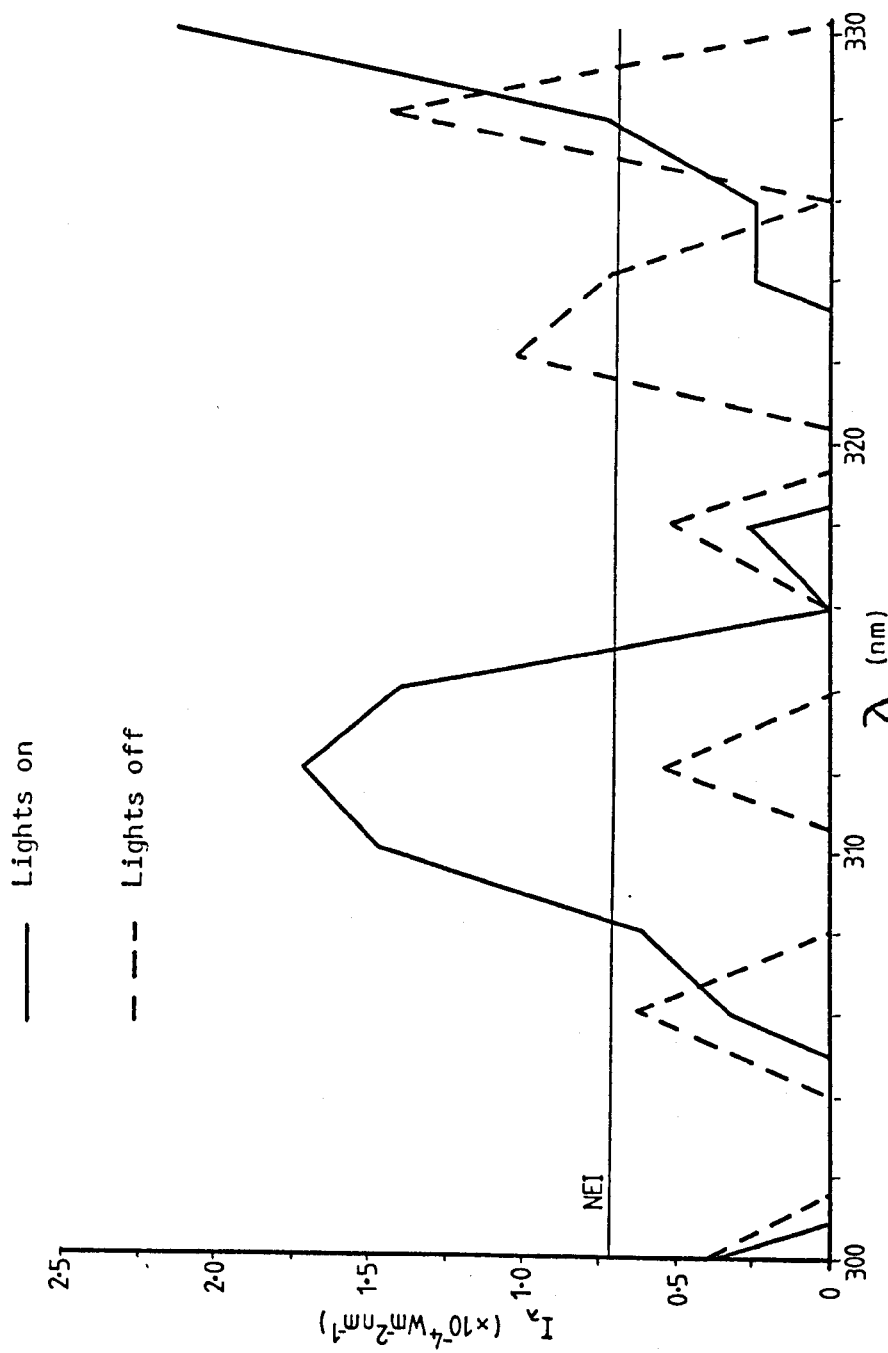


Fig. 7.3 UV radiation spectrum of laboratory lighting.

$$E = \sum_h w_h \bar{I}_h \quad (7.6)$$

where  $w_h$  is the weighting factor for each hour from the grid scale and  $\bar{I}_h$  is the average incident UVB for that hour. The sum was taken over the week during which the badge was worn. The average irradiation per hour was used in the calculation as there was no indication of which period during the hour exposure took place.

Weighting values for the grid scores (0 - 3) were calculated using a Genstat program to find the weighting values that gave the best fit of badge exposure against grid exposure for Week 1 data. The weighting for scores '0' and '3' were constrained to be 0 and 1 respectively. Results of this analysis indicated that a grid score of '1' represented little more exposure than a score of '0'. Similarly a score of '2' was not much different from a score of '3'. Observation and discussion with volunteers supported this theory. A score of '1' often represented a quick dash from one building to another. A score of '2' was a few minutes spent indoors during an hour in the field. On this basis weighting factors  $w_h$  of 0, 0.1, 0.9 and 1 were chosen for the grid scales from 0 - 3. The weighting values were tested on the data of Week 3 and proved to be a suitable interpretation of time spent out of doors.

The data from both weeks were used in a linear regression analysis of badge exposure  $T_B$  (from  $\Delta A_{330}$  measurements and calibration curve) against grid exposure  $E$  (calculated from eqn 7.6) giving

$$T_B = 0.54 (\pm 0.09) E + 0.025 (\pm 0.005) \quad (7.7)$$

Standard errors of the slope and intercept are shown and 54% of the variance was accounted for by eqn 7.7 (Fig. 7.4).

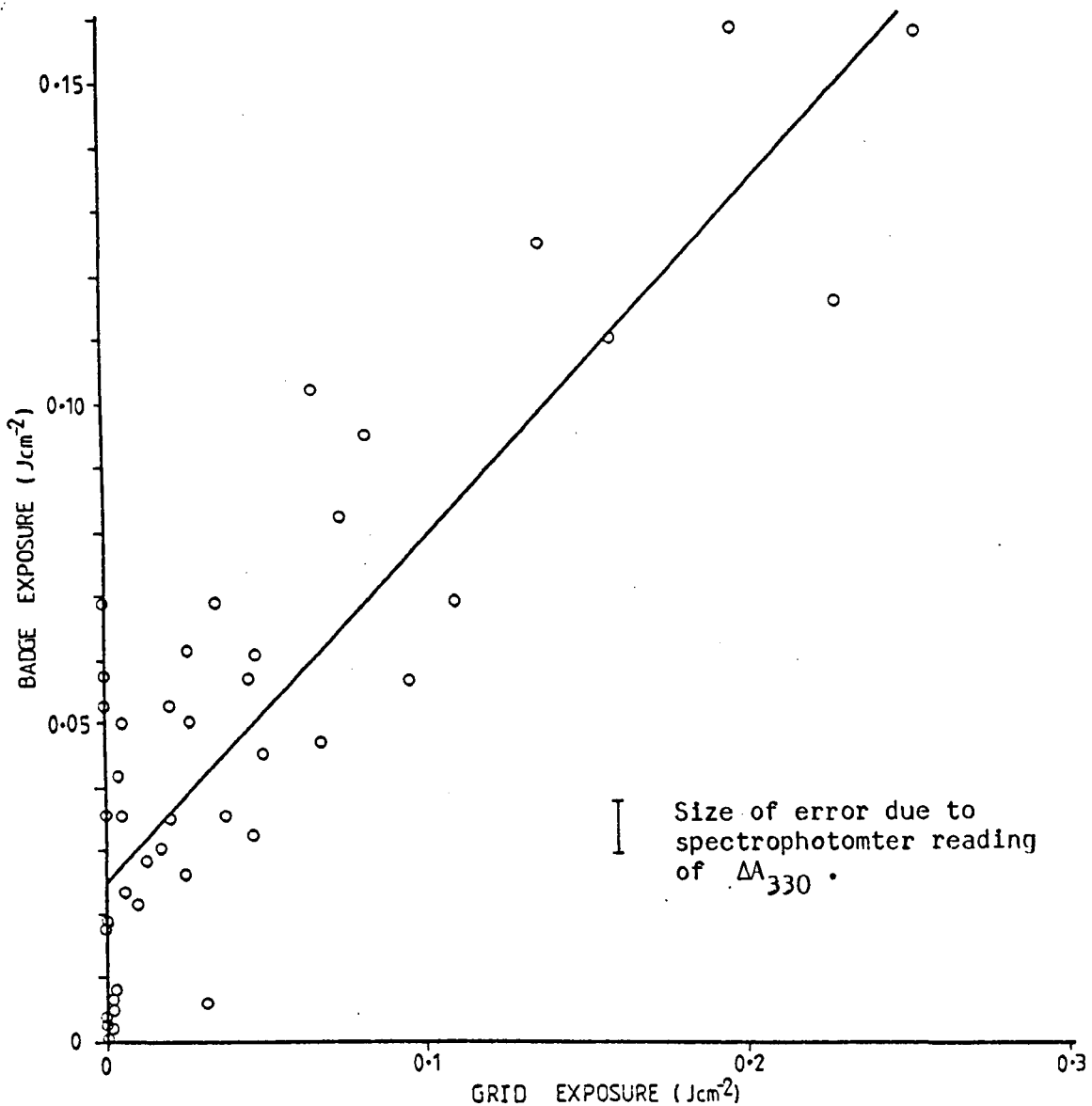


Fig. 7.4 Badge exposure vs grid exposure for Weeks 1 and 3.

The calculated exposures  $E$  estimate the UVB radiation incident on a horizontal surface, while the badge was worn more or less vertically. To assess the proportion of vertical to horizontal irradiation the meteorological site badges were used. The exposures of the four vertical badges were normalised by the exposure of the horizontal badge and the average taken (a volunteer was assumed to be randomly orientated over a period of one week). Results are shown in Table 7.4.

Table 7.4 Normalised vertical irradiance  
for Weeks 1 and 3.

| Normalised irradiance | Week 1 | Week 3 |
|-----------------------|--------|--------|
| Horizontal            | 1      | 1      |
| Vertical S            | 0.766  | 0.785  |
| E                     | 0.471  | 0.549  |
| W                     | 0.364  | 0.549  |
| N                     | 0.364  | 0.653  |
| Average vertical      | 0.491  | 0.634  |

The overall average ratio of vertical to horizontal irradiation for both weeks is 0.562, consistent with the slope of the regression analysis. The intercept is a measure of exposure to indoor lighting. The scatter of measurements with badges worn indoors is large for a number of reasons. Different types of indoor lighting are one source of variation as only fluorescent lights affect the badge measurement. Errors due to the spectrophotometer and contamination, while negligible compared with the response to outdoor exposure, become significant for indoor exposures.

Bearing in mind the low levels of UVB radiation being measured in January, and the errors inherent in calculating grid exposures from subjective judgement on a coarse score scale, the measurements confirmed that polysulphone film badges provide a cheap and easy means of measuring personal UVB exposure in a range of different activities. With values of exposure expected to be far greater in summer, polysulphone film badges were considered to be suitable for use in a more elaborate trial in late spring and early summer.

#### Occupational Exposure to Solar UVB Radiation

The occupational exposure data from the January and May/June trials is presented below. Information from the summer months was gathered as part of a more extended study to investigate the link between UVB exposure and vitamin D status (Chapter 8). It provides an indication of the UVB exposure levels of healthy young adults under the radiation regime of the East Midlands.

#### The volunteers

Most of the subjects in the January trial wore badges again during a 7 week study from 14 May to 29 June 1984. 24 males and 6 females, one female less than in January, took part in the summer study, providing a total population of 30 with an age range (for both trials) of 21 - 63.

Volunteers were asked to record their age, occupation, and whether they considered themselves indoor or outdoor workers. A classification of participants by age and occupation is given in Table 7.5 for the summer study. In January most students and academic staff classed themselves as indoor workers, and the mixed and outdoor technical staff generally spent a smaller proportion of their time outdoors.

Table 7.5 Classification of June volunteers  
by age and occupation.

| Occupation               | Age (year) |       |       |      |
|--------------------------|------------|-------|-------|------|
|                          | < 30       | 30-40 | 40-50 | > 50 |
| Student                  | 9 *6       | 2     | -     | -    |
| Academic staff           | 3 *1       | 5 *2  | 3     | -    |
| Tech. staff<br>(indoor)  | 2 *1       | 1     | 1 *   | 1    |
| Tech. staff<br>(outdoor) | -          | 2     | -     | 1    |

\*x these volunteers classed themselves as mixed indoor/outdoor workers, the remaining students and academics considered themselves to be indoor workers.

Procedure for wearing the badges was as described earlier with a few modifications for the summer months. Volunteers were asked to wear badges from 0800-1800 GMT (0900-1900 BST), and the exposure grid scale was altered to facilitate more accurate assessment of time spent outdoors (Fig. 7.5). Weekend badges were again worn intermittently.

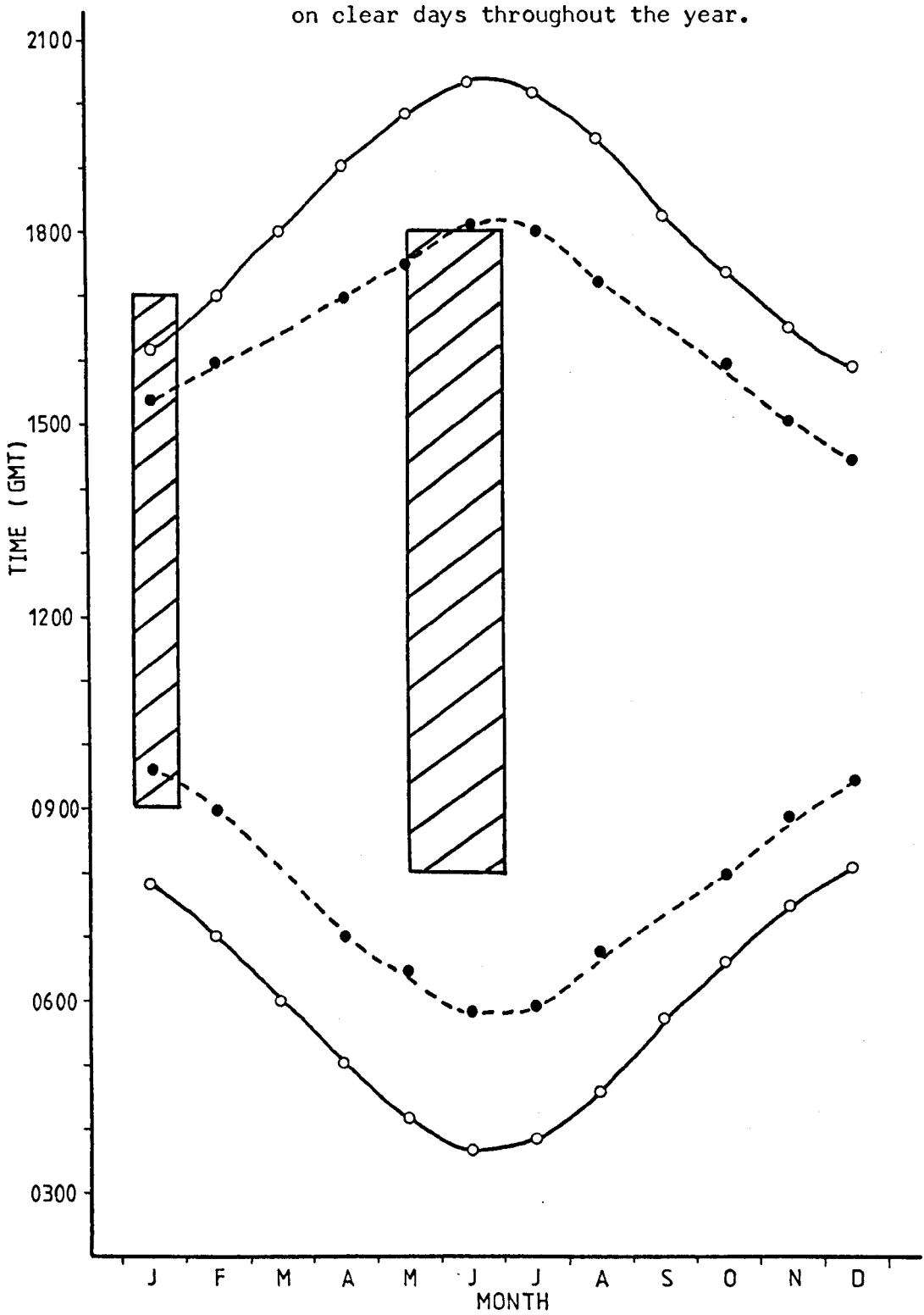
#### UVB sunshine hours for the working day

Fig. 7.6 shows the duration of the solar UVB radiation day throughout the year, and the proportion of this day for which polysulphone film badges were worn. The daylength is for clear days and therefore shows the maximum time for which there is a UVB component in the solar spectrum, the UVB sunshine hours. This follows closely full solar sunrise and sunset, before and after which all solar radiation is diffuse. On overcast days UVB dusk occurs earlier.

Fig. 7.5 Sample exposure grid with summer scale.

| Name                   | Subject No.              |
|------------------------|--------------------------|
| Hourly exposure grid   |                          |
| Hour                   | Mon. Tues Weds Thur Fri. |
| 7-8                    |                          |
| 8-9                    |                          |
| 0800<br>GMT            | 9-10                     |
| 10-11                  |                          |
| 11-12                  | Scale                    |
| 12-1                   | 0 - < 5 min outdoors     |
| 1-2                    | 1 - 5-20 min outdoors    |
| 2-3                    | 2 - 20-40 min outdoors   |
| 3-4                    | 3 - 40-55 min outdoors   |
| 4-5                    | 4 - > 55 min outdoors    |
| 5-6                    |                          |
| 1800<br>GMT            | 6-7                      |
| Additional information |                          |

Fig. 7.6 Daily duration of solar UVB radiation  
on clear days throughout the year.



— Solar sunrise and sunset (Smithsonian Met. Tables)  
also time by which UVB is zero.

- - - Time by which UVB has fallen to 10% of noon value.



Time badges worn.

It was assumed that any exposure before 0900 GMT (0800 in June) was negligible. In January volunteers were asked to wear badges during the working day, 0900-1700 GMT, encompassing the full UVB radiation day. For the summer trial in May and June badges were worn from 0800-1800 GMT during the week. Any exposure after this time would have been to 10% or less of the midday value and have a minimal effect compared with exposure earlier in the day. Weekend badges were worn at the discretion of the volunteers, but provision was made on the exposure grids for long active evenings.

#### Occupation and seasonal exposure

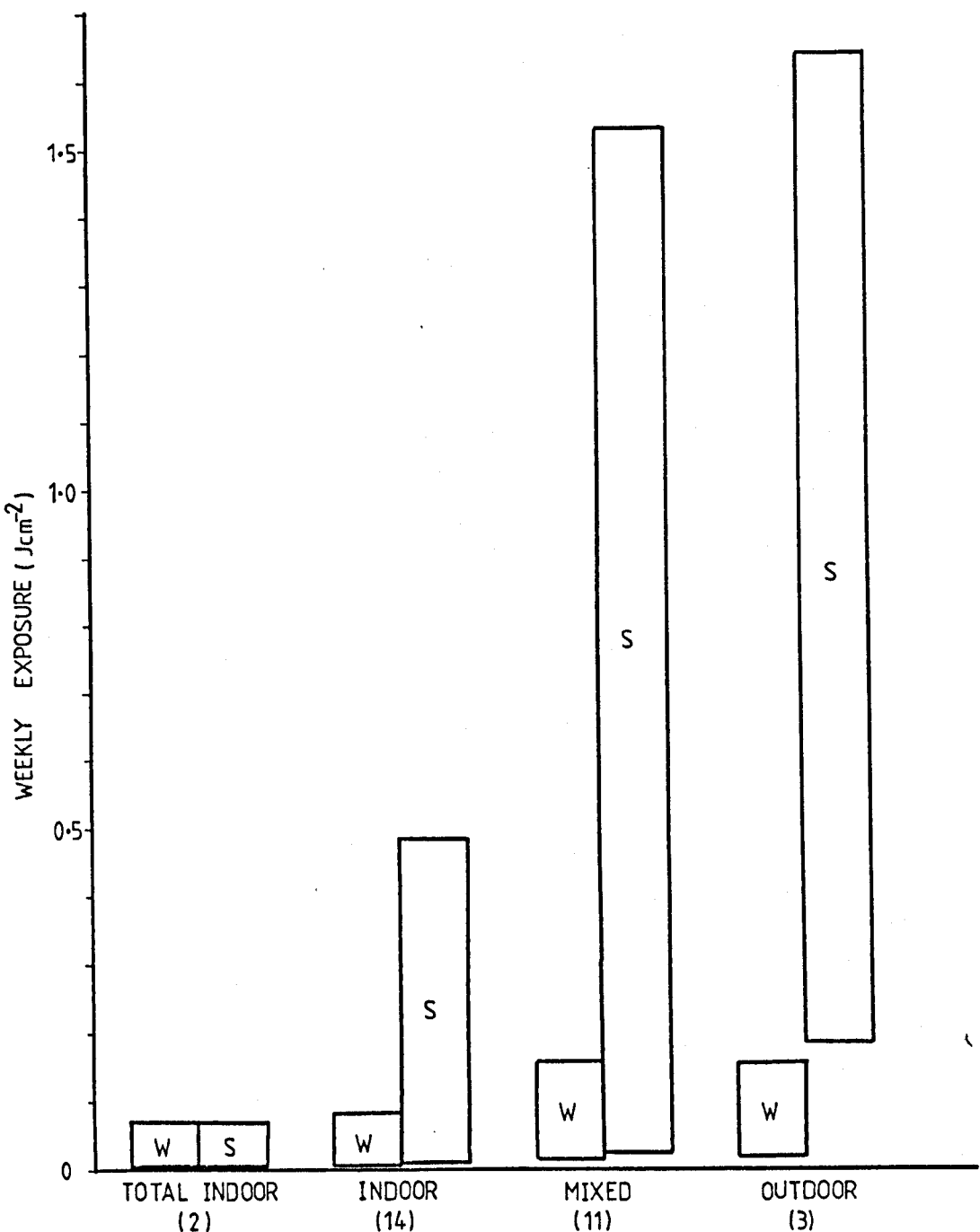
The volunteers were divided into four categories according to their occupation. Two of the volunteers had occupations for which they were indoors for the total <sup>time</sup> that the badges were worn both in January and June. They were classed as total indoor workers. Other participants (14) considering themselves indoor workers nonetheless recorded some outdoor activity, often at midday. Eleven volunteers classified themselves as mixed workers, and three had outdoor occupations.

The range of weekly exposures recorded within each occupational category for the two trial periods is shown in Fig. 7.7.

For the total indoor workers the range is the same in both winter and summer. These values, plus the occasional zero-exposure badge from other subjects, lie within the base level range ( $< 0.07 \text{ J cm}^{-2}$ ) established for an indoor environment by a control group in the extended summer study (Chapter 8).

During January there was no significant difference between exposures for the two indoor groups, or between the two groups with

Fig. 7.7 Working week exposure ranges by season and occupational category.



W      January (2 weeks)

S      May/June (7 weeks)

more outdoor activity. The maximum exposure increased by a factor of 2 from indoor to outdoor categories, and the very lowest values of exposure were not recorded by volunteers claiming to spend time outdoors. Only those with tasks to perform outdoors spent more than brief periods outside, and external activities were timetabled where possible to coincide with the most clement conditions. The similarities within the two pairs of exposure ranges is therefore not surprising.

In May/June the range of exposures increased both between and within occupational categories. Changing weather and workloads from week to week plus personal desires for fresh air all contributed to the extended exposure ranges shown.

The maximum exposures of each occupational range are given in Table 7.6 in relation to the total indoor maximum exposure. The ratio of June to January maxima is also given for each category.

Table 7.6 Maximum exposures by occupation in January and June with respect to total indoor exposure.

|                                      | Category     |        |       |         |
|--------------------------------------|--------------|--------|-------|---------|
|                                      | Total indoor | Indoor | Mixed | Outdoor |
| Occupation/Total indoor<br>(January) | 1.0          | 1.2    | 2.3   | 2.3     |
| Occupation/Total indoor<br>(June)    | 1.0          | 6.9    | 21.8  | 23.4    |
| June/January                         | 1.0          | 5.7    | 9.6   | 10.3    |

At the top end of the exposure range the differences between the two indoor categories and the indoor and mixed occupations increased significantly from January to June. The mixed and outdoor workers remained similar in their maximum exposures, but the outdoor workers did not record exposures in the lowest 10% of the mixed category range.

The discrepancy in UVB exposure between different occupations in this (non random) population may be modified by time spent outdoors in leisure activities.

#### Work and leisure

Volunteers were asked to wear a second polysulphone film badge at weekends, recording time spent outdoors and the type of activity they were engaged upon. Many weekend badges were not worn or suffered damage, therefore results in this section are drawn from a fluctuating population, smaller than the full set of volunteers. As exposure depends so much on individual pursuits it is not possible to give more than a generalised view of the amount of irradiation that may be expected from different pastimes.

In January, weekend badges (2 days) recorded exposures over the same range ( $0\text{--}0.16 \text{ J cm}^{-2}$ ) as the full set of weekday badges (5 days). Weekends spent entirely indoors accounted for the lowest badge records, while the greatest exposure was the result of a full day (0900-1600 GMT) woodcutting in the open air, and a further hour outside the following day. Almost all weekend badge wearers undertook some kind of outdoor activity, often shopping or walking. Short times spent in this way gave indoor workers weekend doses of radiation greater than or equal to their weekday accumulation of UVB. Those with gardens or dogs scored highest over

the weekend. Weekly outdoor workers showed lower exposures for the weekend during January. Where similar occupation was undertaken (gardening) it was for a shorter period of time. In other instances a restful two days resulted in little exposure.

Calculating the full weekly total exposure from the sum of weekday and weekend badges for all volunteers returning their badges and for both January weeks showed a range of full week exposures of 0.006-0.290 J cm<sup>-2</sup>. The maximum was a mixed environment worker with a high weekend exposure, the minimum an indoor worker with an indoor weekend. Of the volunteers falling between the two extremes no demarcation could be made on the grounds of weekday employment, an indoor worker with an active weekend could accumulate the same UVB dose as an outdoor worker spending weekends indoors.

A sunny summer Sunday encourages most people to spend some of their leisure time in the open air, and the May/June weekend badges support this.

Weekend exposures for the indoor workers exceed the weekday values in 33 out of 60 cases. The majority of the exceptions occurred during two weeks with dull weekends. Over the four weeks with fine weather at the weekend 30 out of 39 indoor workers recorded over half their total weekly UVB dose at the weekend. In some cases virtually all exposure was at weekends.

Outdoor workers, by contrast, always showed lower exposures at the weekend than during the week. Those employed in the open air tended to continue to spend time outdoors during their leisure hours. Taking account of the different periods involved (2 days and 5 days) weekends and weekdays provided similar exposures for these volunteers.

Mixed workers, as their name suggests, had mixed dependence on weekend activities for their exposure levels. Weather, workload and preferred pastimes gave each individual a different exposure pattern over the seven week study. The relative importance of weekends for this group covered the full range between indoor and outdoor workers; from providing over half the total exposure to contributing the same daily accumulation rate as the weekdays.

The cumulative UVB radiation received by four volunteers in January and then in May/June is shown in Fig. 7.8 and illustrates the personal and occupational influences on exposure with season.

All exposures were low in January, and no volunteer had any appreciable exposure in the second week. The cumulative exposure shows the expected increase with occupational category, although it should be noted that almost half the outdoor volunteer's total exposure was gained during the first weekend; weekday employment for this subject still produced the highest exposure values, but only marginally so.

In May/June the occupational differences were more pronounced as the total daily available UVB radiation increased 40-fold from the January level and outdoor employment patterns also became more diverse.

The relative importance of weekend exposures is particularly noticeable at this time of year. Weekends 4, 6 and 8 accounted for over 75% of the total indoor workers cumulative exposure, while weekend 2 alone was responsible for 30% of the indoor worker's exposure. In comparison, all six weekends contributed only 10% to the outdoor worker's accumulated UVB. For the particular mixed environment worker illustrated, weekend exposure accounted for just 50% of the total cumulative exposure over the seven weeks of the trial.

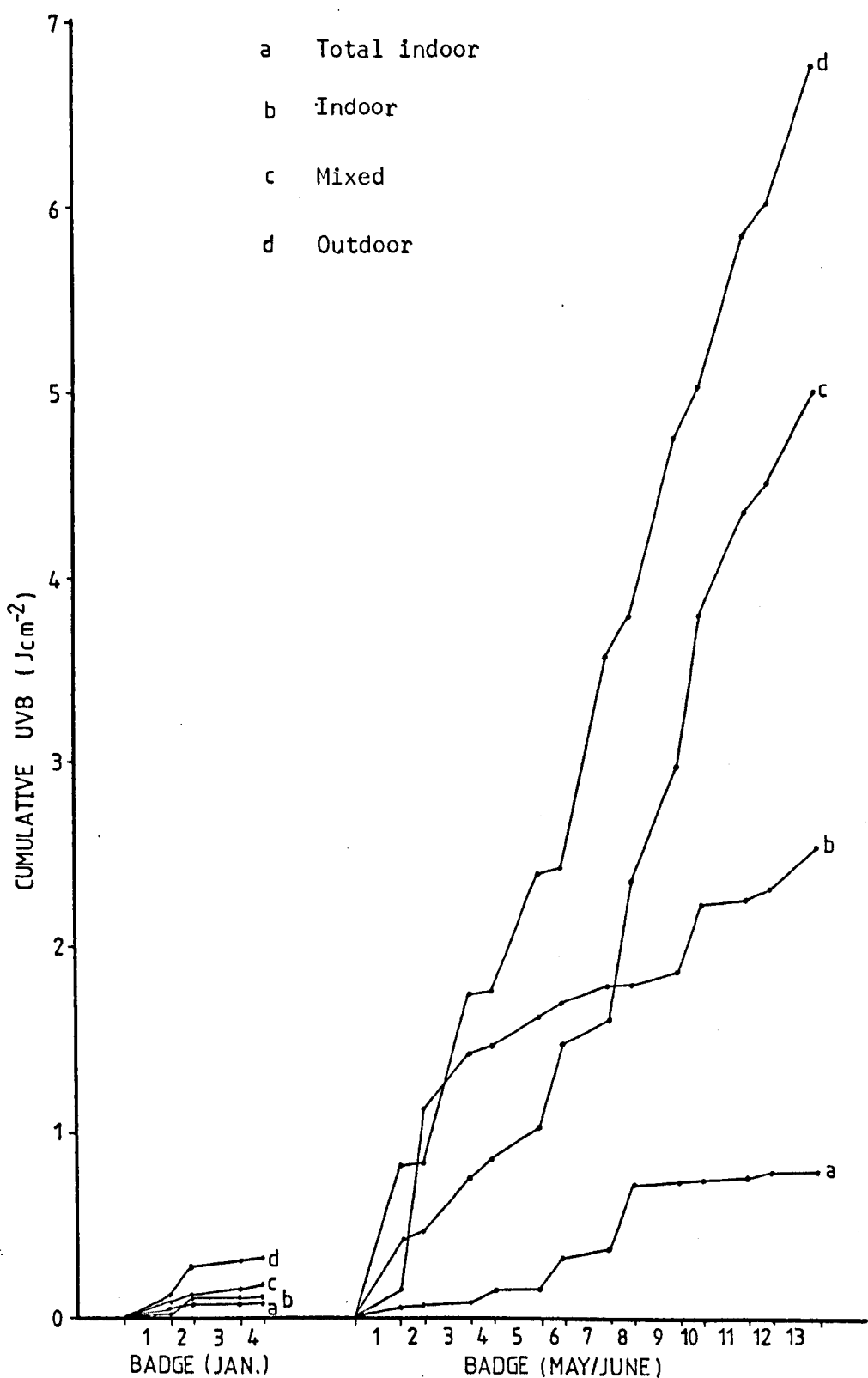


Fig. 7.8 Cumulative UVB exposures for 4 volunteers during the two trial periods.

The UVB exposure in various employments and the relative importance of different weekend activities have been described for workers in the radiation environment of Sutton Bonington. Populations in other climates would require either more or less time outdoors to receive the same dose of UVB radiation. It is therefore instructive to consider personal exposure with respect to the available UVB i.e. that incident on a horizontal surface, a figure comparable under any climate.

A detailed account of the Sutton Bonington UVB climatology is given in Chapters 5 and 6. Personal exposures are compared here with the UVB incident on the horizontal meteorological site badges. These badges were exposed for the hours that volunteers were asked to wear badges, but were covered if it rained. As few people choose to work in the rain these badges represent the 'available workday' UVB radiation. Table 7.7 shows the percentage of available workday UVB radiation received by each category of worker during the weeks of the January and May/June trials.

As expected there was an increase in percentage UVB received with increased outdoor employment, with variation from week to week in any category reflecting that week's particular tasks.

Other workers have measured the UVB exposure received during different activities and results from Challoner, et al (1976)<sup>a</sup>, Leach, et al (1978)<sup>b</sup>, Diffey, et al (1982a)<sup>c</sup>, Larko and Diffey (1983)<sup>d</sup> and Holman, et al (1983)<sup>e</sup> are summarised below (Table 7.8).

The ambient UVB used in these studies was either measured or calculated from Bener's data for the period during which exposure took place.

Table 7.7 Occupational percentages of available workday UVB radiation.

| Date          | Occupation   |        |       |         |
|---------------|--------------|--------|-------|---------|
|               | Total indoor | Indoor | Mixed | Outdoor |
| Jan. 9 - 16   | 10           | 3      | 14    | 22      |
| 23 - 29       | 0.5          | 0.6    | 2     | 4       |
| May 14 - 18   | 2            | 4      | 11    | 21      |
| 21 - 25       | 0.3          | 6      | 6     | 20      |
| 28 - 31       | 0.1          | 3      | 14    | 38      |
| June 4 - 8    | 1            | 2      | 3     | 24      |
| 11 - 15       | 0.1          | 0.4    | 11    | 17      |
| 18 - 22       | 0.2          | 0.4    | 10    | 15      |
| Mean (Summer) | 0.62         | 2.63   | 9.17  | 22.5    |
| ± S.D.        | 0.69         | 1.99   | 3.62  | 7.5     |

Table 7.8 Occupational percentages of ambient UVB received.

| Occupation           | % Ambient UVB received         |   |
|----------------------|--------------------------------|---|
| Gardeners            | 10                             | a |
| (cf. outdoor)        | 46 - 69 dependent on body site | e |
|                      | 10 - 70                        | d |
| P.E. Teacher         | 33 - 63 dependent on body site | e |
| (cf. mixed)          |                                |   |
| Classroom teacher    | 7 - 11 dependent on body site  | e |
| Lab./Office worker   | 2 - 4                          | b |
| (cf. indoor)         | 6                              | d |
| Ward-fast patients   | 0.1                            | a |
| (cf. total indoor)   |                                |   |
| Leisure : Sunbathing | 75 - 80                        | c |
| Skiing               | 20 - 23                        | c |
| Sailing              | 13 - 15                        | c |

Results agree well with the present study for the two classes of indoor workers. For the outdoor workers (gardeners) the Sutton Bonington value lies between the percentages from other studies. Values are lower for the mixed worker category. However these occupations are so dependent on individual work load that this spread of results is not surprising.

For indoor workers who rely on leisure activities and holidays for most of their UVB exposure, Holman, et al (1983) rated ten recreations in order of descending fractional UVB exposure:

1. Boating , Ocean swimming
2. Sunbathing
3. Hiking
4. Golf
5. Fishing
6. Tennis , Pool swimming
7. Cricket
8. Gardening

The little information obtained from the Sutton Bonington trial about weekend pastimes seems to support this order. Very high weekend exposure was recorded by two volunteers after periods spent sunbathing, and the more active sports of hiking and tennis proved better UVB accumulators than gardening.

#### To distant climes

Personal exposures reported thus far have all been received in the English East Midlands. However during the trial periods two volunteers had holidays abroad, and agreed to wear polysulphone film badges during their vacation. A further set of badges was taken to India by a visiting research worker.

27 January 1984, Val d'Isere, French Alps.

Altitude 1400 m, Latitude 45.5°N

Five polysulphone film badges were exposed on 27 January from 0900 to 1530 GMT. One badge was placed horizontally on an unshaded hotel balcony, with a second badge mounted vertically below it with a south-facing aspect. The remaining three badges were worn on the hats of skiers who were active from 0900 - 1200 GMT and 1300 - 1530 GMT. The sky was fully overcast with grey stratus cloud throughout the day. The UVB radiation received is shown in Table 7.9.

Table 7.9 UVB radiation incident in French Alps and intercepted by skiers.

| Badge        | UVB (0900 - 1530) $\text{J cm}^{-2}$ | % Ambient |
|--------------|--------------------------------------|-----------|
| Horizontal   | 0.244 ( $\pm$ 8%)                    | 100       |
| Vertical (S) | 0.244 ( $\pm$ 8%)                    | 100       |
| Skier 1      | 0.110 ( $\pm$ 16%)                   | 45        |
| 2            | 0.141 ( $\pm$ 16%)                   | 58        |
| 3            | 0.161 ( $\pm$ 16%)                   | 66        |

On the same day, 27 January, the ambient UVB at Sutton Bonington (altitude 50 m, 7° further North) was  $0.09 \text{ J cm}^{-2}$ . The meteorological conditions were very similar, and there was patchy snow cover on the ground at Sutton Bonington. The horizontal/vertical (S) ratio for the week at Sutton Bonington (snow cover and 3 days with clear skies) was 0.78 or 78%.

With all radiation diffuse and the high reflective properties of snow the equivalence of the horizontal and vertical (S) exposures in

France is not surprising. More direct beam radiation and less snow reduces the ratio of UVB incident on a vertical surface at Sutton Bonington.

The incident UVB in the Alps was 2.7 times that for Sutton Bonington under similar weather conditions, emphasising the effect of latitude and altitude on radiation climate.

The skiers received from 45 - 66% ( $\pm$  8%) of the available UVB, a higher percentage than that reported by Diffey, *et al* (1982a) who found the percentage of available UVB intercepted by skiers in Austria was 20 - 23%, 22% under light cloud.

The high percentage of the available UVB received by skiers (twice that of an outdoor worker) is probably due to the combination of a number of factors: the high albedo of snow, the length of time spent outdoors and the unshaded nature of ski slopes.

18 - 22 June 1984, Austrian Alps.

Altitude 3000 - 7000 ft, Latitude  $\sim 47^{\circ}$ N

An alpine walking holiday in Austria at mid-summer provided the radiation regime under which a further polysulphone film badge was exposed. The badge was pinned to a rucksack worn while walking for an average of 8 hours per day. No climatological data are available, but the recorded UVB radiation dose of  $2.81 \text{ J cm}^{-2}$  is by far the highest weekly value measured during the trial. The highest exposure for an outdoor worker at Sutton Bonington that week was  $0.84 \text{ J cm}^{-2}$ , the result of long periods ( $\sim$  5 hours) spent outdoors each day of the week. The maximum weekly exposure recorded at Sutton Bonington during the May/June trial was  $1.64 \text{ J cm}^{-2}$ , 58% of the Austrian value.

Once more latitude and altitude appear to have increased the available UVB for this volunteer. A combination of climate, long hours outdoors and hiking scoring high on the 'Interception Scale' of activities (Holman, et al, 1983) explains the high holiday dose.

23 - 29 February, 18 - 24 March 1984, Hyderabad, India

Latitude 17.4°N.

An agricultural research worker spending a study period in Hyderabad, India took two sets of badges for exposure measurements in a subtropical climate.

The badges were exposed a) on a horizontal, unshaded surface surrounded by flat farmland and b) worn on the shorts of the worker throughout the day. The horizontal badges were changed every day, the worker's badge every two days.

Two weekly periods were chosen, during which UVB doses were measured with the polysulphone film badges: 23 - 29 February and 18 - 24 March, 1984.

The weeks of exposure occurred during the dry season, when skies were clear every day. Sunrise was at 0630 and sunset 1820 (local time). Daily values of available UVB radiation incident on a horizontal surface are given in Table 7.10 together with the exposures of the worker, their percentages of the available UVB, and an indication of time outdoors.

The work involved was measuring the growth of various tropical crops, and may be compared with the outdoor workers at Sutton Bonington (gardeners). The percentage of available UVB received is of the same

order as that found in England, although the absolute value of the UVB dose is increased. The dose received in India over two days is at the maximum end of the range received in England, at mid-summer, over a five day period. During February and March in England the available UVB/day is of the order of  $0.18 \text{ J cm}^{-2}$  and  $0.44 \text{ J cm}^{-2}$  for each month respectively. This is only  $\sim 5$  and 10% of the UVB radiation incident on a horizontal surface in India.

Table 7.10 Available and received UVB of outdoor worker in India.

| Date  |    | Available UVB<br>( $\text{J cm}^{-2}$ ) | Received UVB<br>( $\text{J cm}^{-2}$ ) | % Available | Time outdoors                          |
|-------|----|---|--|-------------|--|
| Feb.  | 23 | 3.85                                    | 1.04                                   | 14          | < 1 hr at noon                         |
|       | 24 | 3.70                                    |  |             | $\sim 0.5 \text{ d}^{-1}$ more at noon |
|       | 25 | 3.36                                    |  |             | 1000-1700 in field                     |
|       | 26 | 4.40                                    |  |             | 1100-1430                              |
|       | 27 | 4.28                                    |  |             | All day in field                       |
|       | 28 | 3.95                                    |  |             | All day in field                       |
| March | 29 | 4.41                                    | 1.17                                   | 26          | Most of day                            |
|       | 18 | 4.10                                    | 1.07                                   | 13          | 1.5 h early a.m.                       |
|       | 19 | 4.05                                    |  |             | All a.m., 0.5 p.m.                     |
|       | 20 | 3.80                                    | 0.808                                  | 10          | very little                            |
|       | 21 | 4.05                                    |  |             | > 0.5 each hour                        |
|       | 22 | 4.12                                    | 0.435                                  | 5           | < 0.5 each hour                        |
|       | 23 | 3.95                                    | 0.730                                  | 19          | > 0.5 each hour                        |
|       | 24 | 3.83                                    |  |             | < 0.5 each hour                        |

Summary

Polysulphone film has proved to be a relatively cheap and easy means of assessing personal exposure to solar UVB radiation. The range of exposures of a sample population under the radiation regime of the East Midlands has been studied with respect to occupation and the ambient UVB of the location. Percentages of the available UVB received at Sutton Bonington while engaged in various tasks agree with results at other sites and by other workers.

## 8. UVB AND VITAMIN D

### Introduction

The role of UVB in maintaining a healthy vitamin D status in man was reviewed in Chapter 3. The rate of production of vitamin D in vivo and the amount of exposure to sunlight required for health have not been resolved in the literature and these unknown quantities were investigated as one application of the general UVB measurements described in previous chapters.

### Materials and Methods

A group of long-stay geriatric patients at Nottingham General Hospital were chosen for study and for comparison with a younger, healthy population.

#### Elderly volunteers

Twenty-seven patients gave their informed consent to participate in the study, which was approved by the Hospital Ethical Committee. All volunteers were long-stay patients, their time in hospital ranging from several months to years. 24 of the patients were female, 3 were male. They were aged 70 - 94 years.

The patients were divided into two groups. 14 (to be referred to as Sun-patients) were resident on two ground floor wards with easy access to a terrace facing south-west. The remaining 13 (Control patients) were on wards immediately above, with no outdoor access.

The study took place over a 13-week period, from 26 April to 26 July, 1984. Each patient wore a polysulphone film badge (one per week) to record UVB exposure, and the ward staff were asked to record the times during which patients were outside on the terrace.

A Kipp solarimeter and a SEE 240 UVB sensor were mounted on the hospital terrace to record the total solar radiation and natural UVB available at this location. The UVB radiation was recorded on a printing dose-timer (Appendix B2) and the output from the Kipp was integrated to give the total incident radiation per hour. Both instruments were therefore directly comparable with concurrent measurements made at Sutton Bonington.

Non-fasting venous blood samples (10 ml) were taken by hospital doctors in weeks 2, 4, 6, 8, 10 and 13 of the study. The blood plasma was stored at -20°C and later analysed for 25-hydroxyvitamin D by competitive protein binding assay (Appendix C).

There was no control of the patient's dietary intake of vitamin D other than the exclusion of fatty fish and vitamin D supplements. Analysis of a typical day's food consumption gave a maximum vitamin D intake of 1.41 µg, little more than half the recommended daily dose of 2.6 µg. The average intake of these patients is likely to have been considerably less than the maximum, about 0.4 µg if the daily egg (assumed above) is not included.

None of the patients had liver disease or any condition known to interfere with calcium or vitamin D metabolism.

#### Young volunteers

The UVB exposure of 30 healthy young volunteers was monitored for 7 weeks from 14 May to 29 June, 1984 and is described in Chapter 7. Of these 30 volunteers, 10 agreed to give blood for plasma 25(OH)D analysis. The 3 females and 7 males were aged 21 - 37 years. There was no dietary control of this group and volunteers were assumed to have

a generally balanced food intake. One subject was a vegan with no dietary source of vitamin D.

Non-fasting venous blood samples (10 ml) were taken on 22 May, 13 June and 3 July. The plasma was stored and analysed in the same way as that from the elderly patients.

#### Results and discussion

Of the 27 geriatric patients, five died (from natural causes) during the study. A further two developed conditions affecting their plasma 25(OH)D levels and were therefore excluded from any analysis. A complete set of six plasma 25(OH)D levels was not available for all the remaining patients, due to low recoveries from the assay or missing samples, but only one patient had insufficient data to be included in the results.

One of the original control patients was observed to sit in front of an open window in warm weather, and was also taken on outings by relatives. He was therefore considered as a Sun-patient in the analysis.

The 19 patients for which results are given were divided between Sun and Control patients as shown in Table 8.1. The corresponding information for the young comparison volunteers is also given.

Table 8.1 The volunteer groups.

| Group   | Total subjects | Female | Male | Ages (years) |
|---------|----------------|--------|------|--------------|
| Sun     | 10             | 9      | 1    | 72 - 90      |
| Control | 9              | 8      | 1    | 80 - 94      |
| Young   | 10             | 3      | 7    | 21 - 37      |

### The Available UVB Radiation Climate

The UVB radiation environments to which the different volunteer groups were exposed were measured with SEE 240 UVB sensors. The available UVB radiation is therefore taken to be the radiation incident on a horizontal surface in the waveband 300-316 nm.

The control group, restricted to the wards, had no environmental UVB available to them. Any change in the polysulphone film badges was a result of wavelengths up to 330 nm affecting the film. As fluorescent lighting and aspect of all wards was similar the  $\Delta A_{330}$  changes in badges of the control group were taken as a baseline for zero UVB irradiation. The range of control badge values was consistent with badges for Sun-patients who had not been out on the terrace during the week, and with badges scoring zero from the young volunteer group both in January and during the summer (Fig. 8.1).

The Sun-group had access to a terrace facing south-west with trees along the border at intervals providing intermittent shade (Plate 8.1). The SEE 240 was mounted on a table  $\sim 2.5$  m above the level of the terrace in an unshaded position, and was therefore monitoring the maximum UVB available. Patients sat outside only on warm days between 1000 and 1500 GMT. Exposure grids were completed by ward staff on one of the wards only, but similar practices of patient care were assumed for the second ward. With very few exceptions all exposure took place between the hours of 1300 and 1500 GMT, and in time blocks of 1 to 2 hours.

The available UVB is shown in Fig. 8.2 for two days when many of the Sun-patients were outdoors. The two plots show the incident UVB

● out for 0.5 h.

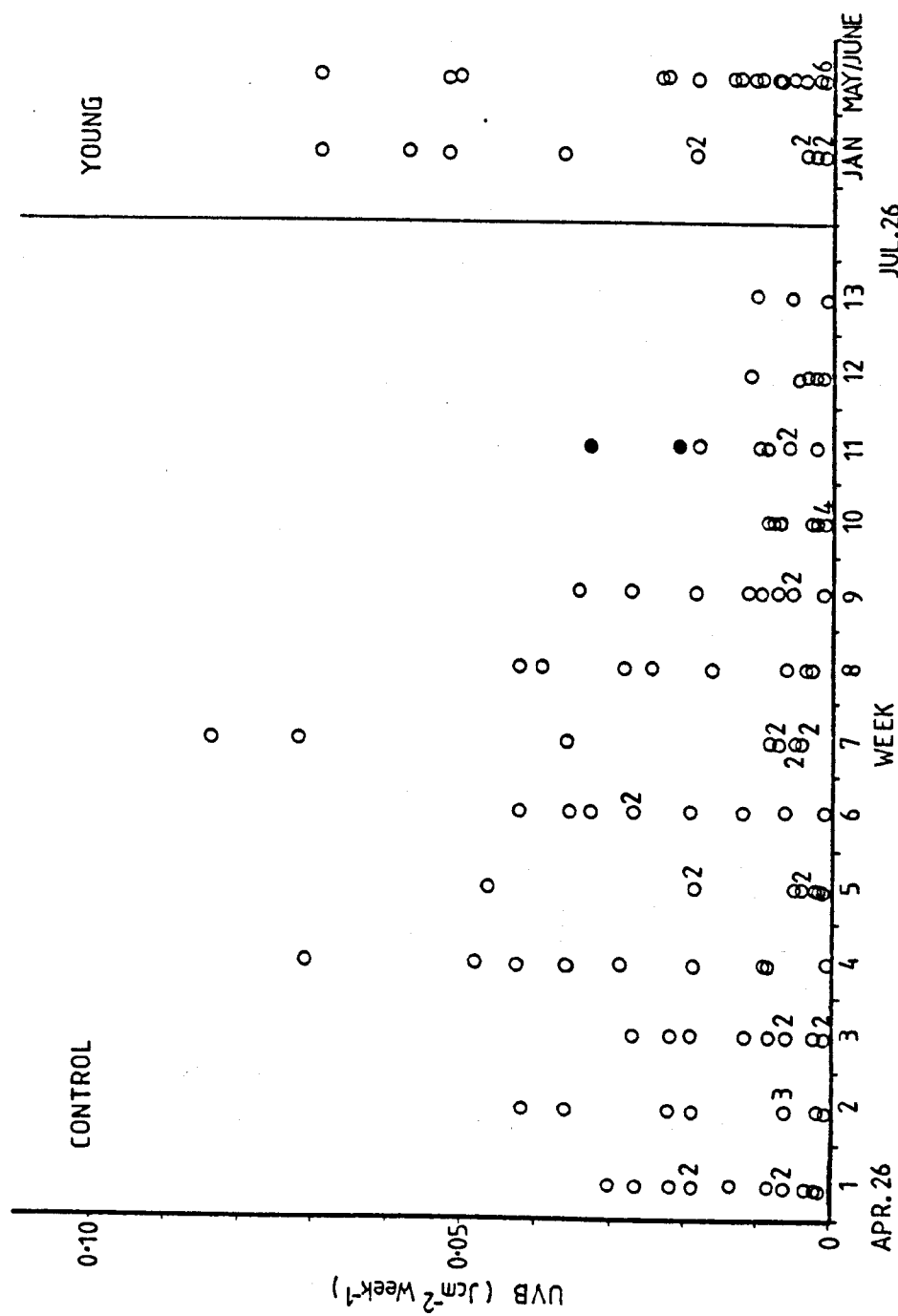
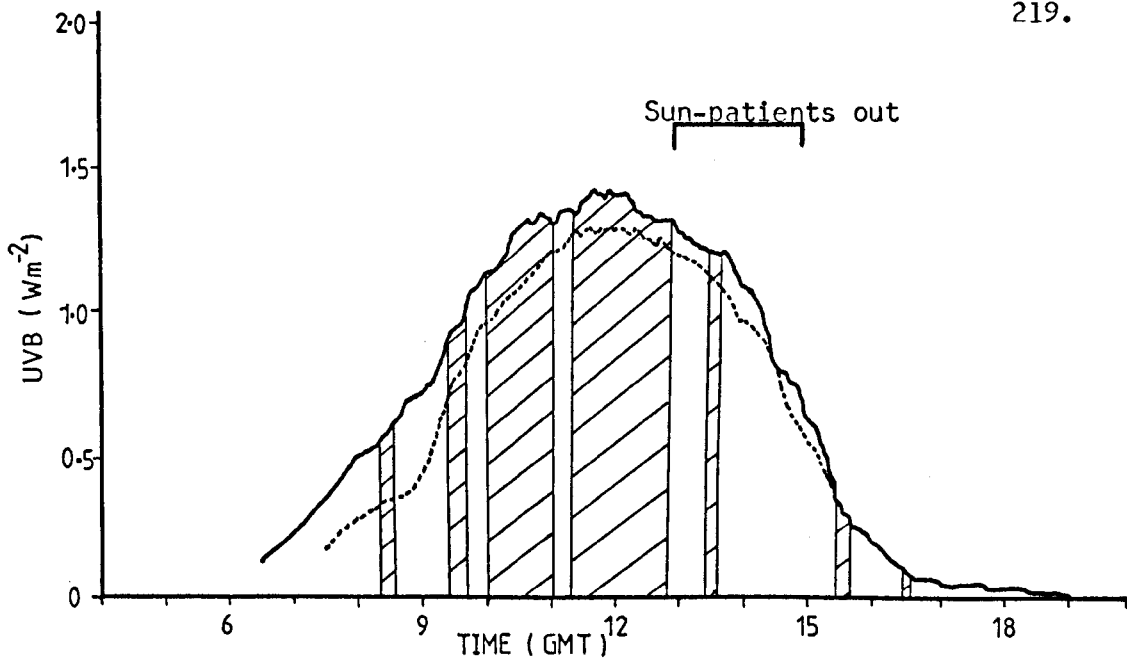


Fig. 8.1 Weekly exposures of Control group badges and indoor badges of young group.

a) 29 May 1984

219.



b) 15 June 1984

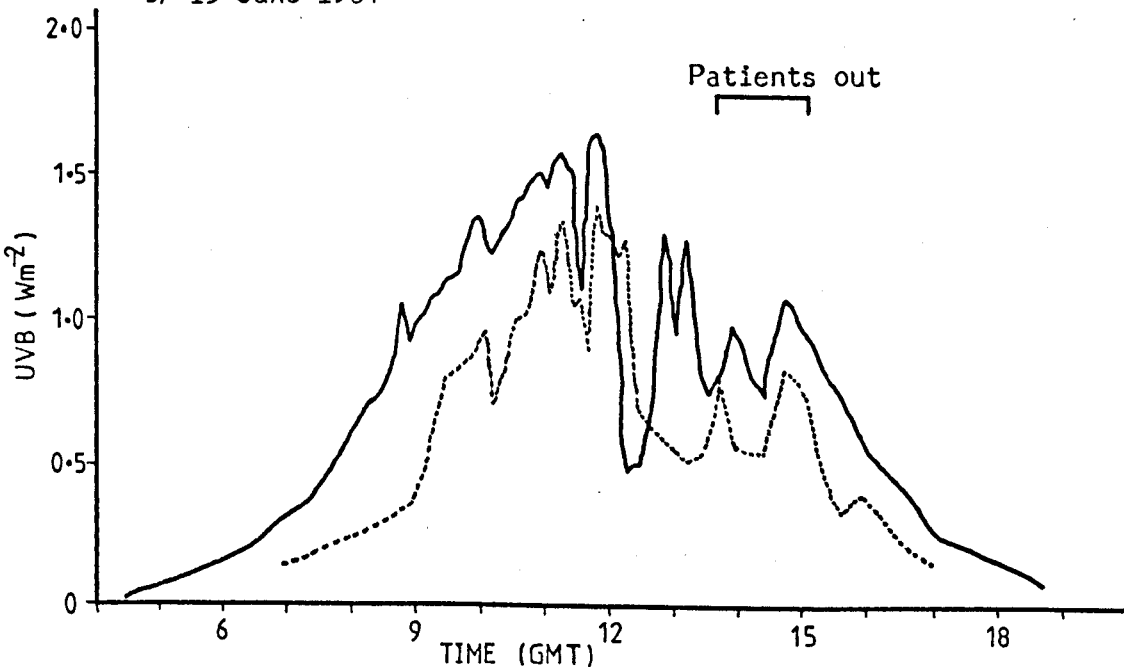


**Fig. 8.2** The available UVB radiation at Nottingham (-----) and Sutton Bonington (—) on a) a clear day, and b) a day with intermittent cloud.



Plate 8.1 The terrace to which the Sun-group had access.

radiation measured by the SEE 240 sensors on the terrace at Nottingham and on the meteorological site at Sutton Bonington. The difference between the two sites reflects their geography and the local weather conditions. Fig. 8.2b for 15 June 1984 shows the effect of varying cloud cover on the relative amounts of available UVB. On days, or part days, when cloud cover was similar at both sites (clear or completely overcast), the incident UVB radiation was always lower at Nottingham. This is illustrated in Fig. 8.2a for 26 May 1984, a clear day.

During that part of a clear day when the exposure of individuals was most frequent at both sites (0900 - 1500 GMT) the UVB at Nottingham was ~ 15 - 20% lower than at Sutton Bonington, a consequence of the restricted exposure of the site. At Sutton Bonington the SEE 240 was about 100 m from the nearest building, and 'viewed' over 99% of the celestial hemisphere. By contrast the sensor at Nottingham was about 6 m from a 3-storey building, which obscured ~30% of the celestial hemisphere. As the UVB radiation is more than 50% diffuse at this latitude even on a clear day in summer (Chapter 6) the hospital building obscures approximately 15% of the global (direct + diffuse) UVB radiation for most of the day. In the early morning (before 0900 GMT) the whole terrace was in the shade of the building, but patients were not outside at this time. Reflection of light from the buildings onto the sensor may contribute to the measured radiation, but by a small amount compared with the blocked radiation: the reflection coefficient for sand (an approximation to red brick) is 9% at 300 nm. Trees around the terrace might also be expected to reduce the incident UVB, although they did not cast direct shade on the radiation sensors.

Measurements of full solar radiation made with the Kipp solarimeter support the architecture-dependent radiation differences between sites. During the central hours of the days studied, global fullband radiation at Nottingham was 5 - 10% lower than at Sutton Bonington, a figure consistent with the UVB waveband when it is considered that the percentage of diffuse radiation over the full solar spectrum is ~ 20%.

A further factor for consideration is the difference in atmospheric pollution between the two sites. The hospital, close to the city, might be expected to have a higher concentration of low level pollutants,

including ozone. No measurements of ground level ozone are available, but the work of Derwent, et al (1976) suggests that the difference in ground level ozone between the sites would not be significant. Derwent, et al monitored low level ozone at a number of sites in southern England from central London to a rural site at Sibton. They found that ozone levels were generally above 8 pphm (the USA Quality Standard) over the whole area on days of high concentration, with little dependence on proximity to a source of precursors. Conditions of warm anti-cyclonic weather favoured high ozone concentrations, but the ozone was transported from the source area to other regions, or may have been transported into the area as a whole from the continent. Any additional absorption of UVB at ground level in Nottingham is considered negligible in comparison with the different architectural aspects of the sites.

#### Individual Exposure

The UVB radiation available to the Sun-patients may have been less than that available at Sutton Bonington, but it is the behaviour of an individual within a given UVB environment which ultimately determines exposure. The radiation dose incident on a body depends on the time of day and the duration of exposure, whether in sun or semi-shade, orientation with respect to the sun, and posture. The biological effectiveness of the intercepted dose to the individual will be governed further by the area of skin exposed. All these individual behaviour traits varied widely within and between the two groups of Sun-patients and Young subjects.

The Sun-patients were most consistent within the group. Patients who chose to go outdoors on a given day were often out at the same time

and for a similar duration. The area of skin exposed was generally only the hands and face, with the occasional bared forearm on very warm days (Plate 8.2). The patients sat in wheel-chairs or on benches and



Plate 8.2 Patients sitting on the terrace.

remained in one position. The chosen attitude of each patient was the greatest variable: some liked to sit facing directly into the sun while others preferred to be in the shade. Polysulphone film badges were worn on the lapel, where it is estimated that they receive a similar dose to the hands and face (Diffey, 1981).

Among the Young subjects behaviour was more diverse. Time of day and duration of exposure differed widely from day to day and person to person, and were not confined to any particular hour of the day. Fig. 8.2a shows the duration and times of exposure for the Young subject most frequently outdoors on 26 May 1984. The subject with least exposure was outside for less than 20 minutes.

Being mobile and usually engaged in some sort of physical activity, the Young subjects were assumed to be randomly oriented over their weekly exposure periods. In the open surroundings of Sutton Bonington they were also considered more likely to be in direct sunshine than in the shade.

Skin area exposed and the resultant biological response of the body was another uncontrolled variable, and depended on the individual and the heat of the day. Arms were frequently bared and under the most clement conditions legs and torsos were also exposed.

The range of exposures measured for individuals in each group is shown in Fig. 8.3 and Table 8.2. Exposures, from the polysulphone film badges, are plotted at the end of the week for which the badges were exposed. The dates for the two groups do not coincide exactly as the hospital badges were changed every Thursday, while the Sutton Bonington week ran from Monday to Monday (the sum of 1 week + 1 weekend badge). The maximum level of the control badges is also shown for comparison. During weeks when no patient went outside (3 - 10 May, 17 - 24 May, 12 - 19 July) all badges were within the control range, as were badges marked 'Indoors' from the Young subjects.

All data for the Sun-patients groups is shown, including patients who did not complete the trial.

The range of exposures for both groups changed tremendously from week to week, an indication of the variable weather during the early summer. The Sun-patients were the most weather-dependent group; if it was cold they remained indoors regardless of the radiation conditions.

Each Sun-patient's weekly exposure range is considered in the context of the two Young-subject weekly ranges that it spans.

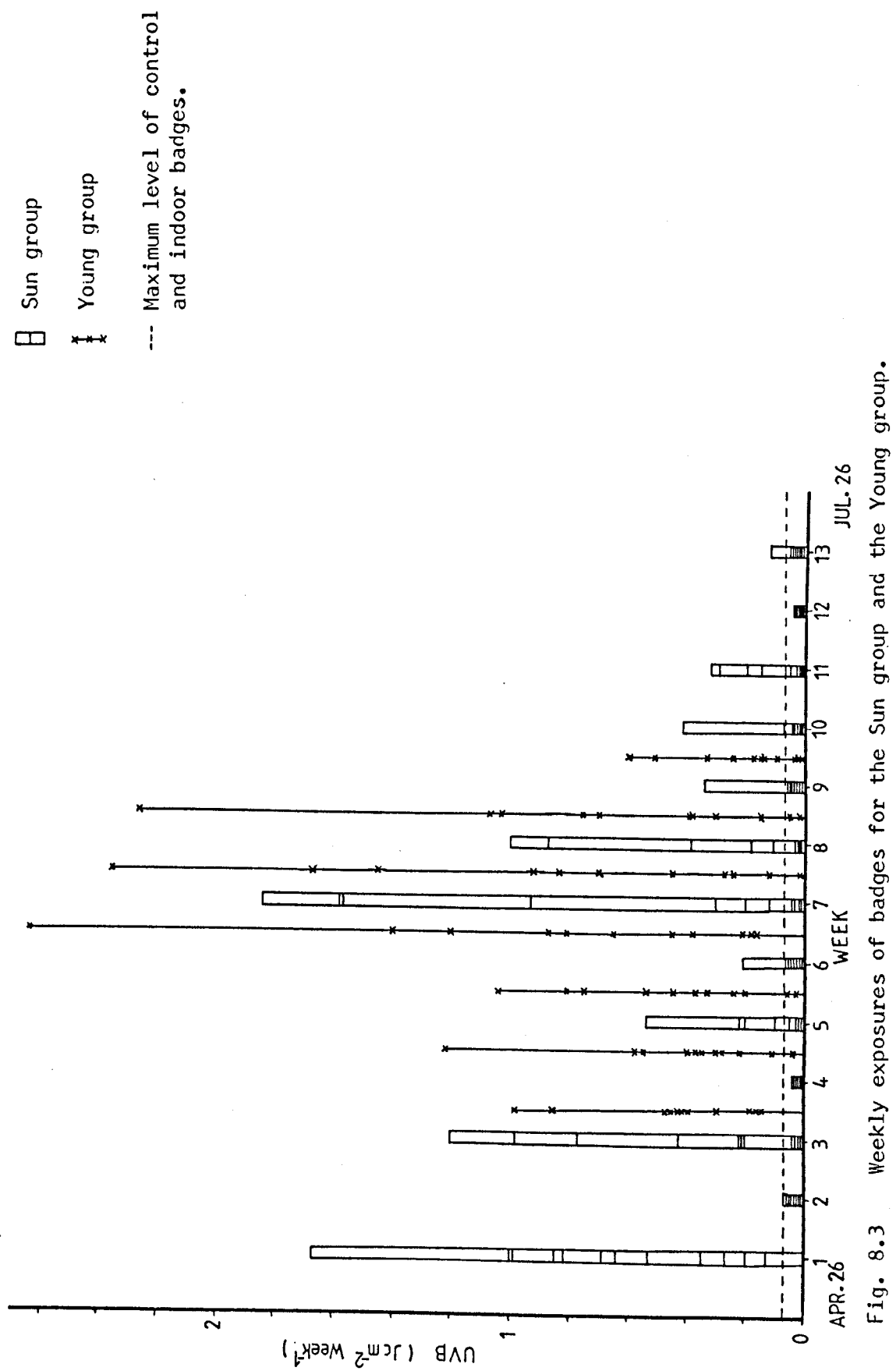


Fig. 8.3 Weekly exposures of badges for the Sun group and the Young group.

Table 8.2A Cumulative UVB exposure ( $\text{J cm}^{-2}$ ) for Sun group by week of trial.

| Week of trial | Patient |      |       |      |                   |      |      |                   |      |      |      |      |                   |      |      |      |
|---------------|---------|------|-------|------|-------------------|------|------|-------------------|------|------|------|------|-------------------|------|------|------|
|               | E1      | E2   | E3    | E4   | E5                | E6   | E7   | E8                | E9   | E10  | E11  | E12  | E13               | E14  | E15  |      |
| 1             | 0.51    | 0.82 | 1.01  | 0.69 | 0.62              | 0.27 | 1.00 | 0                 | 0.86 | 0.12 | 0.34 | 0.01 | 0.69              | 0.20 | 1.67 |      |
| 2             | I       | 0.54 | 0.82  | 1.01 | 0.69              | 0.65 | 0.27 | 1.01              | 0.18 | 0.88 | 0.12 | 0.35 | 0.11              | 0.70 | 0.20 | 1.79 |
| 3             | 1.29    | 0.87 | 2.21  | 0.79 | 0.76              | 0.29 | 1.01 | 0.18              | 0.93 | 0.14 | 0.78 | 0.14 | 0.82              | 1.18 | 1.80 |      |
| 4             | I       | 1.30 | 0.87  | 2.21 | 0.81              | 0.79 | 0.29 | 1.04              | 0.18 | 0.93 | 0.15 | 0.79 | 0.17              | 0.82 | 1.18 | 1.81 |
| 5             | 1.30    | 0.87 | 2.22  | 0.81 | 0.83 <sup>+</sup> | 0.30 | -    | 0.19              | 0.93 | 0.15 | 1.35 | 0.18 | 0.92              | 1.30 | 2.03 |      |
| 6             | 1.30    | 0.87 | 2.22  | 0.82 | 0.83              | -    | -    | 0.19              | 1.13 | 0.15 | 1.39 | 0.18 | 0.92              | 1.33 | 2.06 |      |
| 7             | 2.24    | 0.87 | 3.80  | 0.85 | 0.84              | -    | -    | 0.19              | 1.17 | 0.27 | 2.97 | 0.28 | 1.22              | 3.17 | 2.27 |      |
| 8             | 2.29    | 0.90 | 3.80  | 0.86 | 1.12              | -    | -    | 0.20              | 1.18 | 0.27 | 3.85 | 0.84 | 1.61              | 3.29 | 3.28 |      |
| 9             | 2.29    | 0.90 | 3.82* | 0.87 | 1.16              | -    | -    | 0.22              | 1.52 | 0.29 | 4.08 | 0.85 | 1.61              | 3.29 | 3.28 |      |
| 10            | 2.32    | 0.95 | 3.85* | 0.94 | 1.57              | -    | -    | 0.23              | 1.52 | 0.29 | 4.08 | 0.86 | 1.61              | 3.29 | 3.28 |      |
| 11            | 2.33    | 0.95 | 4.01* | 1.00 | 1.59              | -    | -    | 0.23 <sup>+</sup> | -    | 0.29 | 4.11 | 0.86 | 1.66 <sup>+</sup> | 3.30 | 5.63 |      |
| 12            | I       | 2.33 | 0.95  | 4.01 | 1.00              | 1.59 | -    | -                 | 0.23 | -    | 0.29 | 4.11 | -                 | 1.66 | 3.30 | 5.63 |
| 13            | 2.34    | 0.99 | 4.04  | -    | 1.71              | -    | -    | 0.23              | -    | -    | 4.11 | -    | 1.66              | 3.32 | 5.71 |      |

+ Badge damaged, estimated from grid exposure.

\* Known to be an underestimate.

I All patients remained indoors throughout the week.

**Table 8.2B** UVB exposures ( $J \text{ cm}^{-2}$ ) for Control group by week of trial.

The mean  $\pm$  standard deviation, maximum and minimum for the group is given for each week of the trial, and the cumulative mean throughout.

| Week of trial | Mean  | $\pm$ S.D. | Maximum | Minimum | $\Sigma$ mean |
|---------------|-------|------------|---------|---------|---------------|
| 1             | 0.013 | 0.009      | 0.0266  | 0.002   | 0.01          |
| 2             | 0.015 | 0.014      | 0.0418  | 0.006   | 0.03          |
| 3             | 0.011 | 0.009      | 0.0266  | 0.0     | 0.04          |
| 4             | 0.028 | 0.021      | 0.0710  | 0.0     | 0.07          |
| 5             | 0.011 | 0.014      | 0.0460  | 0.0     | 0.08          |
| 6             | 0.026 | 0.018      | 0.0640  | 0.0     | 0.10          |
| 7             | 0.023 | 0.029      | 0.0700  | 0.0     | 0.13          |
| 8             | 0.020 | 0.015      | 0.0420  | 0.003   | 0.14          |
| 9             | 0.013 | 0.010      | 0.0340  | 0.0004  | 0.15          |
| 10            | 0.003 | 0.003      | 0.0090  | 0.0     | 0.16          |
| 11            | 0.011 | 0.016      | 0.050   | 0.0     | 0.17          |
| 12            | 0.004 | 0.004      | 0.011   | 0.0     | 0.17          |
| 13            | 0.004 | 0.003      | 0.011   | 0.0     | 0.18          |

Table 8.2C Cumulative UVB exposure ( $\text{J cm}^{-2}$ ) for Young subjects by week of trial.

| Date | Subject |      |      |      |      |      |                   |                   |      |                   |      |
|------|---------|------|------|------|------|------|-------------------|-------------------|------|-------------------|------|
|      | S1      | S3   | S4   | S5   | S8   | S9   | S11               | S18               | N1   | N2                |      |
| May  | 14-20   | 0.47 | 0.30 | 0.45 | 0.45 | 0.16 | 0.17              | 1.49              | 0.85 | 0.39              | 0.98 |
|      | 21-27   | 0.87 | 0.35 | 1.31 | 0.80 | 0.71 | 1.33              | 1.60              | 1.22 | 0.61              | 1.28 |
| Ju   | 28- 3   | 1.91 | 0.38 | 1.94 | 1.13 | 1.57 | 1.40              | 1.73              | 1.67 | 1.08 <sup>+</sup> | 1.82 |
| June | 4-10    | 2.78 | 1.00 | 3.14 | 1.32 | 2.97 | 1.78 <sup>+</sup> | 2.19 <sup>+</sup> | 4.20 | 1.26              | 2.64 |
|      | 11-17   | 4.23 | 1.92 | 3.26 | 1.56 | 4.64 | 2.62              | 2.46              | 5.01 | 1.70              | 4.99 |
|      | 18-24   | 4.93 | 2.54 | 4.27 | 1.95 | 5.71 | 2.99              | 2.47              | 5.16 | 1.74              | 7.26 |
|      | 25-29   | 5.44 | 2.69 | 4.29 | 2.12 | 5.72 | 3.14              | 2.56              | 5.86 | 2.08              | 7.29 |

<sup>+</sup> Badge missing, estimated from grid exposure.

The Sun-patients as a group had less exposure in any week than the Young subjects. The weekly mean and median exposures for both groups are shown in Table 8.3. Although individual Sun-patients recorded

Table 8.3 Weekly mean and median exposures ( $\text{J cm}^{-2}$ ) for exposed subjects.

| Week | Sun-patients |               | Young group comparison              |      |                                       |      |
|------|--------------|---------------|-------------------------------------|------|---------------------------------------|------|
|      | Weekly mean  | Weekly median | Weekly means<br>(Mon-Fri) (Sat-Sun) |      | Weekly medians<br>(Mon-Fri) (Sat-Sun) |      |
| 1    | 0.59         | 0.622         |                                     |      |                                       |      |
| 2    | 0.03         | 0.006         |                                     |      |                                       |      |
| 3    | 0.26         | 0.046         |                                     |      |                                       |      |
| 4    | 0.01         | 0.003         | 0.41                                | 0.16 | 0.43                                  | 0.08 |
| 5    | 0.08         | 0.009         | 0.37                                | 0.04 | 0.29                                  | 0.03 |
| 6    | 0.03         | 0.006         | 0.37                                | 0.10 | 0.30                                  | 0.07 |
| 7    | 0.52         | 0.208         | 0.52                                | 0.36 | 0.49                                  | 0.36 |
| 8    | 0.25         | 0.113         | 0.33                                | 0.57 | 0.23                                  | 0.40 |
| 9    | 0.04         | 0.011         | 0.38                                | 0.29 | 0.40                                  | 0.12 |
| 10   | 0.05         | 0.033         | 0.23                                |      | 0.16                                  |      |
| 11   | 0.03         | 0.048         |                                     |      |                                       |      |
| 12   | 0.01         | 0.002         |                                     |      |                                       |      |
| 13   | 0.02         | 0.003         |                                     |      |                                       |      |

exposures higher than many of the Young subjects, there were always some patients who remained indoors, lowering mean and median values for the Sun-patient group.

Maximum exposure levels for both groups were reached during the two weeks 7 - 21 June. The Young subject maximum for an individual was  $2.64 \text{ J cm}^{-2} \text{ week}^{-1}$  and for the Sun-patients was  $1.84 \text{ J cm}^{-2} \text{ week}^{-1}$ . The latter exposure was the result of four afternoons spent outdoors between 1330 and 1500 GMT, giving a total time of 7 hours outside. This particular patient (E14) liked to sit facing the sun, and would therefore receive maximum UVB radiation on hands, face and badge. During the same week another patient (E13), outside for 6 hours during the same period of the day, but preferring to sit in the shade, recorded an exposure of only  $0.3 \text{ J cm}^{-2} \text{ week}^{-1}$ . A further 2 patients (E11 and E1) with exactly the same exposure times (5.5 hours) but different heliophilic tendencies had weekly exposures of  $1.58 \text{ J cm}^{-2}$  and  $0.94 \text{ J cm}^{-2}$ , illustrating the effect of personal habit on the intercepted radiation.

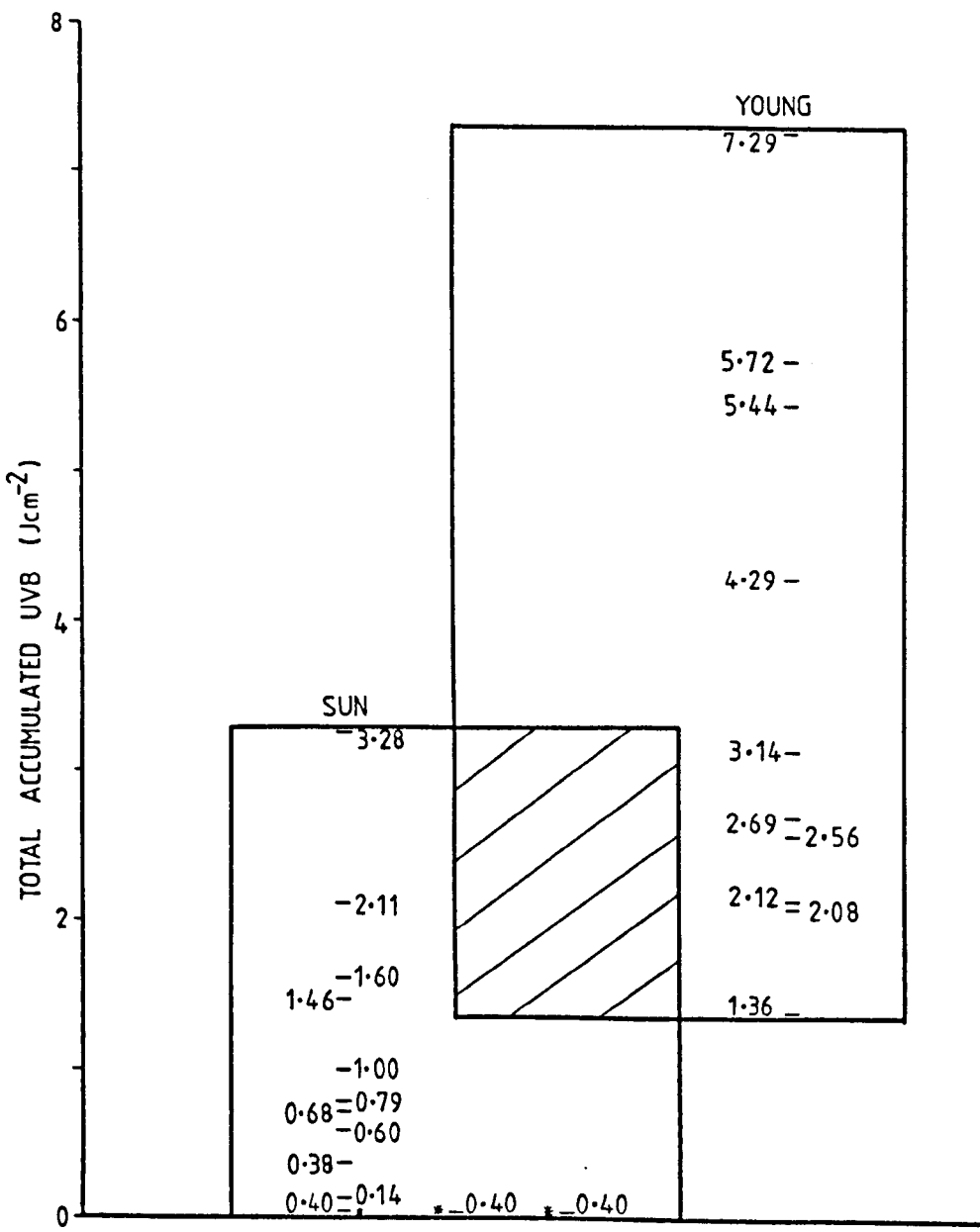
In comparison the Young subject (S18) with maximum exposure ( $2.64 \text{ J cm}^{-2} \text{ week}^{-1}$ ) had spent three full days (0800-1600) and one afternoon (1300-1700) outdoors, and the remainder of the week indoors. The days of exposure were the same as those of Sun-patient E14. The time outdoors was spent gardening (2.5 days) and in other recreational pastimes involving physical activity. Holman, et al (1983) ranked a number of recreations in order of descending average exposure for different body sites. Gardening rated the lowest (8), with sunbathing 2 (after boating), and active sports (tennis and cricket) scoring 6 and 7.

A Young subject (S8) recording 6 hours of sunbathing (1300-1900 on one day) and a further full day working in the field had a badge exposure of  $1.4 \text{ J cm}^{-2} \text{ week}^{-1}$  for the same period as above, with little additional time spent outdoors. Although the available UVB decreases with time from noon, comparing these figures with the elderly subject ( $1.58 \text{ J cm}^{-2} \text{ week}^{-1}$ ) emphasises the reduction in intercepted radiation with activity. The greater area of skin open to interception would however be expected to compensate for the effect of activity when considering the biological implications of exposure. The Young subject was sunbathing in shorts, the elderly lady was more decorously clad in dress, cardigan and stockings.

Over the seven weeks when the two groups were recording outdoor exposure, the total accumulated dose for the Sun-patients covered the range  $0.038 - 3.28 \text{ J cm}^{-2}$ . The comparable figures for the Young subjects were  $1.36 - 7.29 \text{ J cm}^{-2}$ . The overlap between the two group exposures is shown in Fig. 8.4

This diagram illustrates how elderly patients with easy access to a sunshine environment can accumulate a similar dose of incident UVB radiation to healthy younger people engaged in a variety of occupations. A couple of hours spent outside on pleasant afternoons provides the potential exposure (albeit to a lesser area of skin) received by the population in general, at little additional effort to hospital staff, and no expense. The benefits of such excursions from the ward may be apparent not only for vitamin D status (discussed below) but also in the general health and well-being of the patients.

Fig. 8.4 Total accumulated UVB ( $\text{J cm}^{-2}$ )  
for the Sun group and Young group  
from 14 - 29 May 1984.



\* No outdoor exposure.



Dose range common to both groups.

### Vitamin D Status

Plasma samples from all three groups of volunteers were analysed for 25-hydroxyvitamin D (25(OH)D) in November 1984. High pressure liquid chromatography (HPLC) and the protein binding assay set out in Appendix C were used. All the samples for any one hospital patient were measured at the same time to avoid inter-assay variation. Samples from the Young subjects were assayed in 3 sets, one for each sampling date. The assay for 13 June failed, leaving only two plasma 25(OH)D levels for this group, one at the beginning (22 May) and one at the end (3 July) of the recorded exposure period.

The mean and range of the first and last plasma 25(OH)D values for each group are in Table 8.4. Initial and final plasma concentrations for individuals within each group are shown in Fig. 8.5.

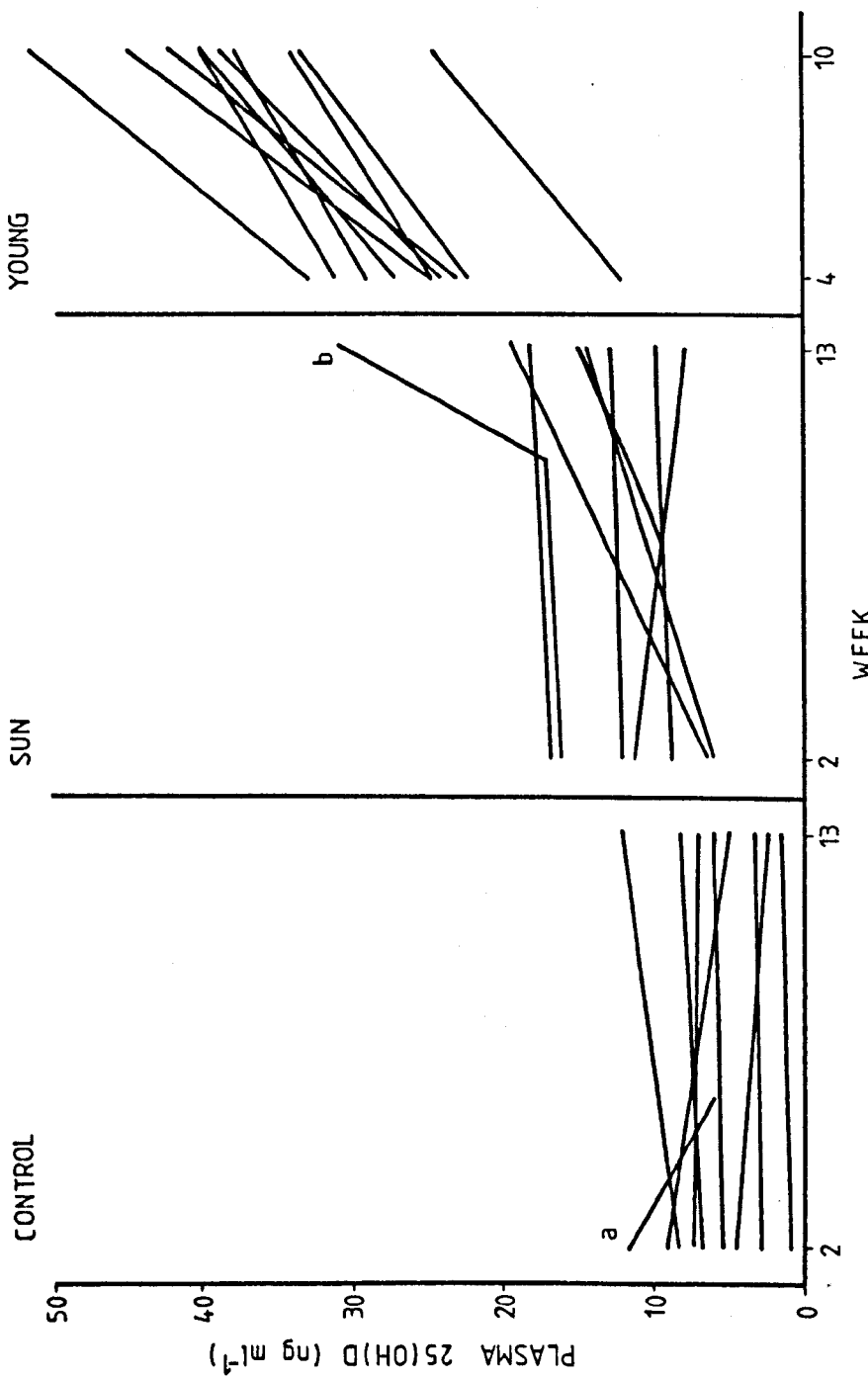
**Table 8.4** First and final plasma 25(OH)D values for the three volunteer groups.

| Group            | First plasma 25(OH)D<br>(ng ml <sup>-1</sup> ) | Final plasma 25(OH)D<br>(ng ml <sup>-1</sup> ) |
|------------------|--|--|
| Control (a)      | 6.68<br>(1 - 12)                               | 5.78<br>(2 - 12)                               |
| Sun-patients (a) | 11.51<br>(6 - 17)                              | 13.05<br>(8 - 20)                              |
| Young (b)        | 26.11<br>(13 - 38)                             | 38.68<br>(25 - 51)                             |

Standard error of difference of means (of combined groups) between first and last sample = 1.4 with 26 degrees of freedom.

(a) 10 May - 26 July. (b) 22 May - 3 July.

Fig. 8.5 First and final plasma  $25(OH)D$  concentrations of the three volunteer groups.



a Out before study began.

b In residential home for last 3 weeks of study.

The Control patients have significantly lower plasma 25(OH)D concentrations than the Sun-patients ( $P < 0.001$ ) both at the beginning and end of the study, with all elderly patients having lower concentrations than the Young volunteers. There was no significant ( $P > 0.05$ ) change in the 25(OH)D status of the control group during the trial period. Analysis of variance showed a highly significant ( $P < 0.001$ ) difference in the response of the groups between sampling dates although most of this difference was due to the Young group. When the Young subjects were removed from the analysis the response with time of the Control and Sun-patients differed only at the  $P = 0.05$  significance level. However no account was taken in this analysis of the amount of UVB radiation received by members of the Sun-group. The great variation in individual exposure introduces large standard errors, and when considering the group as a whole the non-uniformity of "treatment" masks some of the effect of exposure.

In countries with large seasonal variations in solar UVB radiation, and for a population not taking regular dietary vitamin D supplements, a seasonal change of plasma 25(OH)D is observed (Stamp and Round, 1974; Beadle, et al, 1980; Devgun, et al, 1981a in U.K.; Hamberg and Larsson, 1980 in Sweden; Audran, et al, 1984 in France). The minimum vitamin D levels occur in late winter/early spring (February to April) as stored metabolites are depleted during the winter and exposure to increasing UVB radiation has not yet begun. At the commencement of the study the Sun- and Control-patients would normally be expected to have similar winter low plasma 25(OH)D levels. However, April 1984 was unusually warm and sunny and the Sun-patients spent considerable time outdoors

in the fortnight before the trial began. This early exposure probably caused the high plasma 25(OH)D levels for this group at the start of the study (Table 8.5).

Table 8.5 Plasma 25(OH)D levels ( $\text{ng ml}^{-1}$ ) for Control and Sun-patients.

| Patient | Date (1984) |        |        |         |        |                   |                    |
|---------|-------------|--------|--------|---------|--------|-------------------|--------------------|
|         | 10 May      | 24 May | 7 June | 22 June | 5 July | 26 July           | 9 Aug.             |
| Control | C1 < 1      | 1.42   | 3.04   | 2.58    | 2.47   | 1.56              |                    |
|         | C2 3.40     | 3.44   | -      | 3.59    | 3.86   | 5.51 <sup>+</sup> |                    |
|         | C4 4.40     | 3.20   | -      | 3.56    | 5.53   | 2.24              |                    |
|         | C6 11.88    | 8.56   | 5.86   | -       | -      | -                 |                    |
|         | C7 9.60     | 10.67  | 9.40   | -       | 9.83   | 4.72              |                    |
|         | C8 7.53     | 7.20   | 6.50   | 9.70    | 12.80  | 8.50              |                    |
|         | C9 5.60     | 4.01   | 4.76   | 5.51    | 5.86   | 6.00              |                    |
|         | C10 9.50    | 16.77  | 12.00  | -       | 11.70  | 12.40             |                    |
|         | C11 7.43    | 7.30   | 11.37  | 12.30   | 9.17   | -                 | 7.00 <sup>M</sup>  |
|         |             |        |        |         |        |                   |                    |
| Sun     | E1 19.50*   | 64.60* | 12.50* | 9.93    | 11.35  | 14.09             |                    |
|         | E2 11.30    | 8.80   | 8.92   | 10.46   | 8.44   | 7.80              |                    |
|         | E3 6.16     | 4.74   | 11.15  | 10.62   | 13.28  | 19.70             |                    |
|         | E4 12.02    | -      | 13.36  | -       | -      | 12.80             |                    |
|         | E5 16.92    | 15.58  | 17.60  | 16.14   | -      | 17.32             |                    |
|         | E9 12.10    | 12.04  | 10.14  | 14.44   | -      | -                 |                    |
|         | E11 5.96    | 8.60   | 8.60   | 10.28   | 13.90  | 14.10             |                    |
|         | E12 16.51   | 67.20* | 12.20  | 13.89   | 17.09  | -                 | 31.76 <sup>M</sup> |
|         | E13 9.89    | 10.90  | 11.62  | 7.54    | 8.40   | 8.84              |                    |
|         | E14 8.77    | 9.42   | 8.87   | 13.62   | -      | 9.00              |                    |
|         |             |        |        |         |        |                   |                    |

\* Low recovery from protein-binding assay. These samples were not used for analysis.

<sup>M</sup> Male patients, both of whom were out of hospital for two weeks at the end of the trial period. C11 remained indoors, E12 spent many hours outside in the garden. Neither wore film badges during this period of absence.

+ Outside one afternoon 2 weeks before this sample.

The second sample from the Sun-patients, taken two weeks later, showed a drop in plasma concentration for four of the patients (E2, E3, E5, E9) who recorded little UVB exposure in the first weeks of the study. As there appears to be a time lag between exposure to UVB radiation and changes in plasma 25(OH)D status (Davie and Lawson, 1980), this suggests that the April exposure raised plasma levels - evident in the first set of samples - but with no further exposure and in the absence of stored vitamin D, levels had dropped 2 weeks later.

Because plasma 25(OH)D values, especially on the first sampling date, depended on the unknown UVB exposure before the study began, the base level vitamin D status for the Sun-patients was taken to be an average of the first 2 samples. The mean and standard deviation of the base level for Sun-patients are  $10.9 \pm 3.8 \text{ ng ml}^{-1}$ , with a range of 5.5 to  $16 \text{ ng ml}^{-1}$ .

The highest initial plasma concentration in the Control group ( $11.9 \text{ ng ml}^{-1}$ ) was from patient C6, taken out by relatives during April. With no further UVB exposure the 25(OH)D level of this patient fell to  $6 \text{ ng ml}^{-1}$  after 4 weeks. Excluding this anomalous record, the first sample statistics for the Control group have a mean of  $6.03 \pm 2.87 \text{ ng ml}^{-1}$  and a range of 1 to  $10 \text{ ng ml}^{-1}$ .

The plasma values on the first sample for the Young group were higher than both elderly groups. By mid May these subjects, all reasonably fit and active, had been exposed to enough UVB to raise their plasma levels above the winter minimum. All values were within the normal range for healthy young adults (Chapter 3).

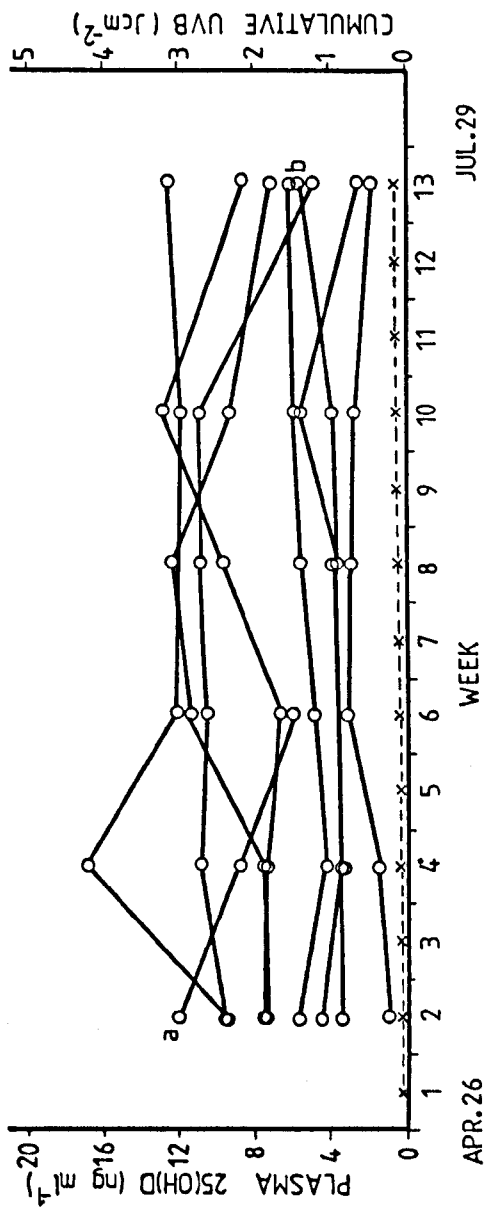
The normal range of 25(OH)D concentrations for the elderly is lower than for young people, and the plateau concentration for the elderly seems to be  $16 - 24 \text{ ng ml}^{-1}$  (Toss, et al, 1980; Dattani, et al, 1984) compared with  $50 - 80 \text{ ng ml}^{-1}$  for young adults (Stanbury, et al, 1980). It has also been suggested that in elderly patients the plasma 25(OH)D level of females is lower than that of males (Omdahl, et al, 1984) although Corless, et al (1979) and Lawson, et al (1979) found no difference between the sexes. Of the two males participating in this study the Control group male had one of the highest plasma values, but this was not significantly greater than the values for females. The male in the Sun-patient group was also at the higher end of the range. In the last 2 weeks of the study, and for a further week, this patient was at home, and exposed to much more (unrecorded) UVB radiation than in the hospital ward. By 9 August when he returned to hospital his plasma 25(OH)D level had risen to  $31.8 \text{ ng ml}^{-1}$ . However, only blood samples and exposure values measured before leaving hospital are used in group analysis.

#### The Relation Between UVB Exposure and Vitamin D Status

##### The Control group

The 9 patients in the Control group were resident in two adjacent wards with no ready access to sunlight. Two of the patients are known to have been outside, one before the study began (C6), and the second (C2) for 0.5 hour in week 11 of the trial. The plasma 25(OH)D values of the Control patients are shown in Fig. 8.6 for the duration of the study. The cumulative UVB exposure is also shown, calculated as the sum of the weekly mean badge readings for the group.

**Fig. 8.6** Plasma 25(OH)D concentrations and mean cumulative UVB dose by week for the Control group.



a Outside before study began.

b Outside for 0.5 hr in week 1.

—x— Cumulative UVB.

Plasma 25(OH)D levels remained constant throughout the trial period for most of the Control group. Two subjects showed an increase in plasma concentration during the study, but both levels fell to the patient's steady state value by the next sampling date. Such anomalies may be due to a change in diet, health or medication of the patient or errors in the assay, but are not correlated with UVB exposure.

The plasma levels for these patients are consistent with those of similar hospital patients studied by Hosking, et al (1983). They expected values of such long-stay geriatrics to be less than  $10 \text{ ng ml}^{-1}$ . At plasma 25(OH)D levels below  $8 \text{ ng ml}^{-1}$  the frequency of osteomalacia increases (Toss, et al, 1980), and at levels below  $3 \text{ ng ml}^{-1}$  a patient is classed as vitamin D deficient (Lawson, 1981).

Three patients in the Control group recorded plasma levels at or below  $3 \text{ ng ml}^{-1}$ . One patient (C1) had been confined to an institution for over a decade; the other two (C2, C4) were very small and frail and probably had very limited storage capacity for any vitamin D they might receive from their diet. Nothing is known about the metabolism of these individual patients. Different absorption, liver and kidney functions can affect the way that each patient utilises supplies of the vitamin, although no patient with obvious renal or liver complaints was included in the survey. It was noticeable that the 4 patients with the highest plasma 25(OH)D concentrations (C7, C8, C10, C11), and the most fluctuation between samples, were the 3 heaviest female patients and the male. Only one patient (C10) maintained plasma concentrations above  $8 \text{ ng ml}^{-1}$  for the entire study period. As the Control group do not usually receive any UVB exposure their vitamin D levels must be maintained by dietary intake, which this study shows to be insufficient to achieve a healthy vitamin D status.

The Sun-patient group

Plasma 25(OH)D concentrations of the Sun-patients increased over the 13-week trial. The increase between first and final samples for the Sun-group as a whole is not significant at the  $P < 0.01$  level, but it is when each patient is considered with respect to her own UVB exposure (Fig. 8.7a - k) that the change with sunlight exposure becomes most apparent.

The base plasma level for each patient (mean of the first 2 sample values) ranged from 5.5 to 16 ng ml<sup>-1</sup>. These base levels were the result of many unknown factors in the patient's history: previous and present medical condition, metabolism, diet, and the amount of UVB radiation received in the weeks before the study.

Two patients had a healthy vitamin D status when the trial began, and maintained this level with small doses of UVB radiation (Table 8.6). All other patients had levels low enough for a rise in plasma 25(OH)D to be expected with UVB irradiation.

The exposure pattern during the 13 weeks varied greatly from patient to patient. When the weather was suitable for patients to be outside, individual choice of whether to leave the ward and where to sit on the terrace resulted in the range of exposures shown in Fig. 8.3.

During the last 5 weeks (24 June - 29 July) of the trial very few of the patients had appreciable exposure. If the vitamin D status reached by the patients due to previous exposure was insufficient, or their metabolism was such that they had no stores of the vitamin, the plasma 25(OH)D concentration would be expected to decrease by the time the final blood sample was taken. Such a decrease was observed for 5 of the patients; no effective store of vitamin D is likely at this time of year when levels are still increasing after the winter depletion.

Fig. 8.7 Plasma  $25(\text{OH})\text{D}$  concentration (—) and cumulative UVB doses (----) by week for the Sun group.

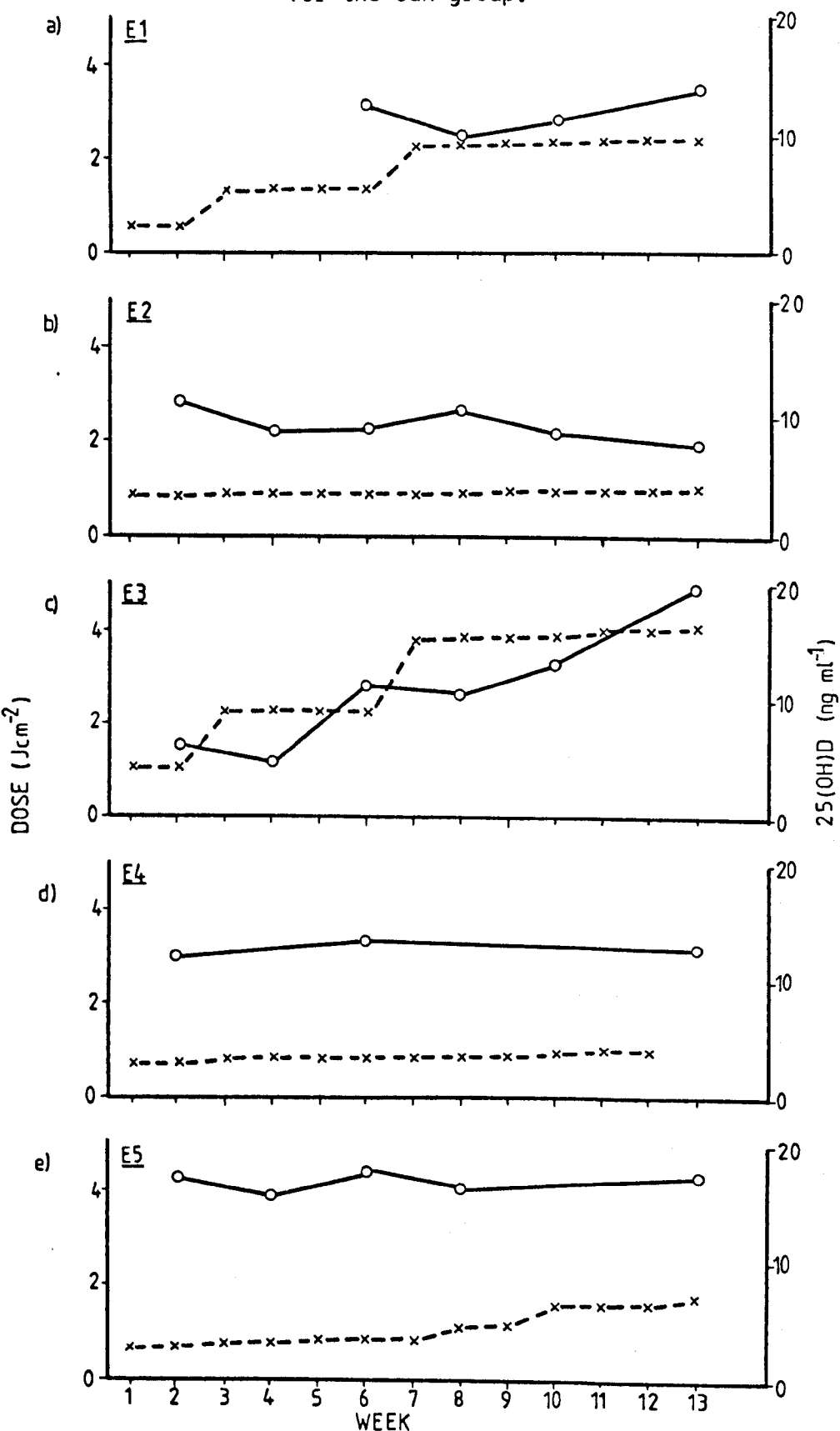
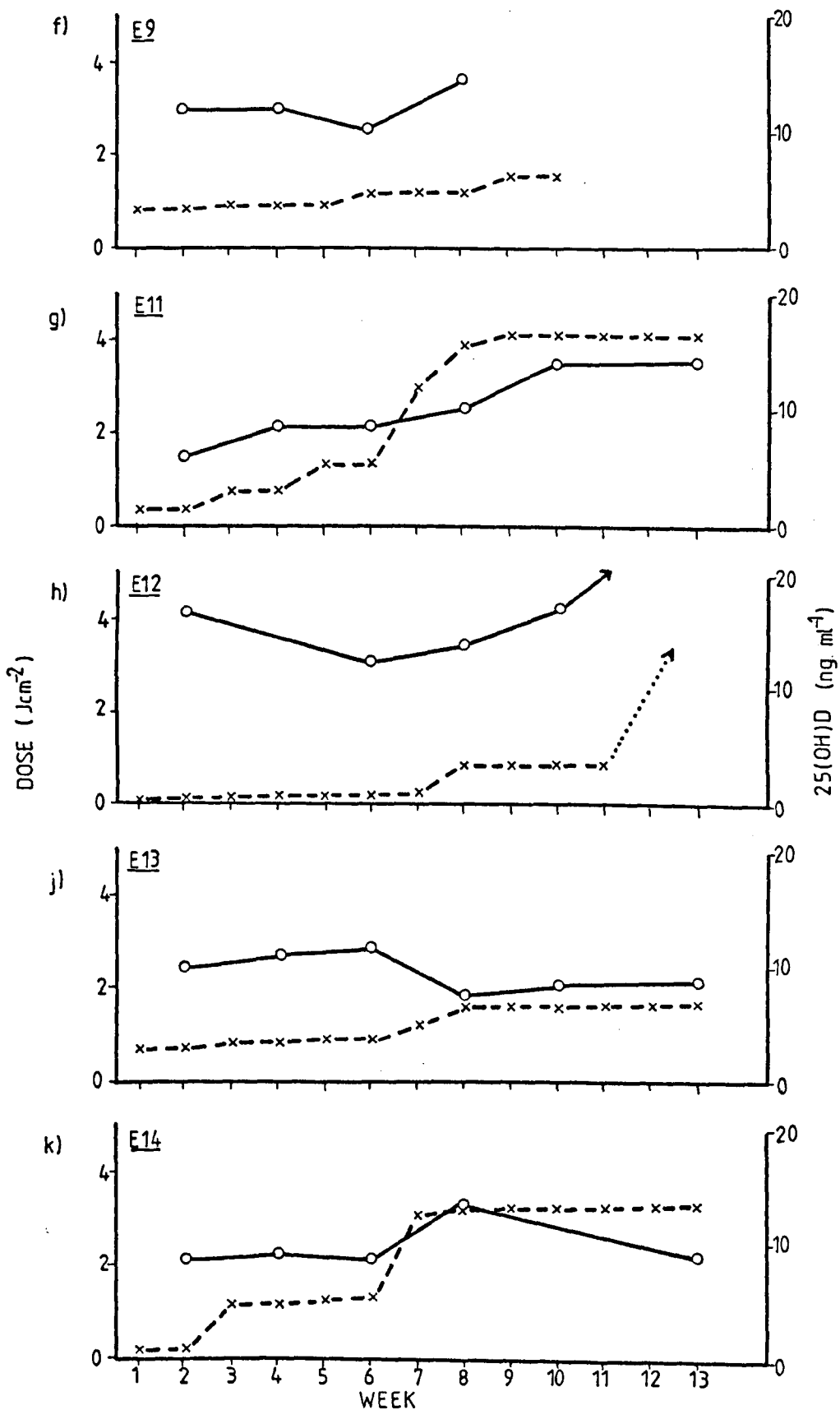


Fig. 8.7 Continued.



**Table 8.6** Plasma 25(OH)D concentrations and cumulative UVB for Sun-patients.

| Patient | 25(OH)D                        |                                |                                 |  |  |
|---------|--------------------------------|--------------------------------|---------------------------------|--|--|
|         | Base<br>(ng ml <sup>-1</sup> ) | Peak<br>(ng ml <sup>-1</sup> ) | Final<br>(ng ml <sup>-1</sup> ) | (Peak-Base) <sub>w</sub><br>(ng ml <sup>-1</sup> ) | (Cumulative UVB) <sub>w-2</sub><br>(J cm <sup>-2</sup> ) |
| E3      | 5.45                           | 19.7                           | 19.7                            | 14.25  | 4.01*  |
| E11     | 7.3                            | 14.1                           | 14.1                            | 6.8  | 4.11   |
| E14     | 8.45                           | 13.62                          | 9.0                             | 5.17   | 3.27   |
| E1      | 9.93                           | 14.09                          | 14.09                           | 4.16   | 2.34   |
| E2      | 10.05                          | 11.3                           | 7.8                             | 1.25   | 0.866  |
| E13     | 10.4                           | 11.62                          | 8.84                            | 1.22   | 0.816  |
| E4      | 12.02                          | 13.36                          | 12.8                            | 1.34   | 0.813  |
| E9      | 12.07                          | 14.44                          | 14.44                           | 2.37   | 1.13   |
| E5      | 16.25                          | 17.60                          | 17.32                           | 1.35   | 0.834  |
| E12     | 16.51                          | 17.09                          | 17.09                           | 0.58   | 0.836  |

w - Week of peak sample.

\* - This patient was known to be outdoors in the final 3 weeks without her badge, therefore this exposure value is low.

Individual charts of personal exposure to UVB and plasma 25(OH)D levels for the 10 Sun-patients supplying sufficient data for analysis are shown in Fig. 8.7a - k. A brief study of each chart will illustrate the efficacy of UVB radiation in determining the plasma 25(OH)D levels in subjects with varying metabolisms and vitamin requirements.

- a) Very low recoveries from the protein binding assay gave unreliable figures for the first two blood samples from this patient, therefore vitamin D status from weeks 6 - 13 only is considered. Weeks 3 - 6 provided no exposure to UVB radiation, and between weeks 6 and 8 the plasma 25(OH)D level declined. From week 8 to week 10 this trend was reversed after a period spent in the sun during week 7. 25(OH)D status continued to improve until the end of the study with only very small additional doses of UVB.

- b) After an initial period of exposure during week 1, patient E2 recorded very little subsequent UVB accumulation, the total cumulative dose from weeks 2 - 13 being only a factor of 1.3 greater than the mean Control group exposure. An overall decrease in 25(OH)D status implies that the primary dose of UVB was sufficient to raise plasma levels above an (assumed) post-winter depletion state, but not enough to provide any stored form of the vitamin to maintain the higher level without further exposure.
- c) As an illustration of the relationship between UVB exposure and vitamin D status, this patient provides the best pictorial example. The plasma 25(OH)D values track the exposure behaviour of the patient with a time lag of approximately two weeks. The recorded UVB in weeks 9, 10 and 11 are known to be underestimates of the true exposure; this is why the 25(OH)D continues to rise to week 13 despite the apparent lack of received UVB radiation.
- d) The only three plasma values available for this patient showed the vitamin level to remain relatively constant. This is consistent with the low degree of UVB exposure, which appears just sufficient to maintain the initial (fairly healthy) value.
- e) Sun-patient E5 had a healthy vitamin D status at the beginning of the study period, with a plasma level approaching the plateau region for an elderly female. Her plasma 25(OH)D response to UVB radiation might therefore be less obvious than for D-deficient subjects. Mawer, et al (1984) found that in young adults who were D-replete, 25(OH)D levels did increase after UVB irradiation, but the increase was negatively correlated with the initial plasma 25(OH)D level. The

only weeks when the patient had a significant dose of UVB are weeks 1, 8 and 10. With no plasma value for week 10 it is not possible to say whether or not the 25(OH)D level continued to decline from week 8 to 10 and then increased more than shown from week 10 to 13, after the exposure. A decrease from the starting plasma value (early April exposure) is evident, following three weeks with little time spent outdoors. The following rise and fall is unexplained by the exposure pattern, although this patient is known to have been outside at least once without a badge during week 5. Lack of information precludes any further conclusions being drawn about this patient's response.

- f) Patient E9 was moved to a residential home towards the end of the study and figures for 8 weeks only are available. For an elderly lady initial plasma values are adequate. A decrease in levels follows three weeks with minimal UVB exposure. Between weeks 6 and 8 the plasma level rises again after UVB irradiation in week 6. The rise is greater than might be expected from the recorded UVB, possibly due to a shaded badge or to some unknown physiological factor.
- g) Another patient showing a good correlation between UVB irradiation and plasma 25(OH)D level is Ell. As for E3 (Fig. 8.7c) there appears to be a two week response time. The overall increase in plasma concentration is less pronounced for this patient, reasons for such differences are discussed later.
- h) A second patient with a satisfactory plasma level from the first sample, was a gentleman who stayed with relatives just before the trial began and spent as much time as possible in the sun. After six weeks with

very small doses of UVB radiation (obtained by sitting immediately in front of an open window on sunny days) his 25(OH)D value had dropped. A further excursion in week 8 was followed by an increase in plasma concentration to week 10. After week 11 the patient was transferred to a residential home for 4 weeks, with easy access to the outdoors. UVB exposure was unrecorded during this time, but conversation with the patient indicated that it was as frequent as possible, and far greater than that normally achieved from the hospital ward. This was supported by the final plasma 25(OH)D level from a blood sample taken on return to hospital. The value was  $31.76 \text{ ng ml}^{-1}$ , within the range of a normal healthy population, and over  $12 \text{ ng ml}^{-1}$  higher than any patient remaining in hospital. Some workers report a sex difference in vitamin D metabolism in the elderly, with healthy males having higher plasma levels than females. This patient was the only male volunteer in the Sun-patient group.

- j) With the majority of the received UVB for patient E13 occurring in the first week of the trial, one might expect (following the  $\sim 2$  week lag period evident for most other patients) that there would be a gradual decline in plasma 25(OH)D from week 4, rather than the rise and steeper fall observed. However individual physiology, diet or medication may explain the behaviour. A fortnight after the next UVB dose (weeks 7 and 8) a small rise in plasma concentration is evident.
- k) The final Sun-patient conforms more to the theory established by study of the previous volunteers, a correlation between plasma 25(OH)D and exposure to UVB to  $\sim 2$  weeks beforehand. The exposure

during week 3 is not reflected in the plasma levels, but the peak may have been missed between the samples at weeks 4 and 6. This patient did not appear to store vitamin D: after rising to more than  $12 \text{ ng ml}^{-1}$  after exposure in week 7, there was a marked decline in plasma concentration with no further UVB irradiation.

To assess the production of vitamin D initiated by solar UVB irradiation the following analysis was employed. The peak plasma  $25(\text{OH})\text{D}$  concentration was found for each patient regardless of its time of occurrence during the trial, and the base level concentration subtracted to give the maximum change in  $25(\text{OH})\text{D}$  level (Fig. 8.8). This change was assumed to be the result of the cumulative UVB irradiation for the period up to two weeks before the peak sample was taken. These data and the plot of change in  $25(\text{OH})\text{D}$  against cumulative UVB are shown in Table 8.6 and Fig. 8.9 respectively.

The patient E3 with the greatest change in plasma concentration showed a far greater increase following UVB radiation than the rest of the group. Four possible factors could contribute to this anomaly. Firstly, the patient is known to have been outside without her badge, therefore the recorded exposure level is low. Secondly, on warm days she removed her cardigan (Plate 2), thereby exposing more skin area to UVB irradiation than patients remaining fully dressed. A third factor may be the starting level of plasma concentration, the lowest in the group, and lastly, as with all volunteers, nothing is known about personal vitamin D metabolism.

Excluding the above patient from analysis, a linear regression performed on this data gave the change in plasma concentration  $\delta P$  as

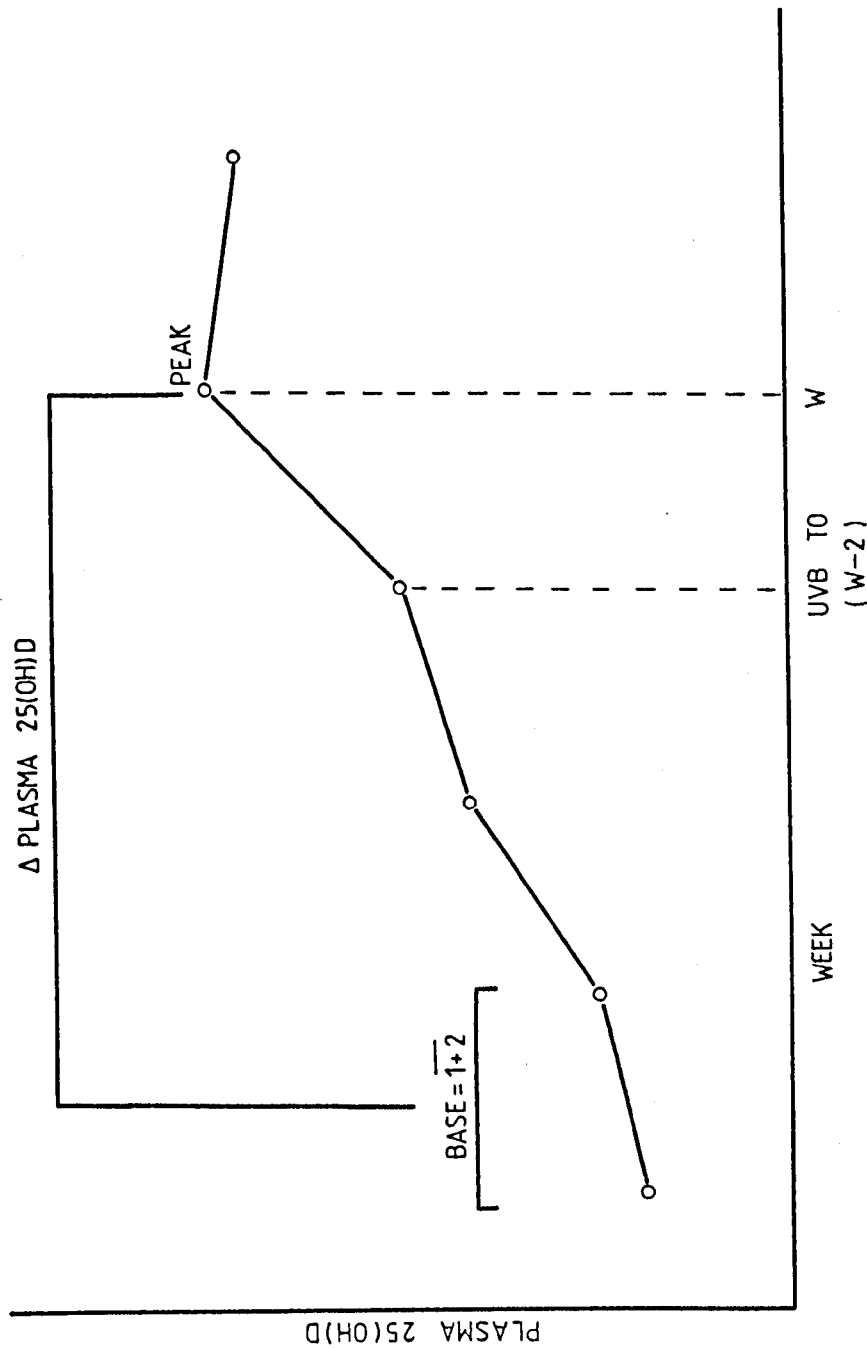


Fig. 8.8 Illustration of the change in plasma 25(OH)D concentration and the UVB irradiation to which it was attributed.

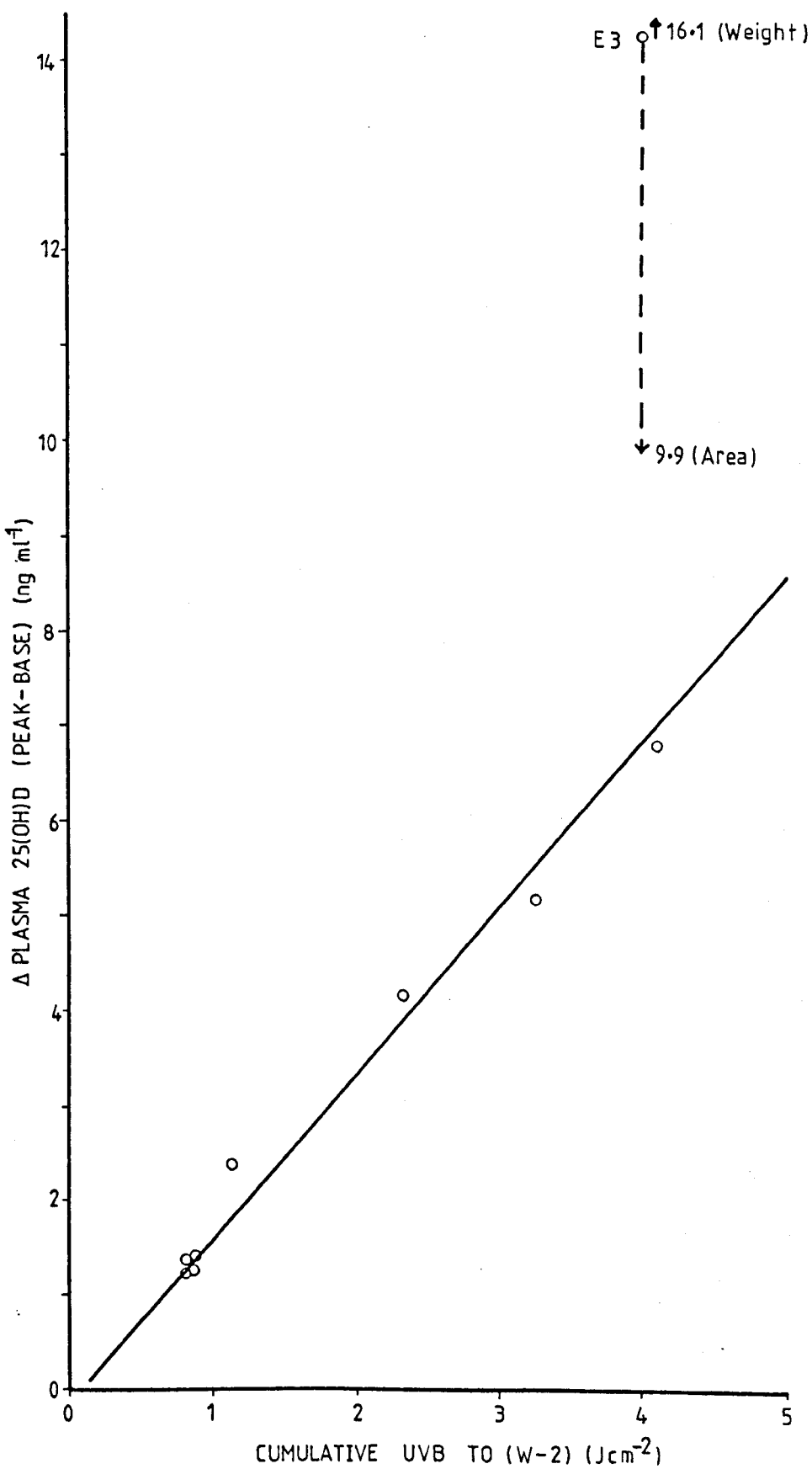


Fig. 8.9 Change in plasma 25(OH)D concentration with cumulative UVB exposure for the Sun group.

$$\delta P = (1.69 \pm 0.11) \Sigma \text{UVB} - (0.13 \pm 0.22) \text{ ng ml}^{-1} \quad (8.1)$$

where  $\Sigma \text{UVB}$  is the UVB exposure accumulated to a date two weeks before the peak plasma concentration. The standard errors of the constants are as shown and the correlation coefficient of the fit is  $r = 0.986$  with 8 subjects.

The intercept on the cumulative UVB axis ( $0.078 \text{ J cm}^{-2}$ ) below which there is no change in plasma  $25(\text{OH})\text{D}$  is of a similar magnitude to the cumulative exposures of the Control group whose mean dose for the full 13 weeks was  $0.15 \text{ J cm}^{-2}$ . If the intercept is attributed to the response of the polysulphone film badges to ward lighting at wavelengths above 316 nm the change in plasma concentration after exposure to solar UVB radiation (300-316 nm) is

$$\delta P / \Sigma \text{UVB} = 1.69 \text{ ng ml}^{-1} \text{ J}^{-1} \text{ cm}^2 \quad (8.2)$$

Eqn. 8.2 quantifies the effect of environmental UVB radiation on vitamin D status for a group of elderly subjects exposing only hands and face to sunlight. However, as plasma  $25(\text{OH})\text{D}$  concentration is a measure of the vitamin status of the whole body blood volume, and in the population at large the area of skin exposed is very variable, eqn 8.2 is not applicable in a general sense unless the volume and area dependences are removed from the relation.

To allow for differences in total plasma volume, the change in plasma  $25(\text{OH})\text{D}$  was expressed in relation to body weight to give the change in total circulating  $25(\text{OH})\text{D}$ ,  $\delta \text{TD}$  as

$$\delta \text{TD} = \delta P \times 40 \times \text{body weight (kg)} \quad (8.3)$$

assuming a plasma volume of  $40 \text{ ml kg}^{-1}$  (Brobeck, 1973).

In order to eliminate the dependence of  $\delta$ TD on exposed skin area a further approximation was made. Adults have a total skin area of between 1.5 and 2.3  $m^2$ , the precise area being a function of height and weight of the individual: the correlation reported by Diem and Lenter (1962) is

$$\log S = 0.425 \log W + 0.725 \log H + 1.896 \quad (8.4)$$

where  $S$  is surface area ( $cm^2$ ),  $W$  is weight (kg) and  $H$  height (cm), and taking the rough approximation that  $H \propto W^{1/3}$  gives the relation

$$S \propto W^{2/3} \quad (8.5)$$

The proportion of total skin area on various sites of the body is given by the 'Law of Nines' (Table 8.7), the hands and face accounting for  $\sim 6\%$  of the total surface area. For a 70 kg subject this would correspond to an area of  $600 \text{ cm}^2$  (Davie, *et al*, 1982). Correcting for the mean weight of the patient (47.2 kg) by eqn 8.5 shows the mean surface area exposed to sunlight for this group to be  $460 \text{ cm}^2$ . Applying these correction factors showed that  $\delta$ TD changed by  $1.69 \times 40 \times 47.2 / 460 = 6.9 (\pm 0.4)$  ng per joule of incident UVB irradiation.

Table 8.7 Proportion of body surface area accounted for by different parts of the body.

| Part of body  | % total body surface area |
|---------------|---------------------------|
| Head          | 9                         |
| Arm           | 9                         |
| Leg           | 18                        |
| Torso , front | 18                        |
| Torso , back  | 18                        |
| Genitals      | 1                         |

Patient E3 was excluded from the general analysis for the reasons given earlier. To investigate how much of the unusually large change in plasma concentration might be attributable to the additional skin area exposed by this patient, an individual correction was made for weight (to make this considerably heavier patient comparable with the rest of the group) and for surface area, taking the front of the lower arms to add approximately  $2 \times 0.5 \times 0.5 \times 7.5\% = 3.75\%$  to the exposed surface area. This correction brings the anomalous value of  $\delta P$  closer to that expected from the group relation (Fig. 8.9), although UVB exposure still appears to be underestimated for patient E3.

#### The Young group

With only first and final blood samples available for this group, the final plasma 25(OH)D concentration had to be assumed to be the peak reached. As UVB exposure accumulated fairly steadily for all but one of the group this is probably a valid assumption.

The cumulative UVB exposure was calculated up to two weeks before the final blood sample (to be consistent with analysis for the Sun-patients), and the change in plasma 25(OH)D plotted against this exposure for each of the 10 volunteers. Fig. 8.10 shows the graph of these data, given in Table 8.8.

The change in plasma 25(OH)D was corrected for weight, normalising to the mean weight ( $67.3 \pm 10.8$  kg) as for the Sun-patient. Excluding the subject marked b, the equation of the line in Fig. 8.10, forced through the origin, is given by

$$\delta P = (3.7 \pm 1.7) \Sigma \text{UVB} \text{ ng ml}^{-1} \quad (8.6)$$

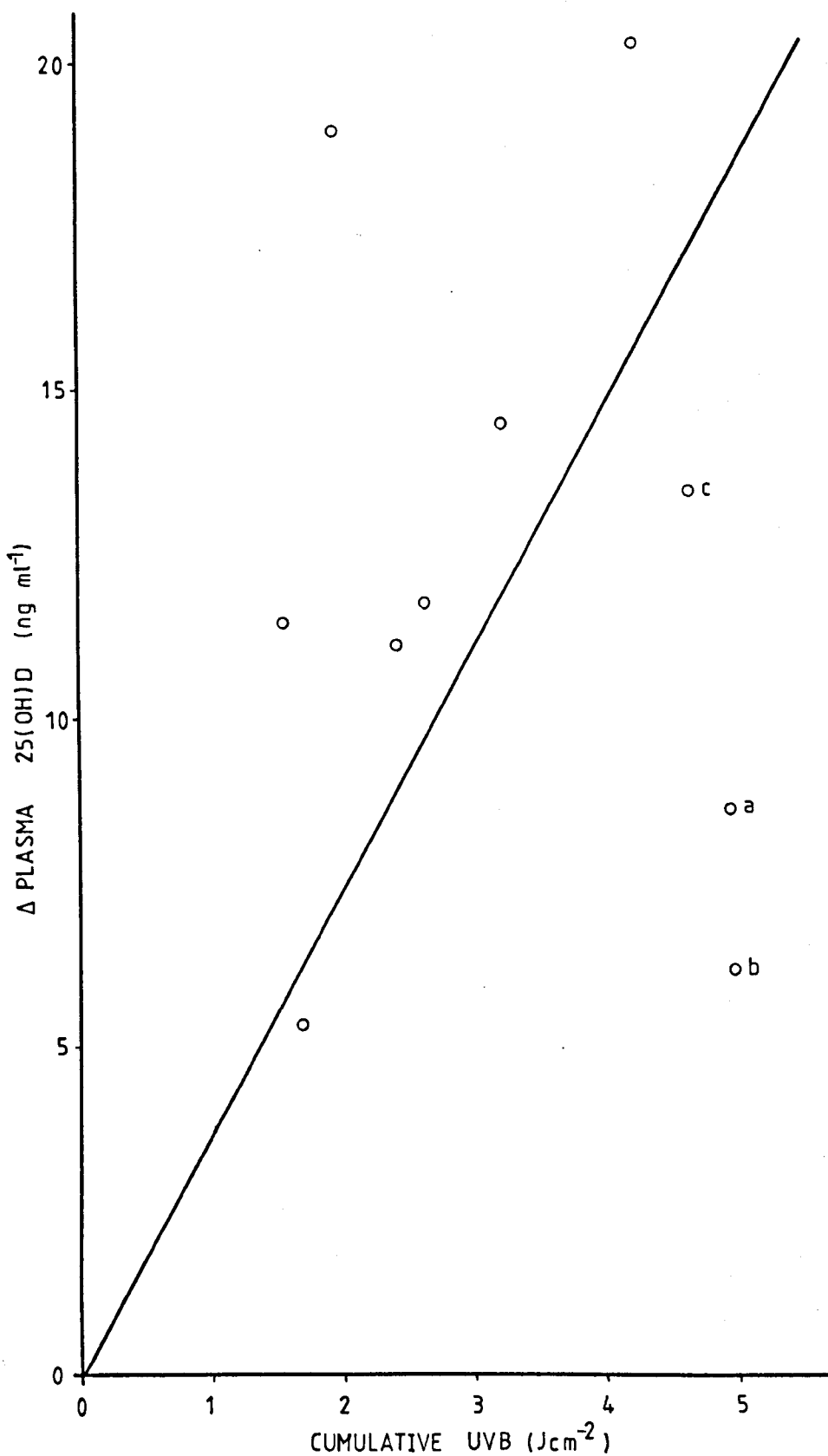


**Fig. 8.10** Change in plasma 25(OH)D concentration with cumulative UVB exposure for the Young group.

**Table 8.8** Plasma 25(OH)D levels and cumulative UVB for Young subjects.

| Subject | First plasma level<br>(ng ml <sup>-1</sup> ) | Final plasma level<br>(ng ml <sup>-1</sup> ) | Change in 25(OH)D<br>(ng ml <sup>-1</sup> ) | $\Sigma$ UVB<br>(J cm <sup>-2</sup> ) | Weight<br>(kg) |
|---------|--|--|---|---------------------------------------|----------------|
| S5      | 12.8   | 24.3   | 11.5  | 1.56                                  | 78             |
| S11     | 22.3   | 33.6   | 11.3  | 2.46                                  | 67             |
| S3      | 23.1   | 42.0   | 18.9  | 1.92                                  | 80             |
| S4      | 24.3   | 38.8   | 14.5  | 3.26                                  | 60             |
| S1      | 24.7   | 45.0   | 20.3  | 4.23                                  | 43             |
| S9      | 28.2   | 40.0   | 11.8  | 2.62                                  | 67             |
| N1      | 28.6   | 34.0   | 5.3   | 1.70                                  | 78             |
| N2      | 29.1 (a)                                     | 37.8   | 8.6   | 4.99                                  | 61             |
| S18     | 33.8 (b)                                     | 39.9   | 6.1   | 5.00                                  | 63             |
| S8      | 38.1 (c)                                     | 51.5   | 13.5  | 4.64                                  | 76             |

Volunteer (b) was taking the anti-convulsant drug phenytoin. Some anti-convulsant drugs have been found to adversely affect vitamin D metabolism. Phenytoin is reported to be associated with low plasma 25(OH)D levels (Stamp and Round, 1972; Toss, et al, 1980; Davie, et al, 1982), although Davie, et al (1983) reported that impaired vitamin D metabolism was more significant in females than males as a result of this drug. The volunteer in this study was male so the low plasma 25(OH)D change could be explained by inhibitory medication, but evidence for this is inconclusive.

The habits of the Young group differed widely, and it is not surprising that Fig. 8.10 shows a large amount of scatter. The dress (and hence skin area exposed) varied widely within the group (Plate 8.3), both between individuals and from day to day.



Plate 8.3 Variation in dress for the Young group.

A further departure from uniform group behaviour was the range of occupations within the group. The Sun-patients all remained seated and inactive during their time on the terrace. The Young subjects undertook many activities when outside, from sunbathing in a prone position, through gardening, to the more energetic tennis and jogging. The positioning of the polysulphone badge and the times spent in various pastimes render the recorded UVB exposure more subjective and prone to error than in the case of the Sun-patients.

Two of the Young subjects (marked a and c in Table 8.8 and Fig. 8.10) have further possible explanations for their deviations from the behaviour of the rest of the group.

Subject (a) received much of the cumulative UVB in one large dose during the 5th weekend of the study, the final exposure record included in this analysis. Clemens, et al (1982) found that after a single dose of UVB radiation vitamin D levels rapidly rose to a peak and then declined by 7 days after irradiation. Davie and Lawson (1980) also suggest that it is the initial exposure to UVB that is most effective and prolonged exposure is less productive than a number of smaller UVB doses over a longer period. The large weekend exposure may therefore distort the effective integrated UVB radiation for this subject.

Volunteer (c) began the study with a high plasma 25(OH)D concentration, and by the end had reached the plateau region of concentration, where no further increase in plasma 25(OH)D would be expected despite additional UVB exposure.

To make a similar analysis to that for the Sun group, the approximate skin area exposed to sunlight was estimated by assuming that the subjects were wearing a short-sleeved, V-neck shirt, thereby exposing face (3%), front of hands and arms (9%) and some torso (2%), corresponding to  $1370 \text{ cm}^2$  for a subject with mean weight of 67.3 kg. This is likely to be a conservative estimate of the average area of skin exposed to sunlight. For the Young group the surface area and weight corrected change in 25(OH)D was calculated on this basis to be  $7.3 (+ 3.4)$  ng per joule of UVB radiation.

Considering the generalisations made in reaching this figure, the result is surprisingly consistent with that calculated for the Sun-patients ( $6.9 \text{ ng J}^{-1}$ ) and provides no evidence for an age related change in the ability to synthesise vitamin D, thus agreeing with the work of Davie and Lawson (1980).

#### Validity of results

The major problem with these calculations is the uncertainty about the relationship between changes in plasma 25(OH)D and the absolute amount of vitamin D synthesised in the skin. There are two unquantifiable variables. Some cutaneously-produced vitamin D will be stored without further metabolism and therefore will not affect plasma 25(OH)D concentrations. Secondly the rate of hepatic hydroxylation is also unknown and this will also affect plasma 25(OH)D levels. Nevertheless, in a relative sense the comparison between young and old in the present study is probably valid. Both groups were studied at the same time of year when plasma 25(OH)D levels are usually at a minimum because of poor sunlight exposure during winter. Therefore a large proportion of

synthesised vitamin D will be 25 hydroxylated and this process is likely to be near its maximum efficiency since there will be little product inhibition by the low plasma 25(OH)D levels (Stanbury, et al, 1980). Moreover, since plasma 25(OH)D is generally recognised to be a good indicator of overall vitamin D status the measurements in the present study give a reasonable indication of what can be achieved in clinical practice.

#### Comparison with other work

The change in total plasma 25(OH)D initiated by exposure to sunlight was taken as  $7 \text{ ng J}^{-1}$  (representative of both young and elderly) and compared with the results of Davie, et al (1982). They found that after irradiation for 32 - 35 days

$$\delta P = 1.21 + 0.08 \times (\text{Daily UV radiation}) \quad (8.11)$$

with UV radiation measured in  $\text{mJ day}^{-1} \text{ kg}^{-1}$ . In the units of Davie, et al the change in plasma 25(OH)D on irradiance was therefore  $0.08 \text{ nmol l}^{-1} \text{ mJ}^{-1} \text{ day}^{-1} \text{ kg}^{-1}$ .

Assuming irradiation for 33 days and taking plasma volume to be  $0.04 \text{ l kg}^{-1}$ , with  $1 \text{ nmol } 25(\text{OH})\text{D} = 400 \text{ ng } 25(\text{OH})\text{D}$ , the UVB induced change in total 25(OH)D becomes  $40 \text{ ng J}^{-1}$ .

Results of the two studies differ by a factor of ~ 6, but this discrepancy must be considered in the context of the two light sources used. In the present work a Joule refers to energy of light in the waveband 300-316 nm; the Joule of Davie, et al is the energy of a Hanovia 7A lamp expressed in terms of the most effective wavelength for

vitamin D synthesis and would therefore be expected to give a higher value for photo-induced synthesis of the vitamin than the solar UVB, a waveband on the declining edge of the vitamin D action spectrum (Fig. 3.2).

Results achieved with artificial light sources may prove misleading if applied under natural lighting conditions and it is more accurate, if less convenient, to use the sun as a light source in studies related to the effects induced by natural exposures within the environment.

#### Sunshine Hours and Vitamin D Health

The exposure time to sunlight required for healthy vitamin D status is estimated below. Calculations are made for an 'average' man, weighing 70 kg and exposing only hands and face (area =  $600 \text{ cm}^2$ ) to sunlight. The change in total  $25(\text{OH})\text{D}$  initiated by solar UVB radiation (300-316 nm) is taken to be  $7 \text{ ng J}^{-1}$  which is consistent with results for both young and elderly.

An estimation of mid-morning or mid-afternoon (1000 - 1200 or 1400 - 1600 BST, 0900 - 1100 or 1300 - 1500 GMT) UVB incident on a horizontal surface was made from SEE 240 measurements for sunny days in the months April to July, giving an average hourly value of  $0.35 \text{ J cm}^{-2}$ . As hands and face are not horizontal surfaces and may be randomly orientated with respect to the solar beam, they were assumed to receive about half the incident solar UVB (Chapter 7) i.e.  $0.17 \text{ J cm}^{-2}$  during one hour outside.

One hour of exposure would produce a change in plasma  $25(\text{OH})\text{D}$  of

$$(0.17 \times 7 \times 600) / (40 \times 70) \approx 0.3 \text{ ng ml}^{-1} \quad (8.12)$$

The recommended daily dietary intake needed to maintain a healthy vitamin D status is 2.6 µg. Thompson, et al (1966) report the normal absorption rate of an oral dose of  $^3\text{H}$  vitamin D to be 62 - 91%, although dietary vitamin D, which may be protein bound, is not necessarily absorbed to the same extent. Taking an absorption rate of 75% and assuming that all plasma vitamin D (cholecalciferol) from diet or skin synthesis is converted to plasma 25(OH)D (Davie, et al, 1982), the recommended daily intake of 2.6 µg vitamin D is equivalent to plasma 25(OH)D of  $0.1 \text{ ng ml}^{-1}$  for a 70 kg man. Two hours per week spent in the sun could therefore provide the equivalent to the dietary requirement for one week.

In addition to maintaining a healthy status, summer exposures to UVB should improve vitamin D levels, increasing plasma 25(OH)D concentrations from the April minimum ( $\sim 15 \text{ ng ml}^{-1}$ ) to a level approaching the plateau value ( $\sim 45 \text{ ng ml}^{-1}$ ). This increase of  $30 \text{ ng ml}^{-1}$  would be produced by 100 hourly exposure periods, which over the months April to July would require 6 hours exposure per week plus 2 hours per week for maintenance.

Increased area of skin exposed, or exposure during the middle of the day (1100 - 1300 GMT; 1200 - 1400 BST), would reduce the time needed in the sun.

Lower plasma concentrations in the elderly mean that a winter minimum to plateau increase might typically be  $6 - 20 \text{ ng ml}^{-1}$ . The number of hours exposure per week needed to achieve this is then 3 (increase) + 2 (maintenance) i.e. 5 hours per week. Once the maximum level of circulating 25(OH)D has been reached further vitamin D

synthesised in the skin is stored for use the following winter.

This study has shown that under the radiation climate of the English Midlands sufficient UVB exposure may be gained during the summer months to maintain a healthy vitamin D status throughout the year. The importance of a cutaneously synthesised source of the vitamin over the dietary source is emphasised by the low plasma 25(OH)D status of individuals with no exposure to UVB radiation.

## 9. SUMMARY and CONCLUSIONS

### Introduction

The main aim of this work was to study the solar UVB climate and its relation to other meteorological variables. The chosen application of the climatological measurements, the cutaneous synthesis of vitamin D initiated by UVB irradiation, required the investigation of two other unknown factors: individual exposure within a specific radiation environment and the production rate of vitamin D by irradiated skin per unit of absorbed UVB.

The solar UVB radiation (300-316 nm) incident on a horizontal surface was recorded over a period of 22 months at Sutton Bonington in the English East Midlands. Global and diffuse radiation were also measured in the waveband 300-3000 nm throughout this period, and diffuse UVB irradiance was monitored for the latter 9 months. Spectral information was collected on clear days.

### Spectral Measurements

The diurnal and annual changes in clear day spectral irradiances were described with reference to atmospheric pathlength and ozone amount, illustrating the relative magnitudes of these two effects with changing wavelength. As wavelength becomes shorter ozone concentration has an increasing influence on the radiation reaching the earth's surface, resulting in an incident UVB spectrum that has a changing slope and short wavelength limit dependent on the interaction between atmospheric pathlength, ozone amount and wavelength.

### Broadband Measurements

At noon on clear days irradiance over the complete UVB waveband was found to change seasonally by a factor of 20, from  $0.09 \text{ W m}^{-2}$  in January to  $1.78 \text{ W m}^{-2}$  in June, compared with a factor of 4 for solar radiation overall. The influence of ozone is seen in the asymmetry of the annual irradiance about the solstices, since the ozone and zenith angle cycles are out of phase. Under clear skies the diurnal changes in UVB are a function of zenith angle. The influence of cloud is briefly described but is too complex to quantify with the limited data available.

Solar UVB radiation is not commonly measured despite the biological importance of this spectral region. To enable estimates of UVB irradiance to be made from more routine radiation measurements, the UVB was studied in conjunction with broader band irradiances.

Comparison with the visible waveband (300-700 nm) on clear days yielded the relation:

$$\frac{I_B}{I_V} = x + y \cos z \quad (9.1)$$

The slope  $y$  was almost constant over all days, complying with the theoretical analysis of Brinkman and McGregor (1983) who showed that  $y$  depends on the ratio of scattered light in the two wavebands, a constant under Rayleigh conditions. The intercept  $x$  by the same analysis is a function of airmass, ozone and spectral turbidities, all of which vary from day to day, as evident from the wide range of  $x$  values observed.

On clear days a proportional relation between  $\ln I_\lambda$  and  $\mu$  was observed. The constant of proportionality varied from day to day but decreased in magnitude towards longer wavelengths for a given day. The value of  $(\partial \ln I_\lambda / \partial \mu)$  should be related to ozone amount by the ozone absorption coefficient  $k_\lambda$  at wavelengths where ozone is the dominant atmospheric attenuator. This relation appeared to hold (within the experimental uncertainty) at 304 nm, but at longer wavelengths where attenuation is governed less by ozone, the experimental data did not agree with these theoretical expectations. Spectral UVB measurements made by Bener (1960) at Davos were consistent with the measurements at Sutton Bonington when analysed in the same manner, suggesting that the simplified theory of dominant ozone absorption loses validity at longer wavelengths and other atmospheric attenuation processes must also be considered. The ratio of global to direct beam radiation  $g$  was taken as an indicator of the Rayleigh and aerosol scattering along the atmospheric pathlength. Originally  $\partial g / \partial \mu$  was assumed to be constant. However, it was found that at 309.2 nm and 316.2 nm  $\partial g / \partial \mu$  changed from day to day, but insufficient measurements were available to establish the controlling factors.

An extended series of measurements is needed over the UVB waveband to gain further insight into the spectrally dependent atmospheric attenuation in this limiting region of the solar spectrum.

When the spectral measurements were compared with a recent model of the UVB clear day irradiances developed by Gerstl, et al (1983), they agreed well, within the constraints to which conditions could be matched.

Following a similar procedure for the full solar waveband, the ratio  $I_B/I_F$  showed a much greater variation in slope  $y$  from day to day. The complete solar spectrum, in contrast with the UVB and visible bands, is subject to attenuation by absorption as well as scattering: water vapour absorption in the infra-red spectral region fluctuates from day to day even in nominally clear conditions and is thought to be responsible for the large range of  $y$  values for the ratio  $I_B/I_F$ .

It has only been possible to quantify relations between the instantaneous flux of UVB and broader solar wavebands on clear days. However, for practical applications the quantity required is often the total radiation dose received over a period of time, under a variety of meteorological conditions. To investigate the possibility of estimating UVB doses from broadband measurements the daily integrated totals of UVB and full solar radiation were calculated for all days for 19 months in 1983 and 1984. Plotting  $\Sigma I_B$  against  $\Sigma I_F$  for each month gave a series of straight lines with gradients which were then normalised from the monthly mean amounts of atmospheric ozone to an arbitrary ozone amount of 350 matm cm. Plotted against the cosine of the zenith angle at noon on the 15th day of each month, these normalised ratios gave the relation

$$(\Sigma I_B/\Sigma I_F)_n = (1.62 \pm 0.12) \cos Z_m - (0.02 \pm 0.077) \quad (9.2)$$

allowing daily incident UVB radiation to be estimated from routine meteorological measurements of the daily integrated global solar radiation to an adequate accuracy. Knowledge of the daily ozone amount

allows a correction factor to be applied to eqn 9.2 to compensate for the difference between actual and arbitrary (350 matm cm) ozone amounts.

This relation was established at Sutton Bonington and cannot be unconditionally applied at other locations where the shape of the solar UVB spectrum is different because of different ozone concentrations and solar angles. Nonetheless, relations for other locations should follow a similar form although the constants in eqn 9.2 might be expected to change. Measurements from other areas of the world are needed to formulate a more universally applicable version of this relation and allow estimates of UVB doses to be made from more commonly measured radiation totals.

#### Diffuse Radiation

Measurements of diffuse UVB radiation showed no consistent relation with any of the other measured radiation quantities. The diffuse component of irradiance is a result of scattering along the atmospheric pathlength below the ozone layer; hence  $(D/I)_B$  is independent of the amount of ozone in the atmosphere and is a function of other varying atmospheric constituents. As scattering effects are wavelength dependent, fluctuating amounts of aerosol affect diffuse radiation to different extents across the solar spectrum and there is no clear correlation between values of  $D$  or  $(D/I)$  in different wavebands.

Clear day values of  $(D/I)_B$  ranged from 0.56 in June to 1.0 in December, and were always higher than the corresponding values of  $(D/I)_F$ , a consequence of the  $\lambda^{-4}$  dependence of Rayleigh scattering.

The shade-ring correction for diffuse UVB measurements made under a standard shade-ring was found to be  $g_r + 0.01$  where  $g_r$  is the geometric correction which may be calculated for any time and place and is the correction required under isotropic conditions. The additional factor (smaller than for the full solar waveband) results from the anisotropy of the diffuse radiation. Anisotropy may be quantified by two parameters: the relative strength of the circumsolar region,  $C_*$ , and the angular width of this region,  $\xi_*$ . Values of  $C_*$  and  $\xi_*$  for the UVB were calculated from shade-ring correction measurements and found to be 0.36 and 0.78 radians respectively. Compared with the corresponding values for the full solar waveband this shows the UVB circumsolar region to be wider but not as strong as for the full solar waveband: diffuse UVB radiation is more isotropic, a consequence of the stronger Rayleigh scattering function at short wavelengths.

Diffuse radiation is particularly important when considering the illumination of oriented surfaces. The total weekly UVB irradiance of vertical surfaces was investigated with respect to the corresponding irradiance on a horizontal surface in January and May/June. South facing slopes on average receive twice the radiation of north facing slopes, east and west faces being intermediate and dependent on the weekly weather pattern. The vertical to horizontal ratio averaged over the four faces ranged from 0.45 to 0.56 independent of time of year, with a maximum of 0.63 when the ground was snow covered. A vertical surface randomly oriented over a period of time

would therefore be expected to receive approximately half the corresponding radiation incident on a horizontal surface - an expression of relevance when considering the exposure of human skin to UVB radiation as the exposed areas on the face and limbs are usually upright.

Further measurements of the incident UVB at other locations are needed to confirm the type of relations mentioned in the previous sections under different radiation regimes, where the short wavelength limit of the solar spectrum may extend beyond, or occur before, that at Sutton Bonington. More detailed atmospheric data, including turbidity measurements for example, are required if the complex processes of spectral attenuation involved across the UVB waveband, from domination by ozone absorption to an increasingly important response to aerosol content, are to be better understood.

Having studied the environmentally available UVB, the other two unknowns required to quantify cutaneous synthesis of vitamin D were investigated.

#### Personal Exposure

Polysulphone film was tested and found suitable as a means of monitoring personal exposure to solar UVB radiation. The film was calibrated against the solar UVB waveband in energy units, rather than as equivalent dose at a specified wavelength, or in biological dose rate units as used previously. Both these methods necessitate detailed knowledge of the illuminating spectrum and the response spectrum of the reaction being studied if measurements are to be used

for more than one application, or compared between workers. As the solar spectrum varies considerably and is not extensively documented below 320 nm, and the response spectrum of vitamin D in vivo in the natural environment is also subject to some uncertainty, a direct measurement of irradiation in standard units provides a more flexible and less ambiguous record of exposure.

Polysulphone film badges were used to measure the exposures of two sample populations: young adults employed in a variety of occupations and a group of elderly long-stay hospital patients.

Exposure measurements from the young population in January and May/June showed UVB received by an individual in the natural environment to depend both on time of year and occupation. The percentage of ambient UVB received while employed in different ways agreed with the findings of other workers, ranging from 3% for office workers to 22% for gardeners, with sunbathing heading a list of recreational activities leading to high UVB radiation doses. The change in exposure with season is most pronounced for outdoor workers, as a result of increases in both ambient UVB and the time spent outdoors. A 10-fold increase was observed from January to June for gardeners; indoor workers showed a corresponding 6-fold increase mainly as a result of additional exposure during leisure hours. These measurements were taken as a representative norm for a healthy population against which to compare the exposures of long-stay hospital patients.

The elderly patients formed two groups, with and without access to an outdoor terrace. There was a marked difference between the UVB exposure of the two groups, the unexposed control group providing a reference zero exposure badge reading.

Vitamin D Status and UVB Exposure

The solar UVB radiation received by the elderly was monitored from April to July, together with plasma 25(OH)D concentrations measured at fortnightly intervals. A subsample of the young population also gave blood at the beginning and end of their May/June exposure trial.

Levels of plasma 25(OH)D were lowest in the control patients, amongst whom there was no sustained increase in vitamin D status during the study. Some of the patients were at or below the plasma level clinically defined as D-deficient. By contrast the patients with access to the terrace showed improved plasma 25(OH)D levels after exposure to sunlight. The change in plasma concentration was proportional to exposure to UVB radiation, the effect of irradiation taking approximately two weeks to become apparent as an increase in the circulating 25(OH)D metabolite. The change in plasma 25(OH)D following solar UVB irradiation (300-316 nm) was calculated to be  $6.9 \pm 0.4 \text{ ng J}^{-1}$  for the elderly. A similar calculation for the young population yielded a production rate of  $7.3 \pm 3.4 \text{ ng J}^{-1}$ , this group being subject to much greater variation in the area of skin exposed. These results suggest that the ability of skin to synthesise vitamin D is not impaired with age.

Taking  $7 \text{ ng J}^{-1}$  as an endogenous synthesis rate representative of both populations, it was estimated that 5 hours per week spent in the sun from April to July would be sufficient to build up plasma 25(OH)D concentrations in the elderly from a state of post-winter depletion to a level providing sufficient bodily stores of the vitamin to maintain a healthy plasma 25(OH)D status throughout the following winter months.

Many questions still remain to be answered about solar induced cutaneous synthesis of vitamin D: the efficacy of different irradiation patterns, large single vs small multiple doses; the productivity of skin on different areas of the body; the possibility of synergistic effects from radiation of different wavelengths; the reduction in efficiency due to UVB screening by increased pigmentation; the annual cycle of vitamin D status and its relation to the status achieved in previous seasons. However, the change in plasma 25-hydroxyvitamin D with exposure to solar UVB has been quantified for the radiation environment of the English East Midlands and it has been clearly demonstrated that sunlight plays the major role in maintaining healthy vitamin D levels in the population. For the elderly confined to institutions sunlight exposure appears to be particularly beneficial. Dietary intake of the vitamin is generally well below the national recommendation for these individuals and inadequate to maintain a desirable plasma 25(OH)D level, but access to sunlight enables a healthy D-status to be achieved.

For the population as a whole UVB remains the over-riding determinant of the vitamin D condition of individuals. Assuming dietary intake to be constant, the increases in plasma 25(OH)D observed in this study were due to irradiation of skin by sunlight. Cessation of UVB exposure results in a declining concentration of the 25(OH)D metabolite in blood indicating that a normal diet is insufficient to maintain the vitamin D status that can be reached by routine activities in the English climate. The vegan participating in the study had a plasma 25(OH)D

concentration mid-way between the extremes of the population range both at the beginning and end of the trial. With no dietary source of the vitamin his D-status is a result entirely of UVB induced cutaneous synthesis, which appears fully adequate.

These conclusions may tentatively be applied to the other main group at risk of D-deficiency, the Asian community. Education to more sunlight exposure would seem to be a better solution to their problem than attempts to alter or fortify the diet. Asians, because of their increased pigmentation, may require more sunlight exposure, and be less inclined to take it, than Caucasians. Improvement of both vitamin sources, dietary and endogenous can be achieved by education to a way of life that is better adapted to the English environment.

Increased pigmentation is a protective mechanism of the skin against damage by short wavelength UV light. More is heard of the hazards of increasing UVB exposure to fair skin, whether by moving to lower latitudes or by artificial means, than of the deficiency effect evident in immigrant rickets. An English summer provides sufficient naturally available UVB to maintain the vitamin D health of the indigenous population without inducing a high incidence of skin cancer; pigmented races remain healthy on both accounts under their own climates of origin. Evolution has found the balance between hazard and benefit from UVB exposure under the latitudinal range of incident radiation levels, but the facility to travel can upset that balance. However, for the environmentally available UVB levels in England the only health hazard connected with solar UVB radiation would appear to be due to lack of exposure.

**PAGE  
MISSING  
IN  
ORIGINAL.**

For nothing worthy proving can be proven  
Nor yet disproven: wherefore thou be wise  
Cleave ever to the sunnier side of doubt.

(The Ancient Sage) 1855 Alfred, Lord Tennyson

REFERENCES

- ABILLON, E. and MERMET-BOUVIER, R. (1973) Effect of wavelength on production of previtamin D. *J. Pharm. Sci.*, 62, 1688
- ANGELL, J.K. and KORSHOVER, J. (1983) Global variation in total ozone and layer-mean ozone: An update through 1981. *J. Clin. Appl. Met.* 22, 1611-1627
- AUDRON, M., JALLET, P., AVENEL, M., BIDET, M., GALLAND, F. and RENIER, J.C. (1984) Variations saisonnières des metabolites de la vitamine D chez l'homme. *Presse Med.*, 13, 661-663.
- BARTON, I.J. and PALTRIDGE, G.W. (1979) The Australian climatology of biologically effective ultraviolet radiation. *Aust. J. Dermatol.*, 20, 68.
- BARTON, I.J. and ROBERTSON, D.F. (1975) Measurements of erythemally effective ultraviolet radiation and total ozone content. *Nature*, 258, 68-69.
- BATCHELOR, A.J. and COMPSTON, J.E. (1983) Reduced plasma half life of radio labelled 25-hydroxyvitamin D<sub>3</sub> in subjects receiving a high fibre diet. *Br. J. Nutr.* 49, 213-216.
- BEADLE, P.C., BURTON, J.L. and LEACH, J.F. (1980) Correlation of seasonal variation of 25-hydroxycalciferol with UV radiation dose. *Br. J. Dermatol.*, 102, 289-293.
- BENER, P. (1960) Investigation of the spectral intensity of ultra-violet sky and sun + sky radiation (between 297.5 m $\mu$  and 370 m $\mu$ ) under different conditions of cloudless weather at 1590 m a.s.l. Contract AF 61(052)-54, Technical Summary Report No. 1. Physikalisch-Meteorologisches Observatorium Davos, Davos-Platz, Switzerland.

- BENER, P. (1963) The diurnal and annual variations of the spectral intensity of ultraviolet sky and global radiation on cloudless days at Davos, 1590 m a.s.l. Contract AF 61(052)-618 Technical Note No.2 Physikalisch-Meteorologisches Observatorium Davos, Davos-Platz, Switzerland.
- BENER, P. (1964) Investigation on the influence of clouds on ultraviolet sky radiation (at 330 m $\mu$  and 370 m $\mu$ ). Contract AF 61 (052)-618 Technical Note No. 3 Physikalisch-Meteorologisches Observatorium Davos, Davos-Platz, Switzerland.
- BIGGS, R.H. (1982) A UV-B radiation transmitting greenhouse for plant studies. In: Biological Effects of UV-B Radiation. Eds. Bauer, H., Caldwell, M.M., Tevini, M. and Worrest, R.C. Proc. Workshop held in Munich-Neuherberg, May 25-27, 1982. Gesellschaft fur Strahler und Umweltforschung mbH, Munchen, Bereich Projektgroer schaften.
- BIGGS, R.H., WEBB, P.G., GARRARD, L.A. and WEST, S.H. (1985) Effects of ultraviolet-B radiation on yield of wheat under field conditions. In: The Impact of Solar Ultraviolet (UV-B) Radiation Upon Terrestrial Ecosystems. Ed. Worrest, R.C. (In Press).
- BOGENREIDER, A. and KLEIN, R. (1982) Does solar UV influence the competitive relationships in higher plants? In: The Role of Solar Ultraviolet Radiation in Marine Ecosystems. Ed. J. Calkins. NATO conference series: Series IV: Marine Sciences 7.

- BRINKMAN, A.W. and McGREGOR, J. (1983) Solar radiation in dense Saharan aerosol in northern Nigeria. *Q.J.R. met. Soc.*, 109, 831-847.
- BROBECK, J.R. (Ed). (1973) Best and Taylor's Physiological Basis of Medical Practice (9th ed.). Williams and Wilkins Co., Baltimore 1973.
- CALDWELL, M.M., ROBBERECHT, R. and BILLING, W.D. (1980) A steep latitudinal gradient of solar ultraviolet-B radiation in the Arctic-Alpine life zone. *Ecology*, 61(3), 600-611.
- CALLIS, L.B. (1979) Solar variability and ozone. *New Scientist*, 84, 532.
- CHALLONER, A.V.J., CORLESS, D., DAVIS, A., DEANE, G.H.W., DIFFEY, B.L. GUPTA, S.P. and MAGNUS, I.A. (1976) Personnel monitoring of exposure to ultraviolet radiation. *Clin. Exp. Dermatol.* 1, 175.
- CLEMENS, T.L., ADAMS, J.S., HENDERSON, S.L. and HOLICK, M.F. (1982) Increased skin pigment reduces the capacity of skin to synthesise vitamin D<sub>3</sub>. *Lancet i* (1982), 74-76.
- COLLINS, B.G. (1973) Ultraviolet radiation at Aspendale, Victoria. CSIRO.
- CORLESS, D., GUPTA, S.P., SATTAR, D.A., SWITALA, S. and BOUCHER, B.J. (1979) Vitamin D status of residents of an old people's home and long stay patients. *Gerontology* 25, 350-355.
- CORLESS, D., GUPTA, S.P., SWITALA, S., BARRAGRY, J.M., COHEN, R.D. and DIFFEY, B.L. (1978) Response of plasma 25-hydroxyvitamin D to ultraviolet irradiation in long-stay geriatric patients. *Lancet ii* (1978) 649-651.

DATTANI, J.T., EXTON-SMITH, A.N. and STEPHEN, J.M.L. (1984)

Vitamin D status of the elderly in relation to age and exposure to sunlight. *Hum., Nutr. Clin. Nutr.* 38C, 131-137.

DAVE, J.V. and HALPERN, P. (1976) Effect of changes in ozone amount on the ultraviolet radiation received at sea level of a model atmosphere. *Atmos. Environ.* 10, 547-577.

DAVIE, M.W.J., EMERSON, C.E., LAWSON, D.E.M., ROBERTS, G.E., BARNES, J.L.C., BARNES, D. and HEELEY, A.F. (1983) Low plasma 25-hydroxyvitamin D and serum calcium levels in institutionalized epileptic subjects: associated risk factors, consequences and response to treatment with vitamin D. *Q.J. Med. New Series LII.* 79-91.

DAVIE, M. and LAWSON, D.E.M. (1980) Assessment of plasma 25-hydroxyvitamin D response to ultraviolet irradiation over a controlled area in young and elderly subjects. *Clin. Sci.*, 58, 235-242

DAVIE, M.W., LAWSON, D.E.M., EMBERSON, C., BARNES, J.L.C., ROBERTS, G.E. and BARNES, N.D. (1982) Vitamin D from skin: contribution to vitamin D status compared with oral vitamin D in normal and anticonvulsant treated subjects. *Clin. Sci.*, 63, 461-472.

DAVIS, A., DEANE, G.H.W. and DIFFEY, B.L. (1976) Possible dosimeter for ultraviolet radiation. *Nature*, 261, 169-170.

DERWENT, R.G., McINNES, G., STEWART, H.N.M. and WILLIAMS, M.L. (1976) The occurrence and significance of air pollution by photo-chemically produced oxidant in the British Isles 1972-1975. Report No. LR 227(AP) Warren Spring Laboratory.

DEVGUN, M.S., PATERSON, C.R., COHEN, C. and JOHNSON, B.E. (1980)

Possible value of fluorescent lighting in the prevention  
of vitamin D deficiency in the elderly. Age and Ageing 9.  
117-120.

DEVGUN, M.S., PATERSON, C.R., JOHNSON, B.E. and COHEN, C. (1981a)

Vitamin D nutrition in relation to season and occupation.  
Am. J. Clin. Nutr. 34, 1501-1504.

DEVGUN, M.S., JOHNSON, B.E., CRUICKSHANK, A.J.M. and PATERSON, C.R.

(1981b) Commercially available sun lamps and vitamin D  
formation. Postgrad. med. J., 57, 159-163.

DEVGUN, M.S., JOHNSON, B.E. and PATERSON, C.R. (1983) Ultraviolet  
radiation, weather and the blood levels of 25-hydroxyvitamin D.  
Clin. Phys. Biochem. 1, 300-304.

DHSS. (1980) Report on health and social security subjects 19.

'Rickets and osteomalacia'. Report of the working party on  
fortification of food with vitamin D.

DIEM, K. and LENTNER, C. (eds) (1970) Documenta Geigy. J.R. Geigy,  
Basle.

DIERMENDJIAN, D. (1969) Electromagnetic scattering on spherical  
polydispersions. Elsevier, New York.

DIFFEY, B.L. (1981) Ultraviolet radiation in medicine (Chapter 7).  
Medical Physics Handbook Series No.11. ISBN 0-9960022-4-3.

DIFFEY, B.L., LARKO, O. and SWANBECK, G. (1982a) UV-B doses received  
during different outdoor activities and UVB treatment of  
psoriasis. Br. J. Dermatol. 106, 33-41.

- DIFFEY, B.L., DAVIS, T. and MAGNUS, I. (1982b) Description and application of a personal dosimeter for measuring exposure to natural ultraviolet radiation. In: The Role of Solar Ultraviolet Radiation in Marine Ecosystems. Ed. Calkins, J. NATO Conference Series: IV, Marine Sciences 7.
- DRUMMOND, A.J. (1956) On the measurement of sky radiation. Arch. Met. Geophys. Biochem. B7, 413-436.
- ELLSAESER, H.W. (1982) Should we trust models or observations? Atmos. Environ. 16, 197-205.
- FARMAN, J.C., GARDINER, B.G. and SHANKLIN, J.D. (1985) Large losses of total ozone in Antarctica reveal seasonal  $\text{ClO}_x/\text{NO}_x$  interaction. Nature 316, 207-210
- FARNSWORTH-LOOMIS, W. (1967) Skin pigment regulation of vitamin D biosynthesis in man. Science 157, 501-506.
- FRAIN-BELL, W. (1979) What is that thing called light? In: Clinical and Experimental Dermatology 4, 1. Ed. Black, M.M. Blackwell Scientific Publications.
- FRASER, D.R. (1980) Vitamin D. In: Vitamins in Medicine. Eds. Barker, B.M. and Bender, D.A. Heinemann, London, 42-146.
- FRASER, D.R. (1983) The physiological economy of vitamin D. Lancet i 969-972.
- GERSTL, S.A.W., ZARDECKI, A. and WISER, H.L. (1983) UV-B Handbook Vol. I. LA-UR-83-728 Draft. Los Alamos National Laboratory, Los Alamos, New Mexico 87545.
- GOEL, K.M., SWEET, E.M., CAMPBELL, S., ATTENBURROW, A., LOGAN, R.W. and ARNEIL, G.C. (1981) Reduced prevalence of rickets in Asian children in Glasgow. Lancet ii, 405-406.

- GOLDBERG, B. and KLEIN, W.H. (1974) Radiometer to monitor low levels of ultraviolet irradiance. *Appl. Opt.* 13, 493-496.
- GOUGH, D. (1980) Climate and variability in the solar constant. *Nature*, 288, 639-640.
- GREEN, A.E.S., SAWADA, T. and SHETTLE, E.P. (1974) The middle ultraviolet reaching the ground. *Photochem. Photobiol.* 19, 251-259.
- GREEN, A.E.S., CROSS, K.R. and SMITH, L.A. (1980) Improved analytic characterization of ultraviolet skylight. *Photochem. Photobiol.* 31, 59-65.
- GREEN, A.E.S. and SHIPPNICK, P.F. (1982) UV-B reaching the surface. In: The Role of Solar Ultraviolet Radiation in Marine Ecosystems. Ed. Calkins, J. NATO Conference Series, IV, Marine Sciences, 7.
- HADDAD, J.G. and CHYU, K.J. (1971) Competitive protein-binding radioassay for 25-hydroxycholecalciferol. *J. Clin. Endocrinol.* 33, 992.
- HALLDAL, P. (1979) Effects of changing levels of ultraviolet radiation on phytoplankton. In: The Ozone Layer. Ed. Biswas, A.K. UN Environment Programme, Environmental Sciences and Applications. Vol. 4. Pergamon Press.
- HARRIS, P.B. (1973) The BRE ultraviolet sensor. BRE Current Paper, Department of Environment.
- HAY, A. (1982) Vitamin D: sunlight and precursors. *Nature*, 297, 364.
- HESS, A., PAPPENHEIMER, A.M. and WEINSTOCK, M. (1922) A study of light waves in relation to their protective action in rickets. *Proc. Soc. Exp. Biol. Med.*, 20, 14-16.

- HOLICK, M.F., MACLAUGHLIN, J.A., CLARK, M.B., HOLICK, S.A., POTTS, J.T.Jr., ANDERSON, R.R., BLANK, I.H., PARRISH, J.A. and ELIAS, P. (1980) Photosynthesis of previtamin D<sub>3</sub> in human skin and the physiologic consequences. *Science* 210, 203-205.
- HOLICK, M.F., MACLAUGHLIN, J.A. and DAPPELT, S.H. (1981) Regulation of cutaneous previtamin D<sub>3</sub> photosynthesis in man: skin pigment is not an essential regulator. *Science* 211, 590-593.
- HOLMAN, C.D.J., GIBSON, I.M., STEPHENSON, M. and ARMSTRONG, B.K. (1983) Ultraviolet irradiation of human body sites in relation to occupation and outdoor activity: field studies using personal UVR dosimeters. *Clin. Exp. Dermatol.* 8, 269-277.
- HOMBERG, I. and LARSSON, A. (1980) Seasonal variation of vitamin D<sub>3</sub> and 25-hydroxyvitamin D<sub>3</sub> in human serum. *Clin. Chim. Acta.* 100, 173-174.
- HOOVER, W.H. (1937) The dependence of carbon dioxide assimilation in a higher plant on wavelength of radiation. *Smithson. misc. Collns.* 95 (21) 13 pages.
- HOSKING, D.J., CAMPBELL, G.A., KEMM, J.R., COTTON, R.E., KNIGHT, M.E., BERRYMAN, R. and BOYD, R.V. (1983) Screening for subclinical osteomalacia in the elderly: normal ranges or pragmatism? *Lancet* ii, 1290-1292.
- KLEIN, R.M. (1978) Plant and near ultraviolet radiation. *Bot. Rev.* 44, 1-127.
- KLEIN, W.H. and GOLDBERG, B. (1978) Monitoring UVB spectral irradiances at three latitudes. *Proc. Int. Solar Energy Soc. Cong.*, New Delhi, India. 1, Pergamon Press, N.Y.

- KNUDSEN, A. and BENFORD, F. (1938) Quantitative studies of the effectiveness of ultraviolet radiation of various wavelengths in rickets. *J. biol. Chem.* 124, 287-299
- KOBAYASHI, T. and YASUMARA, M. (1973) Studies of the ultraviolet irradiation of provitamin D and its related compounds. *J. nutr. Sci.*, 19, 123-128.
- LAMBERG-ALLARDT, C. (1984) Vitamin D intake, sunlight exposure and 25-hydroxyvitamin D levels in the elderly during one year. *Ann. Nutr. Metab.* 28, 144-150.
- LARKO, O. and DIFFEY, B.L. (1983) Natural UVB radiation received by people with outdoor, indoor and mixed occupations and UVB treatment of psoriasis. *Clin. Exp. Dermatol.* 8, 279-295.
- LAWSON, D.E.M. (1981) Dietary vitamin D: is it necessary? *J. Hum. Nutr.* 35, 61-63.
- LAWSON, D.E.M. and DAVIE, M. (1979) Metabolism and function of vitamin D. In: Vitamins and Hormones 37. Eds. Munson, P.L., Diczfalusy, E., Glover, J. and Olsen, R.E. Academic Press, Inc. (London) Ltd. 1-67.
- LAWSON, D.E.M., PAUL, A.A., BLACK, A.E., COLE, T.J., MONDAL, A.R. and DAVIE, M. (1979) Relative contribution of diet and sunlight to vitamin D state in the elderly. *Br. med. J.* 2, 303-305.
- LEACH, J.F., McLEOD, V.E., PINGSTONE, A.R., DAVIS, A. and DEANE, G.H.W. (1978) Measurements of the ultraviolet doses received by office workers. *Clin. Exp. Dermatol.* 3, 77-79.
- LESTER, E., SKINNER, R.K. and WILLS, M.R. (1977) Seasonal variation in serum 25-hydroxyvitamin D in the elderly in Britain. *Lancet i.* 979-980.

- LESTER, E., SKINNER, R.K., FOO, A.Y., LUND, B. and SORENSEN, O.H. (1980) Serum 25-hydroxyvitamin D levels and vitamin D intake in healthy young adults in Britain and Denmark. *Scand. J. Clin. Lab. Invest.* 40, 145-150.
- LINHARES, E.R., JONES, D.A., ROUND, J.M. and EDWARDS, R.H.T. (1984) Effect of nutrition on vitamin D status: studies on healthy and poorly nourished Brazilian children. *Am. J. Clin. Nutr.* 39, 625-630.
- LUND, B. and SORENSEN, O.H. (1979) Measurement of 25-hydroxyvitamin D in serum and its relation to sunshine, age and vitamin D intake in the Danish population. *Scand. J. Clin. Lab. Invest.* 39, 23-30.
- MACLAUGHLIN, J.A., ANDERSON, R.R. and HOLICK, M.F. (1982) Spectral character of sunlight modulates photosynthesis of previtamin D<sub>3</sub> and its photoisomers in human skin. *Science*, 216, 1001-1003.
- MCCARTNEY, H.A. (1975) Spectral distribution of solar radiation within and above crops. *Ph.D. Thesis, University of Nottingham.*
- MAFF (1980) Household food consumption and expenditure: 1978 (Annual Report of the National Food Survey Committee). *HMSO, London.*
- MAWER, E.B., BERRY, J.L., SOMMER-TSITENIS, E., BEYKIRCH, W., KUHLWEIN, A. and ROHDE, B.T. (1983) Ultraviolet irradiation increases serum 1,25-dihydroxyvitamin D in vitamin-D-replete adults. *Miner. Electrolyte Metab.* 10(2), 117-121.
- MENKE, W. (1984) Geophysical data analysis: discrete inverse theory. Academic Press Inc.
- MO, T. and GREEN, A.E.S. (1974) A climatology of solar erythema dose. *Photochem. Photobiol.* 20, 438-496.

- MONTEITH, J.L. (Ed.) (1973) Principles of Environmental Physics.  
Edward Arnold Ltd, London.
- MOORE, J.R. (1980) Sources of error in spectroradiometry. Lighting Research and Technology, 12(4), 213-220.
- NACHTEWY, D.S. and RUNDEL, R.D. (1982) Ozone change: biological effects. In: Stratospheric Ozone and Man Vol. II. Eds. Bower, F.A. and Ward, R.B. CRC Press Inc., Florida, Ch. 4. 103-105.
- NADER, J.S. (1969) Pilot study of UVR in Los Angeles. In: The Biological Effects of Ultraviolet Radiation. Ed. Urbach, F. Pergamon Press.
- NAS, (1976) Halocarbons: effects on stratospheric ozone. Washington, D.C.
- NAS, (1979) Protection against depletion of stratospheric ozone by chlorofluoracarbons. Committee on Impacts of Stratospheric Change, NAS, Washington, D.C.
- NAYAL, A.S., MACLENNON, W.J., HAMILTON, J.C., ROSE, P. and KONG, M. (1978) 25-hydroxyvitamin D, diet and sunlight exposure in patients admitted to a geriatric unit. Gerontology, 24, 117-122.
- OFFERMAN, G. and MANHOLD (1979) Immigrant osteomalacia: occurrence in Turkish guest workers in Germany. In: Vitamin D; Basic Research and Its Clinical Applications. Eds Norman, A.W., Schaefer, K., Herrath, D.V., Grigoleit, H-G., Coburn, J.W., Deluca, H.F., Mawer, E.B. and Suda, T. Walter De Gruyter, Berlin, New York.
- OLSON, R.D. (Ed.) (1984) The photochemical formation of vitamin D in the skin. Nutr. Rev. 42, 341-343.
- OLSON, R.E. (1985) Vitamin D status of the elderly: contributions of sunlight exposure and diet. Nutr. Rev. 43(3), 78-80.

- OMDAHL, J.L., GARRY, P.J., HUNSAKER, L.A., HUNT, W.C. and GOODWIN, J.S. (1982) Nutritional status in a healthy elderly population: vitamin D. Am. J. Clin. Nutr. 36, 1225-1233
- PALM, T.A. (1890) The geographic distribution and etiology of rickets. Practitioner, 45, 270-279; 321-342.
- PALTRIDGE, G.W. and BARTON, I.J. (1978) Erythemal UVR distribution over Australia - the calculations, detailed results and input data. Div. Atmos. Phys. Tech. Paper No. 33, CSIRO, Australia.
- PAUL, A.A. and SOUTHGATE, D.A.T. (1978) McCance and Widdowson's The Composition of Foods. 4th Edition. HMSO, London. Elsevier North-Holland Biomedical Press, Amsterdam, New York, Oxford.
- PARFITT, A.M., GALLAGHER, J.C., HEANEY, R.P., JOHNSTON, C.C., NEER, R. and WHEDON, G.D. (1982) Vitamin D and bone health in the elderly. Am. J. Clin. Nutr. 36, 1014-1031.
- POSKITT, E.M.E., COLE, T.J. and LAWSON, D.E.M. (1979) Diet, sunlight and 25-hydroxyvitamin D in healthy children and adults. Br. med. J. 1, 221-223.
- PRATHER, M.J., McELROY, M.B. and WOFSY, S.C. (1984) Reductions in ozone at high concentrations of stratospheric halogens. Nature, 312, 227-231.
- REINHOLD, J.G., FARAJI, B., ABADI, P. and ISMAILBEIGI, F. (1981) An extended study of the effect of Iranian village and urban flatbreads on the mineral balances of two men before and after supplementation with vitamin D. Ecol. Food Nutr. 10, 169-177.
- REITER, R., MUNZERT, K. and SLADKOVIC, R. (1982) Results of 5 years concurrent recording of global, diffuse and UV radiation at 3 levels (700, 1800, 3000 m a.s.l.) in the Northern Alps. Arch. Met. Geoph. Biocl. Series B, 30, No. 1-2.

ROBERTSON, I., FORD, J.A., McINTOSH, W.B. and DUNNIGAN, M.G. (1981)

The role of cereals in the aetiology of nutritional rickets:  
the lesson of the Irish National Nutrition Survey 1943-48.

Br. J. Nutr. 45, 17-22.

ROBINSON, N. (1966) Solar Radiation. Elsevier Publishing Co.

RUNDEL, R. (1985) Computation of spectral distribution and intensity  
of solar UV-B radiation. In: The Impact of Solar Ultra-  
violet (UV-B) Radiation Upon Terrestrial Ecosystems. Ed.  
Worrest, R.C. (In Press).

SCHMAILZL, U. (1985) Ozone depletion under different scenarios. In:  
The Impact of Solar Ultraviolet (UV-B) Radiation Upon  
Terrestrial Ecosystems. Ed. Worrest, R.C. (In Press).

SCOTTO, J. and FEARS, T.R. (1977) Intensity patterns of solar UVR.  
Environ. Res. 14, 1. Ed. Selikoff, I.J. Academic Press.

SELLERS, W.D. (1969) Physical climatology. The University of Chicago  
Press, Chicago and London.

SIVKOV, S.I. (1971) Computation of Solar Radiation Characteristics.  
Keter Press, Jerusalem.

SMITH, R.G. (1975) Solar ultraviolet radiation in southern England.  
BRE Current Paper. Department of the Environment.

SMITH, R.C. and BAKER, K.S. (1981) Optical properties of the clearest  
natural waters (200-800 nm). Appl. Opt. 20(2), 177-184.

SMITHSONIAN INSTITUTE, (1951) Smithsonian Meteorological Tables.  
(6th Edition). Smithsonian Institution, Washington.

SPINHIRNE, J.D. and GREEN, A.E.S. (1978) Calculations of the relative influence of cloud layers on received UV and integrated solar radiation. *Atmos. Environ.* 12, 2449-2454.

STAMP, T.C.B. (1975) Factors in human vitamin D nutrition and in the production and cure of classical rickets. *Proc. Nutr. Soc.* 34, 119-130.

STAMP, T.C.B. and ROUND, J.M. (1974) seasonal changes in human plasma levels of 25-hydroxyvitamin D. *Nature*, 247, 563-565.

STAMP, T.C.B., ROUND, J.M., ROWE, D.J.F. and HADDAD, J.G. (1972) Plasma levels and therapeutic effect of 25-hydroxycholecalciferol in epileptic patients taking anti-convolusant drugs. *Br. med. J.* iv, 9-12.

STANBURY, S.W., MAWER, E.B., TAYLOR, C.M. and deSILVA, P. (1980) The skin, vitamin D and the control of its 25-hydroxylation. An attempted integration. *Min. Elec. Metab.* 3, 51-60.

STEVEN, M.D. (1977) Standard distribution of clear sky radiance. *Q.J.R. met. Soc.* 103, 457-465.

STEVEN, M.D. (1984) The anisotropy of diffuse solar radiation determined from shade-ring measurements. *Q. J.R. met. Soc.*, 110, 261-270.

STEVEN, M.D. and UNSWORTH, M.H. (1980) Shade-ring corrections for pyranometer measurements of diffuse solar radiation from cloudless skies. *Q.J.R. met. Soc.*, 106, 865-872.

STORDAL, F., HOV, O. and ISAKSEN, I.S.A. (1982) The effect of perturbation of the total  $O_3$  column due to CFC on the spectral distribution of UV fluxes and the damaging UV doses at the ocean surface: A model study. In: The Role of Solar Ultraviolet Radiation in Marine Ecosystems. Ed. Calkins, J. NATO Conference Series, IV, Marine Sciences, 7.

- TATE, T.J. (1979) Applications of polymer films to ultraviolet radiation dosimetry. M.Sc. Thesis, University of Kent.
- TAYLOR, T.G. (1984) Hypovitaminosis D. Bone, 1(1), 11-12.
- TERAMURA, A.H. (1980) Effects of ultraviolet-B irradiances on soybean. I. Importance of photosynthetically active radiation in evaluating ultraviolet-B irradiance effects on soy-bean and wheat growth. Physiol. Plant, 48, 333-339.
- TEVINI, M., IWANZIK, W. and THOMA, U. (1982a) The effects of UVB irradiation on higher plants. In: The Role of Solar Ultraviolet Radiation in Marine Ecosystems. Ed. Calkins, J. NATO Conference Series, IV, Marine Sciences, 7.
- TEVINI, M., THOMA, U. and IWANZIK, W. (1982b) Effect of enhanced UVB radiation on development and composition of plants. In: Biological Effects of UV-B Radiation. Eds. Bauer, H., Caldwell, M.M., Tevini, M. and Worrest, R.C. Proc. Workshop held in Munich-Neuherberg.
- THEKAEKARA, M.P. (1974) Extraterrestrial solar spectrum.  $3000\text{-}6100 \text{\AA}$  at  $1 \text{\AA}$  intervals. Appl. Opt. 13(3), 518-522.
- THEKAEKARA, M.P. (1976) Solar radiation measurement: techniques and instrumentation. Solar Energy, 18, 309-327.
- THOMPSON, G.R., LEWIS, B. and BOOTH, C.C. (1966) Vitamin D absorption after partial gastrectomy. Lancet i, 457-458.
- TOSS, G., ALMQVIST, B., LARSSON, L. and ZETTERQVIST, H. (1980) Vitamin D deficiency in welfare institutions for the aged. Acta. Med. Scand. 208, 87-89.

- TOSS, G., ANDERSON, R., DIFFEY, B.L., FALL, P.A., LARKO, O. and LARSSON, L. (1982) Oral vitamin D and ultraviolet radiation for the prevention of vitamin D deficiency in the elderly. *Acta Med. Scand.* 212, 157-161.
- TSAI, K.S., HEATH, H., KUMAR, R. and RIGGS, B.L. (1984) Impaired vitamin D metabolism with aging in women: possible role in pathogenesis of senile osteoporosis. *Clin. Res.* 32, 411A.
- UNSWORTH, M.H. and MONTEITH, J.L. (1972) Aerosol and solar radiation in Britain. *Q.J.R. met. Soc.* 98, 778-797.
- VAN de HULST, H.C. (1957) Light scattering by small particles. John Wiley and Sons, New York.
- WEBB, A. and STEVEN, M.D. (1984) Measurement of solar UVB radiation in the English Midlands. *Arch. Met. Geoph. Biocl. Ser. B* 35, 221-231.
- WILSON, R.C., GULKIS, S., JANSEN, M., HUDSON, H.S. and CHAPMAN, G.A. (1980) Observations of solar irradiance variability. *Science*, 211, 700-702.
- WMO. (1979) Atmosphere ozone - A survey of the current state of knowledge of the ozone layer. In: The Ozone Layer. Ed. Biswas, A.K. UN Environment Programme. Environmental Sciences and Applications, 4, Pergamon Press.
- WORREST, R.C. (1982) Review of literature concerning the impact of UV-B radiation upon marine organisms. In: The Role of Solar Ultraviolet Radiation in Marine Ecosystems. Ed. Calkins, J. NATO Conference Series, IV, Marine Sciences, 7.

YOUNG, A.R., CHALLONER, A.V.J., MAGNUS, I.A. and DAVIS, A. (1982)

UVR radiometry of solar simulated radiation in experimental  
photocarcinogenesis studies. Br. J. Dermatol. 106, 43-52.

APPENDICES

APPENDIX A1) LICOR LI 1800 Portable Spectroradiometer

|                             |                     |
|-----------------------------|---------------------|
| Manufacturer : LI-COR, Inc. | U.K. Agents :       |
| 4421 Superior Street        | Glen Creston        |
| P.O. Box 4425               | 16 Dalstone Gardens |
| Lincoln                     | Stanmore            |
| Nebraska 68504              | Middlesex           |
| U.S.A.                      | 4LA7 1DA            |

## Specifications :

|                                     |                      |
|-------------------------------------|----------------------|
| Wavelength range                    | 300-1100 nm          |
| Bandwidth ( $\frac{1}{2}$ mm slits) | 6 nm                 |
| Wavelength accuracy                 | $\pm 2$ nm           |
| Wavelength repeatability            | $\pm 0.5$ nm         |
| Linear dispersion                   | 12 nm/mm             |
| Holographic grating                 | 800 grooves/mm       |
| Automatic filter wheel              | 7 filters: wavebands |
|                                     | 300-350 nm           |
|                                     | 350-420 nm           |
|                                     | 420-560 nm           |
|                                     | 560-780 nm           |
|                                     | 780-940 nm           |
|                                     | 940-1100 nm          |
|                                     | Blank                |

## Noise equivalent irradiance:

| Wavelength (nm)                           | 300                | 350                | 400                  | 500-800            | 800-1040           | 1100                 |
|---|--------------------|--------------------|----------------------|--------------------|--------------------|----------------------|
| NEI ( $\text{W cm}^{-2} \text{nm}^{-1}$ ) | $7 \times 10^{-8}$ | $4 \times 10^{-8}$ | $1.5 \times 10^{-8}$ | $8 \times 10^{-9}$ | $6 \times 10^{-9}$ | $1.5 \times 10^{-8}$ |

Maximum irradiance levels ( $\text{W cm}^{-2} \text{nm}^{-1}$ ):

300 - 400 nm  $5 \times 10^{-3}$

400 - 1100 nm  $> 1 \times 10^{-3}$  (dependent on  $\lambda$ )

**Wavelength drive intervals:**

1 , 2 , 5 or 10 nm

**Scanning speed:**

| Speed (nm s <sup>-1</sup> ) | 20 | 30 | 35 | 40 |
|-----------------------------|----|----|----|----|
| Wavelength interval (nm)    | 1  | 2  | 5  | 10 |

Total mean time for 300 - 1100 nm in 2 nm steps is ~ 27 sec.

**Monochromator slew rate:**

55 nm s<sup>-1</sup> (15 sec total reset time for 300 - 1100 nm)

**Scanning:**

Single scan, multiple scans with automatic scan averaging,  
or single wavelength monitoring (sampled once per second).

**Calibration:**

Initially calibrated at factory to NBS standards

| Wavelength (nm) | 300   | 450  | 550  | 650-800 | 1100                               |
|-----------------|-------|------|------|---------|------------------------------------|
| Accuracy        | ± 10% | ± 5% | ± 4% | ± 3%    | ± 5% (under controlled conditions) |

**Detector temperature coefficient:**

| Wavelength (nm)     | 300    | 350   | 400-950 | 1000 | 1100 |
|---------------------|--------|-------|---------|------|------|
| Temp. coeff. (%/°C) | - 0.13 | - 0.1 | 0.05    | 0.5  | 1-2  |

**Long term stability:**

Typically < ± 5% change per year

**Program memory:**

20K bytes ROM, pre-programmed system software for control, data reduction, output and calibration.

System software:

Setup commands:      SYNCH    Initialises monochromator and filter wheel  
                        PARMs    List or set parameters  
                        TIME    List or set internal clock  
                        LABEL   Set up 5 labels for data output  
                        CAL    Calibration against a standard lamp  
                        LI1800 For manually entered lamp data for other lamps

Scanning commands:    SCAN    Executes a scan  
                        PTSCAN Continuous monitoring of one wavelength  
                        PROG    Executes a scan and then up to 4 program  
                               functions on that scan  
                        EX    Performs the functions in PROG on any  
                               named file  
                        RUN    Executes the scan and program in PROG  
                               immediately

Data manipulation commands:    DIV    Divides 2 files and stores result  
                        MULT   Multiples 2 files and stores result  
                        XFRM   Performs transform  $f = aA + bB + c$   
                               where A , B are existing files  
                        CREATE Creates file from terminal input  
                        EDIT   Allows data files to be changed

Graphical output commands:    PLOT   Plots data to plotter/printer  
                        ANA    Outputs file to strip chart recorder

|                          |        |  |
|--------------------------|--------|--|
| Data output commands:    | ITG    | Integrates over selected waveband  |
|                          | SHOW   | Sends data to output device  |
|                          | PPFD   | Photosynthetic flux density  |
|                          | Qx     | Where x is any of last 5 functions.<br>Performs a conversion to quantum data and<br>then executes the function |
|                          | ILLM   | Illuminance  |
|                          | DC     | Set up communications with host computer   |
| File handling functions: | RENAME | Allows file to be renamed and remarks<br>changed   |
|                          | DEL    | Deletes a specific file from memory  |
|                          | LIST   | Lists all files in memory  |
|                          | CLEAR  | Deletes all but protected files from<br>memory   |

#### Internal memory:

Data storage in RAM, up to 32K bytes capacity. A file requires  $3N + 50$  bytes of memory where N is the number of observations in the file.

#### Data output:

RS-232C Device : 1800-03 Plotter/Printer or a computer via the output port

Terminal/Computer: 1800-01 Portable LCD terminal or an RS-232C compatible terminal or computer via the terminal port.

#### Analog device:

Strip chart recorder 0-100 mV.

**Power requirements:**

Internal rechargeable 6V Ni-cad battery, 4 amp hour rating; external 12V DC power; or 100-128/200-256 VAC, 48 to 66 Hz.

Battery capacity is typically 4-8 hours of operation at 25°C.

Recharging time is 12-14 hours, instrument non-operating.

Charging circuit built in and battery can be charged during AC operation.

**Battery voltage sensor:**

Automatic instrument shut-off preserves data stored in memory.

**Operating temperature:**

0-45°C , 0-95% RH.

**Storage temperature:**

- 20-45°C , 0-95% RH.

**Size:**

16.3 x 20.1 x 36.0 cm .

**Weight:**

6.4 kg .

**Long term stability**

The long term stability of the LI1800 calibration is quoted by the Manufacturers as typically <5% per year, with recalibration recommended every 6 months. The instrument arrived in January 1983 with a calibration made in the States and accepted as correct. Calibration of the SEE 240 sensor against the LI1800 then provided a means of checking any change between instruments. There was no deviation from the intercalibration to December 1983.

In January 1984 the LI1800 was sent to Glen Creston, the UK agents for LI-COR, for a calibration check. This was later found to be invalid due to a faulty lamp, and the original calibration continued to be used.

Intercalibration checks with the SEE 240 in February and March 1983 showed a difference between the two instruments in the UVB of  $\sim 10\%$ . with the LI1800 giving the lower values. A sheet of polysulphone film calibrated against the SEE 240 continued to hold its relative calibration.

The recalibration of the LI1800 was repeated in May 1984. Subsequent simultaneous irradiance measurements made with the SEE 240 and the LI1800 showed the LI1800 to be recording UVB values  $\sim 25\%$  lower than the SEE 240. This discrepancy persisted throughout 1984 when using the new calibration. With the original calibration the difference remained at  $\sim 10\%$ .

Early in 1985 a correction factor was received for the May 1984 calibration. Applying this figure to the relevant data brought the LI1800 measurements to  $\sim 10\%$  lower than SEE 240 measurements.

A second LI1800, newly calibrated in the States, was used to make simultaneous measurements with the original instrument on a clear morning in June 1984. The new calibration of the original instrument, corrected by the compensation factor supplied in 1985, was  $\sim 5\%$  lower than the new calibration from the States.

The evidence presented above is insufficient to enable a categorical statement of long term stability to be made, and a range of possible instrumental changes are given below:

- i) During 1983 both the LI1800 and SEE 240 remained stable.
- ii) Early in 1984 sensitivity of the LI1800 decreased by 10%. This is supported by the continuing agreement between SEE 240 and polysulphone film. It is also considered more likely that degradation with time would decrease the sensitivity of the LI1800 rather than increase the sensitivity of the SEE 240. Also the SEE 240 was permanently mounted on the meteorological site while the LI1800 was used in many locations by different workers, rendering it more susceptible to wear and tear.
- iii) Despite the previous statement, sensitivity of the SEE 240 may have increased by 10%, as the original and corrected May 1984 calibrations of the LI1800 agree.
- iv) Both instruments may have changed in opposite directions.  
Statement (iii) is only valid if the calibration lamps in Britain and the States are assumed to have identical outputs. The difference between the two LI1800 instrument calibrations tends to suggest divergent changes, but again the assumption of identical calibration lamps and procedure in the States over an 18 month period is made.

In conclusion, no clear cut decision of stability could be taken. However, as a change of 10% occurred somewhere between the related instruments from 1983 to 1984 a standardising procedure had to be adopted to normalise the data collected before and after the change.

The original (January 1983) calibration of the LI1800 on which calibration of the other sensors was based was taken to be correct. The divergence of measurements was assumed to be due to a decrease in

sensitivity of the LI1800 and all spectroradiometer readings for 1984 were corrected to 1983 levels. The possible error in all readings from this procedure is therefore  $\pm$  10%. The long term stability of the LICOR (States) calibration is  $\pm$  5%, from the measurements made in June 1984.

2) SEE 240 / UVB / W / Probe

Manufacturers: International Light Inc. U.K. Agents:  
Dexter Industrial Green Auriema Ltd.  
Newburyport 442 Bath Road  
Massachusetts 01950 Slough  
U.S.A. SL1 6BB

## Specifications:

## Power requirement:

- 12V stable DC supply for SEE 240 vacuum photodiode

## Calibration:

PIR calibration, traceable to NBS standards, for the actual unit supplied plus typical response spectrum for the SEE 240 with 'W' cosine receptor and UVB phototherapy filter (other filters are available).

The PIR calibration for SEE 240 I was  $4.69 \times 10^{-4} \text{ A cm}^2 \text{ W}^{-1}$   
SEE 240 II  $9.60 \times 10^{-5} \text{ A cm}^2 \text{ W}^{-1}$

## Signal output:

Signal current converted to  $\text{W cm}^{-2}$  and displayed as a digital readout if the unit is used with the IL 700A research radiometer. When connected to the SEE 240 the radiometer also supplies the power for the vacuum photodiode.

## Size:

Diameter 42 mm , height 6.8 cm .

APPENDIX B1) Power supply and current/voltage converter

The 4-core cable from the SEE 240 sensor carried the signals shown in Figure B.1.

An instrument was built to provide a regulated - 12V supply for the vacuum photodiode, and to accept the signal ( $\sim$  nA) from the sensor, converting it into voltage form ( $\sim$  mV) for recording on a Solartron data logger and a printing dose-timer (Appendix B.2). The power supply circuit also provided the power ( $\pm 7\frac{1}{2}$ V) for the printing dose-timer.

During the building and testing of the power supply and current/voltage (C/V) converter a number of components were changed until the long term stability, temperature stability and sensitivity required were achieved.

The circuit diagram of the final configuration is shown in Figure B.2. The components were built onto a printed circuit board and this was then mounted in a metal box  $12 \times 22 \times 9\frac{1}{2}$  cm.

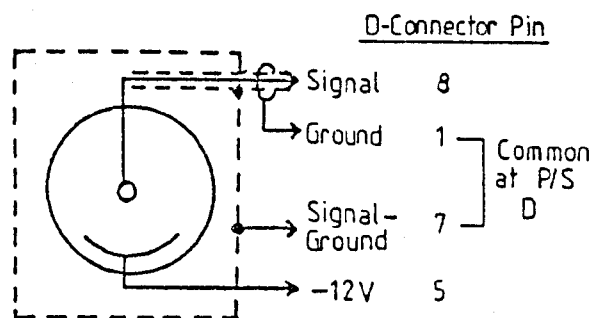
As the mains supply on the meteorological site was subject to some fluctuation the current was passed through a mains filter before connecting the power supply and C/V converter.

The instrument was housed in a box in the field beneath the SEE 240.

Components for power supply and current/voltage converter

Components were from Radio Spares and the RS catalogue numbers are given for identification where necessary.

Fig. B.1 Cable signals for the SEE 240 sensor.



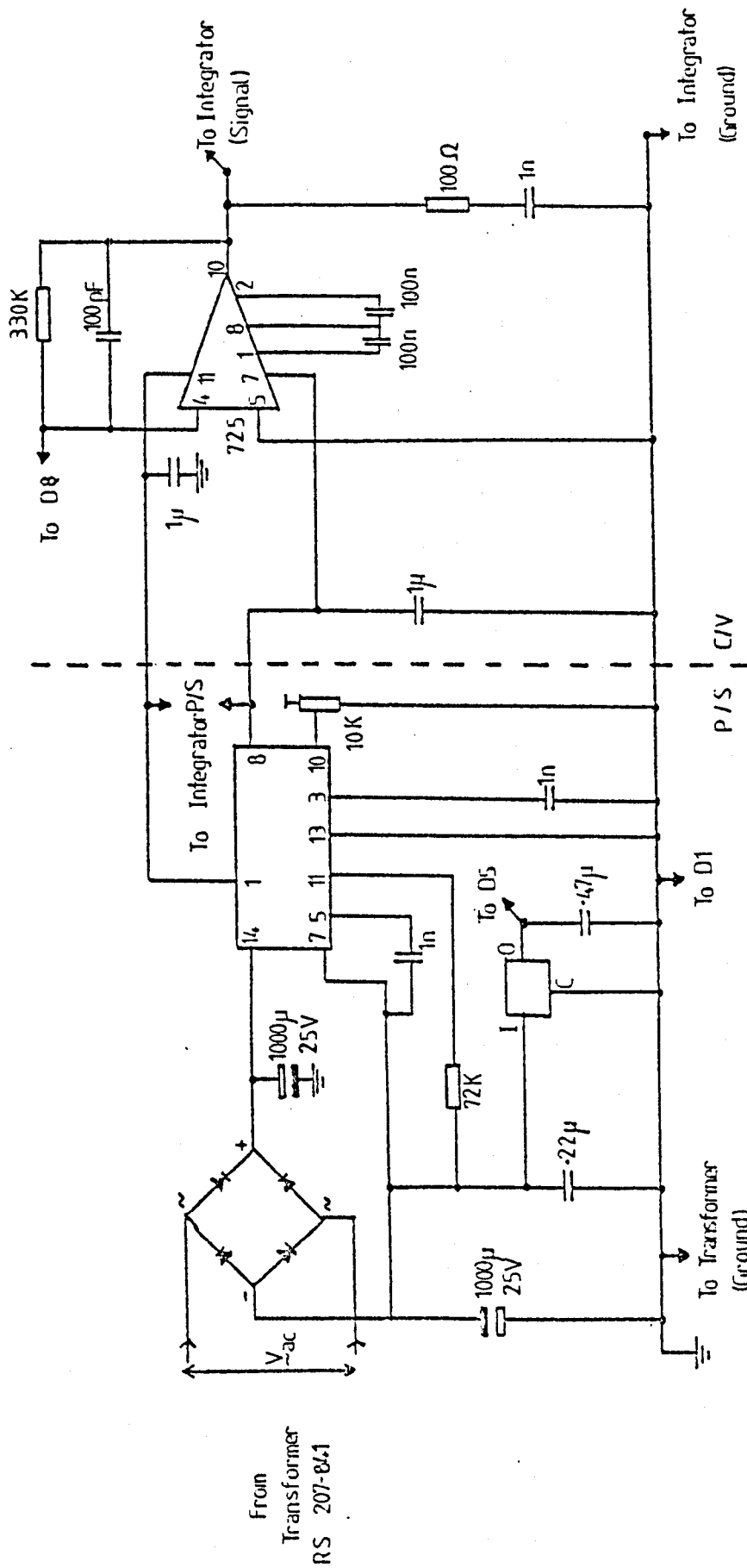


Fig. B.2 Circuit diagram for power supply and current/voltage converter.

|             |  |
|-------------|--|
| Transformer | 207.201  |
| Rectifier   | 261.328  |
| Op. amp.    | 7650 used in photovoltaic mode   |
| Regulators  | 79L12A   |
|             | 306.011  |
| Trimmer     | 50K  |
| Resistors   | 72K $\left\{ \begin{array}{l} 120K \\ 180K \end{array} \right. \text{ in } \parallel \right\}$ High tolerance (1%) |
|             | 330K   |
|             | 100 $\Omega$   |
| Capacitors  | 2 x 1000 $\mu F$ 25V   |
|             | 2 x 1 $\mu F$  |
|             | 1 x 0.47 $\mu F$   |
|             | 1 x 0.22 $\mu F$   |
|             | 2 x 0.1 $\mu F$ polycarbonate  |
|             | 3 x 1 $nF$   |
|             | 1 x 100 $pF$   |
| Connector   | 9 pin D connector  |
| Box         | 12 x 22 x 9 $\frac{1}{2}$ cm   |

## 2) Dose-Timer

A time printing dose integrator was designed and built to record the total UVB radiation incident on a horizontal surface over a period of time. The integrator used a Casio CP10 calculator as a printer. The calculator can be set in 'TIME' mode to act as a clock and will then print the time on a paper tape output when prompted.

The integrator was designed to receive the mV signal from the C/V converter (Appendix B.1) and send a 'Print' signal to the calculator when a set dose of UVB radiation (counts) had accumulated.

The circuit diagram for the integrator is shown in Figure B.3.

The power supply (Appendix B.1) provided  $\pm 7\frac{1}{2}$ V DC to drive the integrator, and this was immediately stepped down to  $\pm 5$ V by the two regulators (78L05, 79L05).

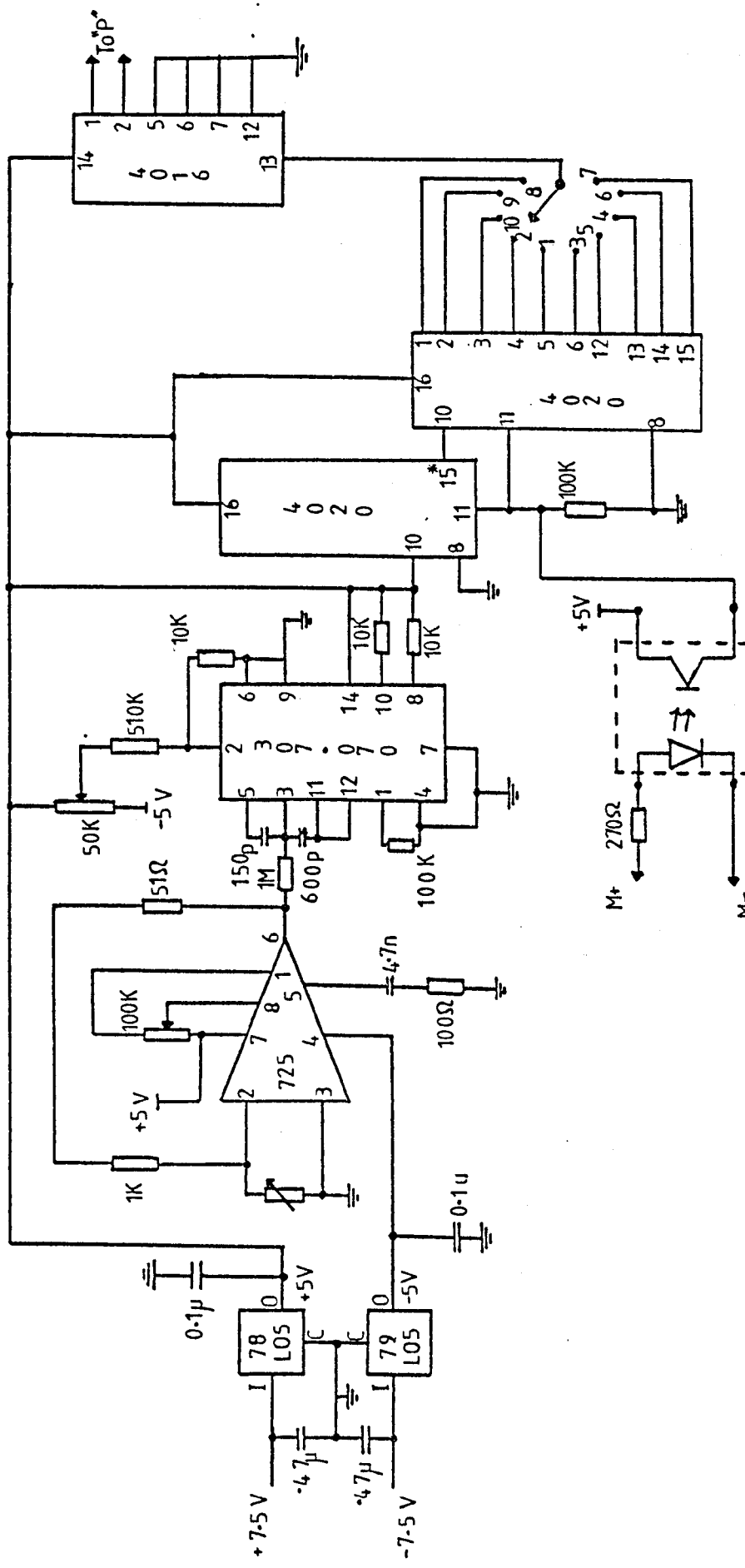


Fig. B.3 Circuit diagram for the dose-timer.

Components for Dose-Timer

## Additional components for Printing Integrator

Casio CP10 printing calculator

Op. amp. 7650

V/F converter 307.070

Frequency divider/counter 2 x 4020

1 x 4020 + 4052 multiplexer

Switch 4016

Regulators 78L05A

79L05A

Opto-isolator 307.979

Trimmers 100K

50K

50 Ω

Resistors 1K } High tolerance

1M }

51 Ω }

510 K }

2 x 100K

3 x 10K

100 Ω

270 Ω

Capacitors 2 x 0.47 μf

2 x 0.1 μf

1 x 4.7 nf

1 x 150 pf

1 x 600 pf (470 pf + 150 pf in ||)

Switch 10 way switch

Connector 9 pin D-connector

Box 9 x 18 x 6 cm

ON/OFF Switch

Timer ZN 1034

Trimmers 5K

2 x 20K

Resistors 2 x 100K

20K

56K

120K

Capacitors 10 μf

0.1 μf

10 nf

The incoming voltage signal from the C/V converter is amplified by the 725 op. amp. and the 307.070 voltage/frequency converter then changes the amplified voltage to a frequency. This resulting frequency is too high for the calculator to cope with so it is stepped down by using two 4020 binary frequencydividers/counters in series. A 10-way switch controls the range on which the dividers work, and hence the range of the printing period.

When the required number of counts has been accumulated at the 4020 counter a signal is sent via the 4016 switch to the 'print' button on the calculator causing it to print the time shown on its display. Activation of the print motor sends a signal to the opto-isolator (RS 307.979) which resets the counters.

Fine wires are soldered to the calculator's printed circuit board on either side of the 'print' button and the print motor terminals are attached to a D-connector on the side of the calculator, which is then connected to the integrator.

The printing dose-timer is calibrated by means of the 3 potentiometers: 50K sets the range of the incoming signal,  $50\ \Omega$  sets the gain and 100K sets the null.

The original calibration was set arbitrarily so that with the 10-way switch set to Range 3 a 10 mV input from a millivolt calibrator gave a print period of 266 seconds (this is equivalent to an accumulated UVB dose of  $280\text{ Jm}^{-2}$  with SEE 240 I).

For subsequent recalibrations the Range and Gain potentiometers were used to bring the calibration back to its original setting. A dark current of 0.3 mV was apparent in the field, but not in the lab.

The interaction of the other apparatus (i.e. the logger) was thought to be responsible for this and the offset was accounted for at the analysis stage.

In August 1984 the dose-timer developed a fault after getting very wet. The instrument was recalibrated compensating for the 0.3 mV offset by using the null potentiometer to offset the dark reading.

A further drift in calibration three weeks later resulted in the 725 op. amp. being changed for the more stable OP07 and a further recalibration was made, again compensating for the 0.3 mV offset.

During long term recording with the printing dose timer the counter range was changed (at the 10-way switch) approximately every 3 months to maintain a reasonable print period of between 2-10 prints per hour around midday. During summer the range was changed to R4 so that a 10 mV input gave a print period of 532 seconds. In winter range 2 gave a print period of 213 seconds for a 10 mV input.

The PCB for the integrating circuit was mounted in a plastic box 9 x 18 x 6 cm with external connections for the power supply and signal (from C/V converter), the 'print' signal (via D-connector to calculator), the range switch and an ON/OFF switch. The calculator was mounted on top of the box, and the whole instrument was kept with the power supply and C/V converter on the meteorological site (Plate B.1).

### 3. Printing Integrator

The dose-timer already described was modified to print the total number of counts accumulated in a given time interval. The input for this integrator was from a Kipp solarimeter mounted at Nottingham General Hospital. The integrated counts were printed out every hour



Plate B.1. Power supply, current/voltage converter and Dose Timer connected for field use.

for comparison with the integrated hourly values from the Kipp on the meteorological site at Sutton Bonington.

The circuit diagram for this integrator is shown in Figure B.4.

The second 4020 frequency divider/counter which acted as the counter for the dose-timer has been replaced by the 4052 multiplexer. This was connected to the '+' and '1' buttons on the calculator (by means of the D-connector and fine wires soldered to either side of the relevant buttons on the calculator PCB), effectively pressing the '+'

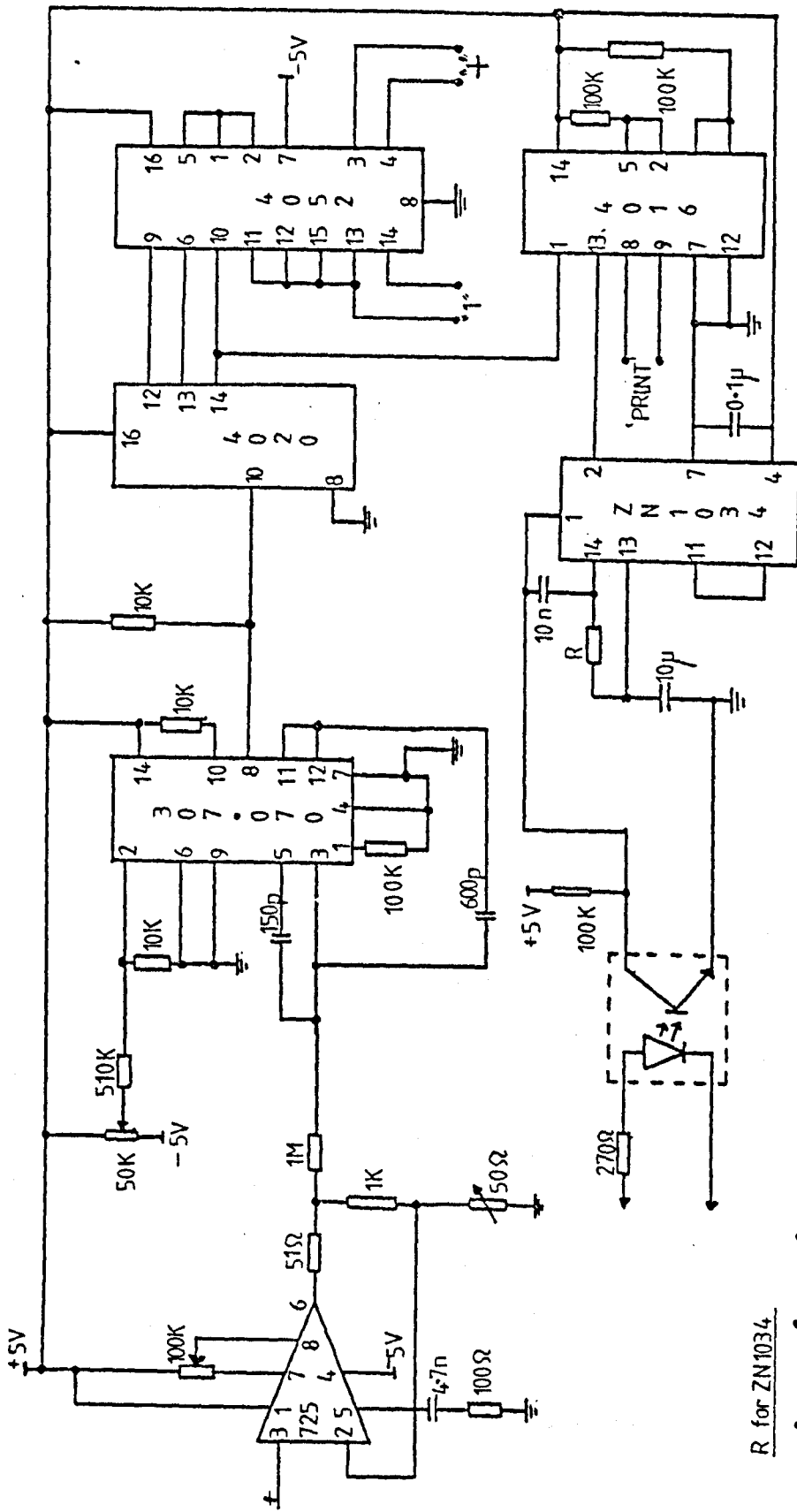


Fig. B.4 Circuit diagram for the printing integrator.

and '1' buttons at a rate proportional to the incoming voltage signal. The calculator, set in 'CAL' mode was therefore counting, and showing the total number of counts on the display.

The ZN 1034 is the timer, which can be set to various time intervals by choosing suitable resistors and capacitors (by a switching device) for the oscillation regulator (Figure B.4). After the given time period the 'print' signal is sent, via the 4016 switch, to the calculator which then prints the total shown on the display. The 'print' signal can only be sent following a '+' signal from the multiplexer so there may be slight time inaccuracies for very slow integration. Activation of the print motor causes the opto-isolater to reset the timer, (and a number of delayed resets can result in the prints being more than a minute after the expected time (say on the hour) although the error in the time between prints is of the order of seconds).

To calibrate the integrator the time period has to be set first. This is done by removing the multiplexer and placing the calculator in 'TIME' mode. The restart timer button and the 'PRINT' button on the calculator are pressed simultaneously and the time is then printed every  $x$  minutes where  $x$  is the time setting. The appropriate resistance is adjusted until  $x =$  desired time period.

Once the time periods have been correctly set the multiplexer is replaced and the calculator set in 'CAL' mode. The counter is then set using the Range and Gain potentiometers.

For a 10 mV input the Gain only is adjusted to give 600 counts/time period. For a 1 mV input the Range only is adjusted to give 60 counts/time period.

The settings for Range and Gain were checked for all time periods (10 min ,  $\frac{1}{2}$  h. , 1 h.).

The integrator was set to print every hour when connected to the Kipp solarimeter. A small power supply provided power for the integrator circuit.

APPENDIX CAnalysis of blood samples for 25-hydroxyvitamin D

Blood samples taken during the summer of 1984 were spun down immediately after collection and the blood plasma stored at - 20°<sup>0</sup>C until November 1984 when the plasma was assayed for the total 25-hydroxyvitamin D metabolite, 25(OH)D.

The technique used follows that of Haddad and Chyu, 1971 and is now a fairly routine procedure for the analysis of 25(OH)D in blood plasma.

Sample extraction

3 ml of each plasma in extraction tubes plus 1 tube containing 3 ml saline solution were spiked with radioactive <sup>3</sup>(H)25(OH)D<sub>3</sub> - 3000 dpm (30 pg) in 20 µl ethanol. The samples were left in the dark for one hour, allowing the radioactive metabolites and serum binding protein to equilibrate. 3 ml of acetonitrile was then added to each sample and the tubes vortex mixed for 30 seconds. The precipitated protein was then centrifuged out of the supernatant at 2000 rpm for 10 min. The supernatants were decanted and further extracted by purification on Sep-Pak C-18 cartridges.

The cartridges were prepared by passing 2 ml methanol through them, followed by 5 ml distilled water, and the vitamin D was then extracted as follows. 2 ml of distilled water (1 ml for the saline solution) plus the 6 ml acetonitrile extract was applied to the cartridge and the eluant discarded. This was followed by exactly 3 ml. methanol:distilled water (65:35), again discarding the eluant. Finally 3 ml acetonitrile was applied and the eluate, containing 90-95% of the

added radioactive vitamin D metabolites, collected in a mini-glass vial pre-rinsed and dried with re-distilled acetone then re-distilled ethanol.

#### High pressure liquid chromatography

The fractions collected from the Sep-Pak cartridges were evaporated under oxygen-free nitrogen, and the residue redissolved in 100 µl isopropanol:methanol:hexane (4:4:92/v:v:v). The samples, with a further 100 µl rinse, were then subjected to HPLC on a stainless steel column (25 cm x 4.6 mm) packed with Zorbax-sil (Dupont U.K. Ltd, Herts).

A constant flow rate of 2 ml min<sup>-1</sup> (1000 psi) gave an elution time of 6-8 min. for 25(OH)D. A standard reference preparation was used to check the elution profile before each run of samples.

The sample fractions collected from HPLC were dried under nitrogen then each fraction was redissolved in 200 µl ethanol and stored in the dark at 4°C.

#### Protein binding assay

The eluants from the HPLC column were blown down under nitrogen at 37°C and the dried fraction made up in 500 µl ethanol. 250 µl of each sample was taken for recovery estimation, suspended in 5 ml fisofluor (Fisons Ltd, Loughborough, Leics) in plastic minivials. The samples were counted on a Packard liquid scintillation counter.

A stock solution of 25(OH)D<sub>3</sub> was sequentially diluted down with 50 µl ethanol to give eight standard concentrations (0.0625, 0.125, 0.25, 0.5, 1, 2, 4, 8 ng/50 µl). Triplicates of each standard, the controls (Table C.1), and duplicates of each serum extract were pipetted into polypropylene assay tubes.

Table C.1. Control tubes (before addition of radioactive ligand).

| Tube    | Content       | Use   |
|---------|---------------|---|
| 0       | 50 µl ethanol | Treated normally  |
| '0 + C' | 50 µl ethanol | Used for non-specific binding (NSB) measurements                            |
| 'B - C' | 50 µl ethanol | Used for total $^{1,25}(\text{OH})_2\text{D}$ free in solution measurements |

7000 dpm ( $\sim$  58 pg) of radioactive  $^3(\text{H})25(\text{OH})\text{D}_3$  in 50 µl ethanol was added to each incubation tube. 1 ml of protein binding solution PBS (Table C.2) was added to each tube except the '0 + C', to which 1 ml buffer solution was added. All tubes were vortex mixed and left to incubate at  $4^\circ\text{C}$  for 30 minutes. Following this, 250 µl Dextran coated charcoal (DCC) suspension (Table C.2) was added to each tube. 250 µl gelatin buffer was added to the 'B-C' tubes instead. After further incubation for 20 min at  $4^\circ\text{C}$  the tubes were centrifuged for 15 min at  $4^\circ\text{C}$  (2000 rpm). 500 µl of each supernatant was transferred to a scintillation vial and 5 ml Fisofluor added. The vials were counted for 10 min to estimate the amount of bound ligand in the 500 ml supernatant.

#### Calculation of Results

##### a) Standard curve

An example of calculation of the standard curve is given below for the assay performed on 17.10.84 for the final Young group samples.

Table C.2. Standard solutions used for assay.

| Solution        | Lifetime   |
|-----------------|--|
| Stock buffer    | 4.86 g Sodium acetate      } Dissolved in 500 ml<br>7.87 g Sodium barbitol      } distilled H <sub>2</sub> O<br>0.05 g Sodium azide added per 500 ml to aid preservation   |
| Working buffer  | 50 ml stock buffer in 850 ml 0.9% NaCl, adjusted to pH 8.6<br>and made up to 1 litre.  |
| Gelatine buffer | 100 mg gelatine in 100 ml working buffer.<br>Stirred on<br>heated stirrer to dissolve gelatine.  |
| PBS             | 1:10,000 dilution of normal human serum.<br>i.e. 10 µl. in 100 ml of gelatine buffer ( $\rightarrow$ ~ 50% max. binding)   |
| DCC             | 750 mg Novit charcoal in 50 ml working buffer. Stirred in<br>cold room for 15 min. 75 mg Dextran T <sub>70</sub> (pharmacia), preswollen<br>with 5 ml out of 50 ml working buffer, is then added and solution<br>stirred in cold room for at least 1 h before use. |

Results from the standard tubes are plotted as  $\%B/B_0$  (% Bound/Total Bound) disintegrations against ng 25(OH)D to give the standard curve. This allows for the recovery counts in the tube and the non-specific binding. The counts are made in disintegrations per minute (dpm) and the efficiency of the counter is corrected for.

Calculation of standard curve

| ng 25(OH)D | Tube    | B' (ave. dpm) | B (= B' - NSB)  | % B/B <sub>0</sub> |
|------------|---------|---------------|-----------------|--------------------|
|            | 'B - C' | 452           |                 |                    |
|            | 'O + C' | 29            |                 |                    |
| 0          | 0       | 305.6         | 264.6 ( $B_0$ ) | 100                |
| 0.0625     | x       | 284.6         | 243.6           | 92                 |
| 0.125      | 1       | 256           | 215             | 81                 |
| 0.25       | 2       | 234           | 193             | 72                 |
| 0.50       | 3       | 172           | 131             | 49                 |
| 1.0        | 4       | 104           | 63              | 24                 |
| 2.0        | 5       | 78            | 37              | 14                 |
| 4.0        | 6       | 51            | 9.6             | 3.6                |
| 8.0        | 7       | 40.6          | 0               | 0                  |

Background = 12 dpm.      'O + C' + BG = 41 dpm.

50% binding at 0.47 ng. The 50% point monitors the sensitivity of the curve by displacement.

The 'B - C' tube is used as a check of counts free in solution.

It does not figure in these calculations.

The standard curve is shown in Figure C.1.

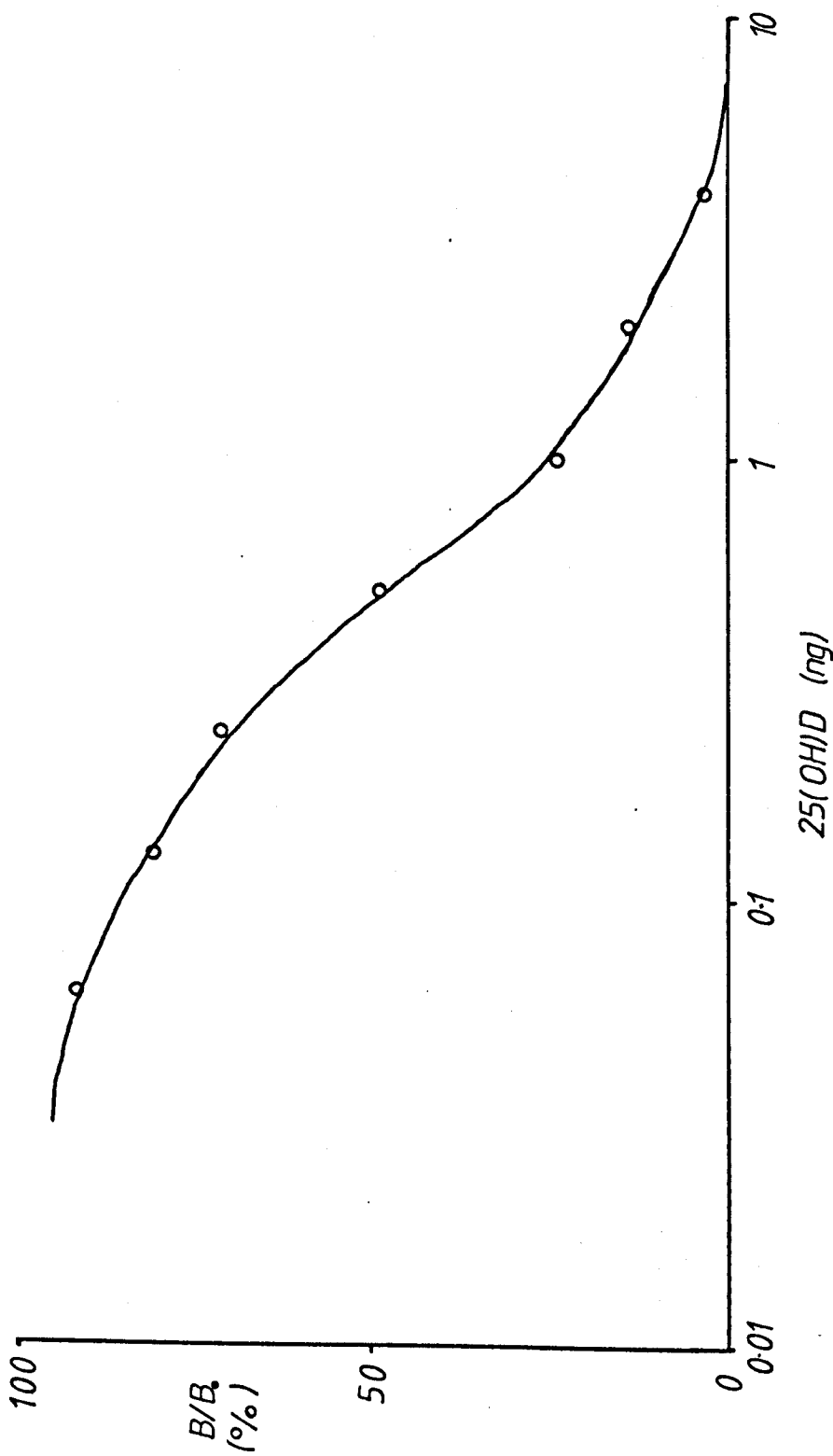


Fig. C.1 Standard curve for 17 October 1984.

The standard curves are very reproducible if fresh buffer, careful pipetting and clean glassware are used each time.

Once the standard curve for the assay has been determined the plasma 25(OH)D concentration for each extract can be calculated as shown below.

#### Calculation of 25(OH)D extract

The recovery for each sample is calculated as the percentage of dpm from the recovery aliquots to dpm from the total radioactive spike added to the sample.

The inter-assay coefficient of variation for the assays was 19.1% (this method normally has an inter-assay coefficient of ~18%).

The intra-assay coefficient of variation was not measured for these particular assays but is normally 11% for the procedure and equipment in the laboratory where the assays were performed.

| Extracts | B' (ave. dpm) | B(B'-lSB) | %B/B <sub>0</sub> | ng 25(OH)D (a) | x 20(b) | / Rec. | Rec. (%) | ÷ 3 (c) |
|----------|---------------|-----------|-------------------|----------------|---------|--------|----------|---------|
| 1        | 105           | 64        | 24.2              | 1.158          | 23.16   | 100.7  | 23       | 33.56   |
| 2        | 112           | 71        | 26.8              | 1.010          | 20.2    | 113.5  | 17.8     | 37.8    |
| 3        | 117           | 76        | 28.7              | 0.94           | 18.8    | 120.5  | 15.6     | 40.1    |
| 4        | 59            | 18        | 6.8               | 2.876          | 57.5    | 119.8  | 48       | 39.9    |
| 5        | 98            | 57        | 21.5              | 1.260          | 25.2    | 126    | 20       | 42      |
| 6        | 110           | 59        | 22.3              | 1.048          | 20.96   | 116.4  | 18       | 38.8    |
| 7        | 96            | 55        | 20.8              | 1.297          | 25.9    | 135    | 19.2     | 45      |
| 8        | 147           | 106       | 40.8              | 0.648          | 12.96   | 72.8   | 17.8     | 24.3    |
| 9        | 112           | 71        | 26.8              | 1.031          | 20.6    | 103    | 20       | 51.5    |
| 10       | 108           | 67        | 25.3              | 1.068          | 21.36   | 101.7  | 21       | 33.9    |
| Blue P.S | 104           | 63        | 23.8              | 1.158          | 23.16   | 105    | 22       | 35.1    |
| Saline   | 90            | 49        | 18.5              | 1.457          | 29.14   | 138.7  | 21       | 46.2    |

- (a) Read from standard curve.  
 (b) The radioactive spike was made up in 50 µl, the sample measured was 1 ml  
 (c) Original plasma sample was 3 ml. ÷ 3 gives plasma concentration of 25(OH)D in ng ml<sup>-1</sup>.  
 Blue P.S. is Blue pool serum and is used as a control for the inter-assay coefficient of variation.  
 The saline is a blank control.